UNIVERSIDAD NACIONAL AUTÓNOMA DE MÉXICO

POSGRADO EN CIENCIAS BIOMÉDICAS

INSTITUTO NACIONAL DE CANCEROLOGÍA
INSTITUTO DE INVESTIGACIONES BIOMEDICAS-ALBERTO SOLS

Estudio de biomarcadores de pronóstico y respuesta a terapia en cáncer gástrico

TESIS

QUE PARA OPTAR POR EL GRADO DE:
DOCTOR EN CIENCIAS BIOMÉDICAS

PRESENTA:
JONE BARGIELA IPARRAGUIRRE

Director de Tesis:
Dra. Mª Isabel Sánchez Pérez
Instituto de Investigaciones Biomédicas-Alberto Sols

Miembros del comité tutor:
Dr. Luis Alonso Herrera Montalvo -Instituto Nacional de Cancerología
Dra. Carmela Calés Bourdet- Instituto de Investigaciones Biomédicas-Alberto Sols

Universidad Autónoma de Madrid, Marzo del 2017

Mª Isabel Sánchez Pérez, Profesora Titular del Departamento de Bioquímica, Facultad de Medicina, de la Universidad Autónoma de Madrid.

CERTIFICA: que **Jone Bargiela Iparraguirre**, Licenciada en Bioquímica por la Universidad de Navarra, ha realizado bajo mi dirección en el Dpto. de Bioquímica de la Facultad de Medicina de la Universidad Autónoma de Madrid-Instituto de Investigaciones Biomédicas "Alberto Sols" del Consejo Superior de Investigaciones Científicas el trabajo de investigación titulado:

"Estudio de Biomarcadores de pronóstico y respuesta a terapia en Cáncer Gástrico"

Y que dicho trabajo reúne todas las condiciones requeridas por la legislación vigente y la originalidad y calidad científica necesarias para poder ser presentado y defendido con el fin de optar al grado de Doctor por la Universidad Autónoma de Madrid.

Y para que conste donde proceda, firmo el presente certificado en,

Madrid, 3 de Enero de 2017

Dra. Mª Isabel Sánchez Pérez

Esta tesis se ha realizado en el Instituto de Investigaciones Biomédicas-Alberto Sols y en el Instituto Nacional de Cancerología de México con la financiación de la beca Isaac Costero Santander-UAM y beca predoctoral CONACYT-UNAM.

A mis padres

A mi abuela

A Mikel

AGRADECIMIENTOS

En primer lugar agradezco a mi directora de tesis, a la Dra. Isabel Sánchez Pérez por ser un referente de trabajo, apoyo y excelente guía en aspectos tanto académicos como personales durante todo este tiempo. Por todo lo que me ha enseñado y me ha ofrecido, sobre todo por inspirarme y motivarme a disfrutar de la ciencia.

Segundo agradezco a mi tutora de tesis a la Dra. Carmela Calés Bourdet, por su implicación constante como tutora, por sus aportaciones, críticas constructivas, enseñanza y el apoyo continúo durante mi proyecto.

Agradezco también a mi tutor el Dr. Luis Alonso Herrera, y a todo su grupo de trabajo del laboratorio de carcinogénesis por haberme acogido en él y darme así la oportunidad de vivir una experiencia única, la cual ha supuesto un enorme aprendizaje laboral y personal.

A la Dra. Rosario Perona y a todo su grupo por su ayuda, colaboración y disponibilidad en todo momento, así como al Dr. Leandro Sastre y su grupo por sus aportaciones y ayuda durante todo este tiempo.

Agradezco al Dr. José Manuel González y a todos y a cada uno de mis compañeros del laboratorio 2.14, Nuria, Laura, Roberto, Natalia y Juan con los que he compartido momentos de trabajo, estrés pero sobretodo alegrías y buenos momentos en estos cuatro años.

RESUMEN

El cáncer gástrico (CG) es una de las principales causas de muerte por cáncer en todo el mundo, la alta incidencia y la falta de un tratamiento eficiente y específico hacen que sea un problema de salud mundial. La gastrectomía complementada con radio-quimioterapia adyuvante es el tratamiento curativo que se aplica a los adenocarcinomas de estómago. Actualmente, la quimioterapia se basa en combinaciones de 5-FU, Cisplatino y Taxanos. Sin embargo, la falta de biomarcadores adecuados para el pronóstico y respuesta a tratamiento hace que nos hayamos planteado estudiar la respuesta molecular a estos agentes en un modelo de líneas celulares de cáncer gástrico. Los adenocarcinomas gástricos comparten las características o hallmarks del cáncer, de las cuales la inestabilidad genómica aparece en más de la mitad de los CG. Dos de los mecanismos celulares que evitan la inestabilidad genómica son el DNA Damage Response (DDR) y Spindle Assemble Checkpoint (SAC), estos además están involucrados en la respuesta al tratamiento, por ello nuestro objetivo ha sido estudiar la implicación de estas dos rutas de señalización en el modelo y su implicación en la respuesta a Paclitaxel (PTX), irradiación (IR) y Cisplatino (CDDP). En primer lugar hemos demostrado que el tratamiento combinado de CDDP y PTX induce la catástrofe mitótica en las células MKN45 siendo más eficaz que los tratamientos por separado. Demostramos que los genes *MAD2L1 y BUB1B*, los cuales codifican proteínas clave de SAC, están sobreexpresados en las líneas celulares derivadas de tumores diseminados, y su disminución afecta a la capacidad de proliferación , migración e invasión de estas células, induciendo el fenotipo senescente y la resistencia a PTX. Además, los niveles elevados de expresión de *MAD2L1* correlacionan con un peor pronóstico en los pacientes con CG. Hemos analizado el papel de CHK1, quinasa principal del DDR, en la respuesta a terapia con IR, identificando una sobreexpresión de la misma en células resistentes a IR y a Bleomicina (BLM). El estudio en una serie de pacientes seleccionados por tumor primario y tratamiento con IR, indica que aquellos pacientes que muestran niveles elevados de CHK1 en el tumor respecto al tejido sano presentan un menor tiempo libre de progresión. Hemos observado que la sobreexpresión de CHK1 no se debe a una regulación diferencial a nivel transcripcional, sino postranscripcional, en la que pudieran estar implicados los miR-195 y miR-503. Por otro lado hemos estudiado la reparación y apoptosis generada por CDDP y BLM en líneas celulares de CG. Las células resistentes a BLM son incapaces de inducir la expresión de la proteína pro-apoptóticas (Bax, Bad and Puma) en presencia del estímulo, mientras que la sensibilidad a CDDP se produce por degradación de MCL-1. Hemos observado que una ineficiente ruta de reparación de NER puede ser la causa de la sensibilidad al CDDP. Todo ello hace que propongamos a CHK1 como un marcador de respuesta a terapia con irradiación y MAD2 un buen candidato de pronóstico en CG y posible diana terapéutica.

SUMMARY

Gastric cancer (GC) still is the fourth main cause of cancer related death in all over the world, its high incidence and lack of efficient personalized treatments makes it a public health problem. In GC adenocarcinomas gastrectomy is the only curative treatment, frequently supplied with adjuvant radio/chemotherapy. The chemotherapy regimen is based on combinations of 5-FU, platinum compounds and Taxanes. There is still an imperative need to improve in GC treatment, since there is a lack of good biomarkers for therapy response and patient prognosis we proposed to study deeply the molecular response to therapy in gastric cancer cell model. Two mayor cellular mechanisms involved in the maintenance of genome stability (DNA damage response and SAC) may be responsible of drug response. Firstly, our results demonstrate that the combined treatment of cisplatin (CDDP) and Paclitaxel (PTX) induces cell death by mitotic catastrophe. We found that the central SAC genes *MAD2L1* and *BUB1B,* were the more prominently overexpressed members in disseminated GC cell lines. Silencing MAD2 and BUBR1 decreased cell proliferation, migration and invasion abilities, induced senescence phenotype and PTX resistance, moreover high *MAD2L1* expression correlated with poor prognosis in GC patients. Since CHK1 is an essential kinase of DDR, plays a critical function in cellular response to genotoxic agents, we aimed to analyze the role of CHK1 in GC as a biomarker for radiotherapy resistance. We demonstrated that CHK1 overexpression specifically increases resistance to radiation in GC cells. Furthermore, we found a correlation between nuclear CHK1 accumulation and a decrease in progression free survival in patients. Moreover, we found that CHK1 expression is controlled by p53 and RB/E2F1 at transcriptional level and miR-195 and miR-503 may be involved in posttranscriptional regulation. On the other hand, in order to understand the role of MAD2 controlling the cell fate in CDDP and BLM response, we analyze the process of apoptosis induction. Our data showed that resistant cells in response to BLM are unable to induce the expression of pro-apoptotic proteins Bax, Bad and Puma. In contrast, in this cells in response to CDDP it is induced the degradation of MCL-1 and increased Bid and Bad levels, as a result they showed BLM resistance and sensitivity to CDDP. Additionally, we found that NER repair is impaired in sensitive cells due to the absence of XPA and XPD translocation to the nucleus. In conclusion, the results presented here suggest that MAD2 could be used as prognostic markers of tumor progression and new pharmacological targets in the treatment for GC, whereas CHK1 as a potential tool for optimal stratification of patients susceptible to receive adjuvant radiotherapy after surgery.

CLAVE DE ABREVIATURAS

5-FU: 5 Fluorouracilo

APC/C: Anaphase promoting complex or ciclosome

BLM: Bleomicina

BUB1B: Budding Uninhibited by Benzimidazoles 1 homolog Beta (Yeast) (Gen)

BUBR1: Budding Uninhibited by Benzimidazoles 1 homolog B (Proteína)

CDC20: Cell division cycle 20

CDDP: Cisplatino

CG: Cáncer gástrico

CHK1: Checkpoint kinase 1

CHK2: Checkpoint kinase 2

CIN: Inestabilidad cromosómica (Chromosome instability)

C-MAD2: Conformación cerrada de MAD2 (close-MAD2)

DBS: Double strand breaks

DDR: DNA damage response

ERCC1: Excision Repair Cross-Complementing group 1

GG-NER: Global Genome –NER

HR: Recombinación homóloga (Homologous Recombination)

IR: Irradiación

MAD2: Mitotic Arrest Deficient 2 (Proteína)

MAD2L1: Mitotic arrest deficient 2–like 1 (Yeast) (Gen)

MCC: Mitotic Checkpoint Complex

MT: Microtúbulos

NER: Nucleotide Excision Repair

NHEJ: Recombinación no homóloga (Nonhomologous End-Joining)

O-MAD2: Conformación abierta de MAD2 (open MAD2)

OS: Supervivencia global (Overall Survival)

PFS: Tiempo libre de progresión (Progression Free Survival)

PTX/PLX: Paclitaxel

RB: Retinoblastoma

SAC: Spindle assembly checkpoint

SASP: Senescence associate secretory phenotype

TC-NER: Transcription Couple –NER

TFHII: Basal transcription factor complex helicase 2

TP53: Tumor Protein 53

XPA: Xeroderma Pigmentosum, complementation group A

XPD: Xeroderma Pigmentosum, complementation group D

XPF: Xeroderma Pigmentosum, complementation group F

XPG: Xeroderma Pigmentosum, complementation group G

INTRODUCCIÓN

1. CÁNCER GÁSTRICO

1.1. Epidemiología

El cáncer gástrico (CG) es una de las neoplasias malignas con mayor incidencia en el mundo, situándose en el cuarto puesto con un millón de nuevos casos diagnosticados en el 2015 y la tercera causa de muerte por cáncer, con 785.558 muertes anuales. La mayor incidencia de esta enfermedad se encuentra en países de Asia del Este seguidos de Europa Central y América del Sur [77].Los factores de riesgo asociados al CG son ambientales y hereditarios. Entre los factores de riesgo ambientales se encuentra en primer lugar la presencia o infección prolongada por la bacteria *H. pylori,* el virus de *Epstein Barr,* así como la dieta (alta en sal y nitratos, baja en frutas y verduras) y el tabaco entre otros [28]. Por otro lado, entre los factores de carácter hereditarios destacan la presencia de pólipos gastrointestinales, historial de cáncer familiar de estómago, mutaciones en BRAC1/2 y anemia perniciosa [21]. El CG por su sintomatología leve en etapas más tempranas puede pasar desapercibida o en ocasiones se confunde con gastritis y malas digestiones. Por ello, un 80% de los pacientes son diagnosticados en etapas avanzadas o metastásicas. En esta situación la supervivencia global a 5 años es de apenas el 20% en cambio en etapas tempranas es de un 90 %. El diagnostico precoz de la enfermedad parece ser una de las maneras más eficaces de reducir la mortalidad por CG. Es el caso de Japón, la incidencia del CG es la más alta del mundo pero presenta una supervivencia global a 5 años del 60%, mientas que en Europa y USA es del 20%.[60] La mortalidad ha disminuido en los últimos años gracias a protocolos de erradicación de la infección por *H.Pylori* y screnningspoblacionales de diagnóstico de la enfermedad , se espera que los efectos sean mucho más drásticos en los próximos 10-20 años.[55]

1.2. Clasificación del cáncer gástrico

El 90% de los cánceres de estómago son de origen epitelial, es decir, adenocarcinomas, el 10 % restante lo componen linfomas, tumores de origen neuroendocrino o carcinoides, tumores de origen estromal (GIST) y de origen muscular. Existen diferentes criterios para clasificar el adenocarcinoma, se pueden agrupar en dos grandes grupos: clasificaciones basadas en la características macroscópicas donde se valora el alcance de invasión o la diseminación a nódulos cercanos y metástasis (clasificación TNM, Bormann) y las basadas en las características microscópicas o histológicas (WHO, Laurens, Ming, Goseki).

La clasificación TNM es hasta el momento la clasificación más universal para el pronóstico del paciente, ya que en base a esta clasificación se determina el estadio del tumor y se decide el abordaje clínico a seguir [121]. La **clasificación TNM** se basa en el grado de invasión del tumor primario así como el grado de metástasis. La letra T describe la extensión del tumor primario (cuanto ha crecido hacia el interior de la pared del estómago y hacia los órganos cercanos). La letra N describe la propagación a los ganglios linfáticos cercanos o nódulos regionales y por último la letra M indica si existe metástasis a partes distantes del cuerpo [121]. Por otro lado, la **clasificación de Laurens** según la apariencia histológica distingue los tumores en intestinales o difusos, y mixtos en el caso de haber un porcentaje de ambos [75]. Esta clasificación está acorde en la mayoría de los casos con el grado de diferenciación, así el tipo **intestinal** suele ser catalogado como bien diferenciado, presenta una histología definida y células más diferenciadas. Son tumores menos agresivos y en general estos pacientes presentan un mejor pronóstico, son más frecuentes en el cuerpo gástrico, presentan metástasis a hígado y metaplásias del epitelio gástrico (úlceras). En cambio los tumores catalogados como **difusos** son tumores más desdiferenciados, presentan una histología más heterogénea, las glándulas han perdido su conformación y aparecen células arriñonadas o con una secreción blanquecina (mucinosa). Los pacientes presentan un peor pronóstico, ya que los tumores son más invasivos, aparecen en personas más jóvenes y presentan frecuentemente metástasis pleural [75].

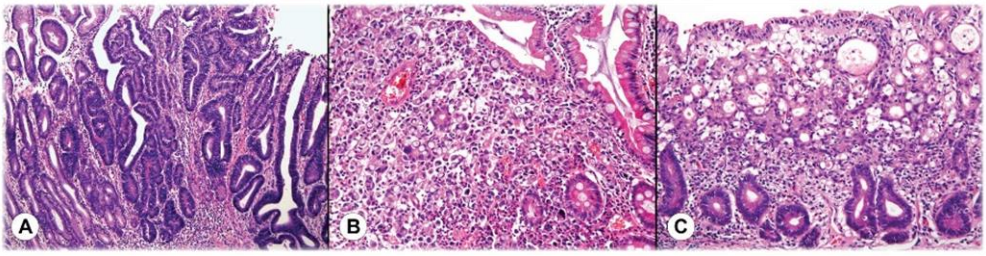

Figura 1. Imágenes representativas de la clasificación histológica de Lauren. A) Intestinal B) Difuso C) Mixto. *Yosep Chong et al.2014*

En el año 2014 se realizó una **clasificación molecular** del CG por parte del Cancer Genome Atlas (TCGA). Teniendo en cuenta la alta heterogeneidad entre tumores de CG pero también la heterogeneidad intra-tumoral observada hasta el momento, se realizó una clasificación integrando la información de la secuenciación masiva de DNA RNA y miRNAs, perfil de metilación , y estudio de inestabilidad microsatelital, agrupando así 295 tumores en los siguientes 4 subtipos: tumores asociados a EBV (*Ebstein Barr* virus), tumores con inestabilidad de microsatélites (MSI), tumores con estabilidad genómica (GS) y tumores con inestabilidad cromosómica (CIN)[20]. Hasta el momento esta y otras clasificaciones moleculares que se han realizado en CG no se han llevado a la práctica en la clínica.

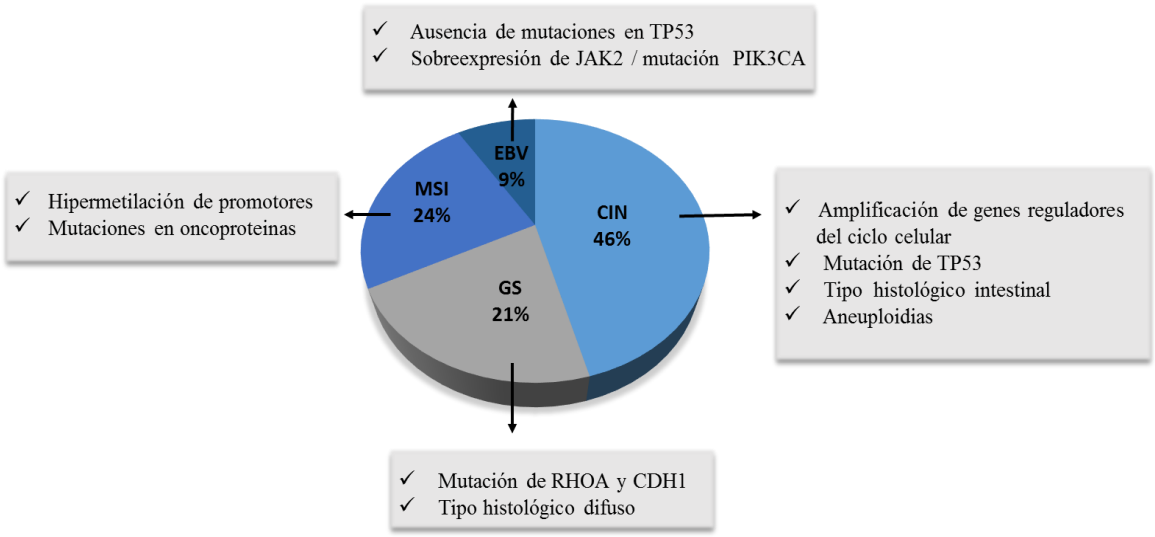

Figura 2: Clasificación molecular de 295 tumores de cáncer gástrico por The Cancer Genome Atlas [11]: 46% chromosome instability (CIN), 24% Microsatelital instability (MSI), 21% Genome stability (GS), 9% Epstein-Barr Virus (EBV).

1.3. Biomarcadores y tratamiento en cáncer gástrico

Un biomarcador es cualquier variable medible que sea indicador de un proceso biológico. En CG se utilizan dos tipos: los de diagnóstico, como son el CEA (carcinoembrionic antigen) y el CA 19-9 (carbohidrates antigens) y de pronóstico, como la inestabilidad de microsatélites. CEA fue utilizado por primera vez en 1980 para el diagnóstico precoz del cáncer de estómago y actualmente es el marcador más valioso a pesar de estar presente en otros tipos de cánceres. CA 19-9 especialmente se relaciona a adenocarcinomas pancreáticos y de estómago.[56] Por otro lado , actualmente se han sugerido como biomarcadores de mal pronóstico la sobreexpresión de las vías de señalización de factores de crecimiento EGFR, HER-2, VEGF, TGF, c-MET, la expresión de citoquinas IL-6,IL-10 y la ciclina E y la sobreexpresión de las proteínas implicadas en apoptosis (Bcl-2 , FasL, survivina) [56]. Cada día surgen nuevos estudios que intentan aportar marcadores de pronóstico para esta enfermedad, con ventajas para la implementación en la clínica. Entre ellos podemos destacar los miRNAs, alteraciones epigenéticas y polimorfismos. Los miRNAs parecen ser biomarcadores prometedores por su expresión estable y robusta tanto en tejido como en plasma, por ejemplo, la diminución de Let-7g y miR-433 especialmente se han relacionado con un mal pronóstico en CG [56]. Aun así, **actualmente no existe un biomarcador único y fiable para predecir el pronóstico del paciente.**

El tratamiento estándar del CG se basa en una gastrectomía subtotal o radical dependiendo de la localización del tumor en el estómago, seguido de radio- quimioterapia adyuvante en la mayoría de casos y quimioterapia paliativa en etapas avanzadas. La quimioterapia por excelencia son combinaciones de 5-Fluororacilo y Cisplatino. En caso de recurrencia (80% de los pacientes en etapas avanzadas) se suelen incorporar fármacos derivados de taxanos como segunda línea de terapia adyuvante [30]. Actualmente se está implementado la quimioterapia neoadyuvante (platinos y radiación) y/o terapia perioperatoria (radiación) con bastantes buenos resultados[1]. A día de hoy la alta resistencia intrínseca o adquirida al tratamiento sigue siendo el mayor obstáculo en el manejo clínico de los tumores sólidos de estómago, los cuales presentan ciertas características comunes que pueden ser responsables de dicho comportamiento ante una terapia clínica.

2. CARACTERÍSTICAS DE LOS TUMORES SÓLIDOS DE ESTÓMAGO

Las características de las células tumorales se definen como el conjunto de capacidades funcionales adquiridas que permiten la supervivencia, proliferación y la diseminación de las células tumorales. Estas funciones se adquieren por mecanismos diferentes en un contexto temporal distinto a lo largo de la carcinogénesis, en un proceso multi-etapa. En el año 2000 Hanahan and Weinberg sugirieron que el crecimiento de las células malignas se debía a la adquisición de seis alteraciones fisiológicas: generación de factores de crecimiento ilimitado, insensibilidad a las señales de inhibición del crecimiento, un potencial ilimitado de replicación, angiogénesis, resistencia a la muerte celular, y la capacidad de invasión y de metástasis [46]. En el año 2011 se añadieron cuatro procesos más: la reprogramación del metabolismo energético, evasión del sistema inmune, ambiente pro-tumoral infamatorio y **la inestabilidad genómica** y mutaciones [47] (Fig. 3)

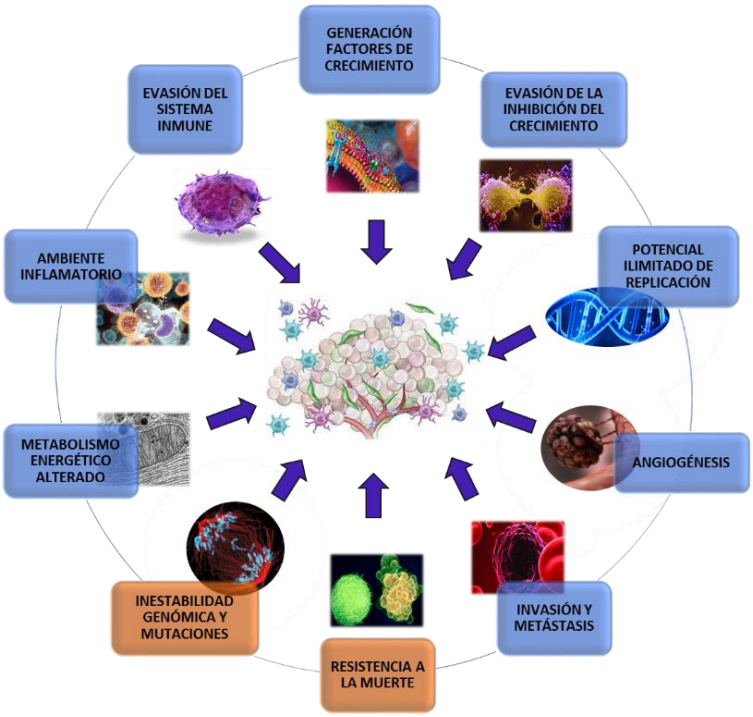

Figura 3. Esquema de los Hallmarks del cáncer descritos por Hanahan en el 2011. Resaltadas las dos características que se van a desarrollar en esta tesis: Inestabilidad genómica y resistencia a la muerte celular.

De todos ellos explicaré en más detalle aquellos relacionados con el contenido de esta tesis: **inestabilidad genómica** (inestabilidad cromosómica) y **resistencia a la apoptosis**.

2.1. INESTABILIDAD GENÓMICA

El DNA está constantemente expuesto a agentes que pueden lesionarlo, agentes externos (luz, químicos ambientales, fármacos…) o agentes internos debido al propio metabolismos celular que genera especies reactivas de oxígeno (ROS)[7]. Las lesiones en el DNA pueden generar **inestabilidad genómica** por acumulación de mutaciones y por el bloqueo de la horquilla de replicación.[7] Para prevenir tales daños las células eucariontes han desarrollado mecanismos de respuesta al daño en el DNA, o DNA Damage Response (DDR), que tiene como función mantener la integridad del genoma, evitando la perpetuación de la lesión y la segregación de cromosomas dañados o incompletos (inestabilidad cromosómica)[74]. Así, DDR actúa como una barrera ante la tumorogénesis [6, 7]. A efectos mecanísticos es una vía de señalización que se compone por sensores que responden ante señales intracelulares de daño en el DNA, quinasas efectoras centrales y quinasas ejecutoras que controlan la parada del ciclo momentánea o permanente (senescencia)[108], e inducen la reparación del daño y/o la apoptosis [135]. La vía DDR es capaz de dirigir el destino

celular ante un estímulo, por lo que es considerado un buen candidato como biomarcador de respuesta a tratamiento.

2.1.1 Respuesta al daño en el DNA (DDR)

La vía de señalización DDR está regulada por dos quinasas altamente conservadas desde levaduras a mamíferos: Ataxia Telangiectasia mutated (ATM) y Ataxia Telangiectasia and Rad3 related (ATR) [15]. ATM se recluta a los puntos de ruptura de doble cadena por el complejo Mre11-Rad50-Nbs1 (MRN) donde se fosforila la variante de histona H2AX, así se genera la señal para el reclutamiento del resto de los participantes de la vía. En paralelo ATM media la reparación de las hebras generando una situación intermedia de ruptura de hebra sencilla lo que a su vez activa a la quinasa ATR [54]. Mediante la fosforilación y la consiguiente activación de las quinasas efectoras CHK1 y CHK2, ATM y ATR son capaces de inducir la parada de ciclo celular y la reparación de la lesión. Cuando el daño es excesivo o irreparable pueden también inducir la senescencia celular y /o la muerte celular. La diana principal de ATR/ATM para la parada del ciclo celular y dictaminar el destino celular es la proteína supresora tumoral p53 (Fig 4). En ausencia de estímulo los niveles totales de p53 se mantienen bajos por la ubiquitin ligasa MDM2 (HDM2 en humanos) que continuamente envía a degradar a p53 vía proteasoma. Una vez activas, ATM/ATR fosforilan a p53, esta se disocia de MDM2 y conlleva a la estabilización de la proteína [80], así el factor de transcripción puede inducir la parada de ciclo, la reparación del daño en el DNA o la inducción de la muerte celular o senescencia controlando la expresión de multitud de genes diana que participen en dichos procesos[62].

Las quinasas efectoras de la vía CHK1 y CHK2 se han relacionado con la resistencia a ciertos agentes antineoplásicos y radiación en cáncer de mama, lo cual ha impulsado el estudio y la generación de inhibidores farmacológicos[5, 40]. Aunque la mayoría se encuentran en etapas iniciales de los ensayos clínicos algunos de ellos presentan resultados favorables en la sensibilización a radiación, pero con gran toxicidad sistémica. La radioterapia y agentes citotóxicos como el Cisplatino (CDDP), activan esta ruta de señalización y los niveles alterados de CHK1 y CHK2 pueden modular la respuesta final a estos estímulos.[93]

2.1.2 Proteína CHK1/ CHK2

La proteína CHK1 es una de las serina/treonina quinasa que se activa en presencia de diversos agentes genotóxicos.[5] La activación se produce mediante la fosforilación en residuos específicos de la proteína. La fosforilación en la Ser-317 y Ser-345 de CHK1 resulta en un incremento en la actividad catalítica de esta. La quinasa CHK1 activa, fosforila a p53 y a proteínas de la familia de fosfatasas CDC25 (A, B, C) induciendo así una parada del ciclo celular. En concreto la fosforilación de CDC25C provoca la inactivación de la fosfatasa, favoreciendo la parada en G2/M del ciclo celular. Junto con la parada de ciclo celular, CHK1 participa en la reparación del DNA, activando la recombinación homóloga (HR) mediante la fosforilación de NEK6 que este as su vez fosforila a RAD51 (proteína clave en HR) haciendo que pueda liberarse de BRCA2 y pudiendo unirse al DNA.[134]

La proteína CHK2 es una serina/treonina quinasa que al igual que CHK1 se fosforila y activa ante diversos estímulos que generan daño en DNA. Hasta el momento se conocen 24 proteínas sustrato de la quinasa CHK2 en humanos, los cuales forman parte de distintas mecanismos celulares que se pueden agrupar de la siguiente manera: reparación de DNA, regulación del ciclo celular, señalización de p53 y apoptosis[133]. CHK2 participa directamente en las primeras etapas de la reparación de rupturas de doble hebra (DBS), fosforando a BRCA1 y BRCA2 [2], con un balance final de activación de HR sobre NHEJ. Ambas quinasas responden ante multitud de lesiones en el DNA y son claves en la vía DDR para evitar la inestabilidad genómica. [2]

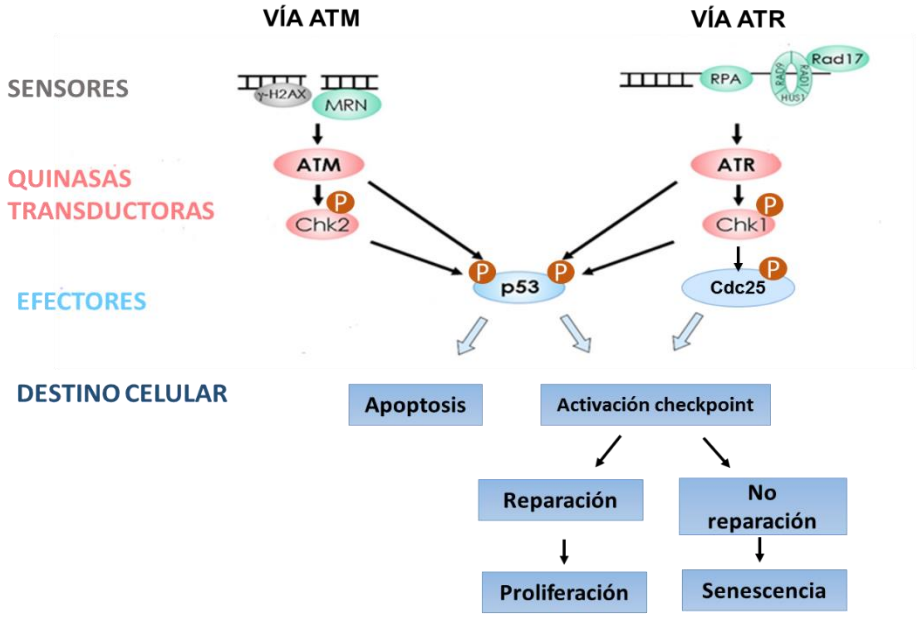

Figura 4: Esquema simplificado de la vía de señalización DDR. Adaptación de *Nature Reviews*[108]

2.2 INESTABILIDAD CROMOSÓMICA

La **inestabilidad cromosómica** (CIN), incapacidad de mantener un número constante de cromosomas en cada división celular, es la disfunción más comúnmente asociada al cáncer en humanos, por lo que se ha convertido en una de las áreas principales en el estudio del cáncer [35]. Las células diploides normales contienen un número invariable de 46 cromosomas. Sin embargo, las células tumorales poseen un número anormal que puede alcanzar entre 60 y 90. Además estos cromosomas suelen presentar aberraciones estructurales que rara vez se encuentran en células normales: inversiones, deleciones, duplicaciones y translocaciones. Las anormalidades numéricas definen la aneuploidía[119].

Por tanto la estabilidad genómica de un organismo depende entre otras cosas, de la segregación precisa de las cromátidas hermanas durante la mitosis. La capacidad de distribuir correctamente los cromosomas replicados es crítico para la transferencia del material genético de una generación a la siguiente. Este proceso está sometido a múltiples puntos de control que aseguran la fidelidad en la trasmisión del material genético y previene la aparición de errores. La segregación de los cromosomas y la división celular dependen de una formación regulada del aparato del huso mitótico que es el responsable de los movimientos de los cromosomas durante la anafase. El huso mitótico es una estructura bipolar formada por microtúbulos (MT) que emanan de dos centros organizadores llamados centrosomas. Los cromosomas condensados se unen al conjunto de MT dinámicos, a través de las estructuras macromoleculares denominadas cinetocoros, que se ensamblan en las regiones centroméricas del cromosoma. Las cromátidas hermanas se mantienen unidas por un mecanismo de cohesión, que debe ser eliminado para que ocurra el anafase.

Por ello, es factible pensar que cualquier fallo en este mecanismo o en sus componentes puede generar aneuploidia y como consecuencia de ello cáncer[107]. El mecanismo de vigilancia de este proceso es el "Spindle Assemble Checkpoint" (SAC) que controla el estado de unión y de tensión entre MT y los cinetocoros.

2.2.1 SAC (Spindle Assemble Chechpoint)

El punto de control SAC es un mecanismo de supervivencia del ciclo celular que detecta la falta de unión entre el cinetocoro y los microtúbulos y/o la falta de tensión entre ellos para retrasar la transición metafase a anafase [114]. SAC se considera el mecanismo principal para evitar la incorrecta segregación de los cromosomas y por tanto la inestabilidad cromosómica. El cinetocoro es la estructura formada por más de 100 proteínas que une los microtúbulos y los cromosomas por el centrómero. Este "andamiaje" proteínico es necesario para que se genere la tensión física adecuada entre los microtúbulos y los cromosomas, así los microtúbulos literalmente tiran de ellos y separan las cromátidas hermanas. Hasta el momento en el que se detecta la correcta unión entre el cinetocoro y el microtúbulo la señal de parada de SAC se encuentra activa (Fig 5A). El paso imprescindible en la activación de SAC es la formación del complejo MCC o Mitotic Checkpoint Complex que incluye a las proteínas BUBR1, BUB1, Cdc20 y MAD2. La formación de MCC conlleva a la inhibición de la E3 ubiquitin ligasa APC/C o complejo promotor de anafase mediante el secuestro de su coactivador, el Cdc20. La inhibición de APC/Cdc20 estabiliza la Securina y la Ciclina B1, así retrasando el inicio de la anafase y por tanto la salida de mitosis. El ensamblaje y desensamblaje de los componentes del complejo MCC son eventos clave en la regulación de APC/C por SAC, ya que en ausencia de MCC el Cdc20 libre activa a APC/C y esta marca para degradación a Ciclina B, activando así a Cdk1 y promoviendo la salida de mitosis. Por otro lado APC/C promueve la degradación de Securina la cual mantiene inhibida a la Separasa, una vez libre la Separasa, ya activa, degrada las cohesinas que mantienen unida los cromátidas hermanas (Fig 5A). Aún no está dilucidado cómo se produce el reclutamiento de las proteínas del MCC al cinetocoro, se conoce que la quinasa BUB1 juega un papel importante en la fosforilación y en el reclutamiento de las proteínas del SAC [19, 73]. En la formación del complejo MCC por un lado se unen BUB1 y BUBR1 y por otro lado MAD2 y Cdc20, se cree que esta última interacción es la etapa limitante del proceso. MAD2 antes de que pueda unirse a Cdc20 debe de cambiar de una conformación abierta (O-MAD2) a una conformación cerrada (C-MAD2). Este cambio conformacional ocurre cuando previamente MAD2 y MAD1 forman un heterotetrámero en el cinetocoro, lo hace posible que un nuevo monómero de O-MAD2 se convierta en C-MAD2. C-MAD2 puede ya unirse a Cdc20 y mantener la parada de mitosis activa[49, 61].La señal de parada del SAC es rápidamente silenciada cuando el último microtúbulo está correctamente unido al cinetocoro. Esto ocurre por varios mecanismos, como es la eliminación de los componentes de SAC del cinetocoro por complejos motores de dineína, o por la inhibición de C-MAD2 mediante la proteína p31comet [120] (Fig 5B).

A

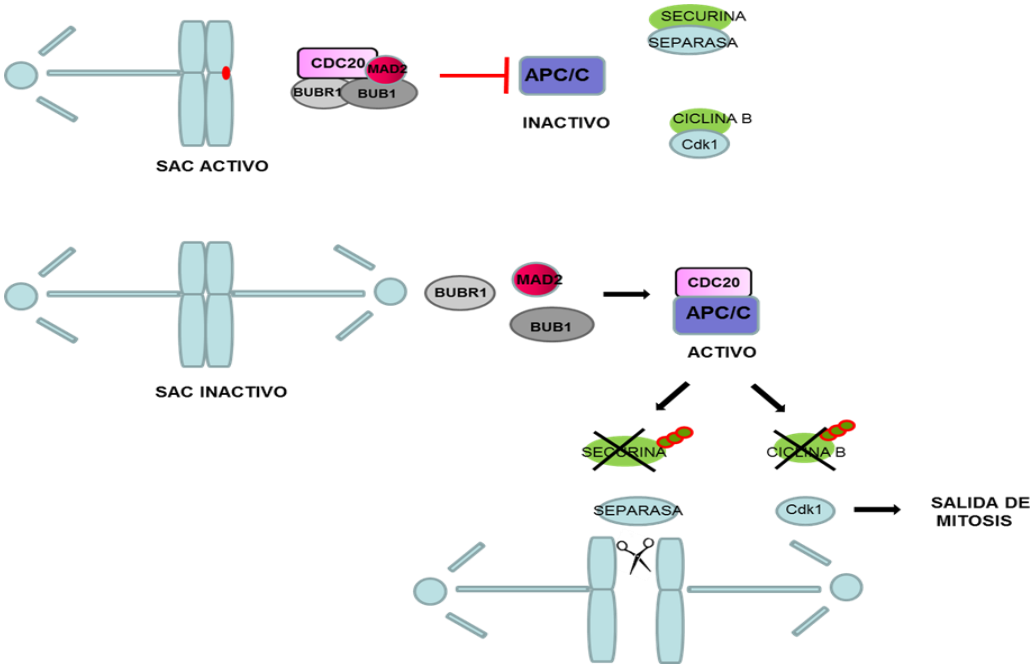

B

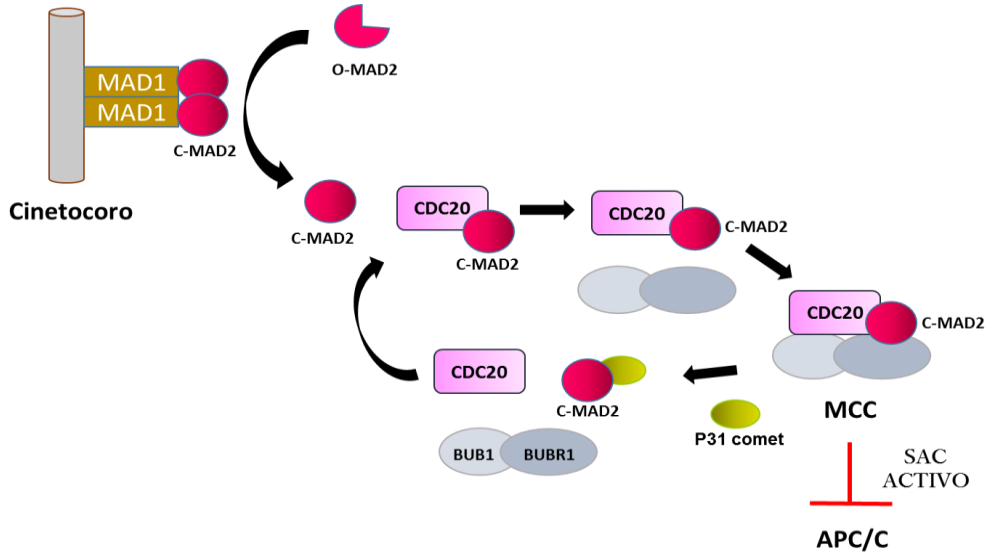

Figura 5:**A)** Activación de la señal de SAC en ausencia de microtúbulos unidos al cinetocoro. En presencia de microtúbulos correctamente unidos Ccd20 libre activa a APC/C, el cual ubiquitina y manda a degradar a Securina y Ciclina B dejando actuar a Separasa y Cdk1 para la segregación de los cromosomas y la salida de mitosis. **B)** Esquema representando el cambio conformacional de MAD2 abierta a cerrada,lo que permite su unión con Cdc20 y la formación del MCC .Inactivación de la señal de SAC por la proteína p31comet desensamblando el complejo MCC. MCC; Mitotic Checkpoint Complex.

En numerosos tipos de tumores como en mama, ovario, pulmón y en tumores gastrointestinales se han observado alteraciones tanto de la expresión de los genes como de los niveles de proteínas implicadas en SAC[10, 131]. Se ha comprobado *in vitro* que la disminución y/o la ausencia de alguna de ellas generan aneuploidías, así como resistencia a fármacos [119]. También se ha observado *in vitro* que una señal débil de SAC puede generar resistencia a fármacos dirigidos contra la dinámica de los microtúbulos, como son los vincaloides y los taxanos [48]. La familia de fármacos conocido como Taxanos comprende al grupo principal de antineoplásicos que tienen como diana a β-tubulina, ampliamente utilizado para tratar tumores sólidos. Estos afectan la dinámica de la tubulina y tienen como objetivo generar una señal de bloqueo prolongada en profase, lo que finalmente provoca la apoptosis por catástrofe mitótica [29]. Dos de la principales proteínas clave de la vía SAC que están alteradas frecuentemente en tumores son MAD2 y BUBR1.

2.2.2 Proteína MAD2

La proteína MAD2 es una proteína esencial en la activación de SAC. Está codificada por el gen *MAD2L1* situada en brazo corto del cromosoma 4. Es un gen altamente conservado desde levaduras hasta mamíferos, siendo una proteína esencial en el desarrollo ya que su ausencia provoca letalidad embrionaria [31]. MAD2 de 111aa y 24 kDa, presenta un dominio HORMA que comprende el 80 % de la proteína, este dominio se ha relacionado con la unión a DNA. Como ya se ha comentado anteriormente MAD2 existe en dos conformaciones relativamente estables, conocidas como O-MAD2 (open-MAD2) y la C-MAD2 (close-MAD2). El cambio conformacional es necesario para que MAD2 se pueda unir a MAD1 y CDC20 y parece ser el mecanismo principal que regula la disponibilidad de MAD2 activa en la célula [49]. La expresión de MAD2 es controlada mediante factores de transcripción como es el E2F1 el cual promueve la expresión del gen, factor que en cáncer se han encontrado sobreexpresado. Además, la proteína p53 y el eje RB/E2F interactúan para regular a MAD2[100].

La expresión de *MAD2L1* así como los niveles de proteína MAD2 están alterados en cáncer. La disminución y la sobreexpresión de MAD2 conducen a una señalización de SAC inadecuada lo que genera aneuploidias tanto *in vitro* como en modelos animales, los cuales desarrollan tumores espontáneos [82, 103]. Existen numerosos trabajos en los que se han relacionado los niveles de MAD2 en tumor con el pronóstico en los pacientes, con resultados contradictorios, así mientras en tumores de colon, boca, endometrio y vejiga los niveles altos de MAD2 correlacionan con un peor pronóstico del paciente, en pulmón y ovario se correlaciona con un mejor pronóstico[39, 59, 67, 111]. Lo mismo ocurre en cuanto a la influencia de MAD2 y la respuesta a tratamiento *in vitro*, ya que dependiendo de la línea celular y del fármaco los resultados en cuanto a resistencia o sensibilidad

varían[48, 118]. Además en los últimos años se han descrito nuevas implicaciones de la proteína en diversos mecanismos celulares como la senescencia[65], apoptosis y una posible relación directa con la vía DDR mediante CHK1[23], lo cual podría explicar su función en la respuesta a genotóxicos como el Cisplatino.

2.2.3 Proteína BUBR1

BUBR1 es otra de la proteínas clave de la ruta de SAC que frecuentemente está sobreexpresada en tumores[18]. Es una proteína multidominio presente a lo largo de todo el ciclo celular, participando en diversas funciones como la segregación cromosómica, la reparación del DNA, la diferenciación de neuronas, ciliogénesis y envejecimiento celular[18]. Existen evidencias de que la reducción de BUBR1 genera un incremento notable en la incidencia de aneuploidías en células hepáticas y acelera el envejecimiento celular, pero los modelos animales no desarrollan tumores espontáneos. BUBR1 está altamente fosforilado durante mitosis por las quinasas Cdk1, Plk1, Mps1 y Aurora B[122]. La fosforilación depende de la tensión de los microtúbulos y /o de la unión del cinetocoro al microtúbulo. Además de su función principal formando parte del SAC, en *D. Melanogaster*, BUBR1 se ha relacionado con CHK1, retrasando la transición de metafase a anafase en respuesta al daño en el DNA por radiación[98]. En mamíferos también existen evidencias de la implicación de BUBR1 en la respuesta a agentes genotóxicos[36].

2.3. RESISTENCIA A LA MUERTE CELULAR

La resistencia a la muerte inducida por fármacos es otro de los “hallmarks” de las células cancerosas[47], debido a una alta tolerancia a la lesión y/o un aumento en la capacidad de reparación por presentar rutas de reparación potenciadas entre otras. La inhibición de la ruta de apoptosis es una de las causas más frecuentes de resistencia a terapia. En esta tesis nos hemos centrado en el estudio de la vía canónica intrínseca de apoptosis y el estudio de la ruta de reparación por escisión de nucleótidos (NER) para evaluar la respuesta al Cisplatino.

2.3.1 La vía intrínseca de apoptosis

La apoptosis es un tipo muerte celular controlada genéticamente. La activación de las proteasas específicas denominadas caspasas es el punto sin retorno de la apoptosis. Existen dos rutas principales de muerte por apoptosis: **extrínseca** (o a través de receptores) e **intrínseca**. Nos centraremos en estudiar la vía intrínseca o vía mitocondrial, la cual se inicia por estímulos de estrés intracelulares como es el daño en el DNA, provocado por antitumorales. Esta ruta de apoptosis está regulada por el equilibrio entre los miembros de la familia Bcl-2. Dicha familia de proteínas se clasifica en tres grupos: proteínas anti-apoptóticas (Bcl-2, Bcl-XL, Mcl-1,) reguladoras (Bim, Bid, Puma, Bad, Noxa ,Bik, Bmf, Hrk) y pro-apoptóticas (Bax y Bak).Estas últimas en presencia de estímulos apoptóticos forman un poro en la membrana mitocondrial externa, permitiendo la salida del citocromo C al citoplasma, el cual junto con la procaspasa 9 y APAF-1 forma el apoptosoma para provocar finalmente la activación de la caspasa-3 y la muerte celular (Fig 6). En CG se ha descrito la resistencia a tratamiento debida a la sobreexpresión de algunos miembros anti-apoptóticos, como Bcl-2.

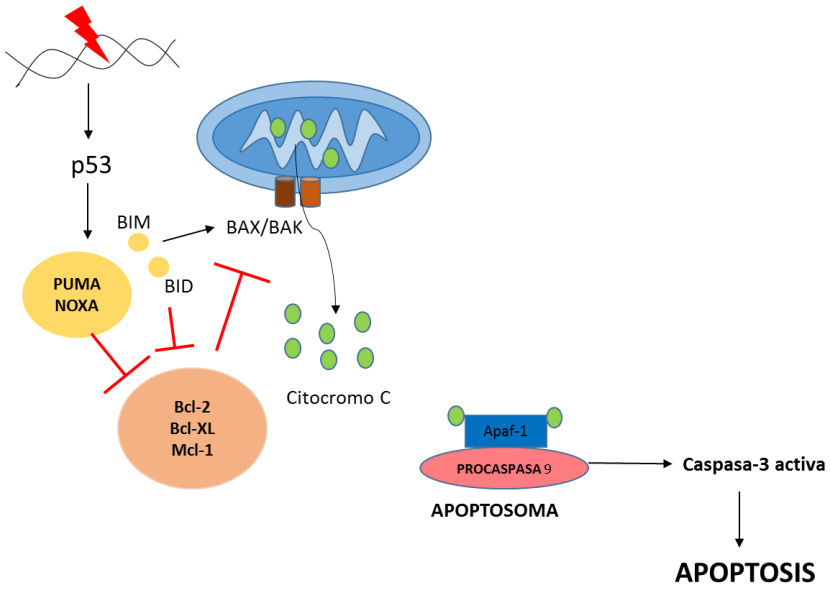

Figura 6: Esquema de la vía intrísica de apoptosis. El daño en el DNA por agentes antitumorales o estrés oxidativo activan la vía mediante un incremento de las proteínas BH3 only reguladoras (Puma , Noxa) que se unen a las proteínas anti-apoptoticas Bcl-2,Bcl- XL, Mcl-1 y las inactivan. Estas una vez inactivas permiten la oligodimerización de las proteínas pro-apototicas Bak y Bax para formar el poro en la membrana mitocondrial y la salida del Citocromo C. La formación del apoptosoma activa la caspasa 3 para que se ejecute la apoptosis.

El Cisplatino activa esta ruta de apoptosis. La resistencia intrínseca o adquirida al Cisplatino es el problema principal actualmente en el tratamiento de tumores sólidos, como ocurre en los tumores gástricos. Los tumores de ovario y testiculares presentan una buena respuesta al tratamiento con platinos[113], pero en cambio otros como el de pulmón, mama, piel presentan una alta resistencia. El Cisplatino en primer lugar activa la vía DDR, la activación de p53 seguido de una activación de la expresión de BAX y BAK conlleva a la muerte celular dependiente de caspasas. En la resistencia a platinos, el nivel de expresión de los miembros de la familia Bcl-2 y caspasas juega un papel muy importante [137]. Solo unos pocos de estos factores se han correlacionado con la resistencia a CDDP en ensayos clínicos, los cuales incluyen BLC-2, BCL-XL y MCL-1 y survivina [24]. La resistencia al CDDP también se ha asociado a defectos en varios transductores de señales pro-apoptóticas como son mitogen-activated proteína kinase 14 conocido como p38MAPK y c-Jun, N-terminal kinase 1 [45] Pero además junto con la pérdida de señalización apoptótica la alta tasa de reparación/eliminación del daño causado en el DNA y/o la tolerancia al daño son también causas de la resistencia a este agente.

2.3.2. Vía de Reparación por Escisión de Nucleótidos (NER)

La vía de reparación de NER o Nucleotide Excission Repair es un mecanismo versátil por el cual se reparan la mayoría de puentes de timidina y fotoproductos producidos por la luz UV, así como aductos o torsiones en el DNA [99]. NER es el mecanismo principal de eliminación de las lesiones provocadas por el CDDP. El CDDP genera principalmente uniones covalentes entre guaninas adyacentes (intra e inter hebra) en el DNA mitocondrial y nuclear formando los denominados "aductos"[8, 25]. Esto conlleva a un bloqueo de la replicación y la transcripción por un impedimento físico para desplazarse la maquinaria por el DNA. Además, estas uniones generan tensiones en la doble hélice, distorsionándola y así creando puntos con alta probabilidad de rupturas de cadena simple o doble en el DNA[116]. La vía de reparación se caracteriza por la participación de las proteínas de la familia XP (Xeroderma Pigmentosum) cuya función se describió al observar que mutaciones en estas proteínas conducían a susceptibilidad a padecer canceres de piel, fotosensibilidad y errores en la reparación de DNA en los pacientes con el síndrome Xeroderma Pigmentosum. El mecanismo de reparación consiste en un primer reclutamiento de proteínas de reconocimiento del daño, señalizan el lugar del daño para reclutar a continuación el complejo de trascripción THFII (con la helicasa XPD) y las endonucleasas (XPG y ERCC1), posteriormente se corta la hebra dañada aproximadamente 20 nucleótidos alrededor del daño y por último la polimerasa por complementariedad con la hebra no dañada sintetiza la nueva hebra [97, 104]. Se conocen dos rutas de reparación NER: la global o GG-NER (Global Genome–NER), la cual repara continuamente zonas transcripcionalmente no activas y en general por todo el genoma, y por otro

lado la acoplada a la transcripción o TC-NER (Transcription Couple –NER) que se encarga de la reparación de genes que se están transcribiendo activamente[86]. La diferencia entre ambas principalmente consiste en las proteínas de reconocimiento del daño, así la presencia de XPC y XPE se restringe a la GG- NER en cambio en TC -NER el bloqueo de la RNA polimerasa III es la señal para el reclutamiento del resto de las proteínas de la vía (Fig 7).

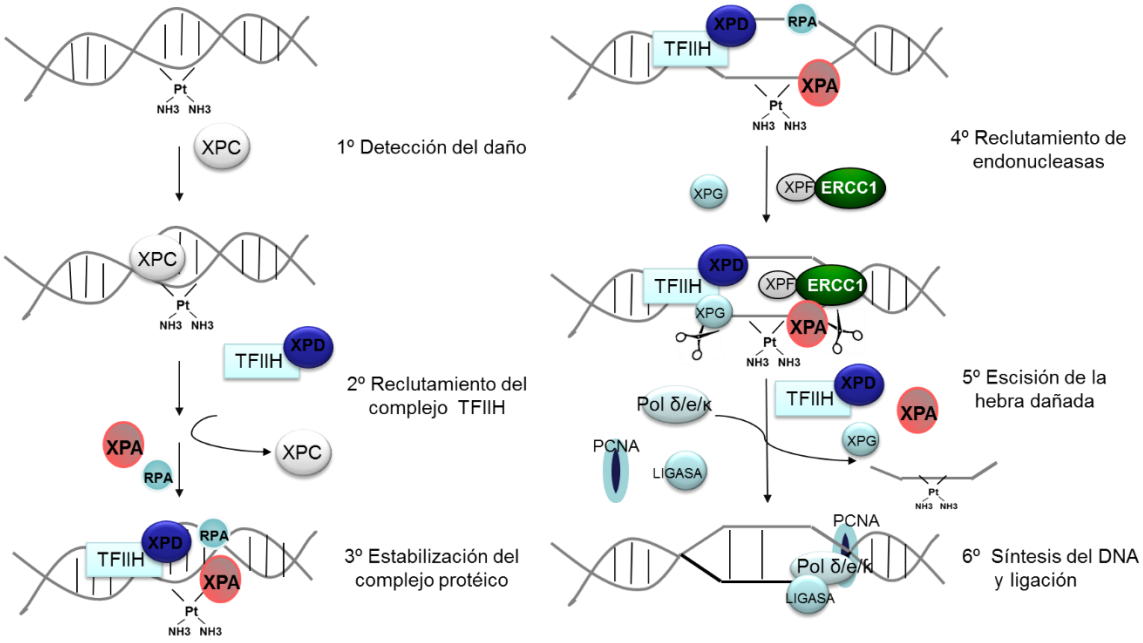

Figura 7: Ruta de reparación GG-NER. Los aductos en el DNA son localizados por la proteína XPC, que recluta al complejo proteico TFIIH, XPA y RPA estabilizan y orientan el complejo mientras la helicasa XPD abre la cadena de DNA .Posteriormente las endonucleasas ERCC1-XPF y XPG cortan la hebra dañada entorno a unos 20 nucleótidos alrededor del daño. Finalmente se elimina la hebra dañada y se sintetiza la nueva por la DNA polimerasa.

En muchos estudios se ha correlacionado la sobreexpresión de alguna de las proteínas de la ruta NER con la resistencia/sensibilidad a platinos [90]. En la mayoría de los estudios se han medido niveles de mRNAs o niveles de proteína en tumores y en líneas celulares[9]. Los niveles elevados de la proteína ERCC1 se han correlacionado con mala respuesta a quimioterapia adyuvante con platino en pulmón y testículo.[53, 113]

La proteína XPA (Xeroderma Pigmentosum group A) participa tanto en TC-NER como en GG-NER, en ambas vías XPA se localiza en la zona lesionada por el complejo de factor de trascripción TFIIH. Tiene como función facilitar el posterior ensamblaje de las proteínas de escisión. XPA en coordinación con RPA (proteína de unión a ssDNA replicación A) facilitan la correcta colocación de las endonucleasas marcando la orientación del daño y su reparación[106]. Así RPA se une a la hebra sencilla no dañada en dirección 5′→3′ mientras que XPA se une a la hebra dañada. La localización de XPA en el núcleo es una de las etapas limitantes de la ruta NER[106] La activación de XPA se produce por fosforilación en la Ser 196 a través de ATR lo que hace que se incremente el paso al núcleo de la proteína[70]. Esta fosforilación aumenta a su vez la estabilidad de XPA, por la inhibición de la ubiquitinación de la E3 ubiquitin ligasa.[124]

La proteína XPD (*Xeroderma Pigmentosunm* grupo D) es una helicasa dependiente de ATP componente del complejo de factor de transcripción TFIIH. Su implicación en la vía NER es fundamental ya que se encarga de abrir la doble hélice del DNA alrededor del daño para el reclutamiento de endonucleasas y demás proteínas de la vía de reparación [51].Estudios *in vitro* han demostrado que los polimorfismos asociados a XPD, por ejemplo, el polimorfismo Lys751Gln afecta a la capacidad de reparación del DNA en respuesta a genotóxicos y en clínica se han validado numeroso SNPs correlacionando con el pronóstico del paciente, en los cuales la mayoría presentan una menor supervivencia global[95, 126].

La proteína ERCC1 (Excision repair cross-complementation group 1) forma un heterodímero con XPF. XPF/ERCC1 es reclutado a la burbuja NER mediante la unión de ERCC1 con XPA. ERCC1–XPF actúa de manera cooperativa con otras proteínas necesarias para generar la incisión como son XPC–RAD23B, XPA, RPA, TFIIH y XPG[99]. Hasta el momento ERCC1 parece ser el biomarcador con mejores resultados para predecir la respuesta a Cisplatino [96]. Aun así los niveles de esta proteína son solo aceptados para dictaminar el tratamiento en cáncer de testículo, en el resto de tumores existen aún resultados controvertidos. En CG se ha observado que los polimorfismos ERCC1 rs3212961 A/C, ERCC5 rs2094258 A/G, DDB2 rs830083 C/G correlacionan con un mejor pronóstico del paciente con tiempos de supervivencia global mayores[72], lo que sugiere que puedan ser considerados buenos biomarcadores de pronostico en CG. En un estudio en la población china se ha demostrado que el polimorfismo en ERCC1 rs11615 C/T y el genotipo CT/TT está asociado significativamente con un peor pronóstico comparado con el genotipo CC en cuanto a la supervivencia global. [57]

OBJETIVOS

El objetivo principal de este trabajo es estudiar el papel de las proteínas clave en el punto de control de ciclo celular G2/M, con el fin de identificar nuevos biomarcadores pronóstico y predictivos de respuesta a tratamiento en cáncer gástrico.

Los objetivos particulares son los siguientes:

1. Evaluar la respuesta al tratamiento con Cisplatino en líneas celulares derivadas de cáncer gástrico durante la fase de mitosis.
2. Investigar la implicación y el valor pronóstico de las proteínas del punto de control de mitosis en la carcinogénesis y respuesta a tratamiento con Paclitaxel en cáncer gástrico.
3. Estudiar otras funciones celulares de MAD2 en respuesta al tratamiento con Cisplatino: Reparación de daño al DNA.
4. Evaluar la regulación de la expresión de CHK1, y su correlación con la respuesta a tratamiento con radiación como biomarcador predictivo de respuesta.

RESÚMENES Y PRUBLICACIONES

RESUMEN

Targeting Chk2 improves gastric cancer chemotherapy by impairing DNA damage repair

Gutiérrez-González A, Belda-Iniesta C, **Bargiela-Iparraguirre J**, Dominguez G, García Alfonso P, Perona R, Sanchez-Perez I.

Apoptosis. 2013 Mar;18(3):347-60. doi: 10.1007/s10495-012-0794-2.PMID:23271172

El Cisplatino (CDDP) es un agente que se utiliza como terapia adyuvante en el tratamiento del cáncer gástrico, sin embargo, muchos pacientes recurren o son resistentes al mismo. En estos casos se utilizan combinaciones de fármacos entre los que se encuentra el Paclitaxel (PTX). El Cisplatino causa parada de ciclo en la fase G2/M, si esta parada falla las células continuaran el ciclo y se activará el punto de control de mitosis (Spindle Assambly Checkpoint- SAC), iniciando la reparación o la muerte celular.

En este trabajo hemos comparado el tratamiento de CDDP con el tratamiento combinado de PTX-CDDP en dos líneas celulares derivadas de adenocarcinoma gástrico, y analizado el mecanismo molecular de inducción de muerte celular. Hemos demostrado que la adición de CDDP en células en mitosis, por el previo tratamiento con PTX, es más efectivo que los estímulos en monoterapia en células de adenocarcinoma (MKN45) pero no en las células derivadas de metástasis en nódulo linfático (ST2957). Los estudios de microscopia "Time-Lapse" indican que esta combinación de tratamiento induce la muerte celular a través de la denominada catástrofe mitótica y apoptosis, ya que el inhibidor de caspasas z-VAD-fmk, protege de la misma. El análisis molecular indica que las células sufren una salida prematura de la parada de mitosis, caracterizada por degradación de Ciclina B, sin que el DNA se haya reparado, puesto que observamos una alta fosforilación de H2AX, indicativo de roturas en el DNA. El análisis de la reparación en cada una de las condiciones, mediante el ensayo de cometa, demuestra que la reparación se encuentra disminuida cuando la lesión con CDDP se induce durante mitosis. Finalmente, observamos que en esta situación se produce la degradación de la proteína CHK2, que participa de forma activa en la reparación en mitosis a través de la fosforilación de BRCA1.

Estos resultados sugieren que la modulación de la muerte celular durante mitosis es una estrategia efectiva en la terapia de cáncer gástrico.

Participación en el trabajo

Análisis molecular mediante WB de la degradación de Chk2 por el proteosoma y su participación en la fosforilación de BRCA1.

Apoptosis (2013) 18:347–360
DOI 10.1007/s10495-012-0794-2

ORIGINAL PAPER

Targeting Chk2 improves gastric cancer chemotherapy by impairing DNA damage repair

A. Gutiérrez-González · C. Belda-Iniesta · J. Bargiela-Iparraguirre · G. Dominguez · P. García Alfonso · R. Perona · I. Sanchez-Perez

Published online: 28 December 2012

Abstract Our results demonstrate that the addition of cisplatin after paclitaxel-induced mitotic arrest was more effective than individual treatment on gastric adenocarcinoma cells (MKN45). However, the treatment did not induce benefits in cells derived from lymph node metastasis (ST2957). Time-lapse microscopy revealed that cell death was caused by mitotic catastrophe and apoptosis induction, as the use of the caspase inhibitor z-VAD-fmk decreased cell death. We propose that the molecular mechanism mediating this cell fate is a slippage suffered by these cells, given that our Western blot (WB) analysis revealed premature cyclin B degradation. This resulted in the cell exiting from mitosis without undergoing DNA damage repair, as demonstrated by the strong phosphorylation of H2AX. A comet assay indicated that DNA repair was impaired, and Western blotting showed that the Chk2 protein was degraded after sequential treatment (paclitaxel-cisplatin). Based on these results, the modulation of cell death during mitosis may be an effective strategy for gastric cancer therapy.

Keywords Cancer · Mitosis · Cisplatin · DNA damage response

A. Gutiérrez-González · J. Bargiela-Iparraguirre · I. Sanchez-Perez
Department of Biochemistry, School of Medicine, UAM, Madrid, Spain

A. Gutiérrez-González · J. Bargiela-Iparraguirre · R. Perona · I. Sanchez-Perez (✉)
Biomedical Research Institute of Madrid, Madrid CSIC/UAM, C/Arturo Duperier 4, 28029 Madrid, Spain
e-mail: misanchez@iib.uam.es

C. Belda-Iniesta
Thoracic, Head & Neck and Brain Oncology Unit, CIOCC Centro integral Oncológico Clara Campal. GHM Grupo Hospital de Madrid, Madrid, Spain

C. Belda-Iniesta · R. Perona
Biomarkers and Experimental Therapeutics Group, IdiPAZ, University Hospital La Paz, Madrid, Spain

G. Dominguez
Department of Medical Oncology, University Hospital Puerta de Hierro, UAM, Madrid, Spain

P. García Alfonso
Department of Medical Oncology, Gregorio Marañon Hospital, Madrid, Spain

R. Perona
CIBER on Rare Diseases (CIBERER), Valencia, Spain

Abbreviations

CDDP	Cisplatin
PXL	Paclitaxel
SAC	Spindle assembly checkpoint
DDR	DNA damage response
DSBs	Double strand breaks
ATM	Ataxia-telangiectasia mutated
ATR	ATM- and Rad3-related
γH2AX	Phosphorylated H2AX
CIN	Chromosome instability
BRCA1	Breast cancer 1

Introduction

Gastric cancer (GC) remains one of the leading causes of cancer mortality worldwide, although its incidence has been decreasing in recent years. Recent epidemiologic studies estimate that approximately 0.9 million cases of GC

are diagnosed annually worldwide. In more than half of all cases, the disease has advanced by the time of diagnosis. Despite potentially curative resection, only 45 % of patients will be free of disease at 5 years [1]. Systemic chemotherapy is therefore essential for the management of advanced GC because it improves survival and quality of life; however, there is no standard patient regimen. Several chemotherapeutic regimens have been established as first-line therapies, and they have contributed to improved survival [2]. After this first therapeutic intervention, 30–70 % of patients receive second-line chemotherapy. Among the various regimens, paclitaxel (PTX) or docetaxel combined with fluorouracil plus cisplatin (PCF), oxaliplatin combined with fluorouracil plus leucovorin (FOLFOX-4) or with capecitabine and epirubicin [3] are the most commonly used therapies [4, 5]. Furthermore, there are patients whose tumors overexpress the epidermal growth factor receptor isotype 2 (Her-2/neu/c-Erb-2) [6, 7]. In these cases, employing a platinum doublet and replacing epirubicin or docetaxel with an antibody directed against the extracellular domain of the transmembrane protein has led to an overall increase in survival of over 30 % in a recent clinical trial [8, 9]. Unfortunately, given that none of these treatments have proven ideal in terms of overall survival, schedule selection is based on patient performance, previous experience with a particular drug combination and potential toxicity studies [10]. The taxanes, paclitaxel and docetaxel, are microtubule-stabilizing agents that induce cell-cycle arrest at the G2/M stage. Both agents have been used to treat advanced gastric cancer. Several clinical trials have shown an improvement in response to drug combinations, using paclitaxel or docetaxel for first-line and cisplatin and 5-FU for second-line treatments [11]. However, the reasons for the positive effects at the molecular level of such combinations are not known, nor is it known which new drugs against given therapeutic targets would further improve the course of the disease.

DNA damage inflicted by genotoxic drugs triggers the DNA damage response (DDR) pathway [12], [13]. The DDR involves a complex network of proteins that cooperate to initiate and coordinate cell-cycle progression, DNA repair and cell death. Two major phosphatidylinositol-3 (PIK)-like proteins, ATM and ATR, act in response to DNA damage. Once activated, these proteins activate the transducer proteins Chk1, Chk2, p53 and BRCA1, among others [14, 15]. Chk1 and Chk2 can phosphorylate several key substrates, such as the Cdc25 family [16–18], leading to G2 phase arrest, which protects cells from entering mitosis in the presence of DNA damage [19]. The decision by the cell to enter mitosis is mediated by a network of proteins that regulate activation of the cyclin B–Cdk1 complex. Cyclin B levels are periodically regulated by transcription and degradation cycles. Thus, Cdk1 must be phosphorylated on its T loop for full activity, and Cdk1 T14 and Y15 phosphorylation is controlled by the balance between Wee1/Myt1 kinases and Cdc25 phosphatases. In human cells, high cyclin B levels are temporally restricted to the G2 phase and early mitosis by regulated transcription and protein degradation. Degradation of cyclin B is regulated by the anaphase-promoting complex/cyclosome (APC/C), a multisubunit E3 ligase that can polyubiquitinate numerous mitotic regulators, and is therefore targeted for destruction by the proteasome. Polyubiquitination of cyclin B starts in the metaphase, when the spindle assembly checkpoint (SAC) is silenced [20]. In addition to direct regulation of Cdk1 T14/Y15 phosphorylation, several feedback mechanisms regulate cyclin B–Cdk1 activation indirectly, such as PlKs and Aurora protein kinases [21].

A number of studies have reported that after prolonged treatment with microtubule-targeted drugs, cells overcome the mitotic delay in a process termed mitotic slippage, adaptation or leakage [22]. The degradation of cyclin B has been shown to play an important role in mitotic slippage, although the details of the molecular mechanisms are not fully understood. Generally, cells treated with microtubule-binding drugs undergo mitotic catastrophe due to mitotic slippage. Mitotic catastrophe is characterized by the appearance of enlarged micronucleated or multinucleated cells [23]. The eventual fate of cells suffering from mitotic catastrophe is usually apoptosis. Mcl-1 is a pro-survival member of the Bcl-2 protein family, and its function is to suppress apoptosis during mitosis. However, under an apoptotic stimulus, this protein is phosphorylated by JNK, p38 and CKII, which promotes degradation by the proteasome and, as a consequence, induces cell death [24]. Cells exposed to genotoxic agents are arrested at different phases of the cell cycle by activation of G1, S or G2/M checkpoints in order to provide sufficient time for DNA repair. In mammalian cells, homologous recombination (HR) and non-homologous end joining (NHEJ) are the two main pathways involved in the repair of DNA double-strand breaks [25]. BRCA proteins act in the DNA repair pathway that involves homologous recombination (HR) and are essential for the repair of double-strand breaks [26].

Previously, we demonstrated that nocodazole sensitizes cisplatin-induced apoptosis in colon carcinoma cells. We showed that these cells suffer from chromosome instability (CIN) due to increased levels of SAC proteins and defects in the DNA damage response [27]. In this study, we used a specific strategy for sensitizing GC cells to cisplatin, which consists of sequential treatment with paclitaxel followed by cisplatin. To gain insight into the molecular parameters that determine cell fate after the mitotic arrest induced by this treatment strategy, we analyzed the mechanisms triggering cell death in tumor cell lines that respond differently to

cisplatin. First, we demonstrated that adenocarcinoma MKN45 cells die due to mitotic catastrophe once they become trapped in mitosis. In contrast, lymph-node metastatic ST2957 cells remained arrested in mitosis. We proposed that MKN45 cells escaped from mitosis, a fact attributable to the inactivation of the cyclin B-Cdk1 complex, and eventually died by apoptosis. Furthermore, we found that Chk2 activity was impaired in response to the treatment, and as a consequence, BRCA1-mediated DNA repair decreases.

Materials and methods

Reagents

Cisplatin, paclitaxel and ChkII were purchased from Sigma Aldrich CO LLC, Spain. z-VAD-fmk was purchased from Vitro S.A., Madrid, Spain.

Cell culture

The MKN45 (poorly differentiated adenocarcinoma) (DSMZ: Deutsche Sammlung von Mikroorganismen und Zellkulturen GmbH) cell line was maintained in RPMI 1640 supplemented with 10 % FBS and 2 mM L-Glutamine. ST2957 cells (lymph node metastases) [28] (ATCC/LGC Standards, Spain) were maintained in high glucose Dulbecco's Modified Eagle Medium (DMEM; Gibco), supplemented with 2 mM L-Glutamine, 1 mM sodium pyruvate and 10 % fetal bovine serum. All cell lines were grown at 37 °C in a humidified atmosphere containing 5 % CO_2.

Cell viability assays

Viability was determined using a crystal violet-based staining method, as described previously [29]. Briefly, 5×10^4 cells per well were seeded in 24 multiwell dishes, treated with various amounts of the selected agent for 24 h and fixed with 1 % glutaraldehyde. After they were washed in 1X PBS, cells were stained with 0.1 % crystal violet. A colorimetric assay using 595 nm Elisa was used to estimate the number of cells per well.

Cell cycle analysis

After appropriate treatment, adherent and non-adherent cells were harvested and fixed overnight in 70 % ethanol in phosphate-buffered saline (PBS). For DNA content analysis, the cells were centrifuged and resuspended in PBS containing 1 μg/ml RNase (Qiagen Ltd., Crawley, UK) and 25 μg/ml propidium iodide, incubated at room temperature for 30 min, and finally analyzed using a Becton–Dickinson Flow Cytometer (Cowley, UK). Data were plotted using Cell Quest software, with 10,000 events analyzed per sample.

Western blotting

Protein extracts (20 μg) were resolved on 4–20 % SDS-PAGE (BioRad) and transferred to nitrocellulose membranes. An immunoblot analysis was performed as described previously [27]. The following antibodies were used in the experiments: cyclin B (Santa Cruz), Chk2 (A-12, Santa Cruz), $Chk2^{Ser19}$, $Chk2^{thr68}$, Histone $H3^{Ser10}$, p-P38, (Cell Signaling, Charlottesville, USA), BRCA1 (Santa Cruz Biotechnology, Inc. Germany), $p53^{Ser15}$, p53, H2A-X^{Ser139} (Upstate), $CDC25C^{Ser216}$, α-Tubulin (Sigma-Aldrich, USA), ATM-^{S1081P} (Rockland Immunochemicals) ATM (Novus Biologicals), Mcl-1 (Santa Cruz Biotechnology Inc., Germany) p-JNK (Promega Corporation, Spain), and secondary antibodies conjugated to horseradish peroxidase (Biorad, Spain). Blots were developed using enhanced chemiluminescence detection system (ECL Santa Cruz Biotechnology, USA).

Immunofluorescence

Cells were fixed and fluorescence microscopy was performed using a NIKON Eclipse 90i. Image analysis was performed with the Nikon NIS-Elements software program and processed using Image J. For high-throughput microscopy, cells were grown on micro-clear-bottom 96-well dishes (Greiner Bio One) and analyzed with a bioimager (Pathway 855; BD). Image acquisition (ORCA 1394; Hamamatsu Photonics) was performed at room temperature using oil as an immersion media and a 40 × 0.75 NA Plan Apo objective (HCX). Image analysis was performed with imaging software (Altovision; BD). All images for quantitative analyses were acquired under nonsaturating exposure conditions. Primary antibodies included γ-H2AX^{Ser139} (Millipore). Secondary antibodies were conjugated with Alexa Fluor 488 (Invitrogen). DAPI (Invitrogen) was used for DNA staining.

Time-lapse microscopy

For live-cell analyses, MKN45 cells were grown in an Ibidi μ-Slide 8-well chamber (IBIDI LLC Martinsried, Germany) transfected with Lipofectamine 2000 (Invitrogen) with 0.5 μg of pBOS-H4B-GFP per well (a gift from Dr. M. Malumbres) followed by time-lapse microscopy using the Cell Observer Z1 (Zeiss) at 37 °C and 5 % CO_2/95 % air, AxioVision 4.8 imaging software and a Cascade 1 k camera. Images were taken every 10 min and further

processed using AxioVision digital image processing software (Zeiss). Cells were filmed during a 24-h period, and every 10 min a bright field and a fluorescent image were captured.

Comet assay

We performed the comet assay under alkaline conditions as described by Singh et al. [30]. CDDP was added at a concentration of 10 μg/mL for 4 h. Cells exposed to the sequential treatment were preincubated for 24 h with paclitaxel and then treated for 4 h with CDDP. For the repair assay, cells were allowed to recover from the induced damage by washing in PBS and incubating at 37 °C with fresh media for 1, 2.5 and 4 h before harvesting. Experiments were performed in duplicate. Fifty comets per duplicate gel were scored and quantified by Komet 5.5 image analysis software (Kinetic Imaging Ltd., Nottingham, UK). Apoptotic cells (nondetectable cell nuclei, ghost cells, clouds or hedgehogs) were not scored.

shRNA lentiviral particle transduction

Chk2 shRNA (h) and control shRNA lentiviral particles were purchased from Santa Cruz Biotechnology, Inc. Transduction was performed according to the manufacturer's instructions. Briefly, cells were seeded in 12 multiwell dishes, and infection was performed in the presence of polybrene (5 ug/ml) overnight. For the selection of stable clones, cells were split and cultured in growth medium containing puromycin 3 μg/ml. Resistant clones were expanded and assayed for stable shRNA expression. Reductions in gene expression were analyzed by quantitative/real-time PCR (QPCR) and compared to non-silencing shRNA. Protein levels were analyzed by immunoblot.

cDNA preparation and QPCR

Total cellular RNA was extracted using Tri-Reagent (Life Technologies, Carlsbad, CA, USA) according to the manufacturer's instructions, and reverse transcription was performed on 2 μg of total RNA using M-MLV reverse transcriptase (Promega, Madison, WI, USA). The primer sets used to amplify specific sequences were 5′- ATCCA AAGGCACGTTTTACG-3′ and 5′- ACAACACAGCAGC ACACACA-3′ for Chk2; and 5′-GAT GGT ACA TGA CAA GGT GC-3′ for GADPH. The quantitative expression of each gene was measured by SYBR Green polymerase chain reaction assay. Statistical analyses were performed for each gene by using a paired t test to compare mean values. Values of $p < 0.05$ were considered significant. Relative quantification (RQ) was achieved using the delta-Ct method in which each 1-Ct difference equals a 2-fold change in transcript abundance.

Statistical analysis

Statistical significance was analyzed using a two-tailed Student's t test; * $p < 0.05$; ** $p < 0.005$.

Results

Paclitaxel sensitizes GC cells to cisplatin by mitotic catastrophe and apoptosis induction

First, we assayed combination modalities of cisplatin (CDDP) with paclitaxel (PXL) in various GC cell lines to assess which treatment was more effective. We studied the viability of MKN45 (poorly differentiated GC cells) and ST2957 (lymph node metastases) adenocarcinoma GC cell lines after exposure to two modalities of treatment. We treated both cell lines either with serial concentrations of CDDP (0–20 μg/ml) or sequentially by pretreating cells with 0.1 μM PXL for 20 h and, after PXL removal, treating them with CDDP as above (PXL-CDDP). We found a modest but statistically significant toxic effect in MKN45 cells after sequential treatment with PXL and CDDP; however, this combination did not have as deleterious an effect on ST2957 cells after 24 h of treatment (Fig. 1a). In order to visualize cell death, we performed immunofluorescence studies with DAPI staining after treatment of GC cells with the various drug combinations. We observed that CDDP and PXL-CDDP led to an accumulation of cells displaying morphological changes characteristic of apoptosis or mitotic catastrophe (MC), such as the formation of apoptotic bodies, chromosome dispersion and micronucleation at 24 h (Fig. 1b). After quantification of the cells showing these morphological features, we found a steep increase in MKN45 cells showing signs of death when compared with ST2957 cells (21 vs 7 %) 24 h after the sequential treatment. In mitotic catastrophe, a cell is destroyed during mitosis or after a faulty mitosis. To follow the behavior of individual cells, we transiently transfected MKN45 cells with GFP-tagged histone H4B (Fig. 1c) and studied the duration of the mitosis. We recorded this information by measuring the duration of the interval between the exact moment when a cell enters mitosis (the interphase-prophase transition or IPT) and the moment when it exits mitosis (the metaphase-anaphase transition or MAT) using time-lapse microscopy. These transition points were chosen because they represent the two key steps in mitotic progression that are regulated by the cell cycle machinery. We showed that the mitotic duration for MKN45-untreated cells is 70 min on average. After

cisplatin treatment the mitotic duration was 90 min. In contrast, paclitaxel, which prolongs mitosis by activating the spindle checkpoint, induced a delay in mitosis up to an average of 120 min. However, sequential treatment with PXL followed by CDDP increased the duration of mitosis to nearly 200 min. We also studied the cells' fate after these treatments and detected that a number of the mitosis processes were accompanied by mitotic catastrophe 4–6 h after the treatments, and overall cell death increased by up to 50 % (Fig. 1d). Collectively, our findings suggest that the PXL-mediated mitotic arrest might have contributed to an increased sensitivity to the proapoptotic actions of CDDP in MKN45 cells.

MKN45 cells suffering from mitotic catastrophe die via apoptosis

To better define the mechanisms of action of PXL-CDDP treatment in inducing MC and/or apoptosis, DNA flow cytometry analysis was performed to determine whether cell cycle perturbations could be responsible for the increase in cytotoxicity induced by the treatment (Fig. 2a). Treatment of MKN45 and ST2957 cells with PXL for 20 h induced an accumulation of cells in the G2/M phase of the cell cycle (around 84 %), but 24 h after PXL removal, the G2/M cell content decreased to 50 %, and the number of apoptotic cells increased (18 %) in MKN45 cells. In contrast, ST2957 cells remained in G2/M (70 %) 24 h after PXL removal. Cisplatin treatment induced apoptosis both in MKN45 (28 %) and ST2957 (9 %) cells. Nevertheless, after PXL-CDDP exposure, only MKN45 cells showed an increase in the percentage of apoptosis (50 %), concomitantly with an important reduction in G2/M cell content (19 %). Although an increase in apoptosis was also observed in ST2957 cells after PXL-CDDP treatment, this effect was not additive, at least at 24 h after treatment, as the majority of cells remained in the G2/M phase (Fig. 2a). Taking into account that these cell lines have chromosomal instability, we did not observe a significant change in aneuploidy population after treatment. Caspase activation is a predictor of cell death and a clear feature of apoptosis. Western blot analysis was used to confirm apoptosis as a mechanism of cell death by analyzing caspase activation through the harvesting of asynchronous cell cultures after treatment with CDDP or PXL-CDDP over a time period of 1–24 h. We studied the activation of caspase-3 by immunoblotting with an antibody against cleaved PARP (a substrate of caspase-3) and observed that CDDP strongly induced PARP's cleavage 24 h after treatment in MKN45 cells, while in PXL/CDDP-treated cells, the cleavage was detected earlier, at only 9 h after drug exposure. In contrast, in ST2957 cells, the kinetics of PARP cleavage were the same regardless of the treatment, and cleavage was almost undetectable in these cells (Fig. 2b, left panel). Accordingly, caspase-3 was strongly activated in MKN45 cells treated with PXL-CDDP (3 h) (Fig. 2b, right panel) and was barely detected, at least at this time, in ST2957 cells (not shown). Mcl-1 is a pro-survival member of Bcl-2 protein family, and its function is to suppress apoptosis during mitosis. However, under apoptotic stimulus this protein is phosphorylated by JNK, p38 and CKII, promoting degradation by the proteasome and, as a consequence, the induction of cell death. The results we present above encouraged us to study the status of Mcl1 in cells treated with PXL-CDDP, where we observed a strong activation of JNK and p38 stress kinases either after CDDP or PXL-CDDP, with the same kinetics for both (Fig. 2c). However, Mcl-1′s small fragment was detected only in MKN45 cells, indicating that the mechanism of apoptotic induction is activated in these cells after PXL-CDDP treatment (Fig. 2c). The additive effect observed in apoptosis induction for PXL-CDDP was abolished by the pan-caspase inhibitor z-VAD-fmk (Fig. 2d). The inhibition of apoptosis correlated with a net increase in the number of cells that accumulated into the G2/M phase of the cell cycle, strongly suggesting that cell death occurred during the mitotic phase of the cell cycle.

Cisplatin-induced mitotic catastrophe is due to mitotic slippage after a prolonged mitotic arrest in MKN45 cells

The results of the flow cytometry analysis did not clearly elucidate the characteristics of the cell cycle arrest in G2/M or mitosis. To determine whether the MKN45 cells were arrested specifically in mitosis or G2 before dying and after PXL-CDDP treatment, we examined the molecular status of the G2/M checkpoint by analyzing the expression of cell-cycle regulatory proteins. Mitotic histone H3 phosphorylation occurs at Ser10, and there is a close correlation between H3 phosphorylation, chromosome condensation and segregation during mitosis. Consistent with these phenomena, $H3^{Ser10}$ phosphorylation, a marker of mitosis, was stimulated (after PXL-CDDP treatment) for approximately 6 h in MKN45 cells and for 9 h in ST2957 cells (Fig. 3a). Next, we analyzed the expression of the cell cycle-related proteins Cdc2, Cdc25c and cyclin B1 that control G2/M transition. Phosphorylated $CDC25C^{Ser216}$ and $Cdc2^{Tyr15}$ downregulate the activation of the cyclin B1-cdc2 complex. Our Western blot analysis showed that PXL induced an increase in Ser216 and Tyr15 inhibitory phosphorylation both on Cdc25C and Cdc2, which was maintained for 6 and 9 h after CDDP exposure in MKN45 and ST2957 cells, respectively, indicating the activation of the G2 checkpoint (Fig. 3b). Another mechanism regulating Cdc2 activity and thus progression into the mitotic

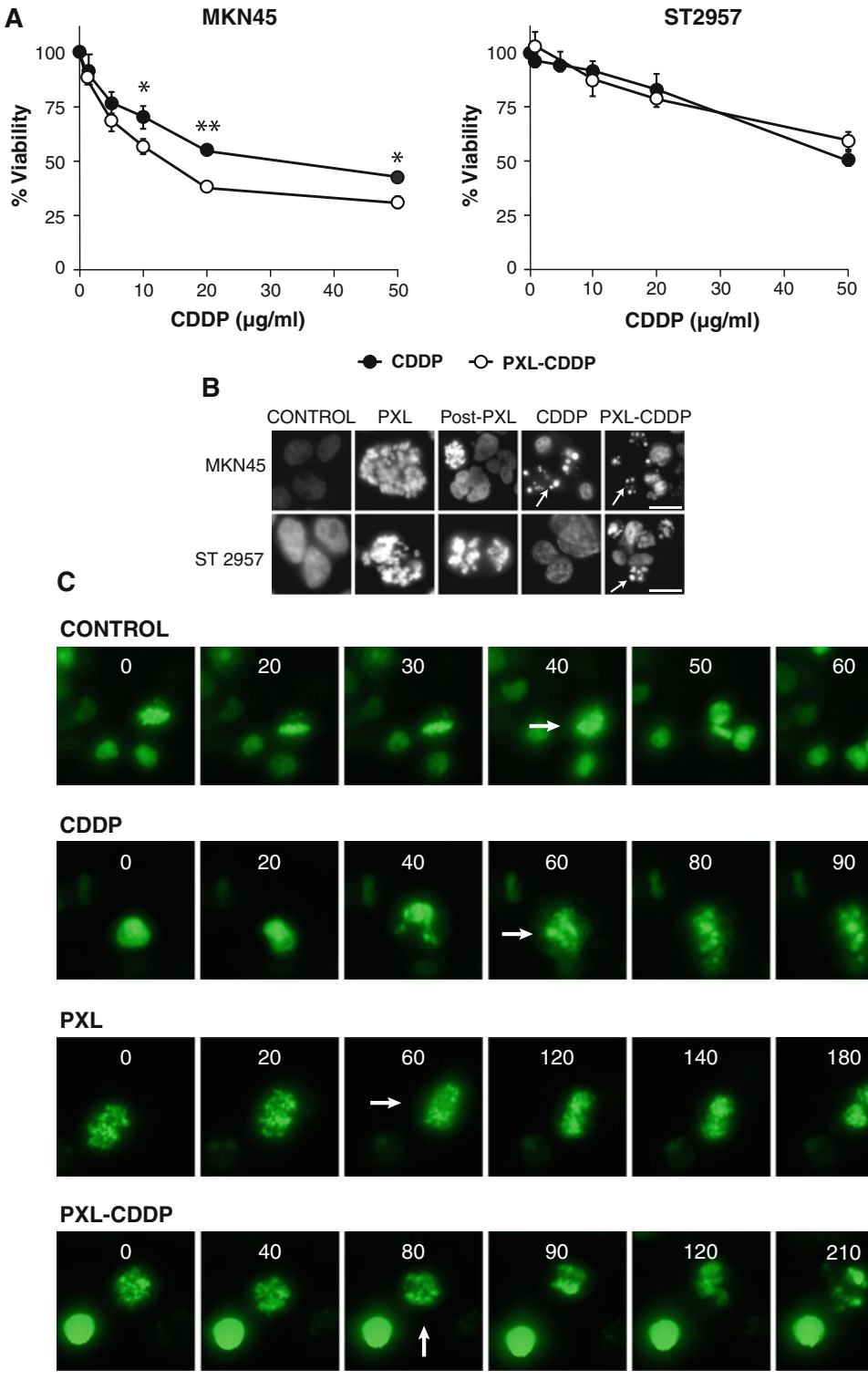

D

	MD (n=20 Movies)	% Cell Death
Control	70 ± 12	3
CDDP	90 ± 10	7
PXL	120 ± 15	20
PXL-CDDP	200 ± 20	53

◀ **Fig. 1** Survival of MKN45 and ST2957 cells after treatment with CDDP or sequential treatment with PXL and CDDP. **a** MKN45 and ST2957 cell lines were treated with increasing amounts of CDDP (0–50 μg/ml) (*filled circles*), or pretreated with PXL (0.1 μM) overnight and then washed and exposed to CDDP (*open circles*). Viability was quantified using the crystal violet method 24 h after treatment. The percentage is shown as relative to the number of cells without treatment. Data represent the means of two experiments performed in quadruplicate. Statistical analysis was performed using Student's *t* test (* $p < 0.05$; ** $p < 0.005$). **b** Cells were treated with CDDP (15 μg/ml), PXL (0.1 μM), PXL-CDDP (0.1 μM–15 μg/ml) for 24 h. Then, cells were fixed with PFA 3.7 % and stained with DAPI. *Arrows* show cell death with fragmented DNA. *Scale bar* 10 μ C. MKN45 cells were transiently transfected with 0.5 μg of pBOS-H4-GFP. 24 h after transfection cells were untreated or treated with CDDP (10 μg/ml); PXL (0.1 μM) overnight, then washed and changed to either fresh medium alone (PXL) or fresh medium plus CDDP (PXL-CDDP). The progression through mitosis of cells expressing GFP-tagged histone H4B was monitored by live-cell microscopy, and typical examples of image sequences are given. *Scale bar* 20 μ. The *graph bar* represents $n = 20$ movies. Table shows the quantification of the mitotic duration (MD) in the studied conditions ($n = 20$ movies) and percentage of cell death in the cells after the various treatments, $n = 100$ cells

phase is the complex formation with cyclin-B1. We then determined endogenous levels of cyclin-B1 and detected an accumulation of this protein after PXL-CDDP treatment in both cell lines. However, in MKN45 cells, a slow and continuous decrease still took place, probably due to the incomplete inhibition of the APC/C, unlike ST2957 cells, which only showed a decrease at 24 h. Together, the data suggests that mitotic slippage in MKN45 cells might be due to the inactivation of the cyclin B1-cdc2 complex after treatment with PXL and then CDDP. This result suggests an exit from mitosis before the cells manage to repair the damage induced by the drugs.

Paclitaxel potentiated cisplatin-induced activation of the DNA damage response (DDR)

To directly assess the consequences of PXL pretreatment in the cellular response to DNA damage, we first analyzed the levels of $\gamma H2AX^{Ser139}$ as a marker of DSBs after cisplatin challenge using high-throughput imaging (HTI) analysis. 6 hours after cisplatin addition, a significant increase in γH2AX foci was observed in PXL-pretreated MKN45 cells, suggesting that these cells are able to detect the CDDP-induced DSBs that remain unrepaired before they enter mitosis, which is in agreement with our in vivo analysis (Fig. 4a, left panel). To further evaluate this result, we studied the kinetics of γH2AX phosphorylation by Western blot comparing asynchronous cell cultures with mitotic cells after cisplatin treatment. In MKN45 cells, DNA damage is detected 9–24 h after treatment with CDDP (Fig. 4a, right panel). However, in PXL-pretreated cells (arrested in the prometaphase), damage is detected earlier (6 h), indicating PXL-potentiated cisplatin induction of DNA damage. Altogether, these findings suggest that MKN45 cells are able to detect DNA damage in mitosis and that this damage is permanent, perhaps because DNA repair was compromised. In contrast, 6 h after the administration of CDDP, ST2957 cells displayed a strong γ-H2AX-signal that declines after PXL/CDDP treatment, suggesting that damage detection by these cells in mitosis may be compromised (Fig. 4a, right panel). Next, we studied other events in the DDR. First, we evaluated the activation of ATM by phosphorylation ($ATM^{Ser1981}$) in GC cells. We did observe CDDP-induced activation of ATM after 3 h of treatment. However, PXL directly activated ATM for at least 24 h. Furthermore, the kinetics of ATM phosphorylation was identical in both cell lines (Fig. 4b). Next, we evaluated the activation of Chk2, and the results showed a significant reduction in both $Chk2^{Thr68}$ and $Chk2^{Ser19}$ phosphorylation levels after PXL-CDDP exposure. The latter was more obvious in MKN45 cells, indicating that this pathway is impaired in this cell line. This impairment may be due to a reduction in Chk2 protein levels, as shown (Fig. 4c). We next analyzed p53 phosphorylation as a measure of ATM activity and found that in both GC cell lines, CDDP treatment induced a drastic increase in $p53^{Ser15}$, in both asynchronous and synchronic cells with similar kinetics (Fig. 4d). Altogether, these results suggest that PXL pretreatment increased chromosomal damage after cisplatin-induced cell death in MKN45 cells, resulting in extensive H2AX phosphorylation and a potentiation of the DDR response in GC cells after cisplatin treatment, which appears to be a direct cause of catastrophic mitosis or apoptosis.

PLX/CDDP treatment induces proteasome-dependent degradation of Chk2

To examine if proteasome activity is involved in the decrease in Chk2 protein levels, we studied whether the proteasome inhibitor MG132 modulated Chk2 protein levels. MKN45 cells showed a reduction in Chk2 in mitotic cells treated with PXL-CDDP, which was inhibited by the addition of MG132 (Fig. 5a). These results prompted us to study whether the application of Chk2 inhibitors improves therapy in GC treatment. In our experience, the selective Chk2 inhibition greatly increased the percentage of apoptosis in GC cells after treatment. In combination with the Chk2 inhibitor (ChkII), cisplatin treatment resulted in approximately a 3-fold increase in apoptosis in MKN45 cells, compared to cisplatin alone. Surprisingly, this effect was not observed in ST2957 cells. However, both cell lines were more sensitive to PXL/CDDP treatment in combination with ChkII (Fig. 5b). These results demonstrate that pharmacological inhibition of the Chk2 pathway may enhance the therapeutic efficacy of platinum compounds in the treatment of GC. To study the contribution of Chk2 in

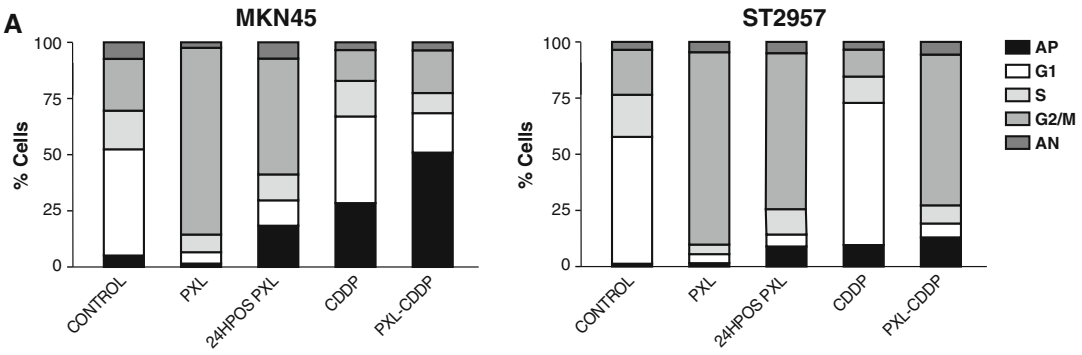

MKN45

	AP	G1	S	G2/M	AN
CONTROL	5.10	47.91	17.43	23.23	6.92
PXL	1.13	5.70	7.61	83.96	1.98
Post-PXL	18.06	12.08	11.52	52.18	6.79
CDDP	28.68	39.26	15.50	14.02	3.00
PXL-CDDP	50.90	18.44	8.51	19.26	2.96

ST2957

	AP	G1	S	G2/M	AN
CONTROL	0.75	57.00	18.48	20.55	3.37
PXL	1.19	4.35	4.17	85.71	4.76
Post-PXL	8.97	5.29	10.53	69.47	5.14
CDDP	9.49	64.44	11.79	12.25	3.35
PXL-CDDP	13.37	6.46	7.56	69.35	5.85

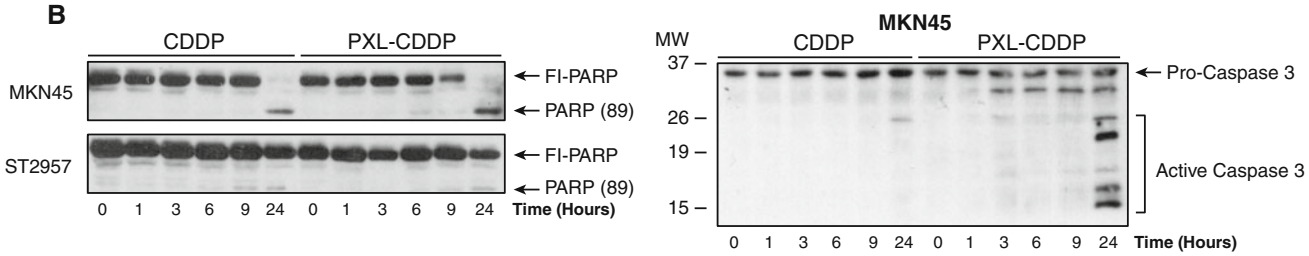

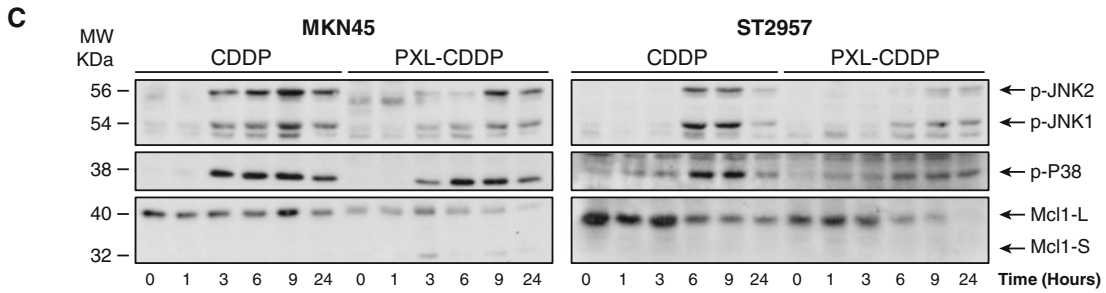

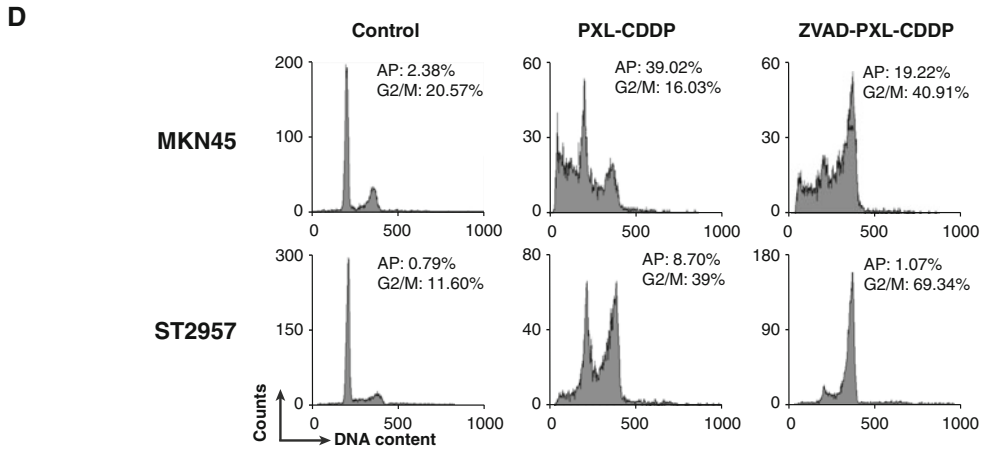

the response to therapy, we abolished Chk2 expression by generating stable cell lines by transduction with Chk2 shRNA (h) lentiviral particles containing a target-specific construct that encodes a 19–25 nt (plus hairpin) shRNA designed to knock down gene expression of Chk2. After selection with puromycin, stable MKN45 cells showed

◀ **Fig. 2** MKN45 cells die during mitosis by mitotic catastrophe and apoptosis induction. **a** Cell cycle analysis of GC cell lines treated with CDDP (10 μg/ml), PXL (0.1 μg/ml) or sequentially treated PXL for 18 h and then treated with CDDP for 24 h. The *graph* represents the percentage of cells in apoptosis (AP), G1, S, G2/M and *aneuploidy >4 N* (AN), indicated in the table below for each cell line in a representative experiment. The experiment was performed three times with similar results. **b** Cells treated with CDDP (10 μg/ml) or cells pretreated with PXL (0.1 μM for 20 h), washed and then treated for 0–24 h with CDDP. Cell lysates were extracted and Western blots were performed using antibodies against PARP and caspase 3. Similar results were obtained in three independent experiments. **c** Mcl-1 is proteolytically processed after sequential treatment in MKN45 cells. Western blots were performed using antibodies against phospho-JNK, phospho-p38 and total Mcl-1 proteins. Similar results were obtained in three independent experiments. **d** Cells were preincubated for 1 h with zVAD-fmk (50 μM) before exposure to the indicated drugs. Cell cycle analyses were performed as in (**a**)

nearly total abolishment of Chk2 mRNA levels and ST2957 showed around 60 % reduction. (Fig. 5c upper graph). This result was confirmed by Western Blot analysis of the cells (Fig 5 lower panel). These cells were used to study the appearance of apoptotic cells after cisplatin treatment. Our results showed that in the absence of Chk2, both cell lines (MKN45 and ST2957) are more hypersensitive to cisplatin, which confirms the pharmacological result. (Fig. 5d).

One of the substrates described for Chk2 during mitosis is BRCA1 [31]. To study the influence of PXL/CDDP treatment on BRCA1-phosphorylation status due to the downregulation of Chk2 during the treatment, we performed Western blot analysis by using a specific antibody against BRCA1. The result showed that both treatments (cisplatin and paclitaxel) individually increased BRCA1 (Ser988) (Fig. 5e, lanes 3 and 4); however, the treatment with PXL/CDDP abolished the phosphorylation of this residue (Fig. 5e, lane 6). To specifically study the contribution of Chk2 to this effect on BRCA1, we used the ChkII inhibitor and observed that the inhibition of Chk2 by ChkII abolished the activation of BRCA1 (Ser988) after CDDP treatment (Fig. 5e, lane 5). These observations suggest that, in the absence of Chk2, the recently identified controller of chromosome segregation, the Chk2-BRCA1 signaling pathway [32, 33], is absent and could increase chromosome instability. The reason for the increased sensitivity of cells to sequential treatment may involve the DNA repair signaling pathway. DNA repair might be impaired in mitosis, and consequently, cytotoxicity may increase after chemotherapy. To investigate whether MKN45 cells were able to repair damage caused by the drugs, we performed a Comet Assay. No differences in either TI or TM were observed in cells where the repair process was not allowed, mainly due to the fact that CDDP-induced adducts are not detected by the Comet Assay. The repair experiments performed at different time points allow the diverse repair systems to detect and excise the induced adducts (these products are now detectable by the Comet Assay). Thus, the values observed in these experiments reflect both the severity of the damage and the repair capability. After 1 h of repair, we observed a higher degree of damage in those cells treated with the sequential treatment than in those treated exclusively with CDDP. These results support the fact that paclitaxel can induce DNA breakage, as has been recently described, thus demonstrating that paclitaxel induces DNA damage due to telomere deprotection during mitotic arrest [34] or to another non-described type of damage [35, 36]. As expected,

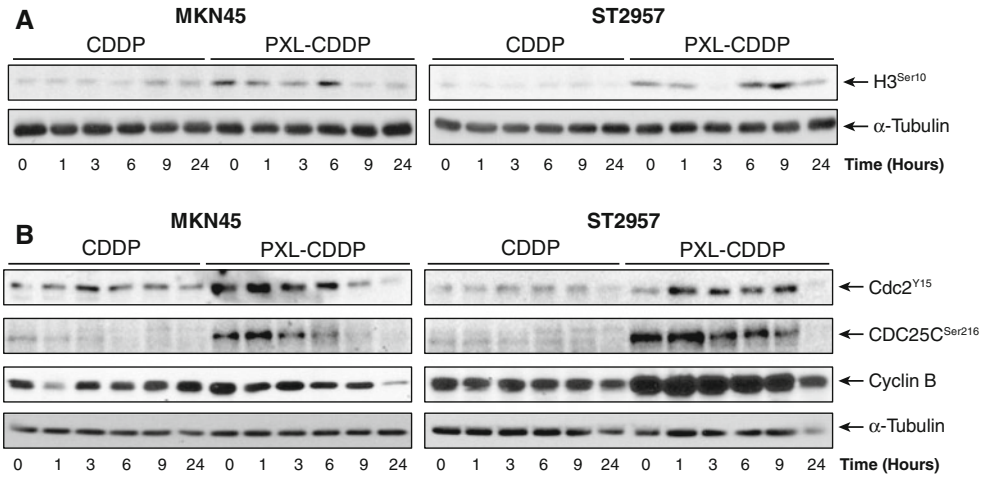

Fig. 3 Cyclin B1 degradation and cdc2 downregulation correlated with mitotic slippage in MKN45 cell after PXL-CDDP treatment. Cells were pretreated or not with PXL (0.1 μM for 20 h), washed and then treated for 0–24 h with 10 μg/ml CDDP. Whole cells extracts were prepared and hybridized with antibodies against **a** HisH3^{ser10,} **b** cdc2^{Y15}, cdc25c^{Ser216} or cyclin-B1. The blots were also probed for α-tubulin to ensure equal protein loading. The experiments were repeated three times with similar results. A representative experiment is shown

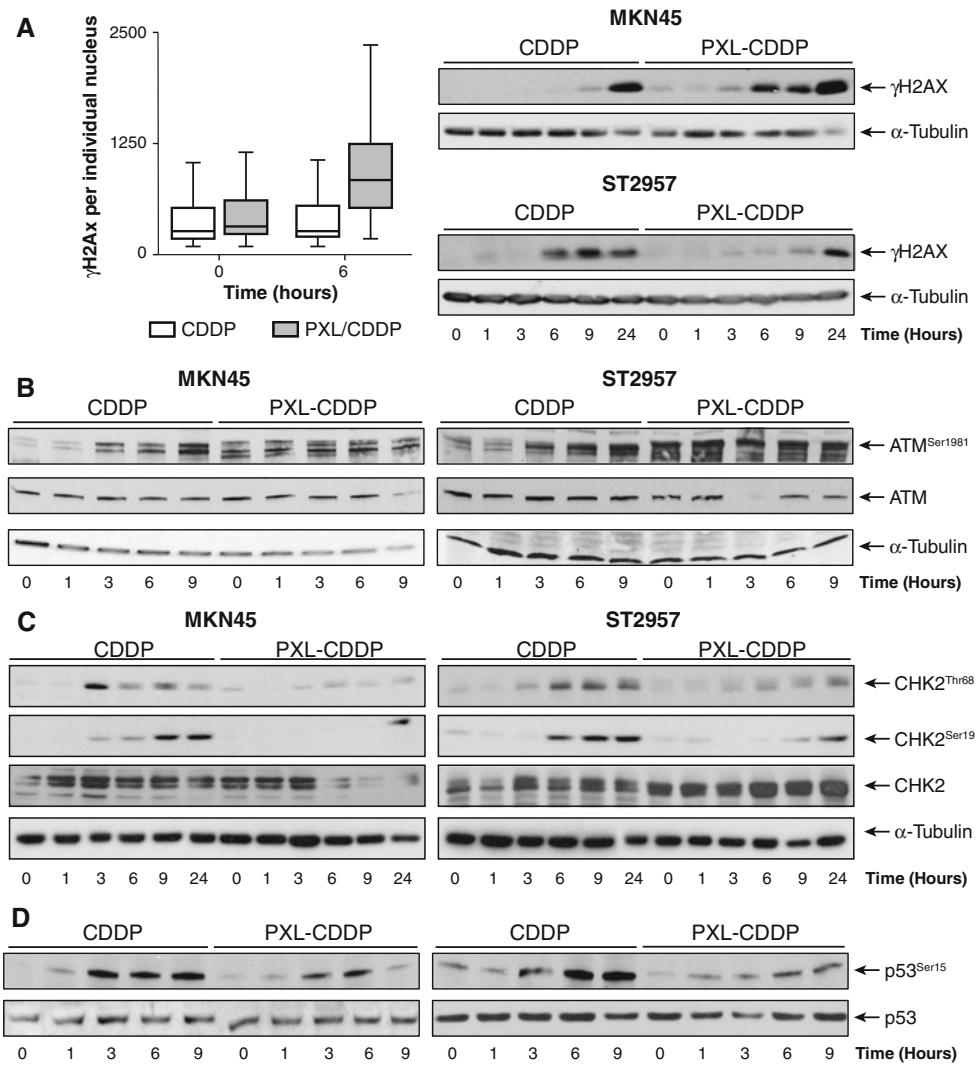

Fig. 4 Paclitaxel potentiated the DNA damage response after Cisplatin treatment in MKN45 cells. **a** Intensity of the γ-H2AX signal per nucleus, measured at the indicated times by high throughput microscopy (HTI). *Each bar* represents the total amount of γ-H2AX found in each nucleus, 6 h after the exposure of MKN45 cells to the treatment. Data are expressed as mean ± SD ($n = 3$). *Right panel*: Extracts from MKN45 and ST2957 cells were harvested at different times after treatment and blotted with antibodies against γ-H2AX. **b** The same extracts from (**a**), blotted with antibodies against $ATM^{Ser1981}$ or ATM. The blots were also probed for α-tubulin to ensure equal protein loading. **c** After treatment with the same schedule, whole cell extracts from MKN45 and ST2957 cells were prepared and blotted against $Chk2^{Ser19}$, $Chk2^{Thr68}$ or Chk2 at the indicated time points. The same extracts from (**a**), blotted with antibodies against $p53^{Ser15}$ and p53. The experiments were repeated three times with similar results. A representative experiment is shown

untreated cells showed the milder degree of damage. As the repair progresses (2.5–4 h), the CDDP-induced damage is almost completely repaired but not the damage induced by the combination of PXL-CDDP, highlighting a deficiency in the repair systems (Fig. 5f). The above results suggest that the increased sensitivity to sequential treatment observed in MKN45 cells is partly due to the inability to induce the homologous repair system mechanism through BRCA1.

Discussion

Despite current advances in the clinical management of GC, there is no therapeutic combination that has proved to be curative for this type of tumor. There have been numerous in vitro studies that predict the prognosis of the disease and studies that reveal molecular targets that, once interfered with, result in increased cell death in response to chemotherapy. However, clinical trials conducted so far, using various combinations of drugs, have not shown an improvement in the management of the disease. The experiments presented here direct us to a novel observation: eliminating cells during mitosis may be an ideal strategy for sensitizing gastric cells to therapy. However, the selected target depends on the subtype of cancer; therefore, understanding the various mechanisms of action of the drugs and discovering new therapeutic targets is crucial to using this strategy successfully. We have demonstrated that gastric adenocarcinoma cells are more sensitive to cisplatin after a prolonged arrest in mitosis due to treatment with paclitaxel; however, no differences were found in lymph node metastases cells. We have attempted to gain insight into the molecular mechanism involved in this process, and our data has revealed that the treatment induced cell death in mitosis (MC) and apoptosis and that the strength of the G2/M checkpoint and the DNA repair pathway are responsible for the fate of the cell.

We found that after sequential PLX-CDDP treatment GC cells acquire gross nuclear alterations that constitute the most prominent morphological traits of MC. MC is a term that has been widely used to describe a form of cell death that occurs during mitosis (as reviewed in [37]). There are controversial data in the literature regarding whether apoptosis is induced during mitosis and, if so, when it is induced. Our in vivo analysis confirms that the above treatment induced cell death during mitosis, in contrast with cells treated with cisplatin alone, which die by apoptosis during the interphase. Our data also indicate that this event is partially a caspase-dependent process, because the use of pan caspase inhibitor z-VAD-fmk reduced cell death in MKN45 cells. The fact that caspase inhibitors fail to completely prevent cell death induced by treatment with spindle poisons led us to conclude that other mechanisms may play a role in mitotic cell death [37, 38]. This hypothesis agrees with recent reports showing that mitotic slippage, due to the slow but progressive cyclin B degradation in the presence of a prolonged mitotic arrest, and caspase-dependent apoptosis are mechanistically independent processes [39]. Accordingly, our present results show that cell fate after mitotic arrest seems to depend on two main factors: the sustained activity of SAC, which prevents cyclin B degradation and slippage, and the ease of triggering the apoptotic machinery. This hypothesis is supported by the fact that ST2957 cells, which showed higher levels of cyclin B during the treatment, did not activate cell death pathways. Another interesting observation is the fact that Mcl-1 is only degraded in MKN45 cells. Mitotic cell death generally occurs via intrinsic or mitochondrial apoptosis, which is regulated by the Bcl-2 family of proteins [40]. Pro-survival members, including Bcl-Xl, Bcl-2 and Mcl1, antagonize apoptosis by blocking the activity of pro-apoptotic regulators. Once Mcl-1 is phosphorylated by JNK, p38 or CKII, it is recruited to the SCF and degraded by proteasome. Mcl-1 has also been reported to be degraded by APC/C-cdc20 when it is phosphorylated by Cdk1 in mitotic arrested cells [41]. Given that we observed an increase in JNK and p38 activities during treatment, it would make sense to test whether other stimuli that activate the stress response pathway could modulate the percentage of cells that die in mitosis.

We demonstrated that sequential treatment in MKN45 cells caused the accumulation of DNA damage over time, indicating the presence of unrepaired DSBs that may lead to cell death. Two questions arise from this observation, the first of which regards the reasons paclitaxel alone induces injury to the DNA. This drug does not directly damage DNA but causes chromosome segregation errors that can increase DNA breaks [42]. The second question concerns the reasons for the lack of repair. New insights are currently emerging on how DDR is controlled during mitosis [43]. We found that BRCA1, a protein required for DNA repair by homologous recombination (HR), is not phosphorylated on the S988 residue. However, we can only hypothesize that Chk2 can phosphorylate BRCA1 on this residue (S988) to mediate the DNA damage response [44] and that this phosphorylation does occur during mitosis [45]. Accordingly, the loss of BRCA1 or impairment of its Chk2-mediated phosphorylation leads to spindle formation defects and CIN in human somatic cells [32]. Our results indicate that the event responsible for the absence of BRCA1 S988 phosphorylation could be the reduction in or the absence of Chk2 activity. The role of BRCA1 during mitosis warrants in-depth study, as does its role in repairing DNA interstrand crosslinks induced by cisplatin, as it has been reported that it plays a role independent of HR in repairing these adducts [46]. One possibility is that if the Chk2-BRCA1 pathway is deficient then there will be increased mis-attachment of spindles or an influence on the activity of the Aurora-B kinase, reducing the ability to repair merotelic attachment. Whatever the mechanism, the consequence may be increased chromosomal instability, which may be incompatible with life. The influence of BRCA1 mutations in GC after sequential PLX-CDDP treatment still needs to be clarified. In this regard, Chk2 reactivation may underlie the absence of radiological responses when bortezomib treatment was evaluated in GC patients [47]. Our data suggest that the inhibition of Chk2 may be a useful therapeutic tool in GC treatment. However, to generalize this concept, it is important to understand the cells' molecular background, given that contradictory results have been described in the literature. For example, antisense inhibition of Chk2 expression enhanced the apoptotic activity of γ-irradiation, and treatment with the topoisomerase I inhibitor camptothecin had a similar effect [48]. Furthermore, inhibition of Chk2 (with siRNA or dominant negative mutants) also enhanced adriamycin-induced apoptosis in a colon carcinoma mice model system [49]. In contrast, it has been shown that inhibition of Chk2 can lead to protection from radio- or chemotherapy [50] [51,], which may indicate that targeting Chk2 may not be beneficial for anticancer treatment. However, our findings refer to the function of Chk2 during mitosis, which has been reported as necessary for proper mitotic spindle assembly and maintenance of chromosome stability [32]. In contrast, it has been demonstrated that the loss of Chk2 promotes MC and cell death and results in suppressed oncogenic transformation and tumor development in a $Mus81^{\Delta ex3-4/\Delta ex3-4}$ background [52].

Further studies are needed to explain the contribution of p53 to cell death induced during mitosis in GC. We have shown that p53 is phosphorylated at Ser15 in GC cells in response to PXL-CDDP. There are various theories about how p53 is activated during mitosis. Our data indicate that

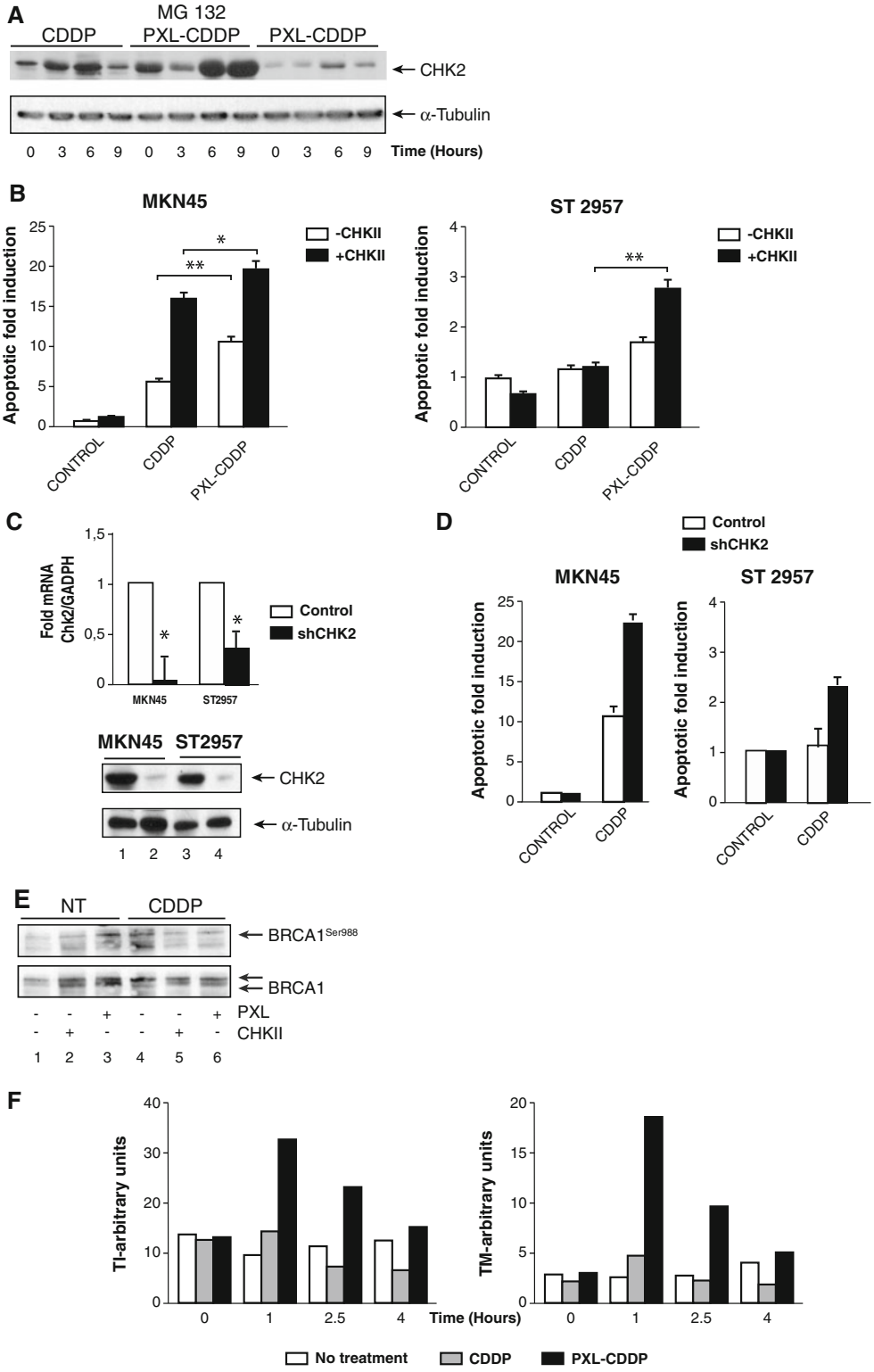

DNA damage causes activation of p53, which could be contributing to the induction of apoptosis. Along these lines, it has recently been reported that doxorubicin causes an increase in chromosome damage during anaphase in cells lacking 14-3-3σ through the activation of the γ-H2AX-path ATM-p53 pathway, which subsequently causes the cells to die [42]. Another possibility is that the cells die due to the increased transcription of pro-apoptotic members of the Bcl2

◀ **Fig. 5** Chk2 abolishment contributes to mitotic death in MKN45 cells. **a** Degradation of Chk2 is proteasome dependent. MKN45 cells were treated with PXL or PXL/CDDP in the presence or absence of the proteasome inhibitor (10 μM MG132) for 3 h, and Chk2 protein levels were detected as in Fig. 4**c**. **b** Cell cycle analyses were performed in the presence or absence of the Chk2 inhibitor (ChkII) 5 μM 1 h before CDDP addition. Cells were then treated with 10 μg/ml CDDP or PXL/CDDP (0.1 μM/10 μg/ml) for 24 h. The graph shows the percentage of apoptotic cells in each condition in the representative experiment. **c** Control and shChk2 stable cells were obtained by lentiviral infection, as described in "Materials and methods" section. Briefly, cells were transduced with lentiviral particles for control or Chk2 gene silencing and selected with 3 μg/ml puromycin. *Graph* shows the relative levels of Chk2 mRNA in the stable cells used in Fig. 5**d** after selection. Western blot is also shown to corroborate the absence of Chk2 (*bottom panel*). **d** Cells were treated with CDDP (10 μg/ml), and apoptotic cells were quantified 24 h later. **e** MKN45 cells were treated with PXL (0.1 μM), CDDP (10 μg/ml) or PXL/CDDP (0.1 μM/10 μg/ml) in the presence or absence of 5 μM ChkII (indicated with *minus* and *plus signals*) and harvested 6 h later. Extracts were probed by using specific antibodies against BRCA1^{Ser988,} and BRCA1. The *positions* of the phosphorylated BRCA1 (pBRCA1) and nonphosphorylated BRCA1 (BRCA1) are indicated. The gel lanes are indicated by *number*. The experiments were repeated twice with equivalent results. **f** The *graphs* show the DNA damage in cells not treated (*black bars*), exposed to CDDP (*grey bars*) or to the sequential treatment with PXL and CDDP (*soft grey bars*) (*left*, TM; *right*, TI) after no repair time, or 1, 2.5 and 4 h of repair. The tail moment (TM) is defined as the product of the percentage of DNA in the comet tail and the distance between the means of the tail and head fluorescence distributions. The tail intensity (TI) is defined as the percentage of DNA (fluorescent) in the tail. TM and TI are expressed in arbitrary units. Experiments were performed in duplicate. Fifty comets per duplicate gel were scored and quantified by Komet 5.5 image analysis software (Kinetic Imaging Ltd., Nottingham, UK). Apoptotic cells (non-detectable cell nuclei, ghost cells, clouds or hedgehogs) were not scored

family of proteins. Our data indicate an increase in ATM activation in response to paclitaxel, very likely a consequence of telomere dysfunction, as recently described [34].

After entering mitosis, the exit is controlled by the spindle assembly checkpoint (SAC). The SAC ensures that metaphase onset takes place when all the kinetochores are properly attached to the mitotic spindle. When bipolar conformation arises, the SAC is inactivated, and the proteolysis of cyclin B and securin allows the chromatids to separate and the cell to exit mitosis. In this study, we have shown that MKN45 cells suffer mitotic slippage, in contrast to ST2957 cells. Mitotic slippage may occur in the presence of an active SAC via cyclin B destruction. Whether bypassing the SAC correlates with cyclin B degradation in MKN45-treated cells and the influence on ST2957 cells, will be the subject of further studies. Our results suggest that GC cells treated sequentially with PLX/CDDP induce degradation of Chk2 and MC. Given that Chk2 is overexpressed in GC (50 % of cases) [53], these results suggest that combining Chk2 inhibitors with CDDP would improve therapeutic responses in this group of patients, leading to a more individualized therapy.

Acknowledgments We are grateful to Javier Perez, Daniel Gomez (photography facility), Diego Navarro and Lucia Sanchez (microscopy facility IIBM) and Diego Mejias (microscopy facility from CNIO) for technical assistance. We also would like to thank Dr. Marcos Malumbres for the GFP-H4B plasmid, R. Sanchez and Marta Fernandez-Fuente for proofreading the manuscript. This work was supported by the following Grants: PS09/1988, PI11-00949 and CCG10-UAM/BIO-5871. The authors declare no competing relationship or commercial affiliations or financial interests.

References

1. Paoletti X, Oba K, Burzykowski T et al (2010) Benefit of adjuvant chemotherapy for resectable gastric cancer: a meta-analysis. JAMA 303:1729–1737
2. Power DG, Kelsen DP, Shah MA (2010) Advanced gastric cancer–slow but steady progress. Cancer Treat Rev 36:384–392
3. Cahill R, Lindsey I, Cunningham C (2009) NOTES for colorectal neoplasia–surgery through the looking glass. Gut 58:1168–1169
4. Im CK, Jeung HC, Rha SY et al (2008) A phase II study of paclitaxel combined with infusional 5-fluorouracil and low-dose leucovorin for advanced gastric cancer. Cancer Chemother Pharmacol 61:315–321
5. Hara T, Nishikawa K, Sakatoku M, Oba K, Sakamoto J, Omura K (2011) Phase II study of weekly paclitaxel, cisplatin, and 5-fluorouracil for advanced gastric cancer. Gastric Cancer 14:332–338
6. Chua TC, Merrett ND (2012) Clinicopathologic factors associated with HER2-positive gastric cancer and its impact on survival outcomes–a systematic review. Int J Cancer 130:2845–2856
7. Yamashita-Kashima Y, Iijima S, Yorozu K et al (2011) Pertuzumab in combination with trastuzumab shows significantly enhanced antitumor activity in HER2-positive human gastric cancer xenograft models. Clin Cancer Res 17:5060–5070
8. Shiroiwa T, Fukuda T, Shimozuma K (2011) Cost-effectiveness analysis of trastuzumab to treat HER2-positive advanced gastric cancer based on the randomised ToGA trial. Br J Cancer 105:1273–1278
9. Sawaki A, Ohashi Y, Omuro Y et al (2012) Efficacy of trastuzumab in Japanese patients with HER2-positive advanced gastric or gastroesophageal junction cancer: a subgroup analysis of the Trastuzumab for gastric cancer (ToGA) study. Gastric Cancer 15:313–322
10. Wagner AD, Unverzagt S, Grothe W, et al. (2010) Chemotherapy for advanced gastric cancer. Cochrane Database Syst Rev:CD004064
11. Van Cutsem E, Moiseyenko VM, Tjulandin S et al (2006) Phase III study of docetaxel and cisplatin plus fluorouracil compared with cisplatin and fluorouracil as first-line therapy for advanced gastric cancer: a report of the V325 Study Group. J Clin Oncol 24:4991–4997
12. Jackson SP, Bartek J (2009) The DNA-damage response in human biology and disease. Nature 461:1071–1078
13. Kastan MB, Bartek J (2004) Cell-cycle checkpoints and cancer. Nature 432:316–323
14. Cha RS, Kleckner N (2002) ATR homolog Mec1 promotes fork progression, thus averting breaks in replication slow zones. Science 297:602–606
15. Ward IM, Minn K, Chen J (2004) UV-induced ataxia-telangiectasia-mutated and Rad3-related (ATR) activation requires replication stress. J Biol Chem 279:9677–9680
16. Ahn J, Urist M, Prives C (2004) The Chk2 protein kinase. DNA Repair (Amst) 3:1039–1047
17. Antoni L, Sodha N, Collins I, Garrett MD (2007) Chk2 kinase: cancer susceptibility and cancer therapy—two sides of the same coin? Nat Rev Cancer 7:925–936

18. Stracker TH, Usui T, Petrini JH (2009) Taking the time to make important decisions: the checkpoint effector kinases Chk1 and Chk2 and the DNA damage response. DNA Repair (Amst) 8: 1047–1054
19. Chen Y, Poon RY (2008) The multiple checkpoint functions of Chk1 and Chk2 in maintenance of genome stability. Front Biosci 13:5016–5029
20. van Leuken R, Clijsters L, Wolthuis R (2008) To cell cycle, swing the APC/C. Biochim Biophys Acta 1786:49–59
21. Lindqvist A, Rodriguez-Bravo V, Medema RH (2009) The decision to enter mitosis: feedback and redundancy in the mitotic entry network. J Cell Biol 185:193–202
22. Rieder CL, Maiato H (2004) Stuck in division or passing through: what happens when cells cannot satisfy the spindle assembly checkpoint. Dev Cell 7:637–651
23. Portugal J, Mansilla S, Bataller M (2010) Mechanisms of drug-induced mitotic catastrophe in cancer cells. Curr Pharm Des 16:69–78
24. Millman SE, Pagano M (2011) MCL1 meets its end during mitotic arrest. EMBO Rep 12:384–385
25. Kass EM, Jasin M (2010) Collaboration and competition between DNA double-strand break repair pathways. FEBS Lett 584: 3703–3708
26. Moynahan ME, Chiu JW, Koller BH, Jasin M (1999) Brca1 controls homology-directed DNA repair. Mol Cell 4:511–518
27. Peralta-Sastre A, Manguan-Garcia C, de Luis A et al (2010) Checkpoint kinase 1 modulates sensitivity to cisplatin after spindle checkpoint activation in SW620 cells. Int J Biochem Cell Biol 42:318–328
28. Vollmers HP, Stulle K, Dammrich J et al (1993) Characterization of four new gastric cancer cell lines. Virchows Arch B Cell Pathol Incl Mol Pathol 63:335–343
29. Sanchez-Perez I, Manguan-Garcia C, Menacho-Marquez M, Murguia JR, Perona R (2009) hCCR4/cNOT6 targets DNA-damage response proteins. Cancer Lett 273:281–291
30. Singh NP, McCoy MT, Tice RR, Schneider EL (1988) A simple technique for quantitation of low levels of DNA damage in individual cells. Exp Cell Res 175:184–191
31. Stolz A, Ertych N, Kienitz A et al (2010) The Chk2-BRCA1 tumour suppressor pathway ensures chromosomal stability in human somatic cells. Nat Cell Biol 12:492–499
32. Stolz A, Ertych N, Bastians H (2011) Tumor suppressor Chk2: regulator of DNA damage response and mediator of chromosomal stability. Clin Cancer Res 17:401–405
33. Sato K, Ohta T, Venkitaraman AR (2010) A mitotic role for the DNA damage-responsive Chk2 kinase. Nat Cell Biol 12:424–425
34. Hayashi MT, Cesare AJ, Fitzpatrick JA, Lazzerini-Denchi E, Karlseder J (2012) A telomere-dependent DNA damage checkpoint induced by prolonged mitotic arrest. Nat Struct Mol Biol 19:387–394
35. Branham MT, Nadin SB, Vargas-Roig LM, Ciocca DR (2004) DNA damage induced by paclitaxel and DNA repair capability of peripheral blood lymphocytes as evaluated by the alkaline comet assay. Mutat Res 560:11–17
36. Sun RG, Chen WF, Qi H et al (2012) Biologic effects of SMF and paclitaxel on K562 human leukemia cells. Gen Physiol Biophys 31:1–10
37. Vitale I, Galluzzi L, Castedo M, Kroemer G (2011) Mitotic catastrophe: a mechanism for avoiding genomic instability. Nat Rev Mol Cell Biol 12:385–392
38. Huang HC, Shi J, Orth JD, Mitchison TJ (2009) Evidence that mitotic exit is a better cancer therapeutic target than spindle assembly. Cancer Cell 16:347–358
39. Huang HC, Mitchison TJ, Shi J (2010) Stochastic competition between mechanistically independent slippage and death pathways determines cell fate during mitotic arrest. PLoS ONE 5:e15724
40. Letai AG (2008) Diagnosing and exploiting cancer's addiction to blocks in apoptosis. Nat Rev Cancer 8:121–132
41. Harley ME, Allan LA, Sanderson HS, Clarke PR (2010) Phosphorylation of Mcl-1 by CDK1-cyclin B1 initiates its Cdc20-dependent destruction during mitotic arrest. EMBO J 29:2407–2420
42. Crasta K, Ganem NJ, Dagher R et al (2012) DNA breaks and chromosome pulverization from errors in mitosis. Nature 482: 53–58
43. Yu B, Dalton WB, Yang VW (2012) CDK1 regulates mediator of DNA damage checkpoint 1 during mitotic DNA damage. Cancer Res 72:5448–5453
44. Okada S, Ouchi T (2003) Cell cycle differences in DNA damage-induced BRCA1 phosphorylation affect its subcellular localization. J Biol Chem 278:2015–2020
45. Zhang J, Willers H, Feng Z et al (2004) Chk2 phosphorylation of BRCA1 regulates DNA double-strand break repair. Mol Cell Biol 24:708–718
46. Bunting SF, Callen E, Kozak ML et al (2012) BRCA1 functions independently of homologous recombination in DNA interstrand crosslink repair. Mol Cell 46:125–135
47. Shah MA, Power DG, Kindler HL et al (2011) A multicenter, phase II study of Bortezomib (PS-341) in patients with unresectable or metastatic gastric and gastroesophageal junction adenocarcinoma. Invest New Drugs 29:1475–1481
48. Yu Q, Rose JH, Zhang H, Pommier Y (2001) Antisense inhibition of Chk2/hCds1 expression attenuates DNA damage-induced S and G2 checkpoints and enhances apoptotic activity in HEK-293 cells. FEBS Lett 505:7–12
49. Ghosh JC, Dohi T, Raskett CM, Kowalik TF, Altieri DC (2006) Activated checkpoint kinase 2 provides a survival signal for tumor cells. Cancer Res 66:11576–11579
50. Carlessi L, Buscemi G, Larson G, Hong Z, Wu JZ, Delia D (2007) Biochemical and cellular characterization of VRX0466617, a novel and selective inhibitor for the checkpoint kinase Chk2. Mol Cancer Ther 6:935–944
51. Pires IM, Ward TH, Dive C (2010) Oxaliplatin responses in colorectal cancer cells are modulated by Chk2 kinase inhibitors. Br J Pharmacol 159:1326–1338
52. El Ghamrasni S, Pamidi A, Halaby MJ et al (2011) Inactivation of Chk2 and mus81 leads to impaired lymphocytes development, reduced genomic instability, and suppression of cancer. PLoS Genet 7:e1001385
53. Shigeishi H, Yokozaki H, Oue N et al (2002) Increased expression of Chk2 in human gastric carcinomas harboring p53 mutations. Int J Cancer 99:58–62

RESUMEN

Mad2 and BubR1 modulates tumourigenesis and Paclitaxel response in MKN45 gastric cancer cells

Bargiela-Iparraguirre J, Prado-Marchal L, Pajuelo-Lozano N, Jiménez B, Perona R, Sánchez-Pérez I.

Cell Cycle. 2014; 13(22):3590-601. doi: 10.4161/15384101.2014.962952. PMID: 25483095

La inestabilidad cromosómica y la aneuploidía son características comunes del cáncer gástrico, pero su contribución en la carcinogénesis y la respuesta a terapia es aún un campo en estudio. La regulación incorrecta de la expresión de las proteínas del punto de control mitótico (Spindle Assebly Chechpoint (SAC) generan errores en la segregación cromosómica y participan en la aneuploidía.

En este capítulo, estudiamos el papel de la inestabilidad cromosómica en la carcinogénesis. Analizamos la expresión de los principales genes que participan en el punto de control de mitosis en una serie de líneas celulares derivadas de cáncer gástrico, y observamos que *MAD2L1* y *BUB1B* están sobreexpresados en líneas células procedentes de tumores diseminados. La disminución de su expresión mediante shRNAs en células MKN45 muestra un descenso en la tasa de proliferación, y menor capacidad de migración e invasión de estas respecto a las células control. Estos datos sugieren la participación de las proteínas MAD2 y BUBR1 en la carcinogénesis. Además, evaluamos el efecto de los niveles de estas proteínas en la respuesta al agente antineoplásico Paclitaxel (PTX). Mediante ensayos de viabilidad y Western Blot observamos que las células con expresión interferida tanto de MAD2 como de BUBR1 muestran una mayor resistencia al agente, y dicha resistencia no se debe a efectos en la inducción de apoptosis, ni a diferencias en la respuesta al daño en el DNA, ya que detectamos la activación de las proteínas principales de cada ruta de forma equivalente en células control o interferidas. Sin embargo, en respuesta a PTX observamos una inducción de la senescencia al disminuir los niveles de las proteínas de SAC, caracterizada por aumento de la tinción β-Gal y un fenotipo secretor asociado a senescencia (SASP), así como por una elevación de las interleuquinas 6 y 8. Nuestros datos sugieren que MAD2 y BUBR1 participan favoreciendo un fenotipo más agresivo del tumor y podrían considerarse como diana terapéutica en el tratamiento del cáncer gástrico. La disminución de sus niveles en situaciones de sobreexpresión podría reducir el crecimiento y la metástasis en los pacientes. Sería muy interesante analizar el efecto fisiológico de la senescencia observada tras la disminución de la expresión de MAD2 y BUBR1, debido a la dualidad existente en la actualidad sobre el papel de la senescencia como supresor tumoral o regulador del progreso del tumor.

Participación en el trabajo: Realizar la parte experimental y análisis de resultados.

Cell Cycle 13:22, 3590–3601; November 15, 2014; © 2014 Taylor & Francis Group, LLC

Mad2 and BubR1 modulates tumourigenesis and paclitaxel response in MKN45 gastric cancer cells

J Bargiela-Iparraguirre[1,2], L Prado-Marchal[2], N Pajuelo-Lozano[2], B Jiménez[1,2], R Perona[2,3,4], and I Sánchez-Pérez[1,2,3,*]

[1]Departamento Bioquimica; Facultad Medicina; UAM; Madrid, Spain; [2]Instituto de Investigaciones Biomédicas Madrid; Madrid CSIC/UAM; Madrid, Spain; [3]Biomarkers and Experimental Therapeutics Group; IdiPAZ; University Hospital La Paz; Madrid, Spain; [4]CIBER on Rare Diseases (CIBERER); Valencia, Spain

Keywords: apoptosis, BubR1, gastric cancer, Mad2, mitosis, paclitaxel, senescence

Abbreviations: BMC, bleomycin; BubR1, budding uninhibited by benzimidazoles 1 homolog B protein (gene BUB1B); CDDP, cisplatin; CIN, chromosome instability; DDR, DNA damage response; Mad2, mitotic arrest deficient-like-1 protein (gene Mad2L1); PTX, paclitaxel; SAC, spindle assembly checkpoint; SASP, senescence associate secretory phenotype; γH2AX, phosphorylated H2AX; Monopolar Spindle kinase, MPS1.

Aneuploidy and chromosomal instability (CIN) are common features of gastric cancer (GC), but their contribution to carcinogenesis and antitumour therapy response is still poorly understood. Failures in the mitotic checkpoint induced by changes in expression levels of the spindle assembly checkpoint (SAC) proteins cause the missegregation of chromosomes in mitosis as well as aneuploidy. To evaluate the possible contribution of SAC to GC, we analyzed the expression levels of proteins of the mitotic checkpoint complex in a cohort of GC cell lines. We found that the central SAC proteins, Mad2 and BubR1, were the more prominently expressed members in disseminated GC cell lines. Silencing of Mad2 and BubR1 in MKN45 and ST2957 cells decreased their cell proliferation, migration and invasion abilities, indicating that Mad2 and BubR1 could contribute to cellular transformation and tumor progression in GC. We next evaluated whether silencing of SAC proteins could affect the response to microtubule poisons. We discovered that paclitaxel treatment increased cell survival in MKN45 cells interfered for Mad2 or BubR1 expression. However, apoptosis (assessed by caspase-3 activation, PARP proteolysis and levels of antiapoptotic Bcl 2-family members), the DNA damage response (assessed by H2Ax phosphorylation) and exit from mitosis (assessed by Cyclin B degradation and Cdk1 regulation) were activated equally between cells, independently of Mad2 or BubR1-protein levels. In contrast, we observed that the silencing of Mad2 or BubR1 in MKN45 cells showed the induction of a senescence-like phenotype accompanied by cell enlargement, increased senescence-associated β-galactosidase activity and increased IL-6 and IL-8 expression. In addition, the senescent phenotype is highly increased after treatment with PTX, indicating that senescence could prevent tumorigenesis in GC. In conclusion, the results presented here suggest that Mad2 and BubR1 could be used as prognostic markers of tumor progression and new pharmacological targets in the treatment for GC.

Introduction

Gastric cancer (GC) is a highly lethal malignancy.[1] Surgery is the main therapeutic option for patients with localized disease, followed by adjuvant chemotherapy, which enhances clinical responses.[2] However, many patients experience disease recurrence and eventually succumb due to chemotherapy resistance and/or metastasis. Paclitaxel (PTX) is widely used in the treatment of GC, usually in combination with other agents, depending on the state of the tumor at diagnosis.[3] This agent targets microtubules and provokes mitotic arrest, causing cell death. However, cells have developed various mechanisms to avoid apoptosis during mitosis through a process called "slippage" and by inducing senescence-like phenotypes due to abnormal mitosis in a variety of tumor cells[4] or through mitotic catastrophe.[5,6] The spindle assembly checkpoint (SAC) is a regulatory mechanism present in all eukaryotes, which prevents chromosome missegregation during mitosis, thereby preventing aneuploidy.[7] SAC is the checkpoint through which PTX and other microtubule poisons exert their effects. The reduced expression of SAC proteins such as BubR1 (budding uninhibited by benzimidazoles 1 homolog B; BUB1B) or Mad2 (mitotic arrest deficient-like-1; Mad2L1) is associated with acquired paclitaxel resistance in ovarian carcinoma cell lines.[8,9]

Chromosome instability (CIN) and aneuploidy are hallmarks of aggressive solid tumors such as GC.[10,11] Aneuploidy can result from inaccurate chromosome segregation; therefore, SAC has a crucial function in genetic integrity. Impaired SAC function has been suggested as one of the causes of aneuploidy in human cancers.[7,12] SAC is a complex of proteins that includes Mad1, Mad2, Bub1, BubR1, Bub3, and MPS1.[13] Among all SAC components, Mad2 and BubR1 have a pivotal function in checkpoint

*Correspondence to: I Sánchez-Pérez; Emails: misanchez@iib.uam.es; is.perez@uam.es
Submitted: 07/16/2014; Revised: 08/28/2014; Accepted: 09/03/2014
http://dx.doi.org/10.4161/15384101.2014.962952

signaling due to their central role in the inhibition of the anaphase-promoting complex/cyclosome (APC/C). The discovery of mutations in BubR1 and Bub1 in a subset of colon cancer cell lines[14] and in mosaic variegated aneuploidy (a rare human disorder characterized by a predisposition to childhood cancers)[15] suggests that a weakened SAC contributes to the oncogenic process. In addition, mouse models that carry mutations in the SAC genes have been reported to develop spontaneous tumors. These heterozygous animals are viable and apparently healthy but develop spontaneous tumors.[16–22] There are examples of no tumor induction, as seen in mice with reduced Bub3[23] or BubR1 expression.[18] However, Mad2[19] or Mad1[21] haploinsufficiency caused a mild increase in the rate of spontaneous tumors. At the other end of the spectrum, Bub1−/H (null over hypomorphic)[24] and Mad2-overexpressing mice[20] all displayed high rates of spontaneous tumourigenesis. Coincidently, aberrant expression of the mitotic checkpoint proteins has been observed in human cancer cells, suggesting that SAC protein levels play an important role in cancer initiation and progression.

Senescence and apoptosis are two important mechanisms that protect cells against cellular transformation and cancer development. Cellular senescence is considered an alternative tumor suppressor mechanism,[25] and a correlation has been reported between senescence cells found in premalignant lesions (but not in malignant tumors) after oncogene activation.[26] However, senescent cells can interfere with their microenvironment by secreting proteases and mitogenic, antiapoptotic and antigenic factors, which can promote carcinogenesis in neighboring cells. This entity was recently described as the senescence-associated secretory phenotype (SASP)[27] and is gaining considerable interest in cancer research.[28]

We have previously demonstrated that pretreatment with PTX, which induces a prolonged arrest in mitosis, increases cisplatin (CDDP) sensitivity in MKN45 GC cells due to impaired DNA repair.[29] In this study, we hypothesized that SAC dysfunction would be associated with GC and with PTX therapy response. We studied SAC protein levels in GC cell lines and found that Mad2 and BubR1 are frequently overexpressed in gastric adenocarcinoma. To clarify whether BubR1 or Mad2 levels play a role in GC, we generated GC gastric cell lines with depletion of these proteins. Our results show that these proteins are involved in proliferation, migration and tumor progression. However, after treatment with PTX the survival ratio of MKN45 cells lacking Mad2 or BubR1 is higher compared with MKN45 parental cells. We attempted to clarify the mechanism by which cells acquired resistance to PTX, and surprisingly, PTX monotherapy induced the apoptotic pathway independently of Mad2 or BubR1 protein levels, indicating that this pathway is unaffected. In the other hand, we observed that PTX treatment induced a senescence phenotype, which is exacerbated in cells that have been silencing for Mad2 or BubR1. The results are promising for the treatment of GC, as senescence could be acting as a suppressor of cancer progression. Although further in vivo studies are needed to clarify the role of senescence in this type of tumor, our results raise the possibility of a new treatment based on Mad2 or BubR1inhibitors in combination with PTX.

Results

mRNA expression levels of SAC components in GC cell lines

One of the characteristics of GC is the presence of a high number of aneuploidies.[30] To analyze the potential role of SAC defects in the generation of aneuploidies, we determined the BUB1B, BUB3, MAD1L1, MAD2L1 expression levels that participate in SAC regulation in 7 different GC cell lines. We also determined the levels of other genes linked to this checkpoint, such as CENPE and AURKB. The transcript levels of the selected genes were quantified by quantitative real time reverse-transcription polymerase chain reaction (qRT-PCR), and represented as fold changes between each GC cell line and the normal human colon fibroblast CCD18Co cell line. We compared the expression levels between primary (AGS and HGC27) and metastatic (SNU1, SNU638, Hs746t, MKN45, ST2957) GC cell lines, and we observed that MAD1L1 and BUB3 transcript levels were variable between all of them. Thus, MAD1L1 is significantly downregulated in HGC27 and BUB3 transcript levels were reduced in HGC27 and MNK45. However, MAD2L1 and BUB1B appeared to be upregulated in metastatic cells. Thus, MKN45 showed 3-fold greater expression of MAD2L1 and 1.5 fold times of BUB1B with respect to control fibroblasts. Moreover, ST2957 cells showed 4 times greater expression MAD2L1 and 2 times greater for BUB1B. Also SNU638 showed an increase of 3 times greater BUB1B expression. (**Fig. 1A**). We analyzed MAD2L1, MAD1L1, BUB1B and BUB3 expression by using several published databases from the publicly available Oncomine database.[31–33] We required a *P*-value of below 0.05 and a fold-change of 2 for gene expression compared to the control. The results indicated that a significant increase in MAD2L1 and BUB1B mRNA level were observed in Gastric Intestinal Type Adenocarcinoma vs. Normal Gastric in 3 different clusters (**Fig. 1B**). CENP-E transcription was reduced in HGC27 and Hs746t and increased in ST2957. Finally, when we studied AURK-B, we observed significantly increased transcript levels in the HGC27 and Hs746t cell lines (**Fig. S1**). These results suggest that MAD2L1 and/or BUB1B overexpression should be a common feature in gastric tumors and could be involved in modulating not only SAC activity but also the ability of adenocarcinoma gastric cells to proliferate and ultimately, their fate after specific drug treatments.

Interference of Mad2 and Bub1R1 expression modulates proliferation and cell migration in GC cells

To study the physiological functions of these proteins, we knocked down Mad2 and BubR1 expression with shRNA lentivirus (shMAD2L1 and shBUB1B) in 2 different cell lines: MKN45 and ST2957. After selecting with puromycin, we were able to obtain stable cultures of cells with reduced levels of Mad2L1 and Bub1B genes. We conducted a qRT-PCR study to select those clonal cultures with the highest knockdown of our genes of interest. We therefore selected the following for further study: MKN45-shBUB1B-2 and MKN45-shMAD2L1–2 from the MKN45 cells and ST2957-shBUB1B-3 and ST2957-shMAD2–

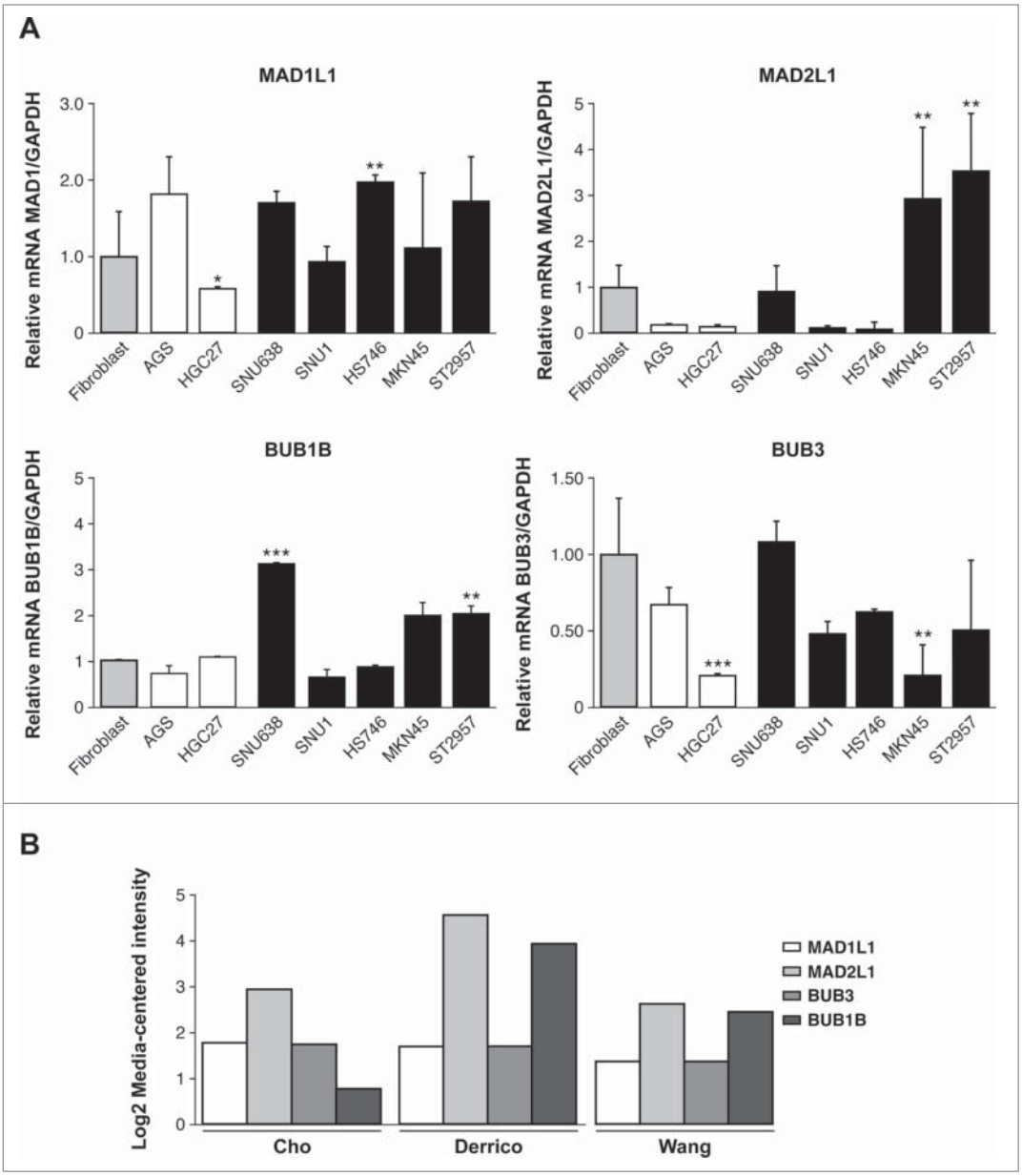

Figure 1. Relative levels of mRNA transcripts for the individual components of SAC. (**A**) Real-time q-PCR was performed to measure the relative levels of MAD1L1, MAD2L1, BUB1B, BUB3 mRNAs in the 7 GC cell lines established from primary tumor (white bars) and disseminated tumor (black bars). Each gene was normalized with GAPDH. Data are shown as relative to CCD18-Co, and the statistical significance was evaluated with ANOVA. ** $P < 0.05$ and *** $P < 0.001$. (**B**) Selected datasets from the Oncomine cancer microarray database were used to determine the alternations of MAD1L1, MAD2L1, BUB3 and BUB1B in mRNA expression levels. The graph represents the fold in gastric intestinal type adenocarcinoma versus normal gastric tissue based on studies reported by Cho et al., Derrico et al. and Wang et al. $P < 0.001$.

1 from the ST2957 cell line. Western blot (WB) analysis corroborated the decrease in protein levels for Mad2 or BubR1, after infection with the specified lentivirus clones (**Fig. S2**).

We evaluated the influence of MAD2L1 and BUB1B downregulation on cell proliferation in 7-day cultures and found that although there were no differences when knocking down BUB1B, the reduction of MAD2L1 appeared to regulate cell growth in both cell lines after 7 d However, there were no statistical differences (**Fig. 2A**). To confirm the role of Mad2 in proliferation, we performed a colony-forming assay. As expected, our results showed that the absence of Mad2 reduced the number of surviving colonies at the end of the experiment (15 days) in both cells lines. We counted 25 colony-forming units (CFUs) in sh-MAD2L1 versus 35 CFUs in MKN45 and 15 CFUs in sh-MAD2L1versus 30 CFUs in control ST2957 (**Fig. 2B**). Surprisingly, although we did not observe a change in proliferation at 7 days, the ability of the cells to form colonies in the absence of BubR1 was also reduced, with the reduction more significant in ST2957 cells (9 vs. 30 CFUs) than in the MKN45 cells (28 vs. 35 CFUs) (**Fig. 2B**). To clarify this contradictory result, we compared the replicative life span of MKN45 cells with that of the cells with diminished Mad2 or BubR1 expression. Our experiment showed that after 15 days, both cell lines achieved lower population doubling levels (PDLs) than the parental MKN45 cells. After another 15 days, however, the cells overcame the crisis and were able to continue growing. Nevertheless, cells without BubR1 achieved lower PDLs than control cells (**Fig. 2C**). These results suggest that Mad2 and BubR1 play a role in proliferation, which indicates that they act on the tumourigenesis process.

SAC downregulation decreases cell migration and invasion in MKN45 cells

The capacity for cells lacking Mad2 or BubR1 to migrate was evaluated with an in vitro wound-healing assay. In control

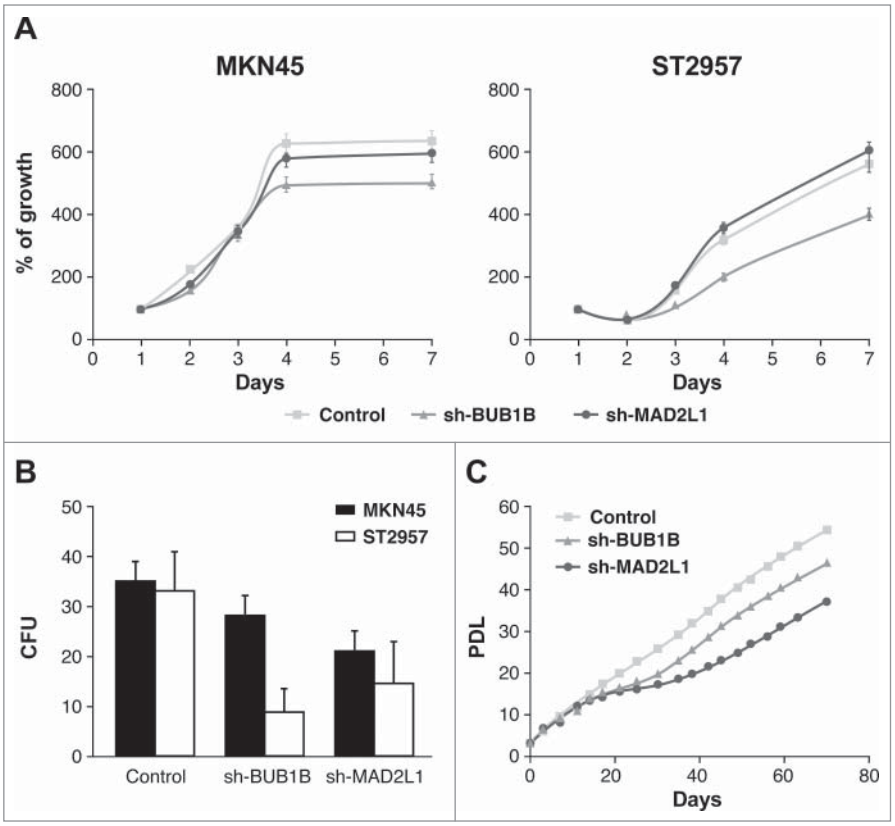

Figure 2. Mad2 and BubR1 regulate cell proliferation. (**A**) The MKN45 and ST2957 cell lines were transduced with lentivirus expressing sh-MAD2L1 and sh-BUB1B. The graphs show the proliferation rate measured every 24 h up to 7 d after infection, measured by crystal violet method. Data were calculated relative to the staining obtained on the first day. The experiments were done in quadruplicate at least 3 times. (**B**) Clonogenic assay. The graph represents the colony counting average at day 14, in 3 different areas per well. The experiment was performed in duplicate. (**C**) Analysis of the accumulated number of duplications over time (PDLs) in the MKN45 cell line and its transduced sh-BUB1R and sh-Mad2 cell lines. Each condition was done in duplicate.

MKN45 cells, 88% of the wound area had been filled within 48 h postscratch. However, when BubR1 or Mad2 expression was diminished in these cells, only 66% of the wound area was filled during that time for both sh-MAD2L1 and sh-BUB1B cells (**Fig. 3A,** Images and left graph). The right graph of **Figure 3A** shows the speed at which cells were able to repopulate the scratched area in arbitrary units: 659 ± 100; 434 ± 160 and 388 ± 95 for MKN45, sh-MAD2L1 and sh-BUB1B, respectively. The ST2957 cell line required more than 50 h to heal the scratch completely. ST2957-shBUB1B and ST2957-shMAD2L1 cells showed impaired migration in the same time period in contrast with the wild type ST2957 cells, with 36% of the area covered compared with 73% for the control cells (**Fig. 3; Fig. S3**). These observations were confirmed by migration assays (**Fig. 3B**). The number of migrating cells was decreased in the absence of Mad2 or BubR1, compared with MKN45 cells. (**Fig. 3B**). Both wound-healing and transwell migration assays revealed that Mad2 overexpression contributed to cell migration in the MKN45 cells. The invasive properties of the cells were assessed by a matrigel-coated transwell assay. There was a basal level of invasion in the control MKN45 cells (30 cells/field). However, the rate was significantly decreased to 18 cells/field in sh-BUB1B and 15 cells/field in sh-MAD2L1 (**Fig. 3C**), demonstrating that the overexpression of Mad2 signaling confers invasive properties to adenocarcinoma parental cell lines. These findings imply that activation of SAC signaling promotes migration and invasion and could be associated with a poor prognosis for GC patients.

Silencing of Mad2 and Bub1R1 increases survival of MNK45 cells treated with PTX

Next, we ascertained whether Mad2 upregulation could play a role in drug responses in GC. First, we studied cell survival after exposure to 3 different antitumoural agents: cisplatin (CDDP), paclitaxel (PTX) and the radiomimetic drug bleomycin (BMC). Our MTS viability assay showed that, in response to increasing amounts of CDDP (0–20 μg/ml), the behavior of all cell lines was almost the same; however, after BMC treatment (0–100 μg/ml), the reduction in Mad2 or BubR1 levels appeared to sensitize cells, given that a reduction in IC50 was observed. Surprisingly, cells with reduced Mad2 or BubR1 levels are more resistant to PTX (0–1 μM) than the control cells (**Fig. 4A**). To support this observation, we studied the viability of cells after exposure to varying doses of PTX using the crystal violet method and we achieved the same result (**Fig. 4C**). To confirm these observations, we performed a colony survival assay. MKN45, sh-MAD2L1 and sh-BUB1B cells were treated with solvent or PTX (100 nM) for 20 h. Ten days later, the number of surviving colonies was recorded. We found that the number of colonies in the absence of Mad2 was similar to MKN45, although the cells with reduced BubR1 had a lower number of surviving colonies compared with the other cultures (574 ± 89, 575 ± 22 and 319 ± 25.5 for MKN45, sh-MAD2L1 and sh-BUB1B, respectively). The number of colonies was higher (also in the absence of Mad2 or BubR1) after PTX treatment than in the control cells (43 ± 1.4, 216 ± 3.5 and 168 ± 8.5 for MKN45, sh-MAD2L1 and sh-BUB1B, respectively) (**Fig. 4B**). However, our data show that migration is not modified by PTX treatment (**Fig. 4D**). These results confirm the crucial role of SAC in cell death induction in response to PTX treatment.

Silencing of Mad2 and Bub1b induces senescence in MKN45 cells treated with PTX

After prolonged arrest in mitosis, cells can die by apoptosis and re-enter on cycle G1 in a tetraploid state, through a process

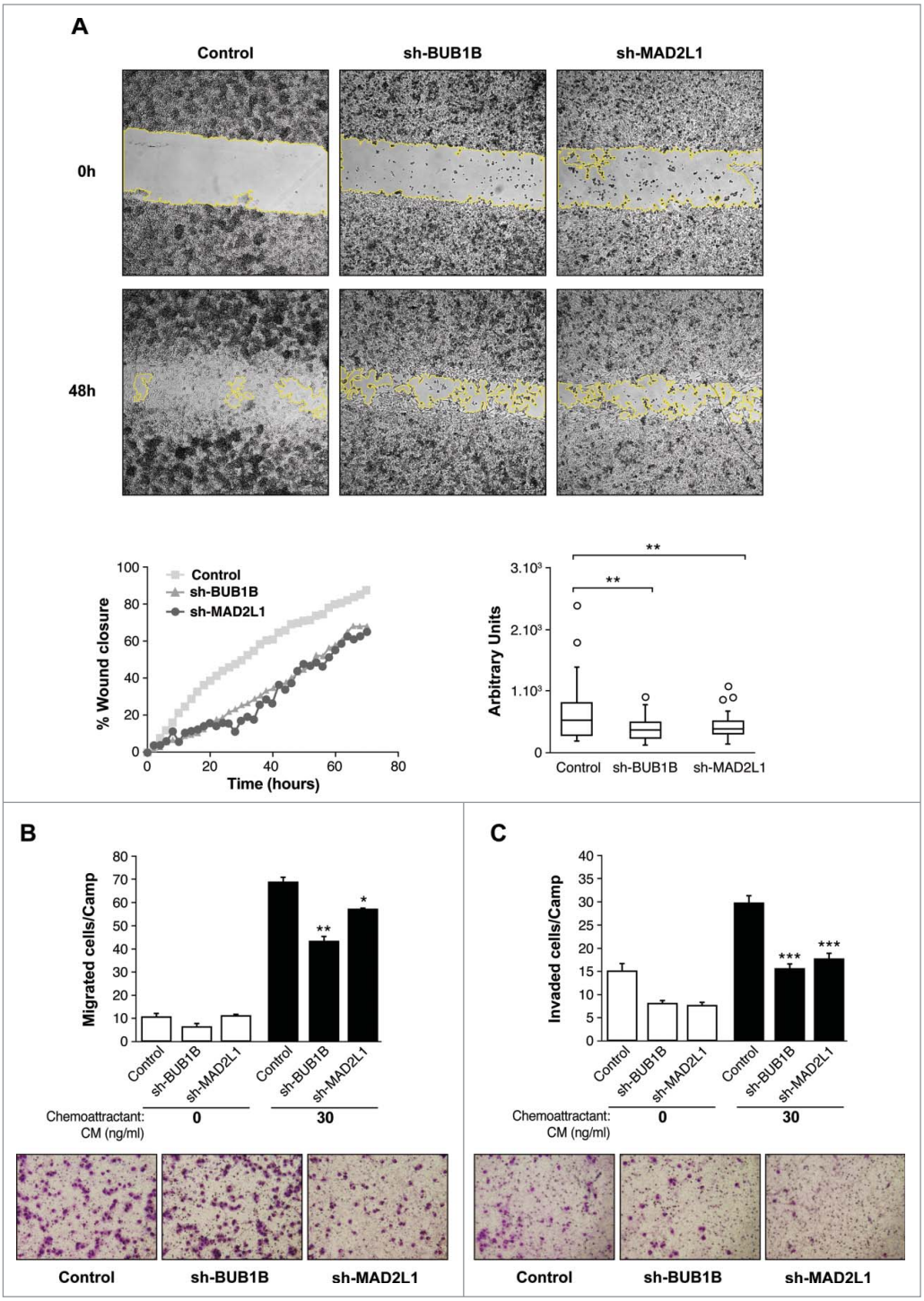

Figure 3. Silencing of Mad2 and Bub1B reduces migration and invasion in MKN45 cells. (**A**) Representative images of the first (0 h) and last picture (48 h) of control MKN45, sh-Mad2L1 and sh-BUB1B cells taken during the wound healing experiment. Images were taken at 10× magnification, every 2 h for 48 h. The yellow line represents the wound border. Left panel: The graph shows the percentage of wound closure over the study time using the ImageJ program. Right panel: Assessment of speed variations within the interfered cell lines and the control. The table shows the average speed for each line. The experiment was performed twice, and statistical differences were assessed by one-way ANOVA (* $P < 0.05$, ** $P < 0.005$, *** $P < 0.001$). (**B**) Transwell migration assay. The graph shows the quantification of stained migratory cells using the transwell assay without chemoattractant (basal migration control) and 30 ng/ml chemoattractant presence at 24 h. Representative photographs of stained cells attached to the bottom membrane of a transwell at the bottom. Statistical differences were assessed by a one-way ANOVA (* $P < 0.05$, ** $P < 0.005$, *** $P < 0.001$) (**C**) Transwell invasion assay. Graph shows the quantification of stained invading cells using the transwell assay with 6 μg of Matrigel, without chemoattractant (basal invading control) and 30 ng/ml chemoattractant presence at 24 h. Representative photographs of stained cells attached to the bottom membrane of a transwell at the bottom. Statistical differences were assessed by one-way ANOVA (* $P < 0.05$, ** $P < 0.005$, *** $P < 0.001$

known as slippage. Death in mitosis is principally mediated by a caspase-dependent apoptotic pathway requiring mitochondrial outer membrane permeabilisation. A flow cytometry analysis demonstrated that the percentage of apoptosis was equivalent in MKN45 cells in response to PTX, independent of SAC (data not shown). We then studied the various molecular markers of apoptosis after PTX treatment in MKN45 cells and those with Mad2 or BubR1 depletion. We found that levels of the antiapoptotic member of the Bcl-2 family Mcl-1 (myeloid cell leukemia-1), a key molecule in cell death during mitosis, decreased 24 h after PTX exposure in MKN45 and sh-BUB1B. However, in the absence of Mad2, the protein remains at basal levels at least 48 h after treatment. Nevertheless, we observed the same behavior in Bcl-xl, with a shift indicative of inhibitory phosphorylation 24 h after PTX treatment (**Fig. 5 A**, left). Mcl1 degradation is controlled by phosphorylation mediated by Cdk1 or the stress kinases p38 and JNK. Our WB analysis showed that Cdk1 is phosphorylated at Y15 (inactive), with the

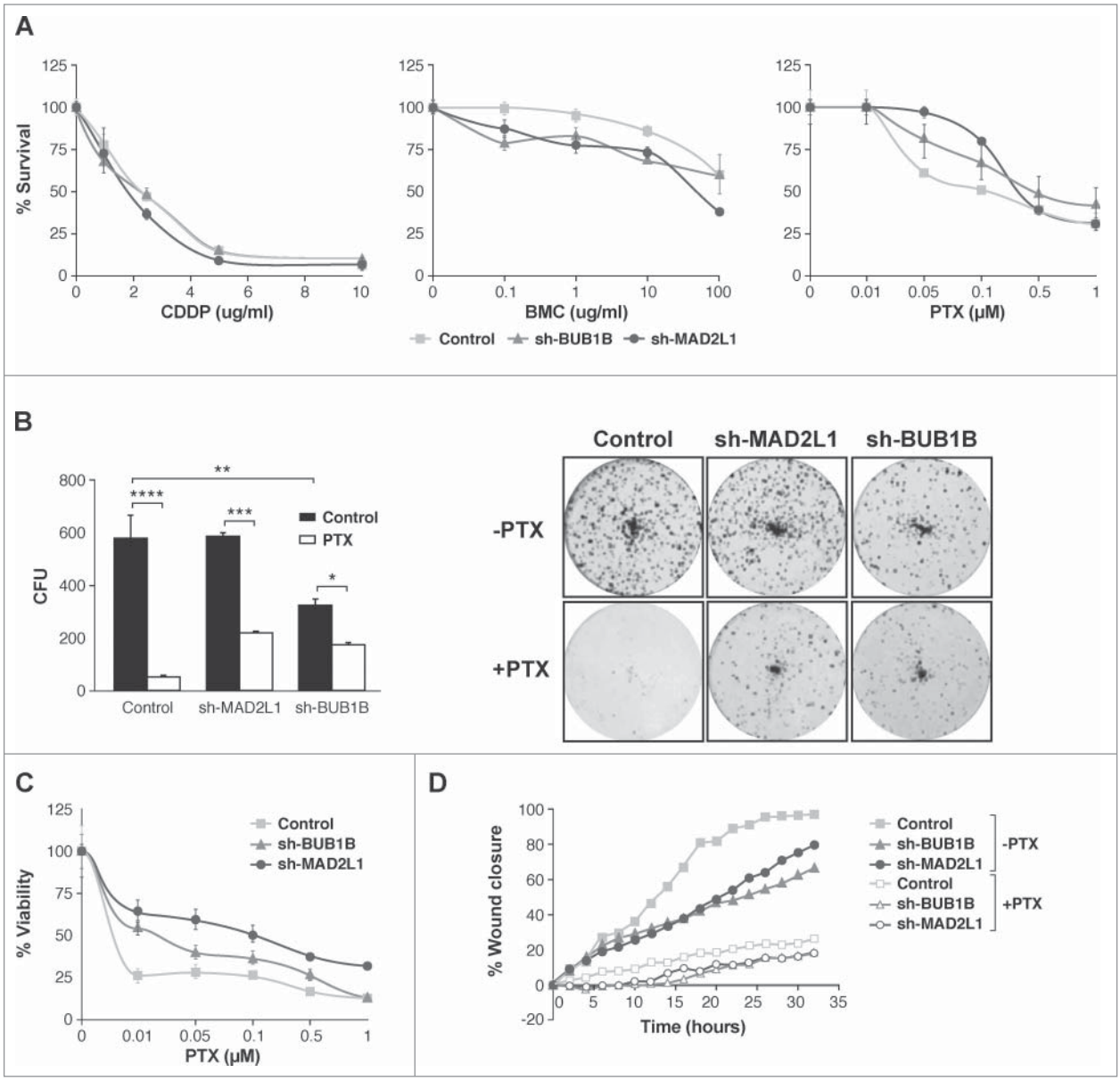

Figure 4. Interference of Mad2 and BubR1 expression increases survival to PTX in MKN45 cells. (**A**) Indicated cell lines were seeded on MW96 and treated with increasing doses of CDDP, PTX or BMC. Graphs show survival curves measured by MTS 48 h after treatment. The experiments were performed in quadruplicate and repeated twice. (**B**) Left panel: Clonogenic assay. The graph represents the average of all clones in each experimental condition, in 3 independent experiments performed in duplicate. Statistical significance was studied by a 2-way anova (* $P < 0.05$, ** $P < 0.005$, *** $P < 0.001$). Cells were plated at low density and treated with 0.05 μM of PTX. Right panel: Representative images of colonies from a 10-day assay in control MKN45, sh-Mad2L1 and sh-BUB1B cell lines. (**C**) Control MKN45, sh-MAD2L1 and sh-BUB1B cells were treated with increasing concentrations of PTX (0–100 nM). Viability was quantified using the crystal violet after 48 h of treatment. Results are presented as percentage of viable cells relative to untreated cells. Data show the results from 3 independent experiments, performed in quadruplicate. Statistical differences were tested using Student's t-test (* $P < 0.05$, ** $P < 0.005$, *** $P < 0.001$). (**D**) The effect of PTX (0.1 μM) on control MKN45, sh-Bub1B and sh-Mad2L1 cell migration in the wound healing assay was measured up to 48 h. The wound closure was quantified every 2 h postwounding by measuring the remaining unmigrated area using ImageJ.

same kinetics in MKN45 cells and cells depleted of BubR1 or Mad2, which achieved maximum levels 24 h after treatment. We then examined the impact of PTX on the stress-related JNK and p38 pathways. Treatment of cells with PTX resulted in a transient increase in phospho-JNK at 24 h after PTX exposure, with a modest increase in Mad2-depleted cells. Moreover, p38 showed persistent activation in MKN45 cells, transient activation in sh-BUB1B and virtually no activation in sh-MAD2L1 cells (**Fig. 5A,** right). Treatment of cells with PTX induced cleavage/activation of procaspase-3 and degradation of PARP to an 85 kDa species in all cell lines 48 h after PTX exposure (**Fig. 5B**). Given that Cyclin B levels control the mitotic state,

we found Cyclin B degradation 48 h after PTX treatment, indicating that apoptosis occurs after exit mitosis. A prolonged arrest in mitosis could also induce DNA damage. Our data showed that the marker of DNA damage H2Ax is activated in MKN45 cells to a lesser degree than in the case of SAC compromised cells. These results suggest that arrest in mitosis increases DNA damage and induces the intrinsic apoptotic pathway in MKN45 cells, regardless of the strength of the SAC. Mcl-1 degradation depends mainly on p38, and its degradation is delayed in depleted Mad2 cells but probably not enough to inhibit apoptosis.

To determine whether senescence was an alternative process to explain the results obtained in survival, we performed an in situ senescence-associated (SA) β-Gal assay. We observed the induction of the senescence-like phenotype of MKN45 cells, manifested by changes in morphology and β-galactosidase (SA-β-gal) activation. With this experiment, we determined that the fraction of SA-β-gal-positive cells increases 3 d after Mad2 or BubR1 depletion (**Fig. 5C,** upper panel). Moreover, SA-β-galactosidase activity staining showed a clear increase in cellular senescence in these cells after PTX treatment compared with control MKN45 cells (**Fig. 5C,** bottom panel). PTX causes a prometaphase arrest cell cycle that, if sustained, generates DNA damage and senescence. p53 is a marker for both events. When we analyzed its activation after 72 h of PTX treatment, we observed an increase in p53 mRNA levels in cells lacking Mad2 or BubR1 (**Fig. 5D**). On the contrary, we observed no increase in $p21^{waf1}$ WB analysis confirmed these results, as well as a sharp increase in $p53^{Ser15}$, induced by PTX. To determine whether the SASP is also under SAC protein control, we monitored SASP IL-6 and IL-8 expression in control cells and after 50 d of gene interference (**Fig. 5E**). Both IL-6 and IL-8 mRNA levels were increased during senescence in the absence of BUB1B, but only IL-6 (and not IL-8) expression was attenuated when Mad2 was decreased. The results of this study suggest that the weaker SAC in MKN45 cells increases the levels of a senescent phenotype involved in the PTX response in these cells.

Discussion

GC is a disease with a very poor prognosis at diagnosis. Finding new targets that increase our understanding of the disease presents a challenge for researchers, but can ultimately contribute to improved and more personalized treatments. However, the biology of this tumor is very complex at the molecular level, and there is no defined pattern of markers.[34] Our results show that GC cells undergo uncontrolled SAC protein expression, which is the case in other types of cancers such as lung, breast, head and neck, ovarian and cervical cancer.[35] This study has shown that two essential proteins in the mitotic checkpoint, Mad2 and BubR1, are overexpressed in the majority of disseminated gastric cancer cell lines, and these results are in agreement with the public database ONCOMINE. (http:oncomine.org). We have characterized the effects of a reduction in Mad2 or BubR1 expression and found that these proteins control cell proliferation, migration and tumor progression in MKN45 and ST2957 cell lines. Accordingly, overexpression of BubR1 in bladder cancer[36] or Mad2 in colorectal mucosa[37] has been associated with high proliferation. Moreover, ovarian carcinoma showed overexpression and correlation of Mad2 and BubR1, which are related to cellular proliferation and time to recurrence[38]. Taken together our data indicated that overexpressed Mad2 and BubR1 participate in the carcinogenesis of GC and high Mad2 and Bub1B could be used as a prognostic marker; in fact BubR1 have recently been suggested as a prognostic marker in ovarian cancer.[39]

There is some controversy in the literature regarding the importance of correct SAC function and therapy response. Mad2 downregulation in MCF7 and A2780 cells[9,40] resulted in resistance to PTX. Similarly, we also detected an increase in cell survival after treatment with PTX in MKN45 cells. Inhibition of apoptosis is a frequent cause of drug resistance, and it has been suggested that Mad2 interference could inhibit anticancer drug-induced apoptosis by upregulating Bcl-2 and interfering with the mitochondria apoptosis pathway.[41] Here, we demonstrated that depletion of Mad2 delay Mcl-1 degradation, suggesting that exit to mitosis is delayed; however, no differences have been found in apoptotic induction because activation/proteolysis of caspase-3/PARP occurs at the same time in cells, regardless of the presence of Mad2 or BubR1. We could say that the difference in survival among MKN45 cells is not due to apoptotic inhibition. More importantly, our data show that the molecular mechanism related to survival correlates with the induction of cellular senescence-like phenotype. The contribution of these proteins to PTX therapy has been previously studied. For example, BubR1 downregulation has been related to PTX sensitivity in esophageal squamous cell carcinoma,[42] but BubR1 inhibition promotes resistance to microtubule inhibitors in colorectal cancer (CRC).[43] Mad2 and BubR1 suppression in PTX-treated ovarian and breast cancer cells results in PTX resistance.[40] Our interpretation is that senescence in GC could act as a tumor suppressor, although in vivo studies are needed in order to confirm the contribution to cell death. Cellular senescence can be induced by oncogenes (oncogene-induced senescence [OIS]) and is a crucial anticancer mechanism that prevents the growth of cells that are at risk of neoplastic transformation. Signaling pathways known to regulate OIS include the p16/RB and p19/p53/p21 pathways. Our results show that Mad2 depletion increases activation of the p53 pathway; however, p53 activation does not result in induction of p21 expression. These results do not agree with those from studies showing that Mad2 partial depletion in IMR90 primary human fibroblasts induces the p53-p21 pathway. However, other cells (such as MCF10 A) show low activation of this pathway when Mad2 is downregulated. Another possibility is that the p53 activation and stability is a reflection of DNA damage in cells, and senescence is associated with the mTORC1 route, through a senescence-associated role for 4E-BP1 in crosstalk with the transcription factor p53.[44] Further studies are warranted to explore

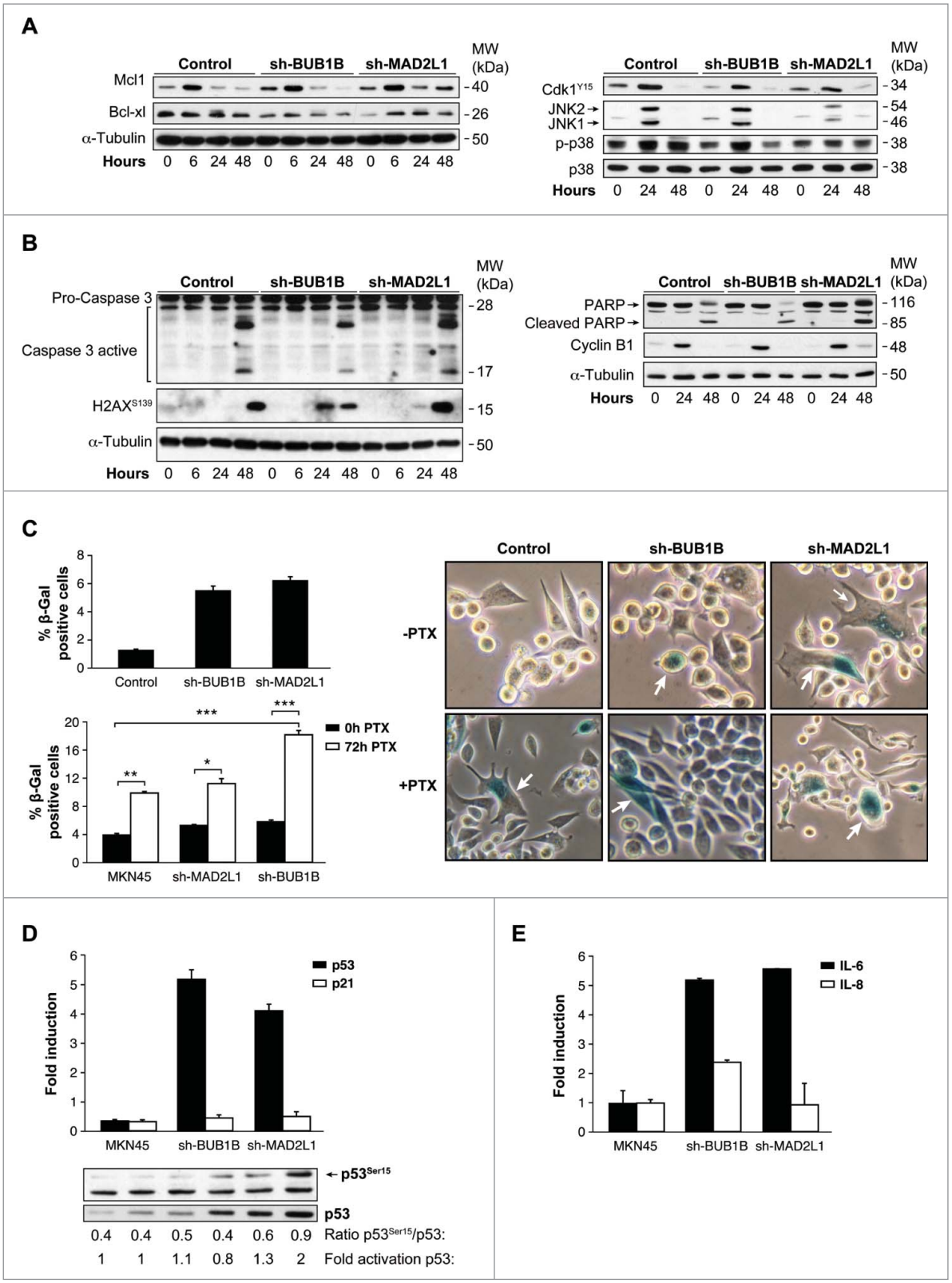

Figure 5. For figure legend, see page 3598.

this possibility. Recent studies have demonstrated that normal human diploid fibroblasts (HDFs) exposed to various senescence-inducing stimuli undergo a mitosis skip before entry into permanent cell cycle arrest. This mitosis skip is mediated by both, p53 and pRb family protein-dependent transcriptional suppression of mitotic regulators,[45] which could be the case in our cells. On the other hand, we can argue that in the absence of Mad2 or BubR1, the PTX treatment leads to a prolonged arrest, probably increasing free radicals, which are crucial for SASP regulation.[46] The secretome of senescent cells is complex, consisting of a range of cytokines, chemokines and proteases, among other substances, and is associated with inflammation, proliferation and modulation of the extracellular matrix (ECM).[47] Our results show that senescent cells with Mad2 or BubR1 depletion undergo IL-6 and IL-8 expression induction. This led us to consider that an increase in IL-6 and IL-8 levels could favor paracrine signaling and increase senescence and ultimately cell death or, by contrast, that SASP contributes to cell transformation, which could ultimately be an advantage for tumor growth.[28] Further studies are needed to clarify the clinical outcome of patients in relation to Mad2 or BubR1 levels and PTX response. On the other hand, a small population of cells could instead become aneuploid, which could ultimately be an advantage for tumor growth.[28] In addition, we should consider studying the relationship between the recently described protein LZTS1 (leucine zipper putative tumor suppressor 1), which plays a critical role in resistance to paclitaxel, by controlling Cdk1 activity, in breast cancer.[48] Therefore, understanding exactly how common environmental and cellular stresses affect mitosis is critical to understanding how and why some cancer cells are sensitive and others are resistant to this important class of chemotherapy. The positive news is that sensitivity to cisplatin or BMC appears to be unaffected in the absence of these proteins, which opens the possibility of using them in combination with new drugs that target Mad2 or BubR1.

In conclusion, we have demonstrated that reduced Mad2 and BubR1 protein levels appear to contribute to cellular senescence induction, a mechanism that could prevent tumourigenesis. This is an exciting result because it opens a new line of research, aimed at designing new drugs that can target these proteins.

Material and Methods

Cell culture and drugs

The MKN45 (poorly differentiated adenocarcinoma; DSMZ: Deutsche Sammlung von Mikroorganismen und Zellkulturen GmbH) cell line was maintained in RPMI 1640, supplemented with 20% FBS and 2-mM L-Glutamine. The ST2957 (lymph node metastases) and HEK293 cells were maintained in high glucose Dulbecco's modified Eagle Medium (DMEM; Gibco), supplemented with 2-mM L-Glutamine, 1-mM sodium pyruvate, 10% foetal bovine serum. All cell lines were grown at 37°C in a humid atmosphere containing 5% CO_2.

Chemicals and antibodies

Antibodies against H2AX phosphorylated at Ser 139, p38, phosphorylated p38, caspase 3, cdk1 Y15, p53 and $p53^{Ser15}$ were purchased from Cell Signaling Technologies (http://www.cellsignal.com). Antibodies against PARP, Cyclin B, Mcl-1 and Bcl-xl were purchased from Santa Cruz Technology (http://www.scbt.com). Antibody Anti-ACTIVE® JNK pAb, Rabbit, (pTPpY) was acquired from Promega Corporation-Spain (http://www.promega.es/). Paclitaxel and puromycin were acquired from Sigma-Aldrich (http://www.sigmaaldrich.com/sigma-aldrich/home.html). BMC was acquired from Calbiochem (http://www.merckmillipore.com/spain/life-science-research), and CDDP was donated from Ferrer FARMA.

Western blotting

Protein extracts (20 μg) were resolved on 4%– 20%– SDS-PAGE (BioRad) and transferred to nitrocellulose membranes. Western immunoblot analysis was performed as described previously.[29]

Viral transduction of cells

Viral particles were generated according to the manufacturer's instructions using GIPZ Lentiviral shRNA for Mad2 or BubR1 (Thermo Scientific Open Biosystems). Briefly, 4.5×10^6 HEK 293 cells/plate in DMEM medium were transfected using lipofectamine 2000 (Invitrogen) with 15 μg of shMad2, 7 μg of envelope plasmid (VSV-G) and 7 μg of Helper plasmid (pCD/NL-BH). The supernatants were recovered 48 h and 72 h after transfection and frozen in small aliquots at -80°C until use.

Figure 5 (See previous page). Interference of Mad2 o BubR1 expression induces senescence phenotype in MKN45. (**A and B**) Western blotting analysis of MKN45, sh-MAD2L1 and sh-BUB1B cultures treated with 0.1 μM PTX during several time intervals. Twenty micrograms (20 μg) of WCE protein were resolved in 15% or 8% SDS-PAGE. Expression/activation of Bcl-xl and Mcl-1 proteins (A-left panel), $Cdk1^{Y15}$, JNK1/2, phosphorylated P38 and total P38 (**A**, right panel), Caspase-3 proteolysis, H2AX (b-left panel), PARP, cleaved-PARP, cyclin-B1 (**B**, right panel) were detected by using specific antibodies against each one. α-tubulin was used as a loading control. (**C**) Left upper panel: β-Galactosidase activity in MKN45 control and cells with Mad2 and BubR1 knockdown in 3-day cultures. Down panel: PTX effect in senescence phenotype was studied measuring β-Galactosidase activity in MKN45 control and interfered cell lines. Cells were treated with PTX (0.1 μM) for 3 d. Bars represent average of 3 independent experiments. (* $P < 0.05$,** $P < 0.005$, *** $P < 0.001$. Representative images of β-Galactosidase stained cell culture with and without PTX in 3 d. Arrows point to senescent cells. (**D**) Q-PCR analysis was performed using Taqman to measure p53 and p21 mRNAs levels in shBUB1B and sh-MAD2L1 knockdown cells referring to MKN45 cells. β-actin was used as endogenous gene control. Western blotting analysis of p53 expression in cells treated with 0.1 μM of PTX for 72 h, using a specific antibody against phosphorylated Ser15 and an antibody against the native protein. α-tubulin was used as a loading control. (**E**) IL-6 e IL-8 expression levels were analyzed by Q-PCR using Taqman in all cell lines in the 3-day culture. β- actin was employed as an endogenous gene control and the graph shows the fold induction referred to the MKN45 control cell line.

Transduction was conducted using 5×10^5 cells per well in a 6-well plate. The cells were examined microscopically 48 hours post-transduction for the presence of GFP reporter expression as an indicator of transduction efficiency. Cells were assayed 72 h later for reductions in gene expression by quantitative/real-time PCR (qRT-PCR) and compared with nonsilencing shRNA.

RT-PCR

Total cellular RNA was extracted using Tri-Reagent, as previously described. One microgram was primed with poly-T and cDNA synthesized with M-MLV reverse transcriptase following the manufacturers' instructions (Promega). The quantitative expression of each gene was measured by SYBR Green polymerase chain reaction assay, using the following specific primer sets: 5′- TCGTGGCAATACAGCTTCAC-3′ and 5′- GGTCAATAGCTCGGCTTCC-3′ for BUB1B; 5′- GCTTGTAACTACTGATCTTG-3′ and 5′- GCAGATCAAATGAACAAGAA-3′ for Mad2L1; 5′-GCTCAGCAACAAACCATGG-3′ and 5′-GGAATATTCAACATAACATG-3′ for BUB; 5′- GGAGCTGGAGAACGAGAG -3′ and 5′- ACTGTGGTCCCGACTCTT -3′ for MAD1L1;5′ GTTGATCTTGCAGGCAGTGA -3′ and 5′- TGAAACCACCAACTTGTCCA -3′ for CENP-E; 5′ GGTGGTTCTGATGGCTTTGT -3′ and 5′- GCAAGCGTAGTCCCATCATT -3′ for BUB3; 5′ GGGAGAGCTGAAGATTGCTG -3′ and 5′- GCACCACAGATCCACCTTCT -3′ for AURK-B 5′-GAG; AGA CCC TCA CTG CTG-3′ and 5′-GAT GGT ACA TGA CAA GGT GC-3′ for GAPDH. Relative quantification (RQ) was performed using the delta-Ct method, where each 1-Ct difference equals a 2 fold change in transcript abundance. qRT-PCR analysis was employed to quantify the expression levels of IL-6, IL-8 and p21 by using Taq-man probes (Life technologies, https://www.lifetechnologies.com).

Cell viability, proliferation, clonogenic assay and PDLs

Viability and growth rate were determined using a crystal violet based staining method, as previously described.[29] Survival was measured using an MTS assay (Promega). For the clonogenic assay, cells were cultured in a 6-well plate at a very low concentration (2000 cells per well). After 14 days, the cells were fixed with 1% glutaraldehyde and stained with crystal violet. The number of colonies was quantified directly using the 10× objective in 3 different areas per well. To measure the population doubling level (PDL), 300,000 cells were plated in p60, and the number of cells was quantified every 4 days. The calculation of the PDL was performed using the following formula: PDL = 3/ln(final no. of cells /300000)+1).

Cell migration and invasion assays

For the wound-healing assay, a confluent monolayer of MKN45 cells and ST2957 controls and knockdown for Mad2L1 or BUB1B cells was scratched into a 24-well plate with a sterile tip. The cell migration's ability to fill the wound was studied up to 50 h. The relative distance traveled by the leading cell edge was assessed by time-lapse microscopy using the Cell Observer Z1 (Zeiss) at 37°C and 5% CO_2/95% air, using the imaging software Axiovision 4.8 and the Cascade 1 k camera. Images were taken every 2 h and further processed using the Digital Image Processing Software AXIOVISION (Zeiss). The wound closure was quantified by measuring the remaining unmigrated area using ImageJ. Migration and invasion assays were performed in modified Boyden chambers with polycarbonate filters (6.5 mm diameter, 8.0 μm pore size) (transwell migration and invasion assays) (Corning Inc., Corning, NY, USA) coated with 0.5% gelatin (migration assay) or 6 μg growth factor reduced Matrigel (BD Biosciences, Bedford, MA, USA) (invasion assay). Prior to the migration and invasion assays, cells were maintained for 16 h in serum-free medium and 1.5×10^6 cells resuspended in serum-free medium were seeded in the upper chamber. Serum-free conditioned medium from NIH3T3 cells at 30 ng/ml was used as chemoattractant and placed in the bottom chamber. Cells were allowed to migrate or invade for 24 h at 37°C with 5% CO_2. Non-migrated and non-invaded cells were removed using a cotton swab, and the filters were stained with Diff Quik (Dade Behring, Newark, DE, USA). Migrated or invaded cells were counted in 10 fields of maximum migration or invasion under a light microscope at 40× magnification.

Senescence Analysis

A total of 150×10^3 cells were seeded on 6 MW plates, and the β-galactosidase (SA-β-Gal) activity was quantify using the Senescence detection kit (Biovision, http://www.biovision.com/)

Oncomine analysis

We searched the public cancer microarray database, Oncomine, to identify studies with MAD1L1, MAD2L1,BUB3 and BUB1B gene expression datasets and compared expression of gastric intestinal type adenocarcinoma vs. normal gastric tissue. In order to be included in our study, a data set was required to have significant gene expression with a P-value < 0.001.

Statistical Analysis

All results were expressed as means ± SD of 3 independent experiments. Statistical analyses were performed using Graph path prims 5.0 ANOVA or Student's 2-tailed t-test. Values of $^*P < 0.05$ were considered significant.

Disclosure of Potential Conflicts of Interest

No potential conflicts of interest were disclosed.

Acknowledgments

We would like to thank Javier Perez (photography facility), Diego Navarro and Lucia Sanchez (IIBM microscopy facility) for their technical assistance. Beatriz Morte for qPCR analysis.

Funding

This work was supported by the following grants: PS09/1988, 595, PI11 -00949 supported by FEDER funds and UAM-Santander CEAL-AL/2013-29. JBI is a fellow of the Programa de Doctorado Doble en Ciencias Biomédicas UNAM, Mexico

City, Mexico/Biociencias Moleculares UAM, Madrid, Spain. JBI was supported by a fellowship from Cátedra Isaac Costero, funded by Banco Santander.

Supplemental Material

Supplemental data for this article can be found on the publisher's website.

References

1. Siegel R, Naishadham D, Jemal A. Cancer statistics, 2013. CA Cancer J Clin 2013; 63:11-30; PMID:23335087
2. Garrido M, Fonseca PJ, Vieitez JM, Frunza M, Lacave AJ. Challenges in first line chemotherapy and targeted therapy in advanced gastric cancer. Expert Rev Anticancer Ther 2014: 14:887-900.
3. Sakamoto J, Matsui T, Kodera Y. Paclitaxel chemotherapy for the treatment of gastric cancer. Gastric Cancern 2009; 12:69-78; PMID:19562460; http://dx.doi.org/10.1007/s10120-009-0505-z
4. Goncalves A, Braguer D, Kamath K, Martello L, Briand C, Horwitz S, Wilson L, Jordan MA. Resistance to Taxol in lung cancer cells associated with increased microtubule dynamics. Proc Natl Acad Sci U S A 2001; 98:11737-42; PMID:11562465; http://dx.doi.org/10.1073/pnas.191388598
5. Nitta M, Kobayashi O, Honda S, Hirota T, Kuninaka S, Marumoto T, Ushio Y, Saya H. Spindle checkpoint function is required for mitotic catastrophe induced by DNA-damaging agents. Oncogene 2004; 23:6548-58; PMID:15221012; http://dx.doi.org/10.1038/sj.onc.1207873
6. Vakifahmetoglu H, Olsson M, Zhivotovsky B. Death through a tragedy: mitotic catastrophe. Cell Death Differ 2008; 15:1153-62; PMID:18404154; http://dx.doi.org/10.1038/cdd.2008.47
7. Kops GJ, Weaver BA, Cleveland DW. On the road to cancer: aneuploidy and the mitotic checkpoint. Nat Rev Cancer 2005; 5:773-85; PMID:16195750; http://dx.doi.org/10.1038/nrc1714
8. Fu Y, Ye D, Chen H, Lu W, Ye F, Xie X. Weakened spindle checkpoint with reduced BubR1 expression in paclitaxel-resistant ovarian carcinoma cell line SKOV3-TR30. Gynecol Oncol 2007; 105:66-73; PMID:17234259; http://dx.doi.org/10.1016/j.ygyno.2006.10.061
9. Hao X, Zhou Z, Ye S, Zhou T, Lu Y, Ma D, Wang S. Effect of Mad2 on paclitaxel-induced cell death in ovarian cancer cells. J Huazhong Univ Sci Technolog Med Sci 2010; 30:620-5; PMID:21063845; http://dx.doi.org/10.1007/s11596-010-0553-y
10. Hanahan D, Weinberg RA. The hallmarks of cancer. Cell 2000; 100:57-70; PMID:10647931; http://dx.doi.org/10.1016/S0092-8674(00)81683-9
11. Hanahan D, Weinberg RA. Hallmarks of cancer: the next generation. Cell 2011; 144:646-4; PMID:21376230; http://dx.doi.org/10.1016/j.cell.2011.02.013
12. Fang X, Zhang P. Aneuploidy and tumorigenesis. Semin Cell Dev Biol 2011; 22:595-601; PMID:21392584; http://dx.doi.org/10.1016/j.semcdb.2011.03.002
13. Lara-Gonzalez P, Westhorpe FG, Taylor SS. The spindle assembly checkpoint. Curr Biol 2012; 22:R966-80; PMID:23174302; http://dx.doi.org/10.1016/j.cub.2012.10.006
14. Cahill DP, Lengauer C, Yu J, Riggins GJ, Willson JK, Markowitz SD, Kinzler KW, Vogelstein B. Mutations of mitotic checkpoint genes in human cancers. Nature 1998; 392:300-3; PMID:9521327; http://dx.doi.org/10.1038/32688
15. Hanks S, Coleman K, Reid S, Plaja A, Firth H, Fitzpatrick D, Kidd A, Mehes K, Nash R, Robin N, et al. Constitutional aneuploidy and cancer predisposition caused by biallelic mutations in BUB1B. Nat Genet 2004; 36:1159-61; PMID:15475955; http://dx.doi.org/10.1038/ng1449
16. Li M, Fang X, Wei Z, York JP, Zhang P. Loss of spindle assembly checkpoint-mediated inhibition of Cdc20 promotes tumorigenesis in mice. J Cell Biol 2009; 185:983-94; PMID:19528295; http://dx.doi.org/10.1083/jcb.200904020
17. Babu JR, Jeganathan KB, Baker DJ, Wu X, Kang-Decker N, van Deursen JM. Rae1 is an essential mitotic checkpoint regulator that cooperates with Bub3 to prevent chromosome missegregation. J Cell Biol 2003; 160:341-53; PMID:12551952; http://dx.doi.org/10.1083/jcb.200211048
18. Baker DJ, Jeganathan KB, Cameron JD, Thompson M, Juneja S, Kopecka A, Kumar R, Jenkins RB, de Groen PC, Roche P, et al. BubR1 insufficiency causes early onset of aging-associated phenotypes and infertility in mice. Nat Genet 2004; 36:744-9; PMID:15208629; http://dx.doi.org/10.1038/ng1382
19. Michel LS, Liberal V, Chatterjee A, Kirchwegger R, Pasche B, Gerald W, Dobles M, Sorger PK, Murty VV, Benezra R. MAD2 haplo-insufficiency causes premature anaphase and chromosome instability in mammalian cells. Nature 2001; 409:355-9; PMID:11201745; http://dx.doi.org/10.1038/35053094
20. Sotillo R, Hernando E, Diaz-Rodriguez E, Teruya-Feldstein J, Cordon-Cardo C, Lowe SW, Benezra R. Mad2 overexpression promotes aneuploidy and tumorigenesis in mice. Cancer Cell 2007; 11:9-23; PMID:17189715; http://dx.doi.org/10.1016/j.ccr.2006.10.019
21. Iwanaga Y, Chi YH, Miyazato A, Sheleg S, Haller K, Peloponese JM Jr, Li Y, Ward JM, Benezra R, Jeang KT. Heterozygous deletion of mitotic arrest-deficient protein 1 (MAD1) increases the incidence of tumors in mice. Cancer Res 2007; 67:160-6; PMID:17210695; http://dx.doi.org/10.1158/0008-5472.CAN-06-3326
22. Dai W, Wang Q, Liu T, Swamy M, Fang Y, Xie S, Mahmood R, Yang YM, Xu M, Rao CV. Slippage of mitotic arrest and enhanced tumor development in mice with BubR1 haploinsufficiency. Cancer Res 2004; 64:440-5; PMID:14744753; http://dx.doi.org/10.1158/0008-5472.CAN-03-3119
23. Baker DJ, Jeganathan KB, Malureanu L, Perez-Terzic C, Terzic A, van Deursen JM. Early aging-associated phenotypes in Bub3/Rae1 haploinsufficient mice. J Cell Biol 2006; 172:529-40; PMID:16476774; http://dx.doi.org/10.1083/jcb.200507081
24. Jeganathan K, Malureanu L, Baker DJ, Abraham SC, van Deursen JM. Bub1 mediates cell death in response to chromosome missegregation and acts to suppress spontaneous tumorigenesis. J Cell Biol 2007; 179:255-67; PMID:17938250; http://dx.doi.org/10.1083/jcb.200706015
25. Courtois-Cox S, Jones SL, Cichowski K. Many roads lead to oncogene-induced senescence. Oncogene 2008; 27:2801-9; PMID:18193093; http://dx.doi.org/10.1038/sj.onc.1210950
26. Collado M, Serrano M. The senescent side of tumor suppression. Cell Cycle 2005; 4:1722-4; PMID:16294043; http://dx.doi.org/10.4161/cc.4.12.2260
27. Young AR, Narita M. SASP reflects senescence. EMBO Rep 2009; 10:228-30; PMID:19218920; http://dx.doi.org/10.1038/embor.2009.22
28. Munoz-Espin D, Serrano M. Cellular senescence: from physiology to pathology. Nat Rev Mol Cell Biol 2014; 15:482-96; PMID:24954210; http://dx.doi.org/10.1038/nrm3823
29. Gutierrez-Gonzalez A, Belda-Iniesta C, Bargiela-Iparraguirre J, Dominguez G, Garcia Alfonso P, Perona R, Sanchez-Perez I. Targeting Chk2 improves gastric cancer chemotherapy by impairing DNA damage repair. Apoptosis 2013; 18:347-60; PMID:23271172; http://dx.doi.org/10.1007/s10495-012-0794-2
30. Sanchez-Perez I, Garcia Alonso P, Belda Iniesta C. Clinical impact of aneuploidy on gastric cancer patients. Clin Transl Oncol 2009; 11:493-8; PMID:19661021; http://dx.doi.org/10.1007/s12094-009-0393-z
31. Cho JY, Lim JY, Cheong JH, Park YY, Yoon SL, Kim SM, Kim SB, Kim H, Hong SW, Park YN, et al. Gene expression signature-based prognostic risk score in gastric cancer. Clin Cancer Res 2011; 17:1850-7; PMID:21447720; http://dx.doi.org/10.1158/1078-0432.CCR-10-2180
32. D'Errico M, de Rinaldis E, Blasi MF, Viti V, Falchetti M, Calcagnile A, Sera F, Saieva C, Ottini L, Palli D, et al. Genome-wide expression profile of sporadic gastric cancers with microsatellite instability. Eur J Cancer 2009; 45:461-9; PMID:19081245; http://dx.doi.org/10.1016/j.ejca.2008.10.032
33. Wang Q, Wen YG, Li DP, Xia J, Zhou CZ, Yan DW, Tang HM, Peng ZH. Upregulated INHBA expression is associated with poor survival in gastric cancer. Med Oncol 2012; 29:77-83; PMID:21132402; http://dx.doi.org/10.1007/s12032-010-9766-y
34. Wu WK, Cho CH, Lee CW, Fan D, Wu K, Yu J, Sung JJ. Dysregulation of cellular signaling in gastric cancer. Cancer Lett 2010; 295:144-53; PMID:20488613; http://dx.doi.org/10.1016/j.canlet.2010.04.025
35. Bharadwaj R, Yu H. The spindle checkpoint, aneuploidy, and cancer. Oncogene 2004; 23:2016-27; PMID:15021889; http://dx.doi.org/10.1038/sj.onc.1207374
36. Yamamoto Y, Matsuyama H, Chochi Y, Okuda M, Kawauchi S, Inoue R, Furuya T, Oga A, Naito K, Sasaki K. Overexpression of BUBR1 is associated with chromosomal instability in bladder cancer. Cancer Genet Cytogenet 2007; 174:42-7; PMID:17350465; http://dx.doi.org/10.1016/j.cancergencyto.2006.11.012
37. Burum-Auensen E, Deangelis PM, Schjolberg AR, Roislien J, Andersen SN, Clausen OP. Spindle proteins Aurora A and BUB1B, but not Mad2, are aberrantly expressed in dysplastic mucosa of patients with long-standing ulcerative colitis. J Clin Pathol 2007; 60:1403-8; PMID:17322345; http://dx.doi.org/10.1136/jcp.2006.044305
38. McGrogan B, Phelan S, Fitzpatrick P, Maguire A, Prencipe M, Brennan D, Doyle E, O'Grady A, Kay E, Furlong F, et al. Spindle assembly checkpoint protein expression correlates with cellular proliferation and shorter time to recurrence in ovarian cancer. Hum Pathol 2014; 45:1509-19; PMID:24792619; http://dx.doi.org/10.1016/j.humpath.2014.03.004
39. Lee YK, Choi E, Kim MA, Park PG, Park NH, Lee H. BubR1 as a prognostic marker for recurrence-free survival rates in epithelial ovarian cancers. Br J Cancer 2009; 101:504-10; PMID:19603021; http://dx.doi.org/10.1038/sj.bjc.6605161
40. Sudo T, Nitta M, Saya H, Ueno NT. Dependence of paclitaxel sensitivity on a functional spindle assembly checkpoint. Cancer Res 2004; 64:2502-8; PMID:15059905; http://dx.doi.org/10.1158/0008-5472.CAN-03-2013
41. Du Y, Yin F, Liu C, Hu S, Wang J, Xie H, Hong L, Fan D. Depression of MAD2 inhibits apoptosis of gastric cancer cells by upregulating Bcl-2 and interfering mitochondrion pathway. Biochem Biophys Res Commun 2006; 345:1092-8
42. Hu M, Liu Q, Song P, Zhan X, Luo M, Liu C, Yang D, Cai Y, Zhang F, Jiang F, et al. Abnormal expression of the mitotic checkpoint protein BubR1 contributes to the anti-microtubule drug resistance of esophageal squamous cell carcinoma cells. Oncol Rep 2013; 29:185-92; PMID:23128493
43. Swanton C, Tomlinson I, Downward J. Chromosomal instability, colorectal cancer and taxane resistance. Cell Cycle 2006; 5:818-23; PMID:16628000; http://dx.doi.org/10.4161/cc.5.8.2682
44. Chao SK, Horwitz SB, McDaid HM. Insights into 4E-BP1 and p53 mediated regulation of accelerated cell senescence. Oncotarget 2011; 2:89-98; PMID:21399233

45. Johmura Y, Shimada M, Misaki T, Naiki-Ito A, Miyoshi H, Motoyama N, Ohtani N, Hara E, Nakamura M, Morita A, et al. Necessary and Sufficient Role for a Mitosis Skip in Senescence Induction. Mol Cell 2014; PMID:24910096
46. Coppe JP, Patil CK, Rodier F, Sun Y, Munoz DP, Goldstein J, Nelson PS, Desprez PY, Campisi J. Senescence-associated secretory phenotypes reveal cell-nonautonomous functions of oncogenic RAS and the p53 tumor suppressor. PLoS Biol 2008; 6:2853-68; PMID:19053174; http://dx.doi.org/10.1371/journal.pbio.0060301
47. Salama R, Sadaie M, Hoare M, Narita M. Cellular senescence and its effector programs. Genes Dev 2014; 28:99-114; PMID:24449267; http://dx.doi.org/10.1101/gad.235184.113
48. Lovat F, Ishii H, Schiappacassi M, Fassan M, Barbareschi M, Galligioni E, Gasparini P, Baldassarre G, Croce CM, Vecchione A. LZTS1 downregulation confers paclitaxel resistance and is associated with worse prognosis in breast cancer. Oncotarget 2014; 5:970-7; PMID:24448468

MATERIAL SUPLEMENTARIO: Mad2 and BubR1 modulates tumourigenesis and Paclitaxel response in MKN45 gastric cancer cells

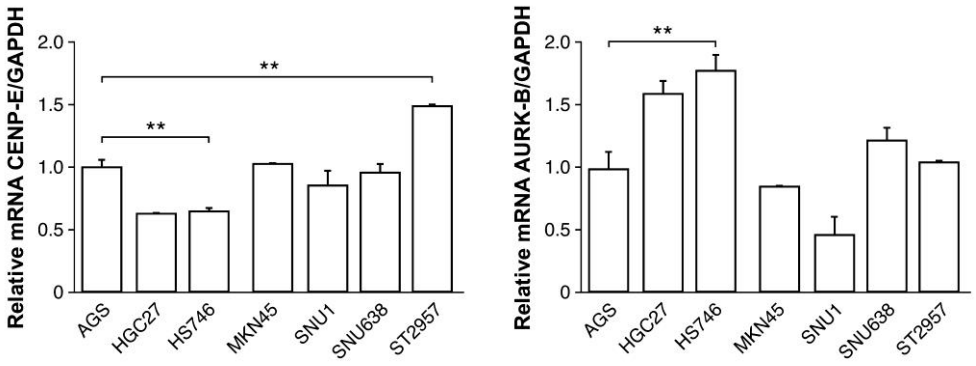

Supplementary figure 1:

Real time PCR (q-PCR) was performed to measure relative levels of CENP-E and AURK-B mRNAs in 7 GC cell lines, each gene normalized with GAPDH. Data are shown as relative to AGS cell line, and statistical significance evaluated by ANOVA ** $p<0.05$ y *** $p<0.005$

A

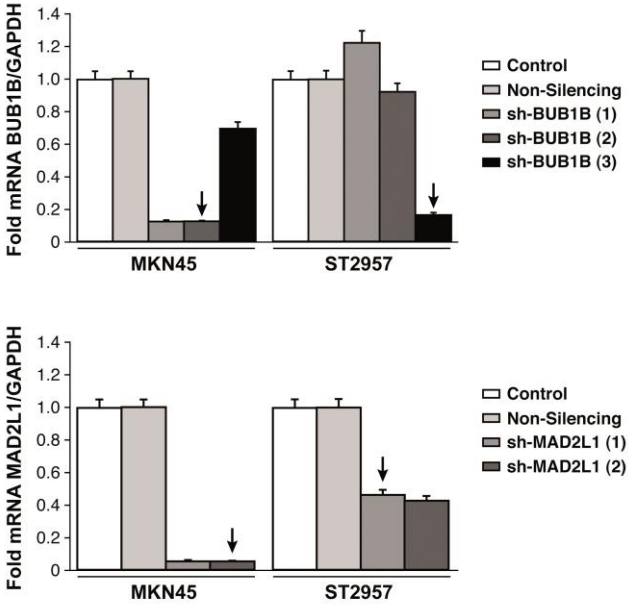

B

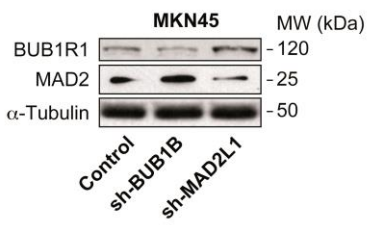

Supplementary figure 2: **A**) Selection of cell lines. ST2957 and MKN45 cell lines were transduced with lentivirus expressing different shRNAs of MAD2L1 or BUB1B (listed form 1 to 3 in BUB1B, 1 and 2 in MAD2L1). Transduced cells were selected by using Puromycin (3µg/ml). Stable cells were analyzed by Q-PCR for MAD2L1 and BUB1B mRNA quantization. The graph represents the average of three different experiments. **B**) Verification by western blotting a decrease of BUBR1 and MAD2 proteins in transduced cell lines comparing to not transduced MKN45 control cells, using specific antibodies against MAD2 and BUBR1. α-tubulin used as loading control

A

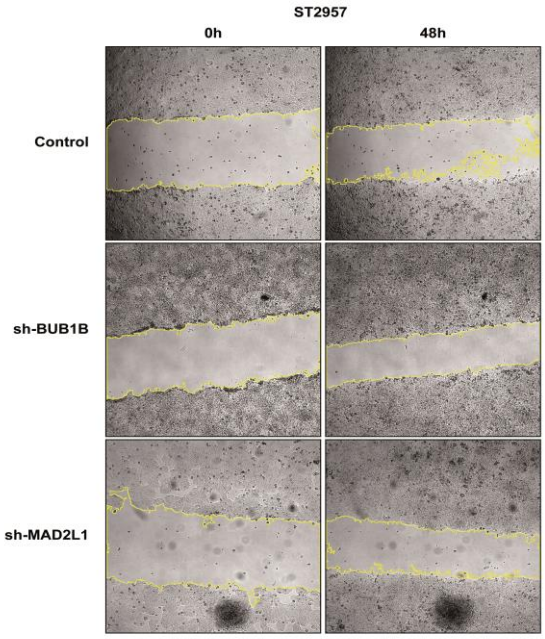

B

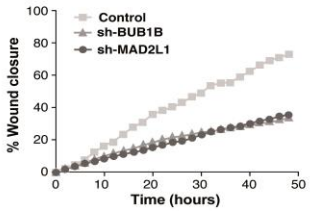

.

Supplementary figure 3: **Donwregulation of MAD2 and BUB1B reduces migration in ST2957**. **A**) Representative images of the first (0h) and last picture (48h) of ST2957 cell line compering control cells and transduced cells, taken during wound healing experiment. Images were taken at 10X magnification, every 2 h for 48 h. Yellow line represents the wound border. **B**) The wound closure was quantified every 2h post-wound by measuring the remaining unmigrated area using ImageJ.

RESUMEN

CHK1 expression in Gastric Cancer is modulated by p53 and RB1/E2F1: implications in chemo/radiotherapy response

Bargiela-Iparraguirre J, Prado-Marchal L, Fernandez-Fuente M, Gutierrez-González A, Moreno-Rubio J, Muñoz-Fernandez M, Sereno M, Sanchez-Prieto R, Perona R, Sanchez-Perez I.

Sci Rep. 2016 Feb 12;6:21519. doi: 10.1038/srep21519. PMID: 26867682

La radiación ionizante (IR) provoca rupturas de doble hebra del DNA y se utiliza como terapia adyuvante en el protocolo clínico del tratamiento del cáncer gástrico. A pesar de sus limitaciones presenta una mejora en el pronóstico de los pacientes con adenocarcinomas gástricos localizados aunque un elevado porcentaje de pacientes presentan resistencia al tratamiento y recurren.

La proteína CHK1 es clave en la vía de señalización intracelular de respuesta al daño en el DNA y se ha demostrado su implicación en la resistencia a varios agentes genotóxicos, por lo que en este trabajo evaluamos la función de la proteína CHK1 en la respuesta a IR en cáncer gástrico. Observamos que la línea celular de adenocarcinoma MKN45 con niveles altos de CHK1 es más resistente a irradiación en comparación con la línea celular AGS, la cual presenta niveles normales de CHK1. Hemos demostrado que inhibiendo la actividad de CHK1 con el compuesto UCN-01 o disminuyendo los niveles de proteína mediante shRNAs se logra sensibilizar a las células tumorales gástricas al tratamiento con irradiación. Además el análisis de los niveles de proteína CHK1 mediante inmunohistoquímica en una pequeña serie de pacientes seleccionados de acuerdo a los criterios de tumor localizado y tratados con IR, indica peor pronóstico (menor tiempo libre de progresión) en aquellos pacientes con altos niveles nucleares de CHK1. Analizamos si la expresión diferencial de CHK1 entre las líneas celulares se debe a diferencias en la activación transcripcional. Nuestros resultados sugieren que la expresión del gen *CHEK1* está regulada por el eje RB/E2F y p53 a nivel transcripcional, sin que existan diferencias entre las líneas que justifiquen las diferencias de expresión. Sin embargo, nuestros resultados sugieren que los niveles elevados de CHK1 se deben a una estabilización del RNA mensajero, sugiriendo que existen modificaciones postranscripcionales implicadas en el proceso. Realizamos un análisis *in silico* para identificar posibles miRNAs implicados en el proceso. Identificamos el miRNA-195 y el miRNA-503, cuya expresión correlaciona de forma inversa con los niveles de CHK1 en las líneas celulares. Estos resultados sugieren que los niveles de expresión de CHK1 podrían utilizarse como criterio de respuesta a irradiación en pacientes de cáncer gástrico. A su vez, sugerimos que los miRNAs 195 y 503 podrían ser buenos candidatos para ser evaluados como biomarcadores de respuesta a esta misma terapia.

Participación en el trabajo: Realizar los experimentos y análisis de resultados.

SCIENTIFIC REPORTS

OPEN

CHK1 expression in Gastric Cancer is modulated by p53 and RB1/E2F1: implications in chemo/radiotherapy response

Received: 08 September 2015
Accepted: 26 January 2016
Published: 12 February 2016

J. Bargiela-Iparraguirre[1,*], L. Prado-Marchal[1,*], M. Fernandez-Fuente[2], A. Gutierrez-González[1], J. Moreno-Rubio[3,4], M. Muñoz-Fernandez[5], M. Sereno[3], R. Sanchez-Prieto[6,7], R. Perona[1,8,9] & I. Sanchez-Perez[1,7,8,9]

Radiation has a limited but relevant role in the adjuvant therapy of gastric cancer (GC) patients. Since Chk1 plays a critical function in cellular response to genotoxic agents, we aimed to analyze the role of Chk1 in GC as a biomarker for radiotherapy resistance. We analyzed Chk1 expression in AGS and MKN45 human GC cell lines by RT-QPCR and WB and in a small cohort of human patient's samples. We demonstrated that Chk1 overexpression specifically increases resistance to radiation in GC cells. Accordingly, abrogation of Chk1 activity with UCN-01 and its expression with shChk1 increased sensitivity to bleomycin and radiation. Furthermore, when we assessed Chk1 expression in human samples, we found a correlation between nuclear Chk1 accumulation and a decrease in progression free survival. Moreover, using a luciferase assay we found that Chk1's expression is controlled by p53 and RB/E2F1 at the transcriptional level. Additionally, we present preliminary data suggesting a posttranscriptional regulation mechanism, involving miR-195 and miR-503, which are inversely correlated with expression of Chk1 in radioresistant cells. In conclusion, Chk1/microRNA axis is involved in resistance to radiation in GC, and suggests Chk1 as a potential tool for optimal stratification of patients susceptible to receive adjuvant radiotherapy after surgery.

Gastric cancer (GC) is the fourth most common human malignant disease worldwide due to its frequency and high rate of mortality[1,2]. Classical adjuvant treatment in GC is based on MacDonald´s protocol including a combination of 5-Fluoruracil (5-FU) and radiation (IR) in stage IB-IVA patients. This regimen demonstrated an increase of progression free survival (PFS) and overall survival (OS)[3,4]. However, this combination is usually associated with increased, severe toxicity[3]. Thus, identification of those patients more prone to benefit from adjuvant radiation and 5-FU after curative surgery for GC to counteract such toxicity is an unmet need[5,6].

Radiation and chemotherapy routinely used to treat cancer do cause a variety of DNA lesions, which in turn activate DNA damage response (DDR)[7]. Checkpoint Kinase 1 (Chk1), a key effector in DDR, is a multifunctional Ser/Thr kinase protein highly conserved through evolution[8] and represents a crucial component in all cell cycle checkpoints. Chk1 activation must be finely regulated to ensure its adequate activity. The major known to date mechanism controlling Chk1 regulation is the phosphorylation of specific residues Ser^{317} and Ser^{345} (both in the C-terminal domain), which leads to catalytic activation. These reactions are catalyzed by ATR and ATM kinases[7–9]. Deregulation of Chk1 expression has been previously described in cancer, i.e. Chk1 is overexpressed[7,10–12] and has been correlated with radiotherapy resistance in some cancer types such as ovarian

[1]Dpto.Bioquímica. Fac. Medicina. Instituto de Investigaciones Biomédicas Madrid CSIC-UAM; Madrid, Spain. [2]The Royal Veterinary College. University of London; London, UK. [3]Medical Oncology Department, Infanta Sofía University Hospital, San Sebastian de los Reyes, Madrid, 28702; Spain. [4]IMDEA-Food Institute, CEI UAM+CSIC, Madrid, Spain. [5]Pathology Department, Infanta Sofía University Hospital, San Sebastián de los Reyes, 28702, Madrid. [6]Unidad de Medicina Molecular, laboratorio de Oncología, CRIB/FPCYT C-LM. Universidad de Castilla-La Mancha, Av. Almansa 14, 02006, Albacete, Spain. [7]Unidad asociada de Biomedicina UCLM-CSIC, Arturo Duperier 4, Madrid Spain. [8]CIBER for Rare Diseases (CIBERER); Valencia, Spain. [9]Biomarkers and Experimental Therapeutics Group; IdiPAZ; University Hospital La Paz; Madrid, Spain. *These authors contributed equally to this work. Correspondence and requests for materials should be addressed to I.S.-P. (email: misanchez@iib.uam.es or is.perez@uam.es)

cancer[13], nasopharyngeal carcinoma[14] and lung cancer[15]. Accordingly, inhibition of Chk1 increases sensitivity to chemo-radiotherapy in multiple tumor models[16,17]. Given this apparent relationship between Chk1 expression and resistance to certain therapies, some groups have made an effort to evaluate Chk1 as a novel target to improve cancer therapy[18] in patients that have been previously exposed to ionizing agents. Besides the well known mechanisms regulating both activation and expression of Chk1 that have already been described[10,19–23], Chk1 is also regulated at the post-transcriptional level by microRNAs (miRNAs)[24,25] which are key regulators of tumor growth and response to chemotherapy[26–28]. In fact, some studies have already begun to identify miRNAs involved in sensitizing or causing resistance to chemotherapy, thus providing potential new targets and mechanisms as optimized treatment options[29–31].

Previous studies from our laboratory suggested that Chk1 levels could be used as a predictive biomarker of therapeutic response in colon cancer[32]. Furthermore, we demostratred that E1A upregulates Chk1 and this correlates with glioblastoma radiosensitivity[33]. Here, we prove that Chk1 is overexpressed in a disseminated GC cell line, MKN45. We have shown that the inhibition of Chk1 results in increased IR sensitivity. Accordingly, we observed nuclear accumulation of Chk1, which correlates with a lower PFS period, in a cohort of patients treated with IR. The results we present here, suggest that Chk1 protein levels are controlled at the transcriptional level mainly through RB1/E2F1 and our preliminary data suggest that at the posttranscriptional level they are likely regulated by miRNA-195 and -503. We conclude that Chk1 is responsible for radiation resistance in GC, and suggest Chk1 as a potential biomarker for the optimal stratification of patients susceptible to receive adjuvant radiotherapy after surgery.

Results

Increased Chk1 expression correlates with resistance to genotoxic agents in GC cells. We studied the sensitivity of the two most common human gastric adenocarcinoma cell lines (AGS and MKN45) to antitumoral agents: cisplatin (CDDP), 5-FU, the radiomimetic agent Bleomycin (BLM) and IR. Dose response curves using this set of drugs showed that after 48 hours of treatment, MKN45 cells are more resistant than AGS cells to both BLM or IR treatment (Fig. 1A), with this increased resistance more evident after BLM treatment. To corroborate this result we conducted a clonogenic assay, and observed that the percentage of colony formation was higher on MKN45 cells than on AGS after 4 Gy irradiation (i.e: 89,6% vs 48.7% respectively) (Fig. 1B). Similarly, when treated with BLM, AGS cells were unable to form colonies at all (Supplementary Fig. 1A); Furthermore, we also observed morphological changes characteristic of cell death in irradiated AGS cells, which were completely absent in MKN45 cells (Fig. 1B). To support this finding we irradiated cells with 4 and 8 Gy for 24 hours. We observed cleavage of PARP, and also a decrease in the full-length form of this protein in AGS cells in a dose dependent manner. However, in MKN45 we only observed basal levels of PARP with no change in proteolysis. Furthermore, the universal marker of apoptosis, activation of Caspase 3, is also observed in the AGS cell line, with particularly strong activity after 8Gy treatment (Fig. 1B).

Given that Chk1 is one of the main effector proteins on the response to IR exposure, we examined the expression levels of Chk1 in MKN45 and AGS cells by RT-QPCR and western blot (WB). Our results showed an increase on Chk1 mRNA and protein levels in both MKN45 and AGS cells when compared to normal tissue. Two different isoforms of Chk1 have been described[34] and our WB analysis indicated that the more abundantly expressed isoform in MKN45 is the classic Chk1 with higher molecular weight (Fig. 1C). We confirmed this result by analyzing the expression of this gene, using public data available on Oncomine database (http//:oncomine.org) (Supplementary Fig. 1B). Our semi-quantitative PCR analysis confirmed the expression of both full-length and short forms of Chk1 in these two cell lines (Supplementary Fig. 1C). Altogether, these results suggest that elevated levels of Chk1 in GC cells correlate with a lack of apoptotic response to IR or BLM treatment.

Chk1 inhibition reduces radioresistance in GC cell lines. To confirm the effect of Chk1 on survival to double strand breaks (DBS) induced by BLM or IR treatment in GC cells, we inhibited Chk1 activity by using the chemical inhibitor UCN-01 prior to treatment. Inhibition of Chk1 with 100 nM UCN-01 (no toxicity observed) increased mortality rate in combination with BLM treatment (0–100 μg/ml). Addition of UNC-01, significantly decreased IC_{50} in both cell lines: from 2.45 to less than 1 μg/ml in AGS and from over 100 to 11 μg/ml in MKN45 cells (Fig. 2A-Left panel). On the other hand, treatment with BLM using 3 μg/ml for AGS cells and 10 μg/ml for MKN45 followed by UCN-01 (0–600 nM) also sensitized both cell lines (Fig. 2A- Right panels); however the dose of UCN-01 required to increase sensitivity to BLM in MKN45 cells was highly toxic (>400 nM). These results suggest a potential synergistic or additive effect upon the combination treatment of BLM with UCN-01. We therefore used the Combination Index (CI) equation method developed by Chou-Talalay[35] using the CalcuSyn program to study combinational synergistic effects. Our studies revealed that in AGS cells both drugs exhibit a synergistic effect ($CI < 1$) at all the UCN-01 doses tested in combination with BLM. By contrast, when using MKN45 cells we only observed that synergistic effect ($CI < 1$) at very high toxic doses of UCN-01. Furthermore, in this cell line our drugs exerted an antagonistic effect ($CI > 1$) at lower doses. To further assess the contribution of Chk1 in the response to therapy, we downregulated Chk1 by pharmacological agents (UCN-01) or silenced it using shRNA lentiviral particles. Next, we analyzed the cell cycle profile after challenge with BLM in cells that had been pre-treated with UCN-01 or after interference on Chk1's expression. We observed a drastic abrogation of the G2/M checkpoint after both treatments, which was even more dramatic when Chk1 is interfered with by our lentivirus (Fig. 2B). Furthermore, we found that the percentage of apoptotic cells was increased in both cell lines after the combination treatment (UCN-01+ IR) (Fig. 2C- Graph). The analysis of the G2/M and S indexes indicated that UCN-01 abolishes the G2/M and Intraphase S checkpoint in GC cells further supporting the contribution of Chk1 to radiation resistance (Fig. 2C- Table). To confirm that UCN-01 inhibits Chk1, we monitored Chk1 autophosphorylation on Ser296 as previously described[36] (Supplementary Fig. 2A). As a control confirming Chk1's silencing we observed that after 72 hours, AGS cells showed almost complete abolishment of Chk1 mRNA

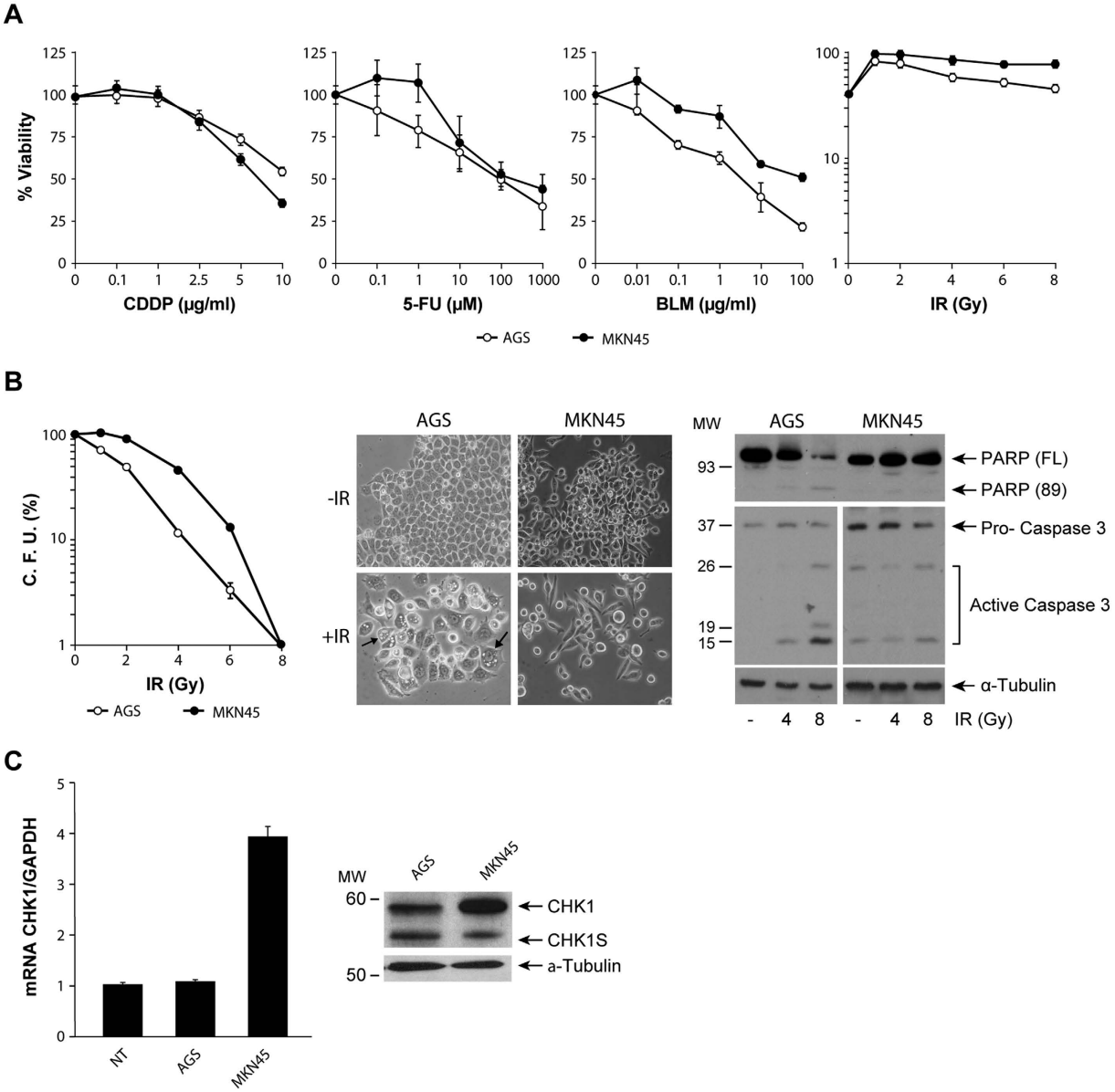

Figure 1. CHK1 mRNA levels are high in GC cells resistant to radiation (IR) and bleomycin (BLM). (**A**) Survival of AGS and MKN45 cells after CDDP, 5-FU, BLM or IR treatment. AGS (○) and MKN45 (●) cells were treated with increasing amounts of CDDP (0–10 μg/ml), 5-FU (0–1000 μM), BLM (0–100 μg/ml) or IR (0–8 Gy). 48 h after treatment, the percentage of viable cells was quantified by the MTS method. Data represent the mean values obtained in two experiments performed in quadruplicate. (**B**) Clonogenic assay in AGS and MKN45 cells 13 days after irradiation with different doses of Gy (0–8); the graph shows the percentage of CFU (colony forming units). Representative images of AGS and MKN45 cells, 13 days after irradiation (4 Gy) are shown. The arrows point to abnormal morphology in AGS cells. Cleavage of PARP-1 was detected by western blot (WB) in cells harvested 24 h after 4 and 8 Gy IR. Activation of Caspase 3 was detected in the same extracts as above, running under the same experimental conditions. (Full length blot is included in supplementary information). α-Tubulin was used as a loading control. (**C**) RT-QPCR analysis of *CHK1* expression in asynchronous cultures of AGS and MKN45 cells. The graph shows the relative levels of CHK1's mRNA compared to normal tissue (NT), and using GAPDH as endogenous control. WB for both Chk1 isoforms (Chk1 and Chk1-S) in whole cell extracts from asynchronous cultures of AGS and MKN cells. α-Tubulin was used as a loading control.

expression and around a 60% reduction for MKN45 cells (Supplementary Fig. 2B). Taken together, the data presented here suggest that Chk1 depletion results in enhanced sensitivity, lower survival rates following exposure to radiation, and altered G2/and intra-S checkpoint responses to DSBs induced damage.

Transcriptional regulation of Chk1 in GC cells. To study whether high levels of Chk1 occur due to alterations at the transcriptional level, we cloned a fragment of Chk1 corresponding to the 5′ Flanking region of the

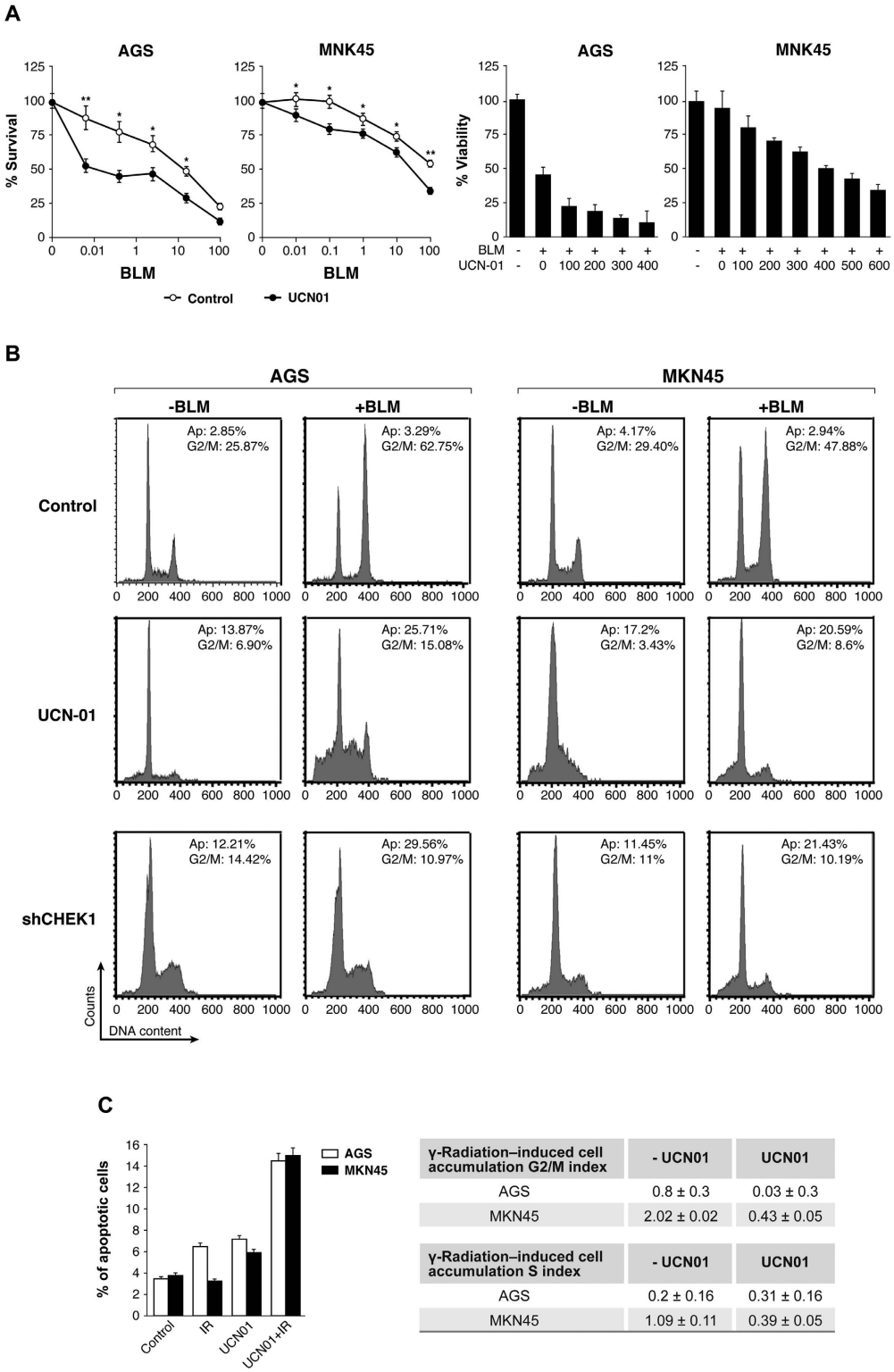

γ-Radiation–induced cell accumulation G2/M index	- UCN01	UCN01
AGS	0.8 ± 0.3	0.03 ± 0.3
MKN45	2.02 ± 0.02	0.43 ± 0.05

γ-Radiation–induced cell accumulation S index	- UCN01	UCN01
AGS	0.2 ± 0.16	0.31 ± 0.16
MKN45	1.09 ± 0.11	0.39 ± 0.05

Figure 2. Chk1 inhibition sensitizes GC cells to BLM or IR. (**A**) Survival rates in AGS and MKN45 cell lines, after treatment with BLM (0–100 μg/ml) and in the presence (●) or absence (○) of 100 nM UCN-01. Histogram: Viability percentage for AGS and MKN45 cells treated with increasing doses of UCN-01 (0–600 nM) in the presence or absence of BLM (3 μg/ml and 10 μg/ml for AGS and MKN45 cells respectively). (**B**) Cell cycle profile after inhibition of Chk1 by treatment with the inhibitor UCN-01 (100 nM for AGS or 300 nM for MKN45 cells) or after silencing Chk1's expression by transient transduction with a lentivirus carrying shRNA- Chk1 for 72 hours. One hour after, cells were treated with vehicle or with BLM (3 ug/ml) for 24 hours. Plots are representative of an experiment performed twice in duplicate. AP: Apoptotic Cells, G2/M: cells in G2 or Mitosis. (**C**) Percentage of apoptotic cells in both cell lines after irradiation, UCN-01 treatment and UCN-01 plus IR. Table containing G2/M and S accumulation index in both cell lines after IR and with or without UCN-01 treatment.

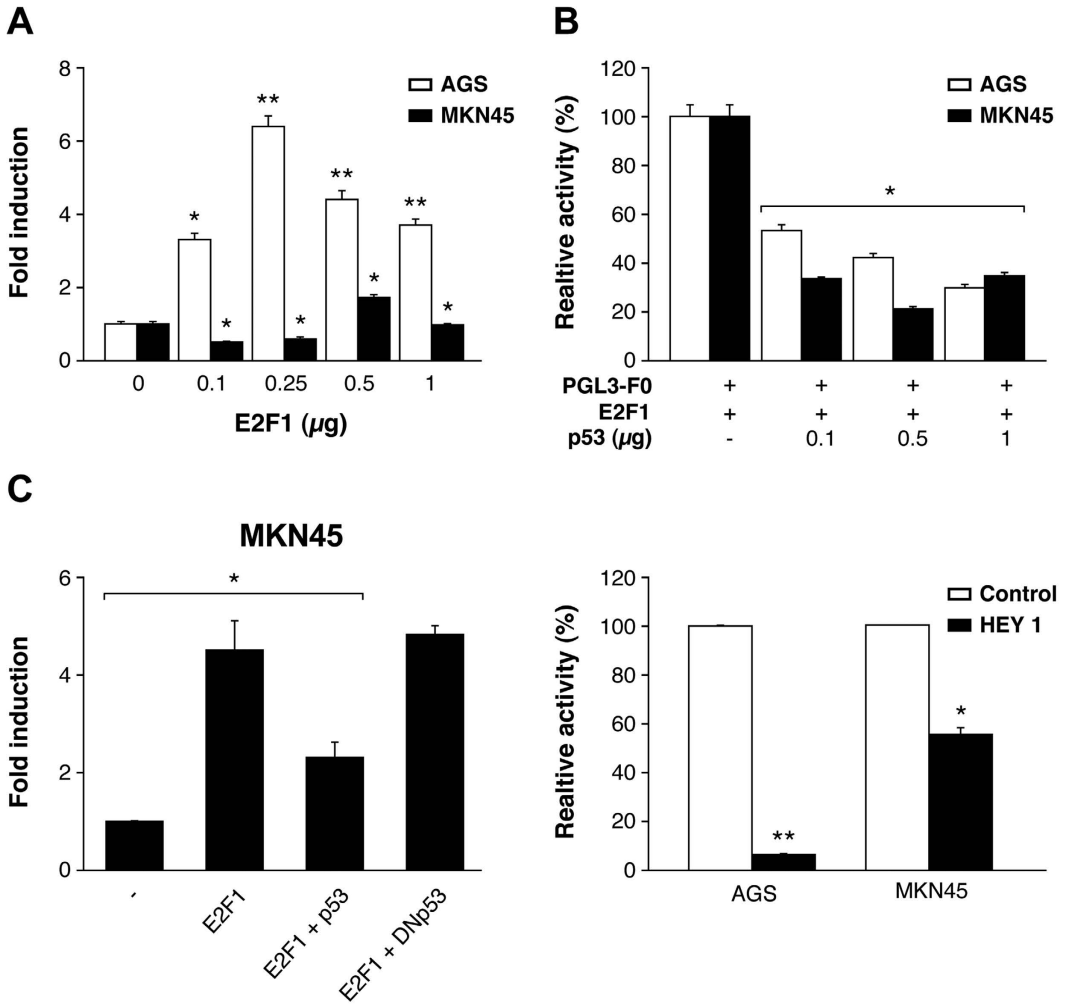

Figure 3. Chk1's promoter activity is regulated by E2F1 and p53 in GC cell lines. (**A**) Cells were transfected with increasing doses (0–1 μg) of an E2F1 expression vector (pCMV-E2F1), the corresponding empty control expression vector, and 200 ng of pGL3-F0. The graph shows activity levels, relative to that of PGL3-F0. (**B**) AGS and MKN45 cells were transfected with 200 ng of PGL3-F0, 500ng pCMV-E2F1 and increasing doses of p53's expression vector (0–1 μg). Results are presented as activity level, relative to that of the empty pGL3-Luc reporter in the presence of E2F1. (**C**) Left graph: MKN45 cells were transfected with 200 ng pGL3-F0 and expression vectors for E2F1 (250 ng), E2F1 plus p53 or E2F1 plus DNp53. Right graph: Both MKN45 and AGS cells were transfected with 200 ng pGL3-F0 and expression vectors for E2F1 (250 ng) or HEY1 (200 ng). All data are presented as the average of at least three independent experiments assayed in triplicate ± SEM. $p < 0,05$ versus empty vector control (Student's *t* test).

gene, (−1823 −284, as predicted by the Transfac tool) which contains the transcription factor (TF) and binds to CHK1's promoter (Supplementary Fig. 3A), in the pGL3-Basic enhanced luciferase plasmid. We detected luciferase activity after transient transfection in AGS and MKN45 cells; this occurred in both cell lines in a DNA- dose dependent manner, confirming that the generated construct is functional (Supplementary Fig. 3B). First, we focused on p53 and E2F1. E2F1 expression in AGS cells reached a 6-fold increase over pGL3-F0; however, only a 2-fold increase was observed in MKN45 cells (Fig. 3A). Next, we analyzed if both E2F1 and p53 cooperate in modulating Chk1 expression in GC cells. We verified that both cells lines are p53 wild type[37,38] and also performed a WB in order to evaluate the status of p53 in our specific experimental conditions, and our results indicated that p53 activation is equivalent in both cell lines. We found a transient activation of p53 4 h after IR (8 Gy) which returns to basal levels 24 hours after. We did not observe differences in p53 basal levels either (Supplementary Fig. 3C). To analyze the contribution of E2F1 and p53 in Chk1 expression, we performed an experiment in which cells were co-transfected with E2F1 (250 ng) and pGL3-F0 (200 ng) expression plasmids and increasing doses of the p53 (0–1 μg) expression vector. Our results showed that p53 was able to inhibit the transcriptional activity induced by E2F1 expression in GC cells, in a dose-dependent manner (Fig. 3C). We also tested the Dominant Negative (DN) form of p53 that was indeed able to revert the p53-dependent down-regulation of Chk1 when co-transfected with E2F1 and pGL3-F0, which further supported the involvement of p53 in Chk1 promoter regulation (Fig. 3D). To confirm that p53 regulates Chk1 promoter *in vivo*, cells were co-transfected with a plasmid

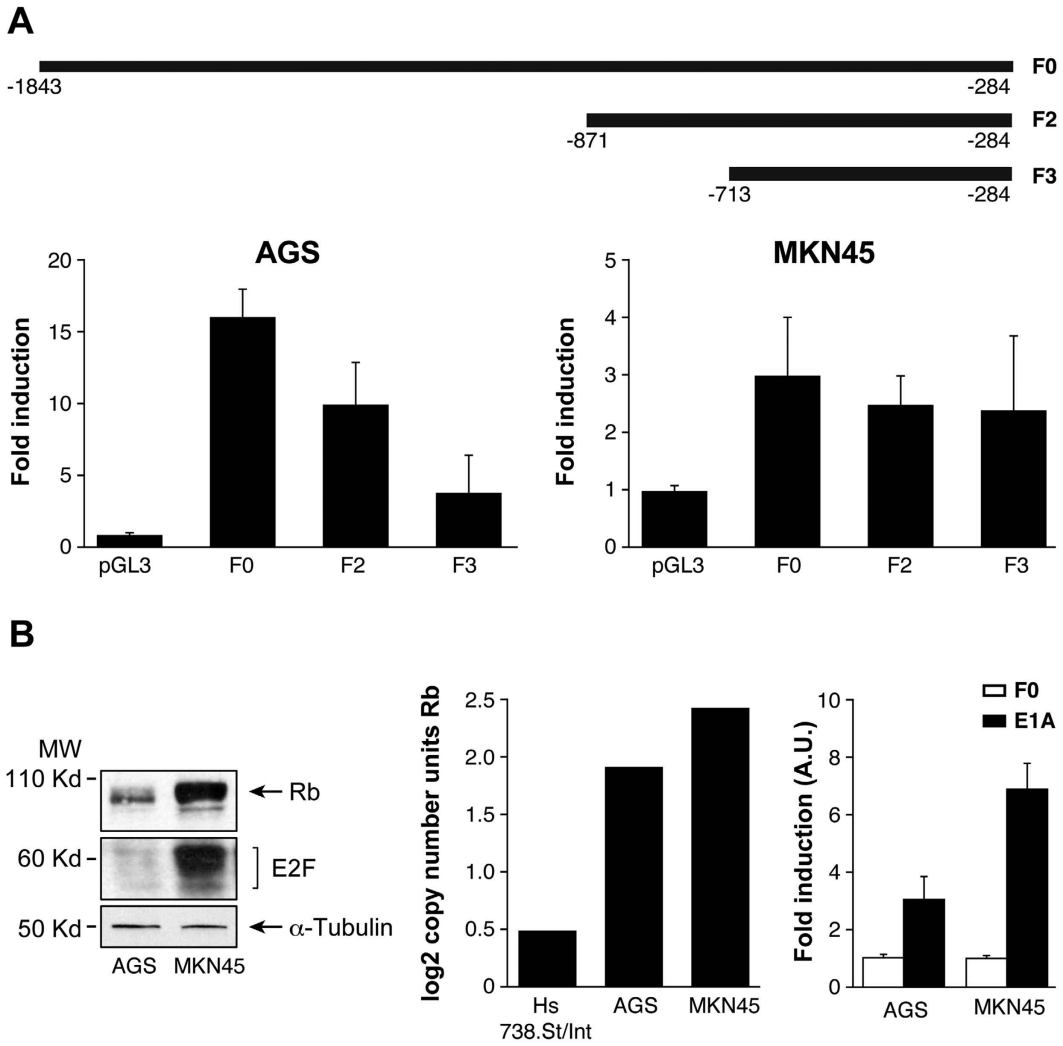

Figure 4. The RB1/E2F1 axis controls activation of Chk1 promoter. (**A**) Schematic representation of the constructs used in the transfection experiments. AGS and MKN45 were transfected with 250 ng of the indicated construction, and luciferase activity was measured 24 h later. The histograms show relative activity normalized to the empty vector in both AGS and MNK45 cells. (**B**) Expression of both RB1 and E2F1 was detected by WB using specific antibodies in AGS and MKN45 cells. α-Tubulin was used as loading control. The experiments were repeated three times with similar results. The graph on the center represents relative expression level (log 2-copy number) of RB1 in control (Hs 738St/Int) and tumoral AGS and MKN45 cells obtained from the Oncomine database. The graph on the right shows luciferase activity measurements in AGS and MKN45 cells after transfection with 250 ng of F0 and 100 ng of PCEFL-E1A. The data are presented as activity relative to the values found for the empty vector in transfected cells. The experiment was performed twice in triplicate.

encoding the Hey1 protein, which is an activator of p53[39] and pGL3-F0. Hey1 completely repressed the activity of Chk1 promoter after E2F1 expression in AGS cells and strongly inhibited it (50%) in MKN45 cells (Fig. 3D). To verify that these TFs control Chk1's expression in AGS cells, we quantified Chk1's mRNA levels under the above conditions. Our results suggest that E2F1 increases Chk1 expression and that activation of p53 reduces it (Supplementary Figure 3D). These results suggest that transcriptional regulation in these cells could be differentially modulated in GC adenocarcinoma through changes on E2F1 protein levels. The "*in silico*" analysis of the promoter sequence, revealed the presence of different E2F1 binding sites; therefore, we performed different deletions of the 5′ UTR (F2) and (F3), taking into account the putative TF binding sites for E2F. F2 and F3 are fragments that contain two and one E2F binding sites respectively (Fig. 4A). We found a drastic decrease in the transcriptional activation in AGS cells dependent on the number of E2F1 binding sites; however, no significant differences were observed in MKN45 cells. This suggests that the two E2F1 binding sites located in the area between −1843 −1201 pb (lost in F2 and F3) play a pivotal role in the induction of the promoter activity, especially in the AGS cell line, which suggests that other mechanisms are involved in the regulation of *CHK1* mRNA levels in MNK45 cells (Fig. 4A).

To further explore the mechanism involved in Chk1 expression by E2F1 and to gain insight into the differences found in E2F1 regulation between these cell lines, we studied the basal expression of RB1 and E2F1 proteins

GC Characteristic	n*	CHK1 Low (%)	CHK1 High (%)	X^2	P
SEX					
Male	19	68,5	31,5	1.709	0.539
Female	4	100	0		
AGE (mean)		63,3	74		0.389
STAGE					
I	3	100	0	2.841	0.417
II	7	57,1	42,9		
III	6	83,3	16,7		
IV	1	100	0		
LAUREN					
Intestinal	8	87,5	12,5	0.410	0.522
Difusse	8	75	25		
HER2/erb-b2					
Positive	2	50	50	0.647	0.421
Negative	17	70	30		
PFS (Months)					
≤18	5	40	60	4.752	0.063
>18	11	90	10		

Table 1. The association of Chk1 nuclear expression with the clinicopathological characteristics of Gastric Cancer patients. Results from a total of 23 patient samples. Correlation between clinicopathological characteristics and Chk1 nuclear expression was assessed by *Chi²* or *Fisher* exact test and *t-test* to compare the mean age between groups. Statistical significance was considered when $p < 0.05$, using IBM SPSS Statistics 22 software. *Patients with missing clinicopathological information in their medical records.

in each cell line. Our results indicate that levels of both RB1 and E2F1 are higher in MKN45 than in AGS cells (Fig. 4B). The expression of the RB gene through the Oncomine database (http//:oncomine.org), confirmed our finding of high levels of RB1 mRNA in MKN45 cells (Fig. 4B middle graph). We took advantage of the ability of adenovirus E1a protein to bind and block this tumor suppressor gene *RB*[40,41]. Transfection of a plasmid encoding the E1a protein in both cell lines, resulted in a clear increase on the activity of Chk1 promoter, which was more dramatic in MKN45 cells (Fig. 4B- right graph). These results indicate that the lack of transcriptional activation of Chk1 promoter in MKN45 cells and to a lower extent in AGS cells, could be due to effects exerted by the RB1 protein through binding to the TF E2F1.

The above results do not completely justify the high level of *CHK1* messenger in MKN45 cells. Therefore, we investigated if the increase on *CHK1* mRNA level in MKN45 cells is a result of post-transcriptional regulation. To investigate this possibility, we treated AGS and MKN45 cells with the transcriptional inhibitor Actinomycin D (Act D). CHK1 mRNA level was reduced 9 hours after Act D treatment in AGS cells (0,75-fold). However, in the MNK45 cell line, mRNA was accumulated at the same time (2,66-fold) (Supplementary Fig. 4A). These results suggest that CHK1 mRNA stability is regulated at post-transcriptional level in MKN45 cells.

Therefore, we decided to investigate the expression of microRNAs in samples from human GC cells in order to find miRNA candidates to regulate Chk1 expression. To this end, we analyzed the gene expression dataset GSE30070[42], and found that the levels of microRNA predicted by the online software TARGETSCAN for *CHK1* were significantly different between cancer and control samples (Supplementary Fig. 4B). From the predicted miRNAs that target *CHK1*, we investigated the potential role of miR-195 and miR-503 in the regulation of the stability of *CHK1* mRNA. miR-195 belongs to the big miR-15 microRNA family. This family has been recently described as radiosensitivity enhancer on breast cancer by targeting *CHK1*[43] and miR-503 has been previously shown to target *CHK1*[44,45]. We then used real-time PCR to detect the expression of miR-195/503 in AGS and MKN45 cell lines. Our results showed that miR-195 and -503 levels were significantly lower ($P \leq 0.05$) in MKN45 cells than in AGS cells (Supplementary Fig. 4B). Taken together, these data suggest an involvement of miR-195 and -503 in the upregulation of *CHK1* mRNA in MKN45 cells.

Prognostic Relevance of Chk1 Expression in gastric tumors. To assess the clinical significance of these findings, we studied the levels of Chk1 protein in a small cohort of patients. The samples were selected from patients that had received adjuvant therapy (Radiotherapy plus 5-FU) after surgery. The overall features of all 23 patients are summarized in Table 1. No significant association between Chk1 levels and age, sex, stage of the tumor, Lauren and Her2+ expression or PFS was observed in patients with GC ($p > 0,05$). However, our analysis detected 6 cases with positive Chk1 nuclear staining *versus* 14 cases that did not show any staining for Chk1 (Fig. 5A). Interestingly, we observed that patients with nuclear Chk1 accumulation tended to have shorter PFS than those with negative nuclear Chk1 staining (17,67 months vs 25,21 months; $p = 0.059$). The Kaplan-Meyer curve showed early differences in PFS between both populations (Fig. 5B). Altogether these results suggest that

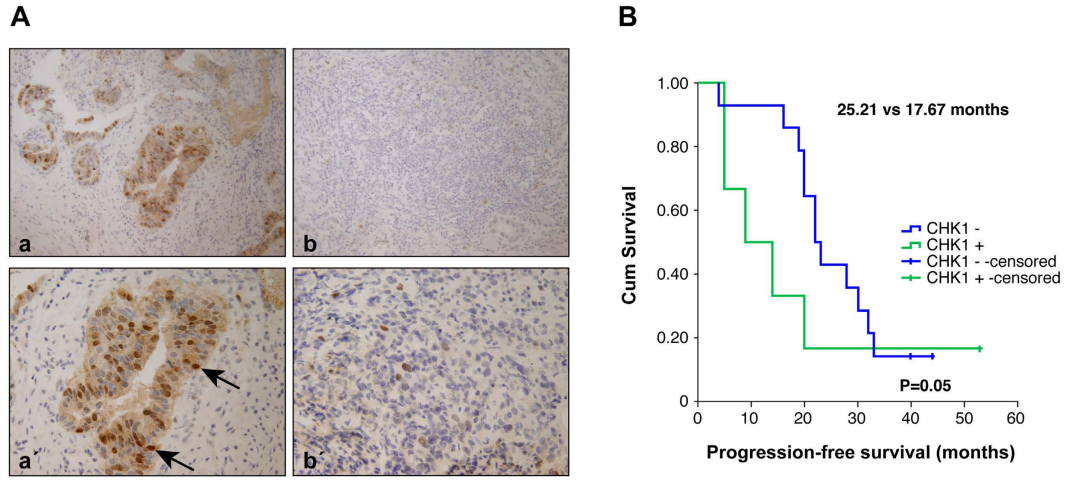

Figure 5. Nuclear Chk1 protein levels correlate with poor clinical outcome in human gastric cancer. (**A**) Immunohistochemical staining of Chk1 in representative carcinoma GC specimens: Nuclear positive and negative staining at 20 HPF (**a,b** respectively); nuclear positive and negative staining at 40HPF (**a',b'** respectively). The arrows point to strong Chk1 staining in the nucleus. (**B**) Kaplan-Meier curves of progression-free survival (PFS) in patients with high or low expression of nuclear Chk1 in their gastric tumors. Survival curves were statistically different when analyzed by the Breslow. IBM SPSS Statistics 22 software.

Chk1 can be considered as a putative biomarker for radiotherapy response in GC patients, since Chk1 protein level correlates with poor clinical outcome in human GC.

Discussion

Combining chemotherapy with radiation improves outcome in GC, but this strategy comes with the price of an increased toxicity rate and furthermore, many of these tumors are resistant to radiation. To overcome this obstacle, it is crucial to identify the key determinants of radioresistance, since this will enable us to develop safer and more effective tumor radiosensitizers.

We have previously reported that CDDP-resistance in colorectal cancer cells correlates with high Chk1 levels[32]. Here, we have demonstrated a relationship between Chk1 expression and IR resistance in GC. Our results indicate that in GC cell lines, Chk1 is upregulated and specifically modulates sensitivity to radiation. This upregulation correlates with poor clinical prognosis in our patient cohort and can be explained by acquired resistance to IR. Taking into account that GC is generally diagnosed at advanced stages, it is difficult to recruit a large cohort of patients meeting our inclusion criteria (gastrectomy plus adjuvant therapy based on 5-FU plus IR). However, it is necessary now to reproduce our results in a larger cohort of patients, to confirm the implication of Chk1 on therapy response and also to clarify other clinical and pathological outcomes. Our data indicate that inhibition of Chk1 activity due to treatment with UCN-01, increases sensitivity to both BLM and IR. This evidence points to Chk1 as a good target in GC treatment. Unfortunately, clinical development of UCN-01 has been halted due to unfavorable pharmacology[46]. However, other inhibitors have been tested such as AZD7762 (a potent and selective ATP-competitive Chk1 kinase inhibitor), which has shown strong chemosensitizing activity when used alongside DNA-damaging agents. This has been evaluated both in *in vitro* and *in vivo* model systems[47]. Increasing evidence indicates that Chk1 inhibitors are able to synergize with antitumoral drugs in an specific molecular context, such as tumors with defects in the DNA damage repair pathway, or those overexpressing specific oncogenes[48].

According with data from the literature, transcriptional regulation of Chk1 is controlled through p53 and E2F1[49,50]. In our experimental model radioresistance of MKN45 cells is not dependent on p53, since in both cell lines used in our study, p53 is wild type[37]. We corroborated that p53 is equally activated and follows the same kinetics in both cell lines after IR treatment. Our luciferase assays demonstrated that p53 regulates negatively the transcriptional activation of Chk1; moreover, we also confirmed that overexpression of p53 by transfection, leads to downregulation of Chk1 mRNA *in vitro*.

We cloned the Chk1 promoter region which contains different E2F binding sites[50]. The RB1-E2F1 pathway is crucial for the regulation of cell cycle progression and tumorigenesis. RB1 is a tumor suppressor gene frequently mutated or deleted in cancer, however in GC it is also amplified in an important percentage of samples[51]. Our results support a definitive role of RB1-E2F1 in the regulation of Chk1 transcription in GC. We suggest that in basal conditions E2F1 is sequestered by RB1, which is then unable to induce the expression of Chk1. This hypothesis is supported by our experiment with E1A oncoprotein, which binds and inhibits RB family members by disrupting E2F-RB1 interactions[52], thus increasing Chk1 promoter activity, especially in MKN45 cells with higher levels of RB1. In addition, in response to E2F1 overexpression these cells are unable to increase Chk1's mRNA.

Several studies have shown that both miR-15 and miR-497 families modulate multidrug resistance in GC cells by targeting BCl-2[53–56]. Furthermore, this family of miRNA controls Chk1 protein levels. For instance, overexpression of the miR-15a/b and miR-16 family affects the radiosensititivity of human breast cancer by regulating Chk1 and Wee1 proteins[43]. On the contrary, it has been shown that downregulation of the miR-15 family

regulates CDDP sensitivity by increasing Chk1 levels[44]. Other studies have demonstrated that dowregulation of miR-424 contributes to cervical cancer progression via upregulation of its target gene Chk1[11]. Along these lines, our results show a significant downregulation of miR-195 and miR-503 expression in MKN45 radioresistant cells. Accordingly, NSCLC (non small cell lung carcinoma) shows lower miR-195 expression in the tumor than in adjacent tissues, and this lower expression has been associated with poorer overall survival[57]. However, in addition to our preliminary results, more experiments are needed to specifically confirm the impact of this family of microRNAs on Chk1's expression and to define its influence on radioresistance. Nonetheless, the inverse correlation between microRNAs and Chk1 would be a promising parameter to consider in the clinical setting. In this regard, recent evidence confirms our findings in lung cancer[57] which supports the universal character of our observations. However, other putative targets of those microRNA should be taken into account, and also their relationship with E2F1-RB[58], in order to describe a possible feedback loop that could be regulating each member.

In summary, in this study we demonstrate that gastric tumors can be stratified into radiation resistant or sensitive, according to the status of Chk1. Chk1 protein levels could be modified by pRB-E2F1, p53 or miRNAs that seem to regulate its expression Thus, the miR-195/Chk1 axis may be used as a new biomarker tool to predict individual response to adjuvant radiotherapy. We previously described the possibility to sensitize advanced tumoral gastric cancer cells by adjuvant chemotherapy based on paclitaxel and cisplatin[59], as an alternative to non-resecable tumors. The data presented here could mark a step forward allowing the design of improved therapeutic interventions for GC patients.

Materials and Methods

Cell lines. AGS and MKN45 human gastric adenocarcinoma cell lines were cultured in F12-Kaings and RPMI mediums respectively (Gibco), and supplemented with FBS (10% for AGS and 20% for MKN45). Cultures were maintained at 37 °C, 5% CO_2 and 95% humidity. AGS and MKN45 are wild type for TP53[37,38].

Cloning. Genomic DNA was extracted from the colorectal cancer cell line HCT116 and the required sequence (−1823 –284) was cloned into a pGL3-enhanced luciferase plasmid vector. *See Supplementary M&M for details.*

PCR. Total RNA was extracted using Tri-Reagent (Life technologies). Gene expression levels were assessed by Q-PCR, by using SYBR green-based chemistries for amplicon detection. For relative quantification (RQ) we used the delta-Ct method. Statistical analyses was performed for each gene by using a paired t-test to compare mean values, where $p < 0.05$ was considered significant.

Reagents and Plasmid Vectors. Cisplatin, 5-Fluorouracile, Actinomycin D and UCN-01 were purchased from Sigma Aldrich. BLM was purchased from Calbiochem. pGL3 Basic and pGEMT easy (Promega), pSG5-HEY1, and pSG5 (Dr. B. Belandia), pCMV-E2F1 (Dra. A. Zubiaga), pcdna-p53DN (Dr. I Palmero), PCEFL-E1A, PEF1-p53 wt and pEF1 Dn (Dr. Sanchez-Prieto).

Luciferase activity assay. Constructs carrying the luciferase gene were cotransfected with 1 ng of Renilla (transfecting control, 1:100) using lipofectamine 2000 (Invitrogen) in 24 well plates following the Manufacter's instructions. 24 hours after transfection, transcriptional activity was quantified using the Dual-Luciferase® Reporter (DLR™) Assay System (Promega) using a Promega luminometer.

Cell viability Clonogenic assay. Viability was determined using a MTS (Promega) staining method, as described[60]. To assess the effects of irradiation, cells were irradiated with different doses of Gy (0–8 Gy) using a ^{137}Cs source (mark 1, model 30, JL. Shepherd & Associates San Fernando CA; Dose rate to 100 mm diameter samples is ~370 R/minute). 15 days after treatment, colonies containing more than 50 individual cells were counted using a microscope and survival fractions were quantified as described[61].

IC50 and Combination Index (CI). IC50 were calculated by using the GraphPad Prism program. We used nonlinear regression to fit the data to the log (inhibitor) vs response (variable slope) curve.

Effects of BLM and UCN-01 combination on growth inhibition were analyzed by the Combination Index (CI) equation developed by Chou-Talalay[35,62] using the CalcuSyn program (Biosoft, Cambridge, UK). The general equation for the classic isobologram is given by: $CI = (D)1/(Dx)1 + (D)2/(Dx)2$ where $CI < 1$ indicates synergism; $CI = 1$ indicates additive effect, and $CI > 1$ indicates antagonism; (Dx)1 and (Dx)2 in the denominators are the doses (or concentrations) of D1 (drug #1, for example, BLM) and D2 (drug #2, for example, UCN-01) alone that gives x% inhibition, whereas (D)1 and (D)2 in the numerators are the doses of D1 and D2 in combination that also inhibits x% The (Dx)1 and (Dx)2 can be readily calculated from the median-effect equation of Chou $Dx = Dm[fa/(1\text{-}fa)]1/m$ where Dx is the median-effect dose, fa is the fraction affected, Dm is the median-effect dose signifying potency and m is the kinetic order signifying the shape of dose-effect curve.

Western blotting. Twenty μg of protein per sample were loaded in SDS-PAGE in 10% (for E2F1,Chk1 and p53) or 8% (for Rb or PARP-1) polyacrylamide gels, and then transferred onto nitrocellulose membranes. Antibody dilutions were as follows: Chk1- 1:500 (sc-377231), E2F1- 1:1000 (sc-193), Rb- 1:200 (sc-102), PARP-1- 1:1000 (H-300: sc-25780), Cleaved Caspase-3 (Asp175) Antibody #9661 1:1000, p53 Antibody #9282 1:1000 (Cell signaling) in 5% fat free milk 0'05% TTBS. HA Antibody- 1:2000 (Boehringer mannheim), Flag antibody-1:2000 (Sigma)

Cell cycle analysis. Cell cycle analysis was performed as previously described[59]. *Supplementary M&M for details.*

Viral transduction of target cells. Viral particles for infection were generated according to manufacturing instructions using GIPZ Lentiviral shRNA for CHK1 (Thermo Scientific Open Biosystems). *See Supplementary M&M for details.*

miRNA analysis. RNA was purified from cultured cells using mirVana™ miRNA Isolation Kit (Ambion; Life Technologies). RT: TaqMan® MicroRNA Reverse Transcription Kit and TaqMan microRNA specific assays (Catalog #: 4427975 ID: 00104; ID: 000494: ID: 001973) were used to perform the RT and quantitative PCR (RT-qPCR) of triplicate samples. Real-time PCR was performed on an Applied Biosystems Step-one plus PCR (Life Technologies) following the manufacturer's instructions. Total RNA input was normalized using RNU6B RNA as an endogenous control.

Gene expression profile analysis. The miRNA expression data in a large set of GC patient samples[42] was downloaded from the Gene Expression Omnibus (GEO, http://www.ncbi.nlm.nih.gov/geo/) and analyzed using custom R scripts for statistical programming http://www.r-project.org/". Briefly, we compared probe values in each sample group ("normal", "pretreatment", "post-treatment") using a Student's t-test and the resulting p-values were adjusted for multiple testing by the Bonferroni method.

Patients and tumor samples. Patients (n = 23) were recruited from the Oncology Department at the Infanta Sofía´s Hospital between 2008 and 2015. We selected those patients diagnosed with GC, who underwent radical surgery and received adjuvant therapy according to the MacDonald´s treatment guidelines (5-FU and radiation). The specimens were collected during tumor resection. Tissue samples were histologically confirmed as tumoral or non-tumoral tissues, and were stored at −80 °C until analysis. This study was approved by the Clinical Research Ethics Committee "IMDEA alimentacion" (code IMD: PI-010). All procedures were carried out in accordance with the approved guidelines and after informed consent was obtained from all subjects included in the study.

Immunohistochemical analysis. Immunohistochemistry was performed in 3-μm sections of paraffin-embedded tissues. Samples were deparaffinized and rehydrated in water, after which antigen retrieval was carried out by incubation in EDTA solution. Endogenous peroxidase and non-specific antibody reactivity were blocked with peroxidase blocking reagent (Dako). The sections were then incubated with the Rabbit Monoclonal Antibody against Chk1 (TA300658. Origene Technologies). Detection was carried out by using Envision Plus Detection System (Dako). Negative controls were performed by replacing the primary antibody with goat serum. The slides were finally mounted with DPX mountant for microscopy (VWR Int). Immunohistochemical analysis was performed by the Pathology department's staff at the same Hospital and the interpretation by a blinded expert pathologist. Chk1 nuclear staining was assessed as a percentage of surface showing positive signal, relative to the percentage of stained cells in the sample per surface area. A semi-quantitative score was assigned, as follows: 0: ≤10%; 1: 10–25%; 2: 25–50%; 3: ≥50%. Positive staining was therefore considered 1, 2 or 3.

References

1. Torre, L. A. *et al.* Global cancer statistics, 2012. *CA Cancer J Clin* **65,** 87–108 (2015).
2. Siegel, R. L., Miller, K. D. & Jemal, A. Cancer statistics, 2015. *CA Cancer J Clin* **65,** 5–29 (2015).
3. Macdonald, J. S. *et al.* Chemoradiotherapy after surgery compared with surgery alone for adenocarcinoma of the stomach or gastroesophageal junction. *N Engl J Med* **345,** 725–30 (2001).
4. Toiyama, Y. *et al.* Administration sequence-dependent antitumor effects of paclitaxel and 5-fluorouracil in the human gastric cancer cell line MKN45. *Cancer Chemother Pharmacol* **57,** 368–75 (2006).
5. Wagner, A. D. *et al.* Chemotherapy for advanced gastric cancer. *Cochrane Database Syst Rev*, doi: 10.1002/14651858.CD004064.pub3 (2010).
6. Viudez-Berral, A. *et al.* Current management of gastric cancer. *Rev Esp Enferm Dig* **104,** 134–41 (2012).
7. Dai, Y. & Grant, S. New insights into checkpoint kinase 1 in the DNA damage response signaling network. *Clin Cancer Res* **16,** 376–83 (2010).
8. Tapia-Alveal, C., Calonge, T. M. & O'Connell, M. J. Regulation of chk1. *Cell Div* **4,** 8 (2009).
9. Smits, V. A. & Gillespie, D. A. DNA damage control: regulation and functions of checkpoint kinase 1. *FEBS J* **282,** 3681–92 (2015).
10. Verlinden, L. *et al.* The E2F-regulated gene Chk1 is highly expressed in triple-negative estrogen receptor/progesterone receptor/HER-2 breast carcinomas. *Cancer Res* **67,** 6574–81 (2007).
11. Xu, J. *et al.* Suppressed miR-424 expression via upregulation of target gene Chk1 contributes to the progression of cervical cancer. *Oncogene* **32,** 976–87 (2013).
12. Cole, K. A. *et al.* RNAi screen of the protein kinome identifies checkpoint kinase 1 (CHK1) as a therapeutic target in neuroblastoma. *Proc Natl Acad Sci USA* **108,** 3336–41 (2011).
13. Liao, Q. *et al.* A preliminary study on the radiation-resistance mechanism in ovarian cancer. *J Cancer Res Ther* **9,** 22–4 (2013).
14. Wang, W. J. *et al.* MYC regulation of CHK1 and CHK2 promotes radioresistance in a stem cell-like population of nasopharyngeal carcinoma cells. *Cancer Res* **73,** 1219–31 (2013).
15. Yang, H. *et al.* Inhibition of checkpoint kinase 1 sensitizes lung cancer brain metastases to radiotherapy. *Biochem Biophys Res Commun* **406,** 53–8 (2011).
16. Morgan, M. A. *et al.* Mechanism of radiosensitization by the Chk1/2 inhibitor AZD7762 involves abrogation of the G2 checkpoint and inhibition of homologous recombinational DNA repair. *Cancer Res* **70,** 4972–81 (2010).
17. Parsels, L. A. *et al.* Gemcitabine sensitization by checkpoint kinase 1 inhibition correlates with inhibition of a Rad51 DNA damage response in pancreatic cancer cells. *Mol Cancer Ther* **8,** 45–54 (2009).
18. McNeely, S., Beckmann, R. & Bence Lin, A. K. CHEK again: revisiting the development of CHK1 inhibitors for cancer therapy. *Pharmacol Ther* **142,** 1–10 (2014).
19. Xu, N. *et al.* Cdk-mediated phosphorylation of Chk1 is required for efficient activation and full checkpoint proficiency in response to DNA damage. *Oncogene* **31,** 1086–94 (2012).
20. Enomoto, M. *et al.* Novel positive feedback loop between Cdk1 and Chk1 in the nucleus during G2/M transition. *J Biol Chem* **284,** 34223–30 (2009).
21. Zhang, Y. & Hunter, T. Roles of Chk1 in cell biology and cancer therapy. *Int J Cancer* **134,** 1013–23 (2014).

22. Zhou, J. *et al.* A kinome screen identifies checkpoint kinase 1 (CHK1) as a sensitizer for RRM1-dependent gemcitabine efficacy. *PLoS One* **8,** e58091 (2013).
23. Yao, H., Yang, Z. & Li, Y. [Expression of checkpoint kinase 1 and polo-like kinase 1 and its clinicopathological significance in benign and malignant lesions of the stomach]. *Zhong Nan Da Xue Xue Bao Yi Xue Ban* **35,** 1080–4 (2010).
24. Bartel, D. P. & Chen, C. Z. Micromanagers of gene expression: the potentially widespread influence of metazoan microRNAs. *Nat Rev Genet* **5,** 396–400 (2004).
25. Xie, Y. *et al.* Checkpoint kinase 1 is negatively regulated by miR-497 in hepatocellular carcinoma. *Med Oncol* **31,** 844 (2014).
26. Croce, C. M. Causes and consequences of microRNA dysregulation in cancer. *Nat Rev Genet* **10,** 704–14 (2009).
27. Bushati, N. & Cohen, S. M. microRNA functions. *Annu Rev Cell Dev Biol* **23,** 175–205 (2007).
28. Garzon, R., Calin, G. A. & Croce, C. M. MicroRNAs in Cancer. *Annu Rev Med* **60,** 167–79 (2009).
29. Cimmino, A. *et al.* miR-15 and miR-16 induce apoptosis by targeting BCL2. *Proc Natl Acad Sci USA* **102,** 13944–9 (2005).
30. Cittelly, D. M. *et al.* Downregulation of miR-342 is associated with tamoxifen resistant breast tumors. *Mol Cancer* **9,** 317 (2010).
31. Ma, J., Dong, C. & Ji, C. MicroRNA and drug resistance. *Cancer Gene Ther* **17,** 523–31 (2010).
32. Peralta-Sastre, A. *et al.* Checkpoint kinase 1 modulates sensitivity to cisplatin after spindle checkpoint activation in SW620 cells. *Int J Biochem Cell Biol* **42,** 318–28 (2010).
33. Valero, M. L. *et al.* E1a promotes c-Myc-dependent replicative stress: implications in glioblastoma radiosensitization. *Cell Cycle* **13,** 52–61 (2014).
34. Pabla, N., Bhatt, K. & Dong, Z. Checkpoint kinase 1 (Chk1)-short is a splice variant and endogenous inhibitor of Chk1 that regulates cell cycle and DNA damage checkpoints. *Proc Natl Acad Sci USA* **109,** 197–202 (2012).
35. Chou, T. C. & Talalay, P. Quantitative analysis of dose-effect relationships: the combined effects of multiple drugs or enzyme inhibitors. *Adv Enzyme Regul* **22,** 27–55 (1984).
36. Clarke, C. A. & Clarke, P. R. DNA-dependent phosphorylation of Chk1 and Claspin in a human cell-free system. *Biochem J* **388,** 705–12 (2005).
37. Nabeya, Y. *et al.* The mutational status of p53 protein in gastric and esophageal adenocarcinoma cell lines predicts sensitivity to chemotherapeutic agents. *Int J Cancer* **64,** 37–46 (1995).
38. Fan, X. M. *et al.* Inhibition of proteasome function induced apoptosis in gastric cancer. *Int J Cancer* **93,** 481–8 (2001).
39. Villaronga, M. A., Lavery, D. N., Bevan, C. L., Llanos, S. & Belandia, B. HEY1 Leu94Met gene polymorphism dramatically modifies its biological functions. *Oncogene* **29,** 411–20 (2010).
40. Liu, X. & Marmorstein, R. Structure of the retinoblastoma protein bound to adenovirus E1A reveals the molecular basis for viral oncoprotein inactivation of a tumor suppressor. *Genes Dev* **21,** 2711–6 (2007).
41. Chellappan, S. P., Hiebert, S., Mudryj, M., Horowitz, J. M. & Nevins, J. R. The E2F transcription factor is a cellular target for the RB protein. *Cell* **65,** 1053–61 (1991).
42. Kim, C. H. *et al.* miRNA signature associated with outcome of gastric cancer patients following chemotherapy. *BMC Med Genomics* **4,** 79 (2011).
43. Mei, Z. *et al.* The miR-15 Family Enhances the Radiosensitivity of Breast Cancer Cells by Targeting G2 Checkpoints. *Radiat Res* **183,** 196–207 (2015).
44. Pouliot, L. M. *et al.* Cisplatin sensitivity mediated by WEE1 and CHK1 is mediated by miR-155 and the miR-15 family. *Cancer Res* **72,** 5945–55 (2012).
45. Pouliot, L. M., Shen, D. W., Suzuki, T., Hall, M. D. & Gottesman, M. M. Contributions of microRNA dysregulation to cisplatin resistance in adenocarcinoma cells. *Exp Cell Res* **319,** 566–74 (2013).
46. Sausville, E. A. *et al.* Phase I trial of 72-hour continuous infusion UCN-01 in patients with refractory neoplasms. *J Clin Oncol* **19,** 2319–33 (2001).
47. Mitchell, J. B. *et al. In vitro* and *in vivo* radiation sensitization of human tumor cells by a novel checkpoint kinase inhibitor, AZD7762. *Clin Cancer Res* **16,** 2076–84 (2010).
48. Maugeri-Sacca, M., Bartucci, M. & De Maria, R. Checkpoint kinase 1 inhibitors for potentiating systemic anticancer therapy. *Cancer Treat Rev* **39,** 525–33 (2013).
49. Gottifredi, V., Karni-Schmidt, O., Shieh, S. S. & Prives, C. p53 down-regulates CHK1 through p21 and the retinoblastoma protein. *Mol Cell Biol* **21,** 1066–76 (2001).
50. Carrassa, L., Broggini, M., Vikhanskaya, F. & Damia, G. Characterization of the 5'flanking region of the human Chk1 gene: identification of E2F1 functional sites. *Cell Cycle* **2,** 604–9 (2003).
51. Cancer Genome Atlas Research, N. Comprehensive molecular characterization of gastric adenocarcinoma. *Nature* **513,** 202–9 (2014).
52. Chellappan, S. *et al.* Adenovirus E1A, simian virus 40 tumor antigen, and human papillomavirus E7 protein share the capacity to disrupt the interaction between transcription factor E2F and the retinoblastoma gene product. *Proc Natl Acad Sci USA* **89,** 4549–53 (1992).
53. Xia, L. *et al.* miR-15b and miR-16 modulate multidrug resistance by targeting BCL2 in human gastric cancer cells. *Int J Cancer* **123,** 372–9 (2008).
54. Zhu, W., Shan, X., Wang, T., Shu, Y. & Liu, P. miR-181b modulates multidrug resistance by targeting BCL2 in human cancer cell lines. *Int J Cancer* **127,** 2520–9 (2010).
55. Zhu, W. *et al.* miR-200bc/429 cluster modulates multidrug resistance of human cancer cell lines by targeting BCL2 and XIAP. *Cancer Chemother Pharmacol* **69,** 723–31 (2012).
56. Zhu, W. *et al.* miR-497 modulates multidrug resistance of human cancer cell lines by targeting BCL2. *Med Oncol* **29,** 384–91 (2012).
57. Liu, B. *et al.* MiR-195 suppresses non-small cell lung cancer by targeting CHEK1. *Oncotarget* **6,** 9445–56 (2015).
58. Mao, A. *et al.* miR-449a enhances radiosensitivity through modulating pRb/E2F1 in prostate cancer cells. *Tumour Biol* doi: 10.1007/s13277-015-4336-8 (2015).
59. Bargiela-Iparraguirre, J. *et al.* Mad2 and BubR1 modulates tumourigenesis and paclitaxel response in MKN45 gastric cancer cells. *Cell Cycle* **13,** 3590–601 (2014).
60. Gutierrez-Gonzalez, A. *et al.* Targeting Chk2 improves gastric cancer chemotherapy by impairing DNA damage repair. *Apoptosis* **18,** 347–60 (2013).
61. Rafehi, H. *et al.* Clonogenic assay: adherent cells. *J Vis Exp* (2011).
62. Ling, X. *et al.* Synergistic effect of allyl isothiocyanate (AITC) on cisplatin efficacy *in vitro* and *in vivo*. *Am J Cancer Res* **5,** 2516–30 (2015).

Acknowledgements

This work was supported by Instituto de Salud Carlos III–Fondo de Investigación Sanitaria (PS09/1988 to ISP; PI11-00949, pI014-1495 and Feder Funds to RP); Comunidad Autónoma de Madrid-Universidad Autónoma de Madrid (CCG10-UAM/BIO-5871 to ISP); Fundación Leticia Castillejo Castillo and Ministerio de Ciencia e Innovación (SAF2012-30862 to RSP), Spain. We are grateful to Dr. L. del Peso Ovalle for the bioinformatics analysis and B. Belandia, A. Zubiaga and I Palmero for kindly providing the relevant plasmids. We are grateful

to Javier Pérez (photography facility), Diego Navarro and Lucia Sanchez (microscopy facility IIBM) for their technical assistance. JBI was supported by a fellowship from Catedra Isaac Costero, funded by Banco Santander-UAM and is a doctoral student from a double doctorate program in Molecular Biosciences (UAM) and in Biomedical Sciences, (UNAM) and received fellowship CVU:607546 from CONACYT.

Author Contributions

B.-I.J., P.-M.L. and G.-G.A. made the experiments and prepared the figures. M.-R.J., M.-F.M. and S.M. developed the clinical protocol and human sample recruitment. F.-F.M., S.-P.R. and P.R. discuss the results and proof reading of the manuscript. I. S.-P. design and wrote the main manuscript. All authors reviewed the manuscript.

Additional Information

Supplementary information accompanies this paper at http://www.nature.com/srep

Competing financial interests: The authors declare no competing financial interests.

How to cite this article: Bargiela-Iparraguirre, J. *et al.* CHK1 expression in Gastric Cancer is modulated by p53 and RB1/E2F1: implications in chemo/radiotherapy response. *Sci. Rep.* **6**, 21519; doi: 10.1038/srep21519 (2016).

CHK1 expression in Gastric Cancer is modulated by p53 and RB1/E2F1: implication in chemo/radiotherapy response.

Bargiela-Iparraguirre J[1†], Prado-Marchal L[1†], Fernandez-Fuente M[2], Gutierrez-González A [1], Moreno-Rubio J [3,4], Muñoz-Fernandez M [5], Sereno M [3], Sanchez-Prieto, R [6,7], Perona R [1,8,9] and Sanchez-Perez I[1,6,7,8,9 *]

[1] Dpto.Bioquímica. Fac. Medicina. Instituto de Investigaciones Biomédicas Madrid CSIC-UAM; Madrid, Spain
[2] The Royal Veterinary College. University of London; London, UK
[3] Medical Oncology Department, Infanta Sofía University Hospital, San Sebastian de los Reyes, Madrid, 28702; Spain
[4]IMDEA-Food Institute, CEI UAM+CSIC, Madrid, Spain
[5]Pathology Department, Infanta Sofía University Hospital, San Sebastián de los Reyes, 28702, Madrid
[6] Unidad de Medicina Molecular, laboratorio de Oncología ,CRIB/FPCYT C-LM. Universidad de Castilla-La Mancha, Av. Almansa 14, 02006, Albacete, Spain
[7]Unidad asociada de Biomedicina UCLM-CSIC[5 6]
[8] CIBER for Rare Diseases (CIBERER); Valencia, Spain
[9]Biomarkers and Experimental Therapeutics Group; IdiPAZ; University Hospital La Paz; Madrid, Spain

Supplementary M&M

Cloning and PCR.

The promoter sequences of interest were amplified by PCR and cloned into the intermediate vector pGEMT-easy (Promega). Fidelity was verified by sequencing. Promoter sequences were then subcloned upstream of the luciferase gene, into the final vector pGL3-Luciferase Basic (Promega), using specific restriction sites for BglII and MluI. The following primer pairs were used:

F0: Fw: 5' GGACGCGTAAGCCATTCTCCTGCCTCGC-3'

F1: Fw 5' GGACGCGTGGTGCAGCCTTTCAGGCCCA-3'

F2: Fw 5'- GGACGCGTGCGCTGTCTTGCTTTACGGC-3'

F3: Fw: 5'- GGACGCGTAGAAGGAGTTCGGGGTCTAG-3'

Rv: 5'- GGAGATCTCCGGCGAACGACTGGGGAAG-3'

Primers used for the short isoform of CHEK1:

1F:5'-GACTGGGACTTGGTGCAAAC-3'

2F: 5'CTGAAGAAGCAGTCGCAGTG-3'

1R: 5'-GCAGGAAGCCAAATCTTCTG-3'

2R: 5'-TGGGAGACTCTGACACACCA-3'

Viral transduction of target cells.

Briefly, 293T cells (4.5 x 10^6 cells/plate) were transfected using lipofectamine 2000 (Invitrogen) with 15 μg of shCHEK1, 7 μg of envelope plasmid (VSV-G), and 7 μg of Helper plasmid (pCD/NL-BH). The supernatants were recovered 48h and 72h after transfection and frozen in small aliquots at -80ºC until used. Transduction was carried out using 5 x 10^5 cells per well in a 6-well plate. 48 hours post-transduction cells were examined microscopically for the presence of GFP-reporter expression as an indicator of transduction efficiency. 72h after, cells were assayed for changes in gene expression by quantitative/real-time PCR (QPCR), compared to non-silencing shRNA.

Cell cycle analysis.

Adherent and non-adherent cells were harvested and fixed overnight in 70% ethanol in phosphate-buffered saline (PBS). For DNA content analysis, cells were centrifuged and resuspended in PBS containing 1 μg/ml RNase (Qiagen Ltd., Crawley, UK) and 25 μg/ml propidium iodide (Sigma-Alcrich), then incubated at room temperature for 30 min, and finally analyzed using a Becton Dickinson Flow Cytometer (Cowley, UK). Data were plotted using Cell Quest software, with 10,000 events analyzed per sample.

Supplementary figure legends

Supplementary Fig. 1

(A) Representative images of a Clonogenic assay of AGS and MKN45 cells at the end of the experiment (13 days) after treatment with IR (0-8 Gy) or BLM (0-7,5 μg/ml). (**B)** *CHK1* mRNA expression in non tumoral cells (Hs 738.St/Int) and GC cell lines (AGS, MKN45, KatoIII and Hs746t) was extracted from deposited CHK1 Copy Number data in Rothenberg Cell Line data sets, analyzed in Oncomine and presented as bars. (C) Schematic representation of the primers used to amplify the two isoforms of *CHK1* (adapted from [1]) by RT-PCR. The picture represents the amplicons detected with each primer set. Only one amplicon was detected using primers set 1 (lane1), whereas two amplicons were obtained when using primer sets 2 or 3. (Lanes 2 and 3). Lane 4 represents the amplification of our endogenous control GAPDH.

Supplementary Fig. 2

(A) UCN-01 (100 nmol/L) was added 30 minutes before bleomycin (10 ug / ml) treatment. Cells were harvested 3 hours later, and phosphorylation of Chk1-Ser296 was studied by WB. (B) mRNA was extracted 72 h after transduction and Q-PCR showed that Chk1 is depleted during the experimental process.

Supplementary Fig. 3

(A) Schematic representation of the constructs used in our transfection experiments. The sequence -1843-287 contains promoter elements and the graph shows the predicted (Transfact tool) transcription factors (TF) that bind to the cloned sequence. (B) Cell lines were co-transfected with 250 and 500 ng of F0-pGL3 plasmid a luciferase reporter construct carrying the Chk1 promoter fragment (-1834-234). The graph shows the expression levels relative to the empty PGL3 vector and normalized by Renilla. Bars represent the average of at least three experiments performed in triplicate (*p<0,05).(C) AGS and MKN45 cells were treated with IR (8 G). Cells were harvested at the indicated times, and p53 stabilization was analyzed by using a specific antibody against p53. α-Tubulin was used as a loading control. (D) AGS and MKN45 cells were transfected as indicated in Figure 3, and mRNAs were extracted 24h after transfection. Chk1 levels were quantified by RT-QPCR. The graph represents the relative levels of Chk1, compared with normal control cells. Transfection of p53 and Hey1 was followed by western blot using a specific antibody against the flag epitope (Hey1) or HA epitope ($p53^{WT}$ or $p53^{DN}$). Tubulin was used as a loading control.

Supplementary Fig. 4

CHK1 is controlled at posttranscriptional level by miRNA-195 and miRNA-503. (A) Cells were treated with Act D (1 μg/ml) for the indicated periods (0-9 h) and *CHK1* mRNA levels were determined by semi-quantitative RT-PCR. Data indicate the intensity of *CHK1* bands normalized with GAPDH, and are presented as mean ± SD of three independent experiments (*$p < 0.05$). (B) Table: differentially expressed miRNAs in GC and normal stomach epithelium with *CHK1* as a potential target. Alignment of the selected miRNAs with the 3'UTR sequence of *CHK1*. Fold changes of miR-195 and miR-503 expression levels in AGS and MKN45 cells. Gene expression is presented as the expression value relative to that of the U6 endogenous control. The experiment was performed in triplicate. Data are presented as mean ± standard deviation (SD).

1 Pabla, N., Bhatt, K. & Dong, Z. Checkpoint kinase 1 (Chk1)-short is a splice variant and endogenous inhibitor of Chk1 that regulates cell cycle and DNA damage checkpoints. *Proc Natl Acad Sci U S A* **109**, 197-202, doi:10.1073/pnas.1104767109 (2012).

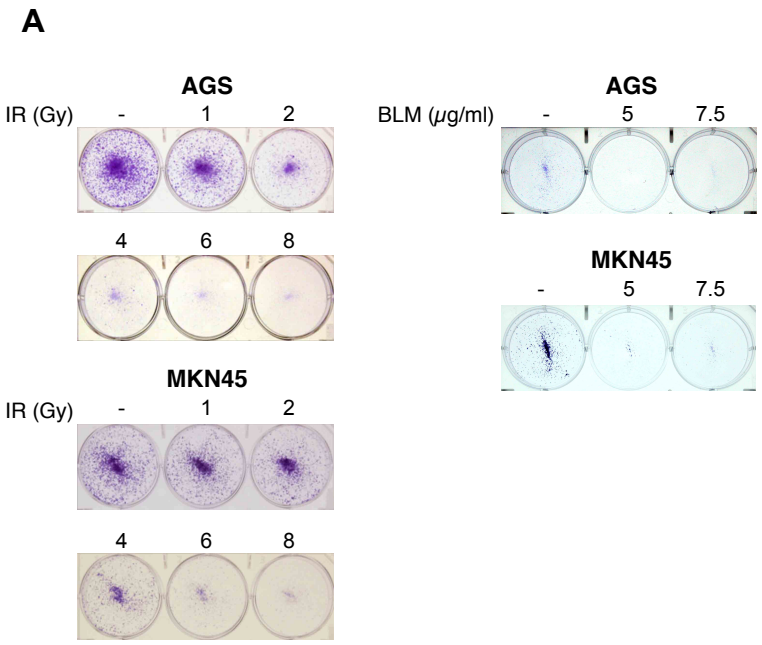

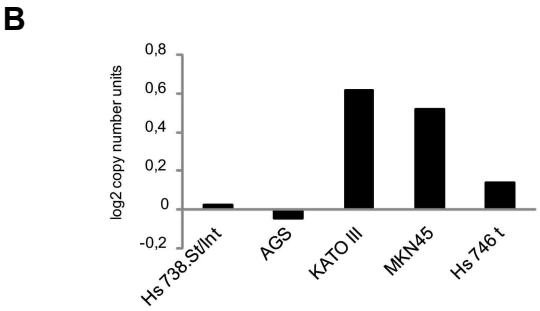

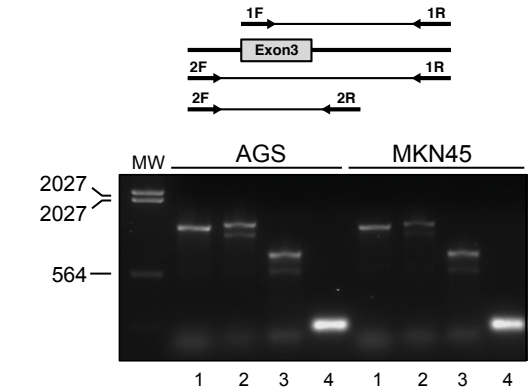

Bargiela-Iparraguirre et al. Figure Supp. 1

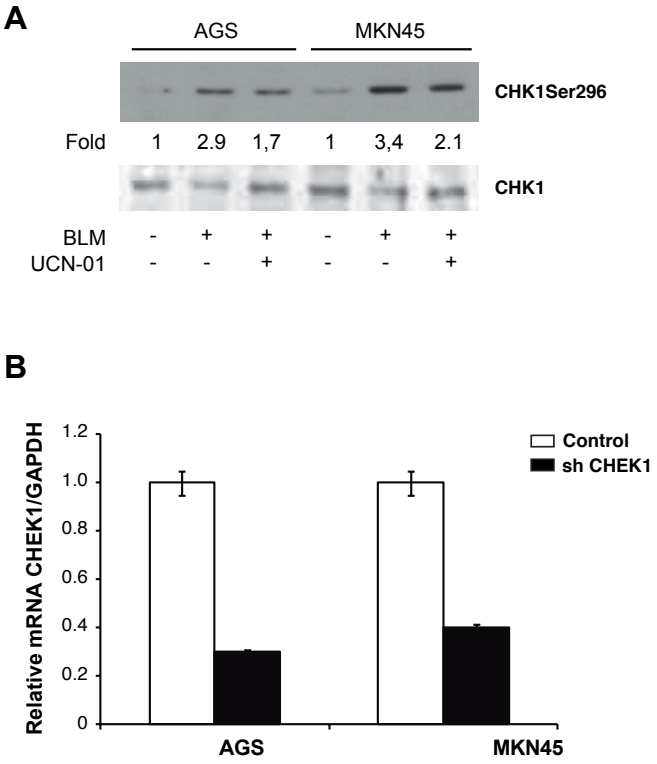

Bargiela-Iparraguirre et al. Figure Supp. 2

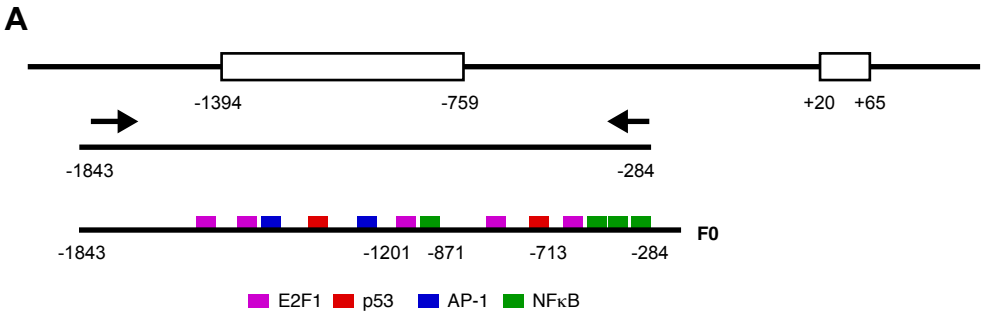
A
-1394
-759
+20
+65
-1843
-284
F0
-1843
-1201
-871
-713
-284
E2F1
p53
AP-1
NFκB

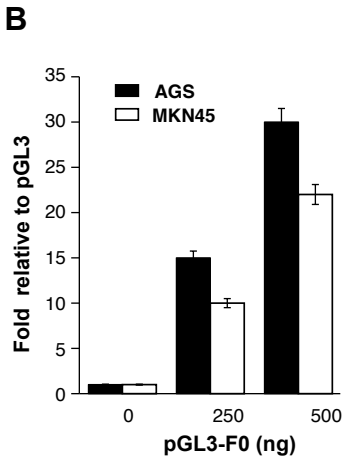
B
AGS
MKN45
Fold relative to pGL3
35
30
25
20
15
10
5
0
0
250
500
pGL3-F0 (ng)

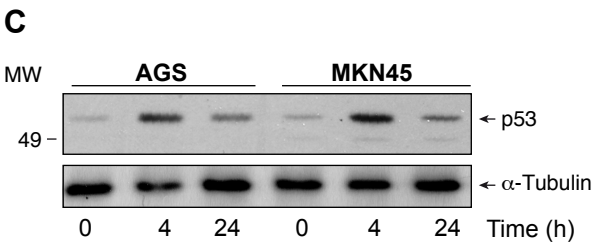
C
MW
AGS
MKN45
49
p53
α-Tubulin
0
4
24
0
4
24
Time (h)

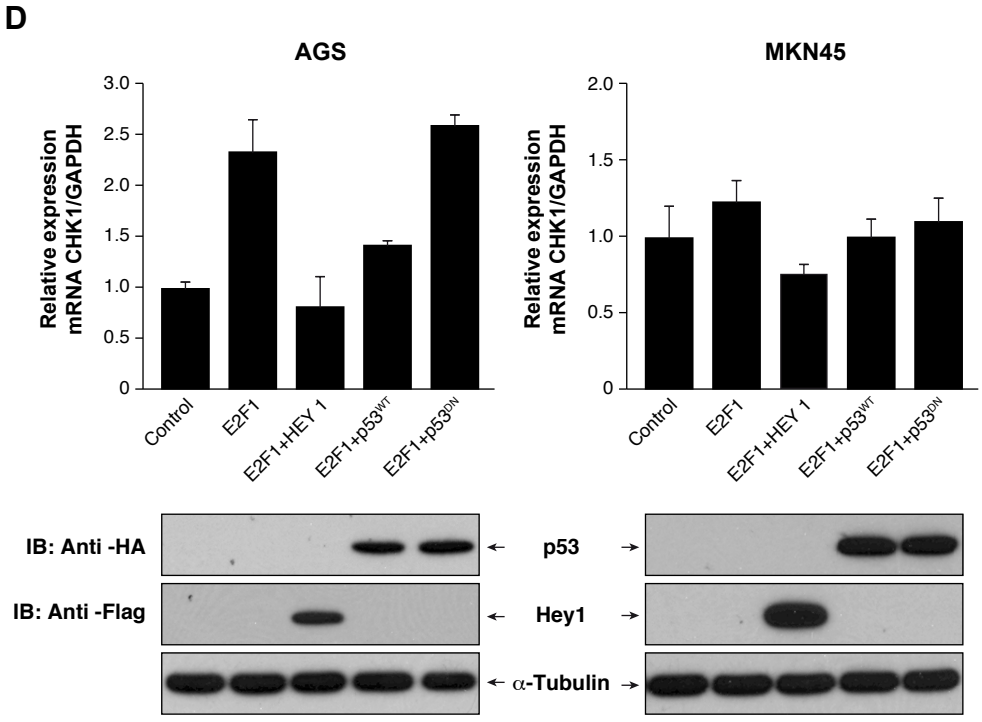
D
AGS
MKN45
Relative expression mRNA CHK1/GAPDH
3.0
2.5
2.0
1.5
1.0
0.5
0
Control
E2F1
E2F1+HEY 1
E2F1+p53WT
E2F1+p53DN
IB: Anti -HA
IB: Anti -Flag
p53
Hey1
α-Tubulin

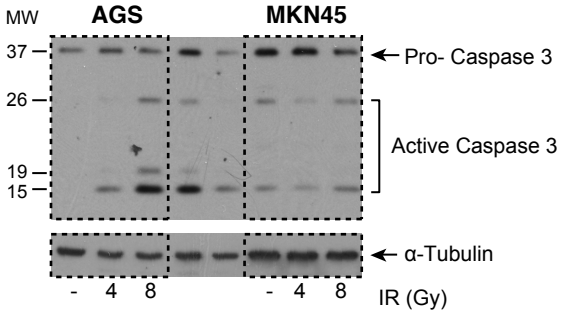
MW
AGS
MKN45
37
26
19
15
Pro- Caspase 3
Active Caspase 3
α-Tubulin
- 4 8
- 4 8
IR (Gy)

RESUMEN

DNA repair proteins, XPA and XPD and the spindle assembly checkpoint Mad2 coordinate cisplatin response in Gastric Cancer cells

Bargiela-Iparraguirre J[1†], Lozano-Pajuelo, N[†], Fernandez-Fuente M[2], Dominguez-Gomez G Perona R [1,8,9] and Sanchez-Perez I[1,,7,8,9]

Enviado a Oncogene 2017-0020

El régimen terapéutico para el tratamiento del cáncer gástrico actualmente no está optimizado para tratar la alta heterogeneidad intra e inter tumoral que presenta la enfermedad. Como se ha comentado anteriormente, Cisplatino y radiación son dos de los agentes más utilizados en la terapia para esta enfermedad. Entender la causa de la resistencia a los agentes antineoplásicos es imprescindible para avanzar en la búsqueda de biomarcadores más efectivos y terapias individualizadas.

En este trabajo hemos profundizado en el estudio de las diferencias que existen en la sensibilidad a Cisplatino y el agente radiomimetico bleomicina en cáncer gástrico. Hemos utilizado dos líneas celulares con sensibilidad opuesta a estos agentes, la línea celular AGS, resistente a Cisplatino pero sensible a Bleomicina, y la línea celular MKN45, sensible a Cisplatino y resistente a bleomicina. Nuestros resultados sugieren que la apoptosis inducida por Cisplatino se produce por la degradación de la proteína anti-apoptótica Mcl-1 y aumento de la expresión de las proteínas pro-apoptóticas Bid, Bim y Bad, mientras la muerte por bleomicina lo rigen el aumento de proteínas pro-apotóticas Bax, Bad. Además con la intención de explicar la distinta sensibilidad al Cisplatino hemos analizado la ruta de reparación por escisión de nucleótidos (NER), encargada de reparar distorsiones grandes en el DNA. Hemos comprobado mediante la cuantificación de aductos y la marca de daño en el DNA, γ-H2AX, así como por ensayo cometa que la línea celular MKN45 presenta una menor eficiencia de reparación del daño en comparación con la línea AGS. Nuestros resultados sugieren que la ausencia de translocación de las proteínas XPA y XPD al núcleo en presencia de Cisplatino influye negativamente en la eficiencia de reparación de la ruta NER en las MKN45.

Con todo ello comprobamos que dependiendo del tipo de estímulo las proteínas implicadas que dictaminan la muerte y la sensibilidad al agente pueden variar, reforzando la idea de la necesidad de conocer las proteínas especificas involucradas en la respuesta para cada agente concreto. Así proponemos que las proteínas de la familia Bcl-2 podrían ser consideradas una buena diana terapéutica y biomarcadores de respuesta en cáncer gástrico. Por otro lado la eficiencia de NER por fallos en la translocación de las proteínas XPA y XPD al núcleo puede ser considerado indicativos de una mejor respuesta al Cisplatino en cáncer gástrico.

Participación en el trabajo: Experimental y análisis de dato

DNA repair proteins XPA and XPD and the spindle assembly checkpoint Mad2 coordinate the response to cisplatin in Gastric Cancer cells.

Bargiela-Iparraguirre J[1], Lozano-Pajuelo, N[1], Dominguez-Gomez G [2] Perona R [1,4,5] and Sanchez-Perez I[1,3,4,5 *]

[1] Dpto.Bioquímica. Fac. Medicina. Instituto de Investigaciones Biomédicas Madrid CSIC-UAM; Madrid, Spain

[2] Dpto. Medicina. Fac. Medicina. Instituto de Investigaciones Biomédicas Madrid CSIC-UAM; Madrid, Spain

[3] Unidad asociada de Biomedicina UCLM-CSIC

[4] CIBER for Rare Diseases (CIBERER); Valencia, Spain

[5] Biomarkers and Experimental Therapeutics Group; IdiPAZ; University Hospital La Paz; Madrid, Spain

* Correspondence should be addressed to.

Isabel Sánchez-Pérez, PhD

Dpto. Bioquímica. Fac. Medicina. Instituto de Investigaciones Biomédicas Madrid CSIC/UAM

C/Arturo Duperier 4

28029 Madrid

Spain

Phone: (+34) 91-5854380

Fax: (+34) 91-5854401

E-mail: misanchez@iib.uam.es; is.perez@uam.es;

RUNNING TITLE: NER in gastric cancer

KEY WORDS: Bcl-2 Family, gastric cancer, apoptosis, bleomycin, cisplatin, Mad2, XPD biomarker.

ABSTRACT

Gastric cancer (GC) is one of the most common cancers worldwide and it is also one with a very poor prognosis. Resistance to apoptosis and impairment of DNA repair mechanisms after therapy are the main causes of a poor response to the available drugs. Heterogeneity between GC tumors makes it difficult to design a standard treatment protocol, which reflects the urgent need to identify molecular biomarkers able to predict therapy response. In this manuscript we aim to analyze the process of apoptosis induction in AGS and MKN45 cells, which show opposite sensitivities to the radiomimetic agent bleomycin (BLM) and cisplatin (CDDP). Our data show that in response to BLM, MKN45 cells are unable to induce the expression of pro-apoptotic proteins such as Bax, Bad and Puma. In contrast, in response to CDDP, these cells induce MCL-1 degradation and also induction of Bid and Bad, resulting in BLM resistance and sensitivity to CDDP in MKN45 but not in AGS cells. Additionally, our experiments show that nucleotide excision repair is impaired in MKN45 cells after CDDP treatment due to the absence of translocation of XPA and XPD to the nucleus. We also show that overexpression of the spindle assembly checkpoint protein Mad2, could be involved in this process. Altogether, our results suggest that Bcl-2 proteins could be good additional targets for GC treatment and Mad2 a good biomarker to predict the response to the drugs used in the clinical setting.

INTRODUCTION

Gastric cancer (GC) is currently the fourth most diagnosed cancer worlwide[25]. Despite recent improvements in survival rates, there are still too many people diagnosed at advanced stages, for which the current clinical regimen is not efficient. The standard therapy regimen consists of gastrostomy and adjuvant radio-chemotherapy with cisplatin (CDDP) and 5-Fluorouracile (5FU) treatment [23, 30].

Radiation (IR) and chemotherapy cause a variety of DNA lesions, which in turn activate the DNA damage response (DDR) [5, 30]. Checkpoint Kinase 1 (Chk1) and Chk2, key effectors in DDR, are multifunctional Ser/Thr kinase proteins, which represent crucial components of all cell cycle checkpoints [4]. They are both involved in drug resistance and also coordinate the crosstalk between different checkpoints to ensure genome stability [3, 6, 9]. For instance, previous *in vitro* studies from our lab have demonstrated that in GC, elevated levels of Chk1 and MAD2 confer resistance to radiotherapy and sensitivity to Paclitaxel (PTX) treatment respectively [3].

CDDP forms special structures upon binding DNA called DNA adducts and IR induces DNA double strand breaks (DSB), leading to cell death by apoptosis [14]. CDDP and IR stimulate the intrinsic apoptotic pathway controlled by the BCL-2 protein family [5, 24]. This family includes: the anti-apoptotic subfamily, (BCL-2, BCL-xL, BCL-w, MCL-1, BFL1/ A-1, and BCL-B proteins), the pro-apoptotic subfamily,(BAK, BAX,) and the BH3-only protein subfamily, (BIM, BID, BIK, BAD, BMF, HRK, PUMA, and NOXA proteins) [8]. Under stress, the relative expression of pro- and anti-apoptotic Bcl-2 proteins is modified [7]. BH3-only Bcl-2 proteins are activated either transcriptionally or post-transcriptionally leading to the initiation of apoptosis. DNA damage and growth factor withdrawal target Mcl-1, which will in turn be degraded by the ubiquitin-proteasome system [22]. Several studies have demonstrated that the overexpression of BCL-2 is associated with chemoresistance to cytotoxic chemotherapeutic agents in patients with GC [29, 36]. The pro-apoptotic protein BAX has been demonstrated to predict clinical responsiveness to chemotherapy in patients with GC [31]. Other BCL-2 family members (BCL-xL, BAK, MCL-1) also have a role in the regulation of chemotherapy induced apoptosis [18, 27].

This indicates that proteins from the BCL-2 family play a pivotal role in the determination of cell fate following chemotherapy, through interactions among its members.

Nucleotide Excision Repair (NER) is the main pathway responsible for the removal of bulky lesions induced by CDDP. The *Xeroderma Pigmentosum* (XP) complementation group of proteins XPA–XPG is involved in NER processes including damage recognition, unwinding, excision, and refilling of DNA [32]. Of particular importance for NER are the two helicase subunits XPB and XPD, which are known to open the DNA helix around the lesion. Then ERCC1 and XPG are recruited and cleave a fragment of the damaged strand. The final step is to fill in the gap thanks to a DNA polymerase and a ligase. The overexpression of some of the components of NER such as ERCC1 has been directly related to increased resistance to CDDP in testicular cancer [33].

DSBs are repaired mainly through two pathways, non-homologous end joining (NHEJ) and homologous recombination (HR). A pivotal role in the choice of NHEJ or HR is played by BRCA1, tumor suppressor proteins involved in several cancers such as breast cancer.

During the development of cancer, tumor cells acquire different characteristics and therefore, this intrinsic heterogeneity of the tumor makes it difficult to predict their response to drugs. We have previously described CHK1 as a biomarker of response to radiotherapy in GC [3]. In this manuscript we have compared the process of apoptosis induction in two gastric adenocarcinoma cell lines (AGS and MKN45), which show opposite sensitivities to the radiomimetic agent BLM and CDDP. Our data strongly suggest that resistance to BLM in MKN45 cells is due to the inability of cells to induce the expression of the pro-apoptotic proteins Bax, Bad and Puma. However, these cells are highly sensitive to CDDP when compared to AGS cells. When we studied the DNA damage repair NER in this cell line, our results suggest that NER is impaired in MKN45 cells due the absence of translocation of two key NER proteins (XPA and XPD) to the nucleus. In addition, the molecular mechanisms suggest that the spindle assembly checkpoint (SAC) protein Mad2, could be involved in this process. Altogether, these results increase the number of targets

that could be used as biomarkers to predict the response to drugs used in the clinical setting.

RESULTS

1. Bcl2-family control CCPD-induced cell death in AGS and MKN45 cells.

We have previously reported that human adenocarcinoma AGS and MKN45 cell lines differ in their sensitivity to some of the most popular antineoplastic agents such as Paclitaxel (PXL) and BLM. MKN45 overexpress both MAD2 and CHK1, checkpoint proteins which are responsible of resistance to PTX and BLM respectively [2, 3]. Here, we study the viability of these cell lines after treatment with CDDP in order to elucidate the main cellular pathways ruling the unequal sensitivity to this agent in GC cells. Our results showed that survival decreases in a dose dependent manner after CDDP exposure in both cell lines but with different sensitivity, being AGS more resistant than MKN45 cells (IC_{50} 7,6 ug/ml vs IC_{50} 2ug/ml in AGS and MKN45 cells respectively) (Figure 1A- upper graph). Then we studied the molecular pathways involved in drug resistance: apoptosis, senescence and autophagy. We detected PARP cleavage 24 hours after CDDP treatment in MKN45 but not in AGS, suggesting that there is a difference in apoptosis induction (Figure 1A lower panel) between cell lines. In order to study senescence we performed a β-galactosidase activity assay in AGS and MKN45 cells treated with CDDP (2, 5 μ/ml) or BLM (3 μ/ml) for 72 hours. Our results showed a significant induction of senescence in both cell lines after CDDP and BLM treatment (Figure 1B). Given that autophagy is also a pro-survival mechanism related to drug resistance, we decided to study the main protein markers involved in this process: p62 and LC3-II. Degradation of p62 occurs when the autophagy process is activated; in our hands, GC cells showed similar behavior after treating with CDDP or BLM in p62 degradation (Figure 1C). These results suggested that CDDP-induced apoptosis in MKN45 is mediated by different molecular targets.

The above results encouraged us to study in depth the involvement of Bcl-2 proteins in apoptosis. To this aim, we investigated whether potential differences in the expression of

the pro-survival BCL2-like proteins (BCL-XL and Mcl-1), the pro-apoptotic factors and BH3 relatives: Bak, Bax, Bid, Bad and Puma could explain the differences in the survival rate observed among the different GC cell lines after treatment with our drugs of study. AGS and MKN45 cells were treated with CDDP and BLM for a number of time points, ranging from 0 to 24 hours. We observed that in response to CDDP, the expression of the anti-apoptotic protein Mcl1 was induced almost 3-fold after 3 hours of treatment in AGS cells. In contrast, this protein was downregulated in MKN45 (almost 70%) after 9 hours of exposure to CDDP. Furthermore, the expression of pro-apoptotic proteins Bak, Bad and Bid was induced after 3 hours (Bak) and 9 hours (Bad and Bid) of treatment in MKN45 cells, whilst no effect was observed in AGS cells. Finally, Puma protein which induction is controlled by p53, was strongly induced in AGS cells and at a lesser extent in MKN45 cells (Figure 2A and Supplementary Figure 1). These results suggest that the higher sensitivity of MKN45 to CDDP is controlled by the downregulation of Mcl1, and by the upregulation of Bid and Bad. Similar studies on BLM reveled that in AGS cells, Mcl-1 levels are not modified by the treatment, while Bcl-XL is transiently decreased in MKN45 but not in AGS cells. In contrast with the regulation of the proapoptotic proteins set by CDDP, BLM strongly increased Bax, Bid, Bad and Puma expression in AGS Cells, while only Bax and Puma increased in MKN45 cells. These results suggest that resistance to BLM is controlled by an inability to upregulate the proapoptotic proteins Puma and Bax (Figure 2B and Supplementary Figure 2). Our data clearly support the hypothesis that specific Bcl2-family proteins control sensitivity to CDDP or BLM depending on the background of each cell line.

Mcl-1 expression is controlled both at transcriptional and posttranslational level. Phosphorylation of MCL-1 via JNK and p38 leads to ubiquitination-mediated MCL-1 degradation. We analyzed MAPKs activity in GC cells after CDDP treatment, and our data indicated that ERK kinases are strongly activated in AGS cells, when compared with MKN45 cells. Surprisingly, CDDP activated the stress kinases JNK and p38 only in MKN45 cells. Finally, we detected the expression of DUSP1, the main phosphatase responsible of inactivation of JNK and p38, and showed overexpression of DUSP1 in AGS cells, which explains the absence of JNK or p38 activation in this cell line. To analyze whether the p38

activity contributes to degradation of MCL1 in MKN45 cells, we used the pharmacological inhibitors SB203580 and PD098059. Our results indicated that in MKN45 cells Mcl1 is degraded in response to CDDP, while inhibition of p38 abolishes its degradation (Figure 2C), but not after JNK inhibition. These results strongly suggest that CDDP-induced apoptosis in sensitive MKN45 cells is modulated by Mcl-1 degradation in a process that depends on p38 expression.

DNA damage repair is impaired in MKN45 treated with CDDP

After an insult, cells induce cell cycle arrest in order to have enough time to repair potential lesions. DNA repair pathways are induced before apoptosis and improper DNA repair is one of the reasons which sensitize cells to drugs. We analyzed the activation of DDR in AGS and MKN45 cells after CDDP treatment and observed a transient activation of CHK1 and CHK2 3 hours after the initiation of this treatment (Supplementary Figure 2). These data indicate that activation of DDR takes place in both cell lines in a similar fashion. Next, we performed a set of experiments to study the DNA repair status in both cell lines. CDDP binds DNA and forms intra and interstrand-crosslinks called adducts. We tested the amount of adducts formed in AGS and MKN45 in order to evaluate the ability of CDDP to reach and react with the DNA, and also the capability of cells to repair from DNA damage. To this end, AGS and MKN45 cells were treated 3 hours with CDDP (10 ug/ml), washed and then allowed to recover for an hour. We quantified the fluorescence intensity of the nuclei by using a specific antibody which recognizes CDDP-adducts, and found that in both cell lines, nuclear intensity increased after 3 hours of CDDP treatment. One hour after CDDP withdrawal, intensity decreased in AGS cells, while no significant differences were observed in MKN45 cells (Figure 3A and Supplementary Figure 2B). To corroborate these data, we also carried out immunofluorescence analysis using antibodies against y-H2AX$^{Ser\ 139}$, which allowed us to quantify the number of DNA damaged foci per cell. Our data showed that 3 hours after CDDP treatment the number of foci per cell increased significantly on a range of 16 to 50 foci per nuclei. However, after 1 hour of recovery, we observed that DNA damage decreased

in AGS (range > 50 foci/nuclei) while it increased even more in MKN45 cells (Figure 3B). Finally, we performed a comet assay to evaluate the repair rate in these cells after CDDP and BLM treatment. Tail moment data showed that AGS cells were able to repair CDDP adducts within one hour; in contrast, MKN45 cells needed at least 3 hours to remove the damage. Accordingly, the percentage of Residual Damage (%RD) reached 7.93± 1.4 in AGS *versus* 65.21±2.9 in MKN45 cells. Taking advantage of the fact that we know that MKN45 cells are more resistant to BLM than AGS cells, we performed the same set of experiments after exposure to BLM, and we observed that 45 minutes after treatment the RD is 10% in MKN45 cells and still 100% in AGS cells (Figure 3C). These results strongly suggest that a potential deficiency on NER repair mechanisms in MKN45 cells could also be one of the reasons of increased sensitivity to CDDP.

In order to assess the occurrence of putative relationships between the expression of NER-associated factors and CDDP resistance, we set out to determine the protein expression levels of the respective DNA repair pathway factors in CDDP sensitive (MKN45) and resistant (AGS) cells. To evaluate NER capacity, we first analyzed the levels of core NER factors XPA, XPD and ERCC1 in both cell lines at different times after CDDP treatment, since previous reports have demonstrated an increase in the expression of core NER factors including ERCC1 in CDDP resistance. We observed a clear induction of ERCC1 from 12 to 24 hours of treatment in both cell lines, with no significant changes in the expression of XPD. Furthermore, XPA increased after CDDP treatment in both cell lines (Figure 4A). Since ATR is known to increase NER activity by phosphorylating and thus stabilizing XPA in response to DNA damage [20], we analyzed ATR kinase activity indirectly by monitoring the level of phosphorylation of its substrate proteins p53 and CHK1. Our results indicated identical ATR activity in both cell lines, as no significant alteration in phosphorylation of p53 or CHK1 was detected regardless of the cells type.

XPA suffers posttranscriptional modifications such us phosphorylation by ATR and MAPKs. In order to determine the effect of these kinases over XPA we treated MKN45 cells with caffeine in the presence or absence of CDDP. Our experiments showed that pretreatment with caffeine reduces the mobility shift of XPA, which points to a phosphorylated state of

this protein. To verify this, AGS and MKN45 cells were transfected with ATR^{WT} and ATR^{DN} expression vector, and consistently with our previous data, XPA was again found to be downregulated. No differences were found between cells treated with JNK or P38 inhibitors (Supplementary Figure 2).

After damage, XPA translocates to the nucleus in order to exert its action. We therefore examined XPA localization, and also that of other members of the NER pathway. Subcellular fractionation and western blot analysis revealed that XPC was highly expressed in AGS cells and its localization is restricted to the nucleus independently of CDDP challenge; however the amount of XPC in MKN45 cells was considerably reduced. The same result was obtained for XPD, which is concentrated in nucleus and increased after CDDP treatment in AGS cells; However, in MKN45 cells the protein was strongly reduced, and no translocation to the nucleus was observed. Finally, we observed that XPA, the key rate-limiting factor for NER [17], was translocated from the cytosol into the nucleus after DNA damage induced by CDDP in AGS cells. Interestingly, we did not find relocalization of XPA in MKN45 cells where this factor remains localized in the cytoplasm (Figure 4C and Supplementary Figure 2B).

It has been described that the SAC protein Mad2 interacts with XPD after CDDP treatment in 293T cells. We therefore preformed co-inmunoinfluorescences to study MAD2 and XPD localization and its possible interaction in AGS and MKN45 cells in the absence or presence of CDDP. According with our subcellular localization results, we found that in AGS cells Mad2 is mainly localized in the nucleus and colocalized with XPD after CDDP treatment. However, in MKN45 cells Mad2 showed cytoplasmic and nuclear distribution, and in the presence of CDDP its expression appeared to decrease in the nucleus without any signs of translocation of XPD to the nucleus (Figure 4D).

Altogether, our results suggest that the different NER efficiency between these cell lines is based on the absence of XPA and XPD translocation to the nucleus in the sensitive cells to CDDP, in a process that is modulated by Mad2.

Discussion

Resistance to therapy is a main obstacle for the effective treatment of GC. Even when we face the same type of tumor, we have to consider that the response to a given drug could be dramatically different from one patient to another. It is therefore imperative to gain insight into the mechanisms that drugs use to kill cells in order to increase our arsenal of biomarkers which allow us to personalize the treatment for every specific patient.

In this manuscript, we demonstrate that CDDP induces apoptotic cell death through the inhibition of the anti-apoptotic protein Mcl-1, and an induction of the pro-apoptotic BH3-only protein Bad and Bid in sensitive GC cells (MKN45). Our findings are in agreement with recent reports, revealing that suppression of the FoxM1/Mcl-1 pathway impairs cell viability and thus increases sensitivity to CDDP in GC cells [22]. In contrast, sensitivity to BLM is controlled by induction of the proapoptotic proteins Bax, Bad, Bid and Puma. We found that the induction of Puma and Bax is crucial in this process, because the absence of these proteins correlates with the BLM resistant phenotype of MKN45. Puma protein is a direct target of p53; the status of p53 in MKN45 cells is WT (wild type) and it is activated in both cell lines (AGS and MKN45) [3]. One possibility could be an epigenetic silencing of the Puma promoter in these cells as it has been reported for other types of cancer [12]. These data reinforce the need to identify specific Bcl-2- family targets specific for the treatment. The development of compounds mimicking the function of BH3-only proteins is an emerging area of research. Thus, huge amounts of inhibitors had been developed in the last decade, and a number of clinical trials are currently being performed to study their effects in combination with chemotherapy [8].

Since NER is the major mechanism for removing intra-strand crosslinks induced by CDDP, NER factors have been widely studied [16]. However, the contribution of NER to CDDP resistance is not well defined, and the effect of NER factors down-regulation on CDDP sensitivity has remained contradictory. Our results show that the expression and translocation of XPD and XPA to the nucleus in MKN45 cells is abolished, and as a consequence, DNA repair in response to CDDP is impaired, due to a lack of ability to reach the DNA damage and NER machinery. Furthermore, our results strongly suggest that this is not due to a postranslational modification of XPA, as it is equally controlled by ATR after CDDP treatment in both GC cell lines.

XPD plays an essential role in DNA repair within the NER pathway. Additionally, it may also interact with specific targets to mediate a diverse set of biological functions including cell cycle regulation, mitosis, and mitochondrial function [15]. The loss of XPD expression caused asynchronous cell division and chromosome instability and it also has been shown that the absence of XPD, leads to improper chromosome segregation [21] .We observed that in sensitive cells, XPD is not able to increase its levels inside the nucleus after CDDP treatment as it does on resistant cells. In addition, we only detected colocalization of Mad2 and XPD in AGS cells. This interaction has previously been described in 293T cells [11]. Mad2 is a protein which can adopt different structures thanks to the flexibility of its HORMA domain. During mitosis, Mad2 switches between its opened and closed conformations, and during interphase it resides at the nucleoporin complex (NPCs), where it interacts with Nup153 and Trp [28]. Our data support the idea that high levels of the SAC protein Mad2 abolishes the proper interaction with XPD in MKN45 cells, which then either interferes with the access to the DNA lesion or abolishes the helicase activity on XPD. Interestingly, we have demonstrated that MKN45 cells, which show high levels of Mad2, are resistant to IR and this correlates with high levels of CHK1 [3 2]. Here we show that the DNA repair in response to the radiomimetic agent BLM is highly efficient. We do suggest an important role of SAC proteins in the control of the processes of DNA repair; although further studies should be carried out in order to clearly identify their direct or indirect contribution. In favor of this new function we propose for SAC proteins, the role of Bub1 in promoting NHEJ activity in response to DNA damage has recently described, and it is consistent with the existence of synergistic interactions between DSB repair and SAC genes [10], as well as with the known role of Bub1 in DDR signaling [35].

The relationship of these proteins with cancerogenesis further supports a broad applicability of our findings to support future studies aimed at characterizing the mechanistic function for these variants in gastric tumors and in the development of target- and mechanism-based therapeutics. Therefore, targeting the key DNA repair pathways involved in CDDP resistance may constitute an effective strategy for surmounting CDDP resistance in GC cells.

MATERIAL AND METHODS

Cell lines. AGS and MKN45 human gastric adenocarcinoma cell lines were cultured in F12-Kaings and RPMI mediums respectively (Gibco), and supplemented with FBS (10% for AGS and 20% for MKN45). Cultures were maintained at 37 °C, 5% CO2 and 95% humidity. AGS and MKN45 are wild type for TP53. [3]

Chemicals and plasmid Vectors

BLM was acquired from Calbiochem (http://www.merckmillipore.com/spain/life-science-research), and CDDP was kindly donated from Ferrer FARMA. Hidroxyurea was purchased from Sigma Aldrich. DAPI (used for DNA staining) was purchased from Invitrogen.

ATR and ATR-dn were kindly donated by Dra. P. Muñoz-Cánoves [34]. Crystal violet used for cell viability studies was purchased from Promega.

Cell viability.

Viability and growth rate were determined using a crystal violet based staining method, as previously described [1]. To assess the effects of irradiation, cells were irradiated with different doses of Gy (0–8 Gy) using a 137Cs source (mark 1, model 30, JL. Shepherd & Associates San Fernando CA; Dose rate to 100 mm diameter samples is ~370 R/minute.

Senescence assay.

A total of $15x10^3$ cells were seeded on 6 MW plates. Cells were stimulated with CDDP Doses and BLM for 48 and 72 hours. After the treatment period, cells were transferred fresh medium and 3 days later β-galactosidase (SA-b-Gal) activity was quantified using the Senescence detection kit (Biovision, http://www.biovision.com/). Ten areas were counted with the objective 20x in a microscope Nicon Eclipse TS100 and ANOVA1 was performed with IBM SPSS 22 software.

Western blotting.

Twenty µg of protein per sample were loaded in SDS-PAGE in 15% (for Bcl2-family), 10% (MAPKs and NER Factors or 8% (PARP-1) polyacrylamide gels, and then transferred onto nitrocellulose membranes, followed by inmunodetection using appropriate antibodies, as

follows: . Antibodies against Chk1 (1:500, sc-377231), PARP-1 (1:1000, sc-7150), MAD2L1 (1:1000, sc-28261) and Mcl-1 (1:1000, sc-819) were purchased from Santa Cruz Technology. The following antibodies were all purchased from Cell signaling: Cleaved Caspase-3 (Asp175) (#9661), p53 (#9282). Bad (#9942), Bax ,(#9942), Bak (#9942), Puma (#9942), BID (#9942), XPD (#4636), p62 (#5114) . The polyclonal Antibody Anti-ACTIVE® JNK pAb, Rabbit, (pTPpY) was acquired from Promega Corporation-Spain. Finally, we purchased our Flag antibody (1:2000) from Sigma. Unless otherwise specified, all the above antibodies were used at a working dilution of 1:1000.

Inmunoflorescence.

Cells were fixed in formaldehyde for 20 min, washed with PBS and permeabilized with Triton 0,5% for 10 min, blocked with BSA 5% for 1 hour. Samples were incubated overnight with the primary antibody at 4C, followed by a 1 hour incubation with the adequate secondary antibody at room temperature. DNA was stained with DAPI**.** Fluorescence microscopy was performed using a NIKON Eclipse 90i, and for the image analysis the software program Nikon NIS-Elements and Image J were used. The primary antibodies used in our study were γ-H2AXSer139, purchased from Millipore, Mad2 -D8A7 (1:300; #4636) from Cell Signaling and XPD (1:100; #1284) from Sigma Aldrich. All Secondary antibodies, conjugated with Alexa Fluor 488, (1:500) were purchased from Invitrogen. γ- H2ax foci were quantified with Cell Profiler software and analyzed with IBM SPSS 22 with 2 way ANOVA test.

Comet assay.

We performed the comet assay under alkaline conditions as described by Singh et al [19].

Briefly, cells were treated for 3 hours with CDDP (10 ug/ml) or BLM (3 ug/ml). After embedding in agarose, cells were irradiated at a dose of 2 Gy on ice and immediately immersed in lysis buffer. For the repair assay, cells were then allowed to recover from the induced damage by thorough washes in PBS and incubation at 37C in 5% fresh media for 30 minutes, 1, 2 and 3 hours for CDDP and 45 minutes, 90 minutes and for 3 hours when BLM treatment was used. TM was calculated with ImageJ OpenComet plugin, data were analyzed with IBM SPSS 22 with Kruskal-Wallis and Mann-Whitney tests

Scoring DNA damage. Immediately before imaging analysis, slides were stained with 60 μl of a 1μg/mL ethidium bromide solution for 10 minutes and covered with coverslips before imaging using a 20X objective under a fluorescence microscope (NIKON90i). Experiments were performed in duplicate. One hundred consecutive cells (50 from each duplicate slide) were randomly selected (carefully avoiding the borders of the slides), scored and quantified by Image J analysis software. The extent of the damage was measured quantitatively by the tail moment (TM), defined as the product of the percentage of DNA in the comet tail and the tail length[13] .For the analysis of repair kinetics, the percentage of residual DNA damage (%RD) at time *t* after irradiation was calculated as follows: % RD=100 X [(DNA damage at time *t* after irradiation – DNA damage in control cells before irradiation)/ (DNA damage immediately after irradiation - DNA damage in control cells before irradiation)] [26].

Statistical analysis. The Kruskal-Wallis test, a non-parametric procedure was used to compare responses, as measured by TMs. Repair ability was measured as the percentage of residual damage at time *t* which was calculated as described above. All statistical analyses were conducted using SSPS software. At least 100 nuclei were measured per condition in inmunofluorescences assays. Statistical significance (at $p < 0.05$) was obtained using IBM SPSS 22 software.

ACKNOWLEDGMENTS

This work was supported by PI1401495 (supported by FEDER funds) from Fondo de Investigaciones Sanitarias, Instituto de Salud Carlos III, Spain. We are grateful to Javier Pérez (photography facility), Diego Navarro and Lucia Sanchez (microscopy facility IIBM) for their technical assistance. We appreciate the comment, suggestions and proof reading of the manuscript to the Dr. Marta Fernandez-Fuente. JBI is a fellow of the Programa de Doctorado Doble en Ciencias Biomedicas UNAM, Mexico City, Mexico/Biociencias Moleculares UAM, Madrid, Spain. JBI was supported by a fellowship from Catedra Isaac Costero, funded by Banco Santander-UAM and Beca Nacional de Posgrado CONACYT. NPL is a fellow of the Programa de Doctorado Biociencias Moleculares UAM, Madrid, Spain. NPL was supported by a fellowship Programa de Formación de Profesorado Universitario REF: FPU15/04669,

Ministerio de Educación, Cultura y Deporte. The authors declare that they have no competing relationship, commercial affiliations or financial interests.

Figure 1. AGS and MKN45 show different sensitivity to CDDP. A) Survival percentage of AGS and MKN45 cells after 48h of CDDP treatment. Cells were treated with increasing concentrations of CDDP (0- 20ug/ml). The percentage of viable cells was quantified by the crystal violet method. Data represent the mean values obtained in three experiments performed in quadruplicate. Lower panel: Cleavage of PARP-1 detected by western blot (WB) in cells harvested at the indicated times after CDDP treatment (10 μg/ml). α-Tubulin was used as loading control. B) Representative images of AGS and MKN45 senescence cells after 72h of CDDP (2,5 μg/ml) and BLM at its IC50 dose (3 μg/ml for AGS and 10 μg/ml for MKN45). The graph represents the percentage of senescent cells for each experimental condition. C) AGS and MKN45 cells were treated with CDDP (10 μg/ml) or BLM (10 μg/ml) for the indicated periods of time. Immunodetection of p62 protein was carried out by using specific antibodies. $\alpha-$ tubulin was used as a loading control.

Figure 2. Bcl2-family controls CDDP and BLM induced apoptosis in AGS and MKN45 cells. A) Bcl-2 protein family members were detected by western blot in AGS and MKN45 cells treated with CDDP (10 μg/ml) at the indicated periods of time. B) Bcl-2 protein family members detection performed by western blot in AGS and MKN45 cells treated with BLM (10 μg/ml) at the indicated time points. C) Cells were treated as in A) ERK, JNK, p38 and DUSP1 were detected by using specific antibodies. D) AGS and MKN45 cells were pretreated during 30 minutes with 10 μM inhibitor p38 (SB203580) or JNK Inhibitor II before CDDP treatment. Mcl-1 was detected by WB at the indicated times after treatment. α-tubulin was used as loading control and for protein quantification.

Figure 3. DNA repair is impaired in MKN45 cells. A) Graph represents nuclear fluorescent intensity of DNA adducts formed after treating AGS and MKN45 with CDDP (10 μg/ml). Control cells (white bars) were untreated, CDDP (grey bars) cells were treated with CDDP for 3 hours. Repair (black bars) represents cells treated with CDDP for 3 hours and then allowed to recover in normal media for 1h before harvesting. B) AGS and MKN45 cells were treated as in A), and y-H2AX foci were detected by Immunofluorescence, using DAPI to stain nuclear DNA. Graphs represent the percentage of nucleus within less than 15, between 15-

50 and more than 50 y-H2Ax/nuclei for each condition. D) Graphs represent the mean Tail Moment ™measured in at least 50 cells per duplicated in each condition after CDDP treatment (left graph) and BLM treatment (right graph). Tables present the percentage of residual damage (RD) after the repair period that follows CDDP (left table) or BLM treatment (right table)..

Figure 4. Nuclear translocation of XPA and XPD proteins is abolished in MKN45 cells after DNA damage. A) XPD, ERCC1 and XPA were detected by western blot in AGS and MKN after CDDP (10 μg/ml) treatment at the indicated times. α-tubulin was used as a loading control. B) XPA levels in AGS and MKN45 cells after 6 hours of CDDP treatment (10 μg/ml) in the presence of caffeine (80mM) and transfected with ATR^{WT} or ATR^{DN} plasmids. C) Nuclear and cytoplasmic localization of NER proteins and MAD2 were detected by western blot in AGS and MKN45 cells after 6 hours of CDDP treatment (10 μg/ml) and cellular fractioning. α-tubulin was used as citoplasmatic protein loading control, and Lamin B1 was used as nuclear protein control. D) Cellular localization of MAD2 and XPD in AGS and MKN45 control cells, and cells treated with CDDP (10 ug/ml) for 6 horus were studied by immunofluorescence by using specific antibodies. Images were taken with a 63X objective. Graphs represent nuclear fluorescence quantification. A.U= Arbitrary Units.

References

1 Bargiela-Iparraguirre J, Prado-Marchal L, Jiménez-Lozano N, Jiménez B, Perona R, Sánchez-Pérez I. Mad2 and BubR1 modulates tumourigenesis and Paclitaxel response in MKN45 gastric cancer cells. Cell cycle 2014: 00-00.

2 Bargiela-Iparraguirre J, Prado-Marchal L, Pajuelo-Lozano N, Jimenez B, Perona R, Sanchez-Perez I. Mad2 and BubR1 modulates tumourigenesis and paclitaxel response in MKN45 gastric cancer cells. Cell cycle 2014; 13: 3590-3601.

3 Bargiela-Iparraguirre J, Prado-Marchal L, Fernandez-Fuente M, Gutierrez-Gonzalez A, Moreno-Rubio J, Munoz-Fernandez M *et al*. CHK1 expression in Gastric Cancer is modulated by p53 and RB1/E2F1: implications in chemo/radiotherapy response. Sci Rep 2016; 6: 21519.

4 Bartek J, Lukas J. Chk1 and Chk2 kinases in checkpoint control and cancer. Cancer Cell 2003; 3: 421-429.

5 Basu A, Krishnamurthy S. Cellular responses to Cisplatin-induced DNA damage. Journal of nucleic acids 2010; 2010.

6 Chila R, Celenza C, Lupi M, Damia G, Carrassa L. Chk1-Mad2 interaction: a crosslink between the DNA damage checkpoint and the mitotic spindle checkpoint. Cell cycle 2013; 12: 1083-1090.

7 Delbridge AR, Strasser A. The BCL-2 protein family, BH3-mimetics and cancer therapy. Cell Death Differ 2015; 22: 1071-1080.

8 Delbridge AR, Grabow S, Strasser A, Vaux DL. Thirty years of BCL-2: translating cell death discoveries into novel cancer therapies. Nat Rev Cancer 2016; 16: 99-109.

9 Dillon MT, Good JS, Harrington KJ. Selective targeting of the G2/M cell cycle checkpoint to improve the therapeutic index of radiotherapy. Clin Oncol (R Coll Radiol) 2014; 26: 257-265.

10 Dotiwala F, Harrison JC, Jain S, Sugawara N, Haber JE. Mad2 prolongs DNA damage checkpoint arrest caused by a double-strand break via a centromere-dependent mechanism. Current biology : CB 2010; 20: 328-332.

11 Fung MK, Han HY, Leung SC, Cheung HW, Cheung AL, Wong YC *et al*. MAD2 interacts with DNA repair proteins and negatively regulates DNA damage repair. Journal of molecular biology 2008; 381: 24-34.

12 Garrison SP, Jeffers JR, Yang C, Nilsson JA, Hall MA, Rehg JE *et al*. Selection against PUMA gene expression in Myc-driven B-cell lymphomagenesis. Molecular and cellular biology 2008; 28: 5391-5402.

13 Gutierrez-Gonzalez A, Belda-Iniesta C, Bargiela-Iparraguirre J, Dominguez G, Alfonso PG, Perona R *et al*. Targeting Chk2 improves gastric cancer chemotherapy by impairing DNA damage repair. Apoptosis : an international journal on programmed cell death 2013; 18: 347-360.

14 Ho GY, Woodward N, Coward JI. Cisplatin versus carboplatin: comparative review of therapeutic management in solid malignancies. Crit Rev Oncol Hematol 2016; 102: 37-46.

15 Houten BV, Kuper J, Kisker C. Role of XPD in cellular functions: To TFIIH and beyond. DNA repair 2016; 44: 136-142.

16 Jung Y, Lippard SJ. Direct cellular responses to platinum-induced DNA damage. Chem Rev 2007; 107: 1387-1407.

17 Kang TH, Reardon JT, Sancar A. Regulation of nucleotide excision repair activity by transcriptional and post-transcriptional control of the XPA protein. Nucleic acids research 2011; 39: 3176-3187.

18 Kubo T, Kawano Y, Himuro N, Sugita S, Sato Y, Ishikawa K *et al*. BAK is a predictive and prognostic biomarker for the therapeutic effect of docetaxel treatment in patients with advanced gastric cancer. Gastric Cancer 2016; 19: 827-838.

19 Landi S, Norppa H, Frenzilli G, Cipollini G, Ponzanelli I, Barale R *et al*. Individual sensitivity to cytogenetic effects of 1,2:3,4-diepoxybutane in cultured human lymphocytes: influence of glutathione S-transferase M1, P1 and T1 genotypes. Pharmacogenetics 1998; 8: 461-471.

20 Lee TH, Park JM, Leem SH, Kang TH. Coordinated regulation of XPA stability by ATR and HERC2 during nucleotide excision repair. Oncogene 2014; 33: 19-25.

21 Li X, Urwyler O, Suter B. Drosophila Xpd regulates Cdk7 localization, mitotic kinase activity, spindle dynamics, and chromosome segregation. PLoS Genet 2010; 6: e1000876.

22 Li X, Liang J, Liu YX, Wang Y, Yang XH, Bao H *et al*. Knockdown of the FoxM1 enhances the sensitivity of gastric cancer cells to cisplatin by targeting Mcl-1. Pharmazie 2016; 71: 345-348.

23 Macdonald JS, Smalley SR, Benedetti J, Hundahl SA, Estes NC, Stemmermann GN *et al*. Chemoradiotherapy after surgery compared with surgery alone for adenocarcinoma of the stomach or gastroesophageal junction. N Engl J Med 2001; 345: 725-730.

24 Maier P, Hartmann L, Wenz F, Herskind C. Cellular Pathways in Response to Ionizing Radiation and Their Targetability for Tumor Radiosensitization. Int J Mol Sci 2016; 17.

25 Mandeville KL, Krabshuis J, Ladep NG, Mulder CJ, Quigley EM, Khan SA. Gastroenterology in developing countries: issues and advances. World J Gastroenterol 2009; 15: 2839-2854.

26 Marcon F, Andreoli C, Rossi S, Verdina A, Galati R, Crebelli R. Assessment of individual sensitivity to ionizing radiation and DNA repair efficiency in a healthy population. Mutation research 2003; 541: 1-8.

27 Matsumoto M, Nakajima W, Seike M, Gemma A, Tanaka N. Cisplatin-induced apoptosis in non-small-cell lung cancer cells is dependent on Bax- and Bak-induction pathway and synergistically activated by BH3-mimetic ABT-263 in p53 wild-type and mutant cells. Biochemical and biophysical research communications 2016; 473: 490-496.

28 Mossaid I, Fahrenkrog B. Complex Commingling: Nucleoporins and the Spindle Assembly Checkpoint. Cells 2015; 4: 706-725.

29 Nakata B, Muguruma K, Hirakawa K, Chung YS, Yamashita Y, Inoue T *et al*. Predictive value of Bcl-2 and Bax protein expression for chemotherapeutic effect in gastric cancer. A pilot study. Oncology 1998; 55: 543-547.

30 Orth M, Lauber K, Niyazi M, Friedl AA, Li M, Maihofer C *et al*. Current concepts in clinical radiation oncology. Radiat Environ Biophys 2014; 53: 1-29.

31 Pietrantonio F, Biondani P, de Braud F, Pellegrinelli A, Bianchini G, Perrone F *et al*. Bax expression is predictive of favorable clinical outcome in chemonaive advanced gastric cancer patients treated with capecitabine, oxaliplatin, and irinotecan regimen. Transl Oncol 2012; 5: 155-159.

32 Spivak G. Nucleotide excision repair in humans. DNA repair 2015.

33 Usanova S, Piee-Staffa A, Sied U, Thomale J, Schneider A, Kaina B *et al*. Cisplatin sensitivity of testis tumour cells is due to deficiency in interstrand-crosslink repair and low ERCC1-XPF expression. Mol Cancer 2010; 9: 248.

34 Vidal B, Parra M, Jardi M, Saito S, Appella E, Munoz-Canoves P. The alkylating carcinogen N-methyl-N'-nitro-N-nitrosoguanidine activates the plasminogen activator inhibitor-1 gene through sequential phosphorylation of p53 by ATM and ATR kinases. Thromb Haemost 2005; 93: 584-591.

35 Yang C, Wang H, Xu Y, Brinkman KL, Ishiyama H, Wong ST *et al*. The kinetochore protein Bub1 participates in the DNA damage response. DNA Repair (Amst) 2012; 11: 185-191.

36 Zhuang M, Shi Q, Zhang X, Ding Y, Shan L, Shan X *et al*. Involvement of miR-143 in cisplatin resistance of gastric cancer cells via targeting IGF1R and BCL2. Tumour Biol 2015; 36: 2737-2745.

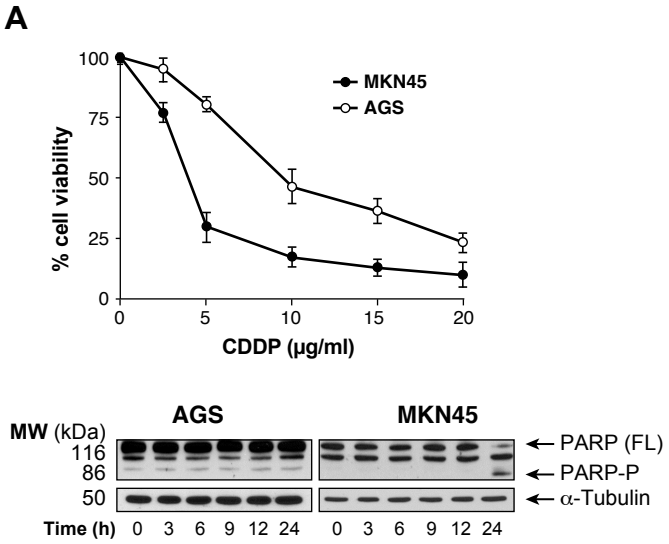

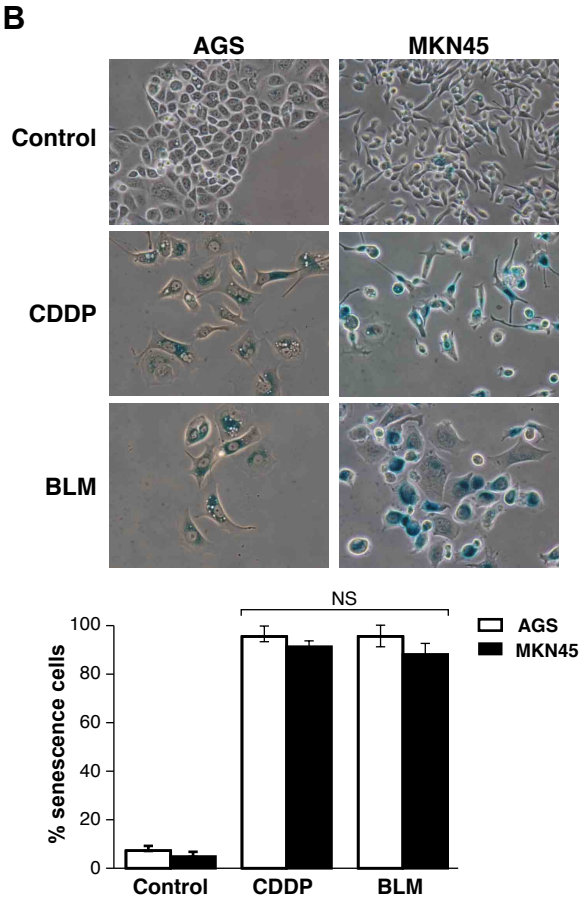

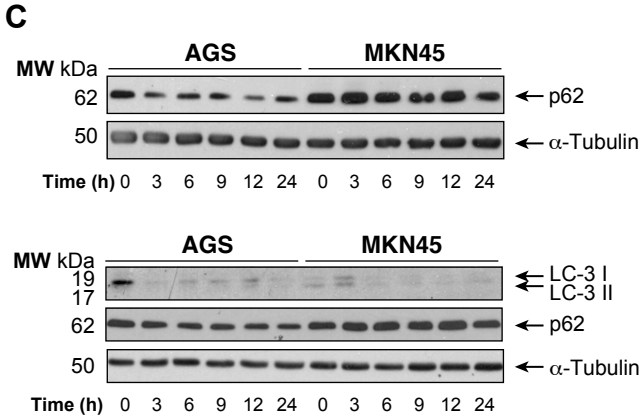

Bargiela-Iparraguirre et al. Figure 1

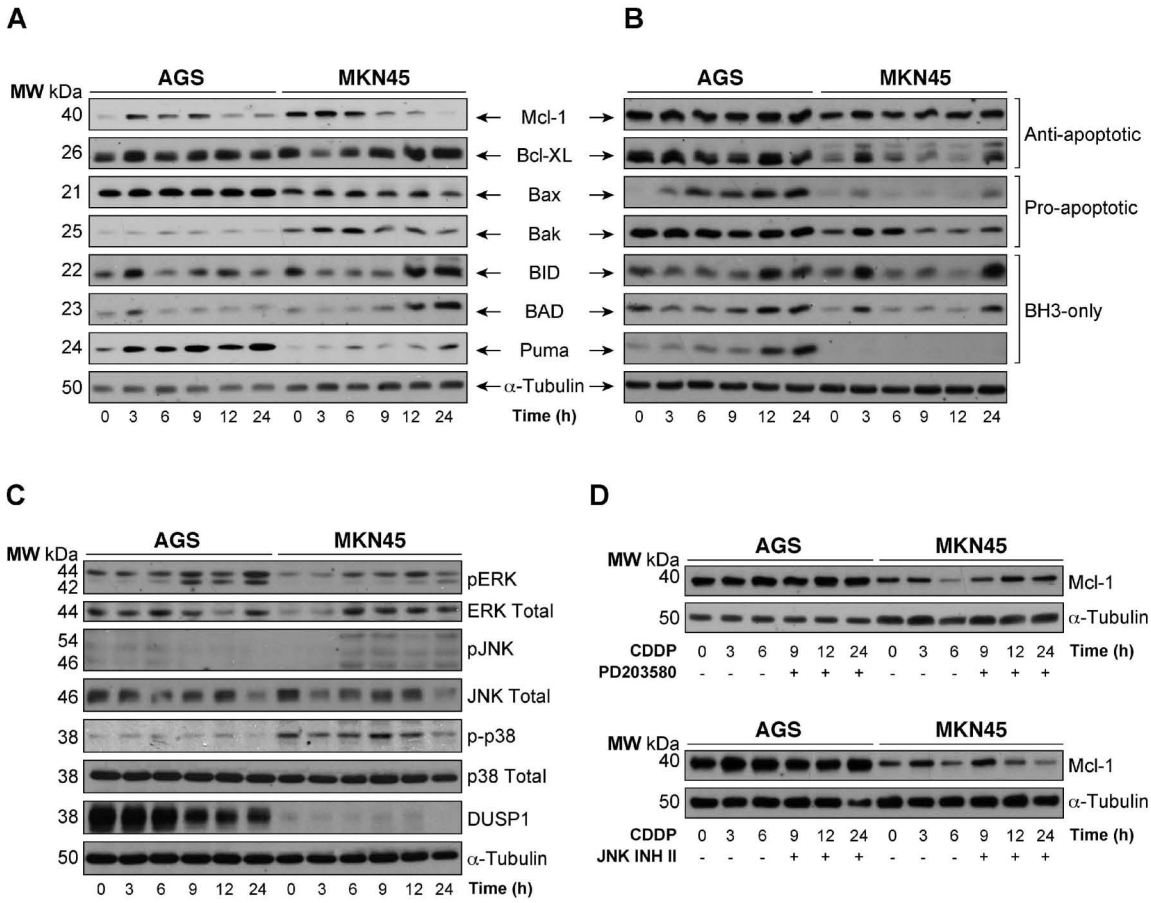

Bargiela-Iparraguirre et al. Figure 2

A

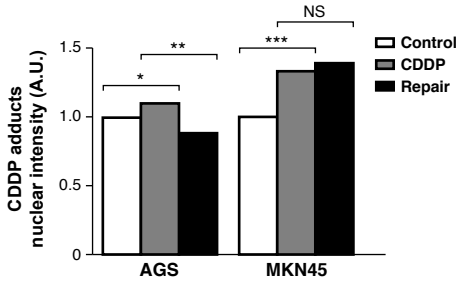

B

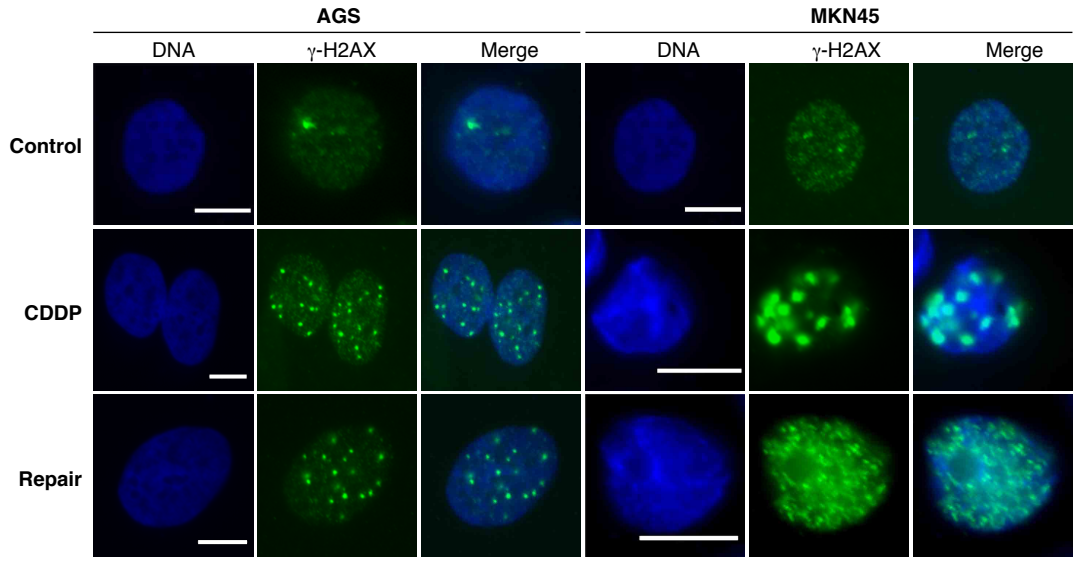

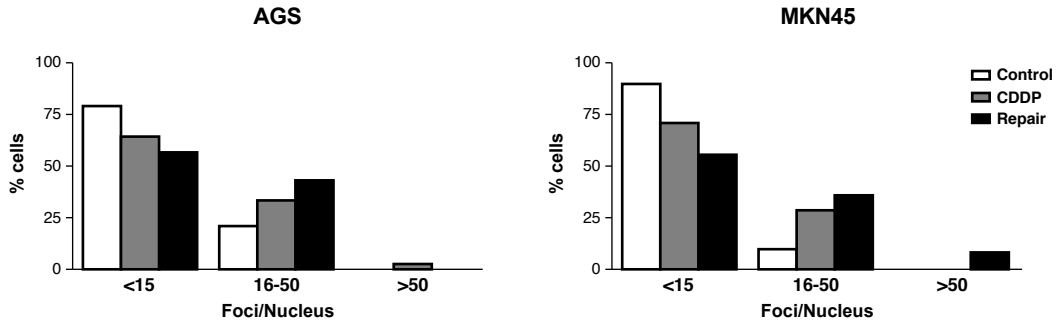

C

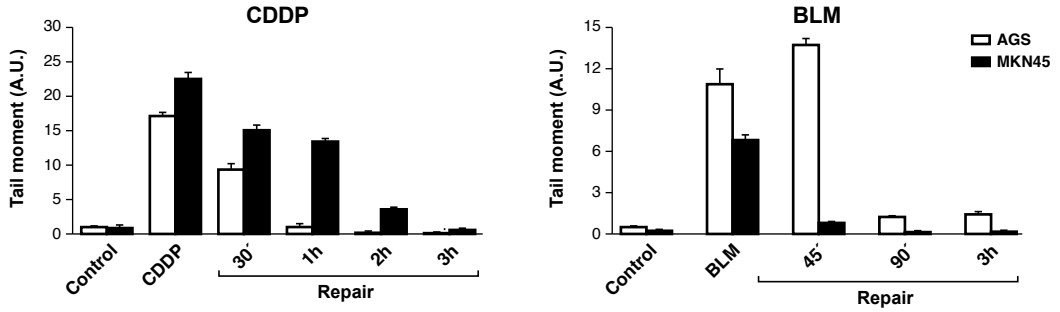

% RD CDDP	AGS	MKN45
30´	76.82±5.3	100±7.5
1h	32.28±2.8	99.94±4.7
2h	20.35±2.2	36.54±3.5
3h	7.93±1.4	65.21±2.9

% RD BLM	AGS	MKN45
45´	100±5.9	10.44±2.1
90´	6.73±1.4	1.49±0.5
3h	8.65±1.2	0.89±0.5

Bargiela-Iparraguirre et al. Figure 3

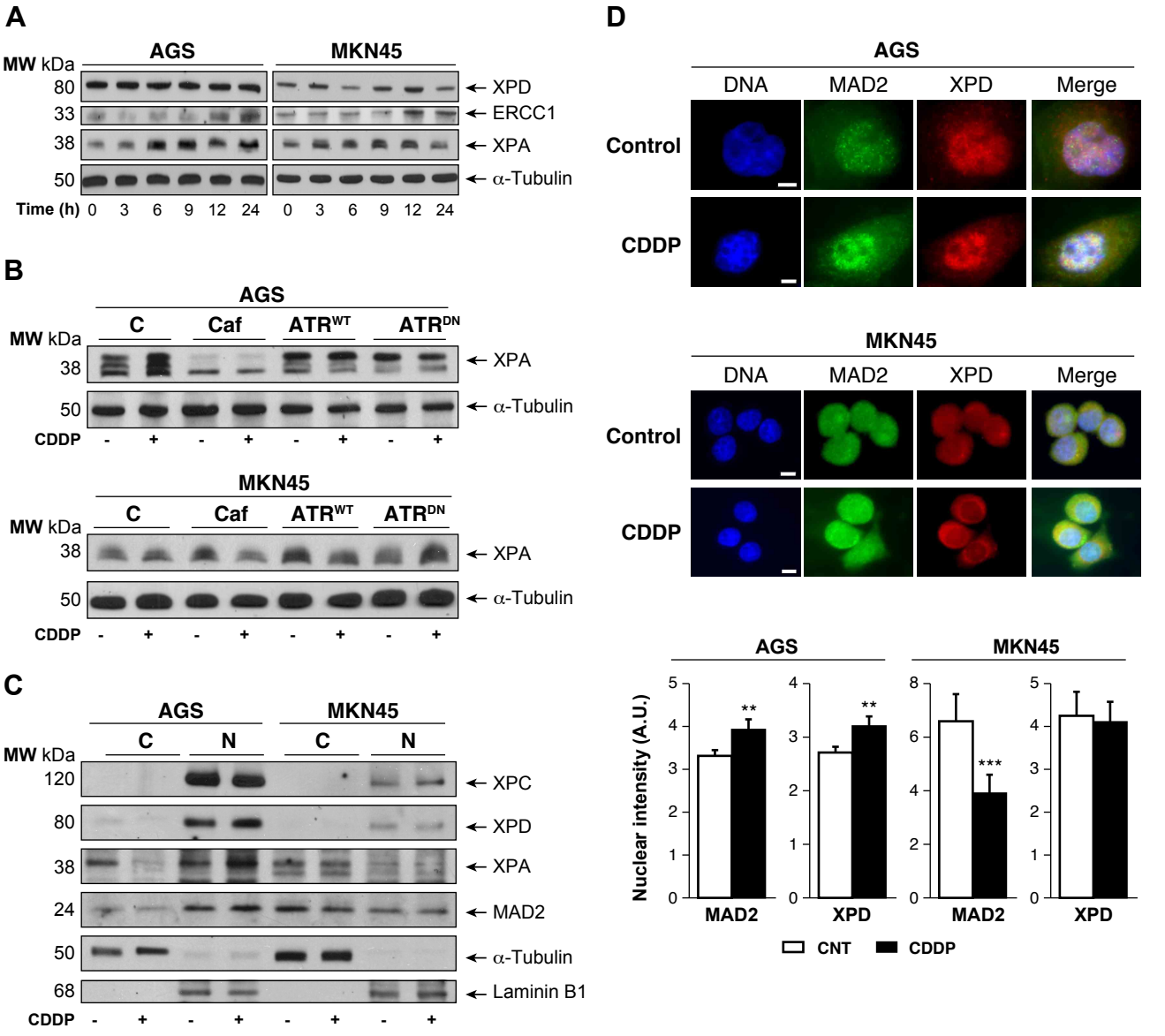

Bargiela-Iparraguirre et al. Figure 4

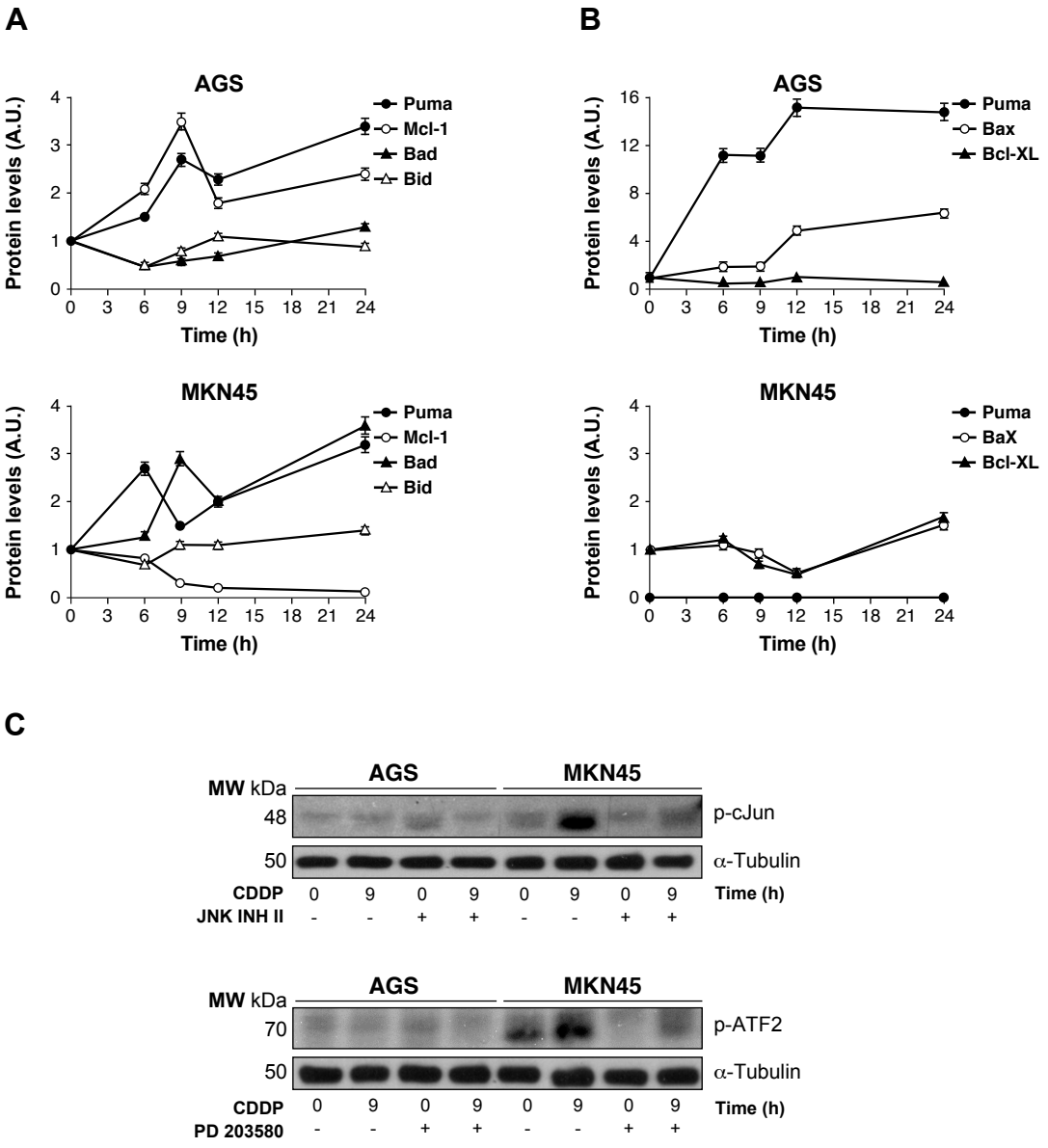

Bargiela-Iparraguirre et al. Supplementary Figure 1

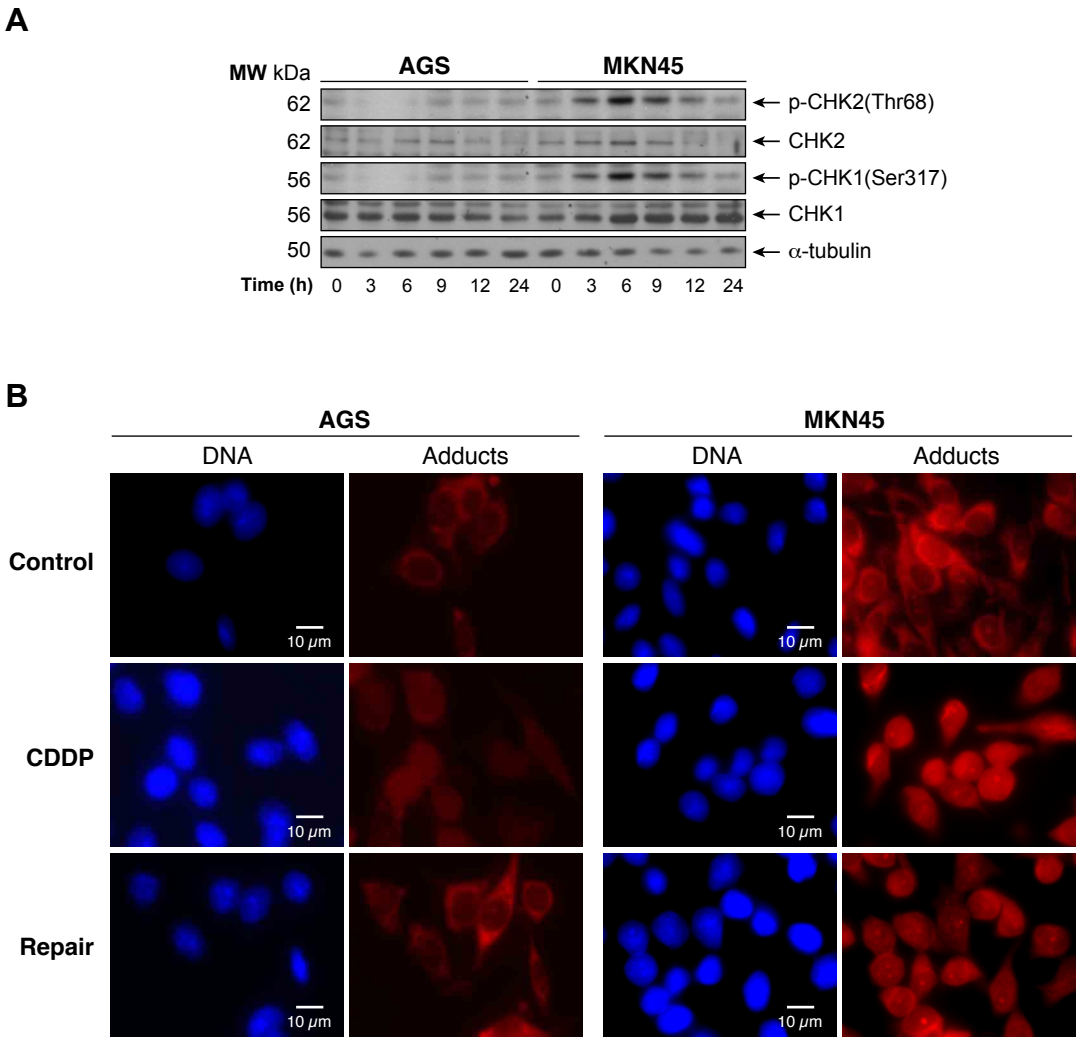
A
MW kDa
AGS
MKN45
62
62
56
56
50
p-CHK2(Thr68)
CHK2
p-CHK1(Ser317)
CHK1
α-tubulin
Time (h) 0 3 6 9 12 24 0 3 6 9 12 24
B
AGS
MKN45
DNA
Adducts
DNA
Adducts
Control
CDDP
Repair
10 μm
C
MW kDa
C
Caf
INH. P-JNK
INH. 203580
PD
38
50
XPA
α-Tubulin
CDDP - + - + - + - + - +

Supplementary figures:

S 1: Bcl2-family controls CDDP and BLM induced apoptosis in AGS and MKN45 cells.

A) Graphs represent the mean protein level quantification normalized with α-tubulin at each time point after CDDP treatment of three independent experiments. B) Graphs represent the mean protein level normalized with α-tubulin amount at each point after BLM treatment on triplicate experiments. C) Western blots detecting ATF2 and p- cJUN in AGS and MKN45 cells as SB203580 or JNK Inhibitor II control.

S 2. **CDDP induces equivalent stress signaling in AGS and MKN45**.

A) DDR proteins were detected by western blot in AGS and MKN after CDDP (10 μg/ml) treatment at the indicated times. α-tubulin was used as a loading control. B) Immunofluorescence images of CDDP adducts formed in the DNA of AGS and MKN45 cells. Control cells were not treated, CDDP cells were fixed after 3h of CDDP treatment and allowed to recover in normal media for one extra hour. Images were taken with 63x objective NIKON Eclipse 90i . C) Western blots detecting phosphorylation of XPA in AGS and MKN45 after caffeine (80mM), SB203580 , JNK Inhibitor II and ERK inhibitor

DISCUSIÓN

El cáncer gástrico en una enfermedad con mal pronóstico y difícil diagnóstico. El régimen del tratamiento actual es un protocolo estándar de radio y quimioterapia, poco efectivo si tenemos en cuenta el alto porcentaje de recaídas y la mortalidad de la enfermedad [28]. La heterogeneidad de la enfermedad hace que sea difícil encontrar una clasificación molecular idónea que permita estratificar a los pacientes para elegir un tratamiento específico y eficiente. La búsqueda de nuevas dianas terapéuticas y biomarcadores pronóstico y de diagnóstico, es un reto imprescindible para el avance hacia tratamientos más personalizados. Este hecho indica la necesidad de encontrar nuevas dianas terapéuticas que actúen solos o en combinación para sensibilizar a las células tumorales. El primer paso, es comprender el mecanismo molecular activado por los fármacos relacionados con la inducción de la muerte celular y la resistencia. En este sentido, nosotros hemos estudiado el papel de ciertas proteínas clave implicadas en puntos de control del ciclo celular y en el mantenimiento de la integridad del genoma en respuesta a genotóxicos, con el fin de identificar nuevos biomarcadores pronóstico y predictivos de respuesta a tratamiento en cáncer gástrico.

Catástrofe mitótica como estrategia para sensibilizar células de CG

El punto de control de mitosis es la última fase del ciclo celular en la que las células tienen la posibilidad de reparar las lesiones antes de dividirse y dar dos células hijas. Por ello, inducir la catástrofe mitótica es una estrategia atractiva para lograr una mayor eficiencia de muerte en las células tumorales. [78] Nosotros hemos demostrado que el tratamiento secuencial de Paclitaxel-Cisplatino sensibiliza a las células tumorales gástricas induciendo la catástrofe mitótica. Acorde con este resultado, en pacientes diagnosticados de carcinoma nasofaríngeo escamoso se observa un mejor pronóstico clínico en aquellos enfermos que reciben Paclitaxel en el protocolo estándar de quimioterapia (Cisplatino y 5FU) comparando con los que solo reciben Cisplatino y 5FU [66]. Nuestros resultados demuestran que las lesiones que provoca el Cisplatino en células mitóticas no se puede reparar debido a una degradación de la proteína CHK2, y por tanto una menor activación de BRCA1 proteína fundamental en el proceso de reparación de DBS [110]. La proteína CHK2 es clave para coordinar el proceso de parada de ciclo y la inducción de la vía de DNA Damage Response (DDR) para reparar DBS, fosforila y activa a sus dianas BRCA1/2 favoreciendo así la reparación por recombinación homóloga [133]. Además acorde con nuestros resultados en células HCT116 la inhibición de CHK2 o el descenso de sus niveles incrementa la muerte por catástrofe mitótica ante el agente doxurrubicina [12]. Estos resultados apoyan la muerte por catástrofe mitótica como una estrategia efectiva para sensibilizar a células de cáncer gástrico, y una coordinación entre el punto de control G2/M y la vía de señalización DDR. Así como la idea de que inhibidores de la quinasa CHK2 puedan potenciar la catástrofe mitótica producida por

agentes genotóxicos, y conseguir sensibilizar a células resistentes en las que la activación de CHK2 en mitosis este favoreciendo la supervivencia de estas [115].

CHK1 biomarcador de respuesta a irradiación

La sobreexpresión de las proteínas de la ruta DDR, CHK1 y CHK2 está ampliamente descrita en un gran número de tumores y se ha correlacionado con la resistencia a fármacos antineoplásicos y a irradiación [76]. Nuestros resultados, demuestran que las líneas celulares con elevados niveles de CHK1 presentan una mayor resistencia a la radiación en comparación con las células sin sobreexpresión. Acorde con esto, líneas celulares radioresistentes de pulmón presentan también niveles elevados de CHK1 y el inhibidor de CHK1, AZD7762, es capaz de sensibilizarlos[102]. Por otro lado hemos estudiando una pequeña cohorte de pacientes seleccionados por tratamiento con radiación, los niveles elevados de CHK1 en tumor correlacionan con un peor pronóstico del paciente (menor tiempo libre de progresión). Acorde con nuestro resultado, en tumores de cerebro niveles elevados de CHK1 fosforilada se han correlacionado con un menor tiempo libre de progresión [102]. Sin embargo, es necesario ampliar el tamaño muestral de nuestro estudio y verificar el resultado en otra serie independiente de pacientes, para determinar la potencia de las correlaciones clínicas-patológicas que permitan describir a CHK1 como una buena diana terapéutica o utilizarla como criterio de selección de tratamiento de esta enfermedad. Por otro lado, hemos observado que la inactivación de CHK1 por el compuesto UCN-01 incrementa la sensibilidad a BLM e IR. Desafortunadamente el fármaco UCN-01 no ha tenido muy buenos resultados farmacológicos por su alta toxicidad, inespecificidad y mala farmacocinética. [84]. Sin embargo, se están evaluando otros inhibidores en diversos ensayos clínicos, como es el AZD7762, un potente y específico inhibidor de CHK1, el cual ha demostrado la capacidad de incrementar la sensibilidad a agentes genotóxicos [76]. Los resultados obtenidos con el compuesto AZD7762 tanto *in vitro* como *in vivo*, refuerzan la idea de que inhibidores de CHK1 son capaces de sinergizar con los efectos de otros antitumorales en un contexto molecular concreto, por ejemplo en tumores con defectos en la reparación de DNA o con mutaciones de ciertos oncogenes como RAS [44]. Actualmente están en curso 6 ensayos clínicos en fase I y II de los inhibidores de CHK1/CHK2 LY2606368 (Prexasertib) y CCT245737, solos o en combinación con Cisplatino en diferentes tumores sólidos como boca, mama, próstata, páncreas y pulmón. (*www.clinicaltrials.gov*)

La sobreexpresión de la proteína CHK1 puede producirse por amplificación génica, aumento de la transcripción o modificaciones postranscripcionales [134]. Entender la causa por la cual CHK1 está sobreexpresada en líneas celulares de cáncer gástrico puede ser fundamental para comprender la respuesta y la resistencia a irradiación. En la inducción de la expresión de CHK1 a nivel transcripcional participan p53 y el factor de transcripción E2F1 [43], puesto que p53 se encuentra mutado en el 50% de los tumores sólidos, podría afectar a la expresión de CHK1. En nuestro

sistema modelo ambas líneas celulares (AGS y MKN45) presentan p53 wild type, y observamos que la activación transcripcional se produce a través de p53 y E2F1 tal y como está descrito. Sin embargo, el mRNA de CHK1 tiene una vida media muy larga, lo cual sugiere la existencia de una regulación postranscripcional como responsable del aumento de la expresión. Actualmente, se considera a los miRNAs como uno de los principales responsables de este proceso y cada vez existen más evidencias que muestran su capacidad de modular prácticamente cualquier proceso celular. Varios trabajos han demostrado que los miR-15 y miR-497 modulan la resistencia a fármacos en cáncer gástrico, teniendo como diana a Bcl-2 [125, 136] La sobreexpresión de la familia de los mir-15 afectan a la radiosensibilidad en cáncer de mama mediante la regulación de punto de control G2 [16, 81]. Al contrario también se ha observado que la sobreexpresión de la familia miR-15 incrementa la sensibilidad a Cisplatino al disminuir los niveles de CHK1 [94] Otros estudios han demostrado que la disminución del miR-424 contribuye a la progresión tumoral del cáncer de cuello de útero mediante el aumento de los niveles de CHK1[127]. Nosotros hemos identificado al miR-195 y miR503 como posibles responsables de la expresión de CHK1, de tal manera que los niveles bajos de estos podrían explicar la alta expresión de CHK1 en las MKN45. De acuerdo con esto, en NSCLC (non small cell lung carcinoma) niveles bajos de miR-195 en tumor respecto al tejido adyacente sano se correlaciona con un peor pronóstico del paciente, y con una menor supervivencia global [71]. Es necesario realizar otros estudios bioquímicos y moleculares que permitan evaluar el efecto de estos miRNAs en la expresión de CHK1 y en la respuesta a radiación. Además, sería de gran interés poder correlacionar los niveles de los miRNAs y CHK1 con el pronóstico y respuesta a IR en pacientes.[89] Una ventaja del uso de miRNA en la clínica es la estabilidad de los miRNA en sangre periférica y muestras parafinadas, lo que permitiría un método menos invasivo y eficaz de medición del biomarcador y posiblemente más fácil para aplicarlo en clínica.

Nuestros resultados abren un campo de estudio interesante, como es explorar nuevas posibles dianas de miRNA-195 y miRNA-503 y su relación con el eje E2F1-RB, podría describir un "loop" de regulación entre ellos y en consecuencia de la expresión de CHK1. Así la expresión de CHK1 podría ser modulada al ser inducida también la expresión de estos miRNAs por E2F1 o RB. En este sentido ya se conocen miRNAs cuya expresión está reguladas por RB, como por ejemplo la familia de miRNA106 en mama[112]. La regulación por RB genera expresiones aberrantes de miRNAs en tumor y niveles bajos del miRNA-106 en concreto se relacionan con tumores más agresivos. Esto familia de miRNAs presentan además como diana a p21, lo que podría explicar un mecanismo de regulación de RB. Es decir, en una situación en donde hay niveles bajos de miRNAs que regulan p21 y por tanto niveles más elevados de esta proteína, puede suponer un incremento en la fosforilación de RB, la liberación de E2F1 e inducción de diversos genes diana que pueden estar relacionados con resistencia y/ agresividad del tumor, como es el caso de CHK1.

Otros miRNAs cuya regulación sería interesante estudiar son aquellos que presentan como diana a varias proteínas claves de la vía, como es el miRNA-16 ya que tiene como diana a CHK1 y a su regulador E2F1[91]. Por otro lado también resultan interesantes el miR-15 el cual regula a CHK1 y Bcl-2 [125] [94], así como el miR-503 que se ha descrito como regulador de Bcl-2 y nosotros sugerimos que también pueda regular los niveles de CHK1. Estos miRNAs pueden jugar un importante papel en la resistencia al tratamiento y en el pronóstico del paciente.

Proteínas del SAC: biomarcadores pronóstico y dianas terapéuticas

La aneuploidia e inestabilidad genómica son características que distinguen a células tumorales de las normales, lo que hace que sean considerados también dianas terapéuticas, ya que un excesivo nivel de inestabilidad genómica es insostenible y por tanto letal incluso para la célula tumoral[15]. En este sentido, actualmente se están desarrollando inhibidores específicos de AURKA, PLK4 y Mps1, los cuales comprometen los centrosomas y SAC induciendo la muerte por catástrofe mitótica.[32]. De acuerdo con esto, nuestros resultados demuestran que las células de cáncer gástrico presentan una expresión alterada de las proteínas del SAC, como ocurre en otros tumores sólidos pulmón, mama, ovario y cabeza y cuello [79]. Nosotros hemos observado que MAD2 y BUBR1, están sobreexpresados en la mayoría de las líneas celulares derivadas de adenocarcinomas diseminados, favoreciendo la proliferación celular, migración e invasión celular [3]. Existen evidencias en la literatura que indican como la sobreexpresión de BUBR1 está relacionada con la diseminación del tumor, la progresión de la enfermedad y una menor supervivencia de los pacientes con cáncer de pulmón [18]. Además, la sobreexpresión de MAD2, en colon, pulmón y en linfoma gastrointestinal está relacionada con la alta proliferación celular y peor pronóstico de los pacientes [59]. En relación con la proteína MAD2, se ha observado que ratones con genotipo (MAD2 con sobreexpresión de MAD2) desarrollan tumores espontáneos y metástasis en pulmón [103]. Nosotros hemos realizado el análisis de la expresión de *MAD2L1* en tumores gástricos resecados respecto al tejido normal contiguo, en una serie de pacientes con adenocarcinomas gástricos primarios que no habían recibido tratamiento previo a la gastrectomía. Hemos comprobado que los niveles elevados de *MAD2L1* en el tumor correlacionan con un menor tiempo de supervivencia global en estos pacientes (ANEXO I). Este resultado también se ha observado en otros tipos de tumor como osteosarcoma, cáncer bucal o endometrial [67, 111, 130].Sin embargo, no hemos encontrado correlación significativa con la respuesta al Cisplatino, lo que puede deberse al reducido número de pacientes que hemos sido capaces de recopilar que hubieran recibido CDDP como única terapia. La gran mayoría de los casos reciben IR y como hemos demostrado otros factores como los niveles de CHK1 pueden estar influyendo en la resistencia a este tratamiento, lo que puede interferir con la correlación entre la respuesta al CDDP y los niveles de expresión de *MAD2L1*. A pesar de que se ha descrito el estudio de los niveles de proteína de

MAD2 en cortes de tejido parafinados mediante técnicas de inmunohistoquimica [111] nuestros datos indican que no es la técnica más adecuada para valorar a MAD2 como biomarcador, ya que no hemos encontrado una buena correlación con los resultados obtenidos mediante QPCR. Sin embargo, tal y como hemos mencionado anteriormente, consideramos que los miRNAs específicos de MAD2 y CHK1 podrían dar una solución al problema, por sus características de expresión robusta, estable y de fácil medición hace que tengan más probabilidad para la incorporación a la práctica clínica.[89] Todos los datos en la literatura y los nuestros propios indican la posibilidad de considerar a MAD2 como una buena diana terapéutica, tanto es así que ya se está estudiando la eficiencia en la disminución de la expresión de MAD2 mediante la incorporación de siRNAs en nanopartículas y su efecto en la inducción de la muerte en células de cáncer de pulmón [87, 88].

La contribución de las proteínas del SAC a la respuesta a antitumorales se ha estudiado previamente por otros grupos, en ocasiones con resultados contradictorios, así la disminución de BUBR1 se ha relacionado con la sensibilidad a Paclitaxel en carcinoma escamoso de esófago pero la inhibición de esta proteína induce la resistencia en cáncer colorectal [52, 109]. Recientemente, se han empezado a identificar funciones celulares de MAD2 independientes de mitosis o SAC. Se ha descrito su posible papel en la respuesta a daño al DNA, o en el destino celular induciendo apoptosis y senescencia [65, 117] , así en cáncer de ovario y mama la supresión de MAD2 y BUBR1 resulta en la resistencia a Paclitaxel [105]. Nosotros también hemos observado que la disminución de MAD2 y BUBR1 confiere resistencia a Paclitaxel en líneas de cáncer gástrico [3]. Aun así cabe resaltar que resultados contradictorios respecto a la respuesta a terapia y los niveles de estas proteínas en tumores [117], ponen de manifiesto que la heterogeneidad intra e inter tumoral está detrás de estos resultados. Por ello el estudio del "background" o estado basal global de estos mecanismos (SAC y DDR) y de sus reguladores es necesario para poder explicar el destino celular en un contexto concreto. En este sentido hemos demostrado que en nuestro modelo hay una inducción de la senescencia como resultado de la bajada de las proteínas MAD2 y BUBR1, la cual se potencia en respuesta al Paclitaxel. La implicación de MAD2 en senescencia ya se había observado previamente, en la línea celular IMR90 [65]. Además también se ha visto que la sobreexpresión de p31comet, inhibidor de SAC, induce la senescencia mediante la acumulación de p21 (Waf1/Cip1) y la disrupción de MAD2 [132]. Nuestros resultados muestran que la senescencia inducida es independiente de p21. Al contrario de lo que ocurre en las células IMR90, fibroblastos primarios donde una disminución de MAD2 induce la senescencia mediante un incremento de p53 y p21[17, 65]. Nosotros interpretamos que en nuestro modelo la disminución de los niveles de MAD2 y BUBR1 provoca una parada en mitosis prolongada, el cual aumenta el estrés energético y oxidativo induciendo la senescencia [14]. Además observamos una potenciación en la inducción de la senescencia al tratar las células interferidas con PTX, ya que supone un

doble reto y estimulo de estrés ante la incapacidad organizar el huso mitótico. Podemos considerar que la inducción de senescencia en cáncer gástrico puede ser un mecanismo supresor tumoral ante una situación en la que la mitosis está comprometida, impidiendo así que se incremente la inestabilidad genómica o trascienda a las células hijas. Aun así, el secretoma de las células senescentes es complejo, consiste en una gran variedad de citoquinas y proteasas, y está relacionado con la inflamación, proliferación y la modulación de la matriz extracelular[13]. Nuestros resultados demuestran que el descenso en los niveles de MAD2 y BUBR1 induce un incremento en la expresión de IL6 e IL-8 lo que nos hace pensar que los niveles elevados de IL pudieran está favoreciendo la señalización paracrina y el incremento de la senescencia[4]. Este resultado es interesante, aunque hacen falta más estudios para explicar la consecuencia fisiológica de esta senescencia prematura. Nuestros resultados sugieren que la incapacidad resolver la segregación cromosómica por la alteración de los niveles de MAD2 es detectada como señal de estrés lo que genera una inducción prematura de la senescencia. Este fenómeno en tal situación actúa como barrera ante la carcinogénesis evitando la ganancia de inestabilidades. Pero por otro lado la senescencia podría tener efectos negativos en cuanto a la respuesta al tratamiento, ya que esta población de células tumorales no está siendo eliminada como tal y podrían contribuir a la resistencia que otros grupos y nosotros hemos observado ante PTX. El tratamiento adyuvante con agentes antimitóticos en estos casos podría resultar contraproducente, ya podría conllevar a una selección positiva de estas células y su capacidad secretora por el fenotipo SASP. Esto puede contribuir a crear un ambiente tumoral favoreciendo la transformación celular de las células adyacentes y el crecimiento tumoral y recurrencia en los pacientes [42]. Para demostrar esto, serian interesantes ensayos *in vivo* mediante xenotransplantes en ratones inmunosuprimidos, en los que comparásemos tumores con sobreexpresión de MAD2 o BUBR1 frente a tumores que no presenten tal sobreexpresión y estudiar la influencia de la inducción del ambiente inflamatorio y la población de células senescentes en respuesta a PTX en cuanto a la recurrencia tumoral.

Implicación de la familia BCL-2 en la apoptosis inducida por Cisplatino

La inhibición de la apoptosis, hallmark de las células tumorales, es una de las principales causas de resistencia a fármacos. Se ha sugerido que la disminución de MAD2 genera resistencia al inhibir la apoptosis mediante la elevación de Bcl-2 [34, 117] así como la reducción de los niveles de las proteínas pro-apoptóticas y disminución de la actividad de las caspasas [34]. Se ha descrito también la correlación entre bajos niveles de MAD2 y la inhibición de apoptosis en la línea celular de tumor germinal 1411HP [37]. Además en líneas de cáncer nasofaríngeo la disminución de MAD2 incrementa la resistencia a Cisplatino por una modulación en el ratio entre las proteínas Bcl-2/Bax y los niveles de la caspasa activa [22]. En cuanto a la respuesta y muerte inducida por el Cisplatino,

hemos demostrado que se produce por una disminución de la proteína anti-apoptótica MCL-1 en la línea celular sensible a este agente, al contrario que con el agente BLM el cual provoca la muerte celular mediante la inducción de la proteína proapoptótica Bax y Puma en la misma línea celular. Este hecho está acorde con el reciente resultado en el que la supresión de la vía FoxM1/Mcl-1 afecta a la viabilidad celular e incrementa la sensibilidad a CDDP células de cáncer gástrico[69]. Puma es sustrato de p53, el estado de p53 es *wild type* en ambas líneas celulares por lo que se esperaría el mismo comportamiento, aunque también se ha descrito que puede inducir la apoptosis independientemente de p53 ,en respuesta a ROS y estrés del retículo endoplásmico, en cuya situación factores de trascripción como E2F1 regulan su expresión [123, 129]. Sería interesante estudiar la regulación de Puma en nuestro modelo así como el estado de metilación de su promotor ya que podría estar silenciado epigenéticamente en las células MKN45, como se ha observado en linfomas y correlacionarlo con la sensibilidad a este agente [41]. Nuestros resultados fortalecen la idea de que dianas específicas de la familia Bcl-2 para cada tratamiento pueden ser una buena estrategia terapéutica. Actualmente están en curso varios ensayos clínicos en distintas etapas en las que se estudia el efecto de varios mimics de las proteínas BH3 only con numerosos inhibidores[27]. Algunos con buenos resultados como es el caso del inhibidor de BCL-2 , ABT-199 o Venetoclax, el cual ha pasado a ensayos de fase III por presentar buenos resultados reduciendo el tamaño del tumor y con menores efectos secundarios que otros inhibidores de BCl-2[26] .En nuestro modelo sería interesante probar los inhibidores de Mcl-1 en líneas resistentes a Cisplatino o inhibidores de Bax y Puma para las líneas resistentes a irradiación, pero el hecho de que Mcl-1 sea esencial para la supervivencia de muchos tipos celulares así como la toxicidad que presenta hace que hasta el momento el uso en clínica está restringido [27]. Además la combinación con quimioterapéuticos que producen daño en el DNA puede generar diversos efectos secundarios en tejidos sanos[27].

MAD2 y la eficiencia de NER como biomarcador de sensibilidad a Cisplatino

La vía de reparación NER es el principal mecanismo que elimina el daño producido por el Cisplatino, por ello las proteínas que participan en la ruta han sido ampliamente estudiadas en relación a la resistencia al agente [58]. Nuestros resultados apoyan que los niveles y la localización de XPA y XPD son las principales proteínas que modulan la eficiencia de reparación de la ruta NER en MKN45. Los resultados sugieren que la falta de translocación al núcleo de estas está comprometiendo la eficiencia de reparación de los aductos. Precisamente la capacidad de estas proteínas de llegar al DNA parece ser determinante en la ruta NER[106], pacientes con la enfermedad Xeroderma Pigmentosum que sufren de fotosensibilidad y un exceso de daño en el DNA presentan principalmente mutaciones en los dominios de unión al DNA, como es el caso de XPA[106]. La helicasa XPD participa en diversos procesos celulares además de la reparación en la

vía de NER[51]. La pérdida de expresión de XPD genera divisiones asincrónicas e inestabilidad cromosómica [68]. En un estudio previo se demostró que XPD interacciona con MAD2 en la línea celular 293T [38], nosotros solo hemos observado colocalización entre MAD2 y XPD en la línea AGS. Se ha sugerido que niveles elevados de MAD2 pueden sensibilizar a CDDP por el hecho que esté interfiriendo en el reconocimiento del daño por las proteínas de reparación NER[38]. Sería interesante analizar esta interacción con técnicas de ligación por proximidad o PLA, la cual permite observar la interacción de proteínas mediante anticuerpos unidos a sondas, estas a una distancia menor a 40 A generan la denominada reacción de amplificación de circulo rodantes, una señal fácilmente medible por microscopio de fluorescencia. Nuestro trabajo acorde con lo anterior también refuerza la idea de que los niveles elevados de MAD2 interfieren en la acumulación nuclear de XPD pudiendo por tanto influir en su unión al DNA y haciendo que estas células sean más sensibles al CDDP. De cualquier forma hacen falta más estudios para profundizar en el mecanismo por el cual MAD2 pueda estar modulando la localización de XPD. MAD2 es una proteína flexible capaz de adoptar distintas conformaciones, durante la mitosis MAD2 cambia de una conformación abierta a una conformación cerrada, estos distintos estados de la proteína regulan claramente la disponibilidad para interaccionar con unas u otras proteínas, por lo que el estudio del estado conformacional de MAD2 podría esclarecer la influencia de sus niveles en distintos procesos celulares. Recientemente se han desarrollado anticuerpos monoclonales específicos que reconocen las distintas conformaciones de MAD2 lo que podría ser de gran ayuda en este área[101].Durante la interfase, MAD2 interacciona con el complejo de nucleoporinas (NPCs), concretamente con Nup153 y Trp .[85]. Experimentos in vivo para hacer un seguimiento de la movilidad de MAD2 así como para estudiar la interacción con proteínas en el paso al núcleo podrían ser interesantes. Profundizar en los mecanismos que regulan la disponibilidad intracelular de las proteínas de reparación e incluso el tiempo de reclutamiento al punto del daño por técnicas de foto-bleaching podría ser de ayuda para estudiar la eficiencia de estas rutas. En este sentido se ha observado que la disminución de la nucleoporina NUP53 produce un descenso de la internalización de MAD1 al núcleo [50], lo que sugiere que podría ser posible también modular la disponibilidad de MAD2 en el núcleo y de esta manera influir tanto en SAC como en mecanismos de reparación de daño.

Interesantemente y acorde a lo que ya habíamos encontrado en trabajos previos, la línea celular MKN45 presenta también niveles elevados de CHK1 lo que le confiere la resistencia a IR, hemos observado que la eficiencia de reparación del daño causado por el agente radiomimético BLM es más alta, pero dicho daño se repara por otra vía de reparación [3], lo que podría estar indicando que la misma línea celular tenga una robusta reparación de HR o NHEJ pero deficiente en NER. Es necesario profundizar en el papel que puedan presentar las proteínas involucradas en la estabilidad genómica en las vías de reparación del daño en el DNA. Recientemente se ha observado que la proteína BUB1 juega un papel induciendo la reparación por NHEJ en respuesta al daño en el DNA

lo cual apunta también en una sinergia entre las proteínas SAC y la reparación por DSB[33]. En *C. Elegans* en presencia de daño MAD1 y MAD2 co-localizan en la periferia nuclear, y son necesarios para una reparación eficiente [63]. También MAD2 se localiza en esta zona en células de mamíferos, lo que podría sugerir una función conservada en el cual MAD2 participa en la reparación del DNA.

Cada vez son más las evidencias de la interconexión entre las rutas de señalización DDR y SAC, no son mecanismos independientes sino que cooperan para un mismo fin [63, 92]. El daño en DNA induce la señalización conjunta entre DDR y SAC para que se dé la parada en mitosis. En *Saccharomyces cerevisiae*, uno de los modelos más utilizados para el estudio de los "checkpoints", se vio por primera vez que existe una parada en mitosis por SAC en respuesta al daño en el DNA. Así, recientemente se ha comprobado la necesidad de ciertos componentes de DDR (ATR, RAD9, BRCA1, ATM) para la correcta activación de SAC en metafase [64]. Por ejemplo la proteína BRCA1 podría contribuir a la activación de SAC induciendo la transcripción de BUB1, BUBR1, y MAD2. La falta de CHK1 conduce a la perdida de cromosomas, alineaciones y células binucleadas. Por otro lado CHK1 también se localiza en el cinetocoro y la ausencia de esta hace que Aurora B baje su actividad catalítica y Cdc20 y MAD2 no se localicen en el cinetocoro [128]. También se ha demostrado que CHK1 interacciona y fosforila *in vitro* a MAD2 [23], todas estas evidencias refuerzan la idea de la participación de DDR en la vía canónica de SAC y viceversa ante agentes que generan fallos en la segregación cromosómica [83]. Con todo ello nuestros resultados refuerzan la idea de continuar en la búsqueda de nuevas estrategias terapéuticas ampliando la perspectiva de las interacciones entre distintos mecanismos celulares que en un principio parecían ser independientes, para así abordar el problema de la resistencia a terapia de una forma más efectiva y con una visión más global.

CONCLUSIONES

1. La muerte inducida en mitosis es una estrategia efectiva para sensibilizar la línea celular MKN45 a Cisplatino. El daño en el DNA causado por el Cisplatino en mitosis induce la degradación de CHK2 vía proteasoma impidiendo una reparación del DNA efectiva y por tanto induciendo la catástrofe mitótica.
2. Los genes *MAD2L1 Y BUB1B* están sobreexpresados en las líneas celulares procedentes de adenocarcinomas gástricos avanzados/diseminados. La sobreexpresión de *MAD2L1* en el tumor correlaciona con un menor tiempo de supervivencia global en los pacientes con cáncer gástrico.
3. La sobreexpresión de MAD2 y BUBR1 favorece la proliferación celular, migración e invasión *in vitro*. El descenso de los niveles de MAD2 y BUBR1 confiere resistencia a Paclitaxel e induce la senescencia en la línea celular MKN45.
4. Niveles elevados de CHK1 confieren resistencia a irradiación en las líneas celulares de cáncer gástrico. La expresión nuclear elevada en el tumor correlaciona con un menor tiempo libre de progresión en los pacientes con cáncer gástrico.
5. Los niveles elevados de CHK1 en la línea celular MKN45 se deben a la estabilización del RNA mensajero. Los miR-503 y miR-19 son candidatos como reguladores de CHK1.
6. La muerte causada por Cisplatino mediante la vía intrínseca de la apoptosis requiere la degradación de la proteína anti-apoptótica MCL-1 y aumento de las proteínas pro-apoptóticas Bad y Bid. La muerte inducida por bleomicina ocurre por la elevación de las proteínas pro-apoptóticas Bax, Bad, Bid y Puma.
7. La sensibilidad a Cisplatino en MKN45 se debe a una ineficiente reparación del DNA provocada por la falta de translocación de XPA y XPD al núcleo tras el estímulo.

BIBLIOGRAFÍA

1 Badgwell B. Multimodality Therapy of Localized Gastric Adenocarcinoma. J Natl Compr Canc Netw 2016; 14: 1321-1327.

2 Bahassi EM, Ovesen JL, Riesenberg AL, Bernstein WZ, Hasty PE, Stambrook PJ. The checkpoint kinases Chk1 and Chk2 regulate the functional associations between hBRCA2 and Rad51 in response to DNA damage. Oncogene 2008; 27: 3977-3985.

3 Bargiela-Iparraguirre J, Prado-Marchal L, Pajuelo-Lozano N, Jimenez B, Perona R, Sanchez-Perez I. Mad2 and BubR1 modulates tumourigenesis and Paclitaxel response in MKN45 gastric cancer cells. Cell cycle 2014; 13: 3590-3601.

4 Bargiela-Iparraguirre J, Prado-Marchal L, Fernandez-Fuente M, Gutierrez-Gonzalez A, Moreno-Rubio J, Munoz-Fernandez M *et al*. CHK1 expression in Gastric Cancer is modulated by p53 and RB1/E2F1: implications in chemo/radiotherapy response. Scientific reports 2016; 6: 21519.

5 Bartek J, Lukas J. Chk1 and Chk2 kinases in checkpoint control and cancer. Cancer Cell 2003; 3: 421-429.

6 Bartek J, Bartkova J, Lukas J. DNA damage signalling guards against activated oncogenes and tumour progression. Oncogene 2007; 26: 7773-7779.

7 Bartkova J, Horejsi Z, Koed K, Kramer A, Tort F, Zieger K *et al*. DNA damage response as a candidate anti-cancer barrier in early human tumorigenesis. Nature 2005; 434: 864-870.

8 Basu A, Krishnamurthy S. Cellular responses to Cisplatin-induced DNA damage. Journal of nucleic acids 2010; 2010.

9 Bowden NA. Nucleotide excision repair: why is it not used to predict response to platinum-based chemotherapy? Cancer Lett 2014; 346: 163-171.

10 Cahill DP, Lengauer C, Yu J, Riggins GJ, Willson JK, Markowitz SD *et al*. Mutations of mitotic checkpoint genes in human cancers. Nature 1998; 392: 300-303.

11 Cancer Genome Atlas Research N. Comprehensive molecular characterization of gastric adenocarcinoma. Nature 2014; 513: 202-209.

12 Castedo M, Perfettini JL, Roumier T, Yakushijin K, Horne D, Medema R *et al*. The cell cycle checkpoint kinase Chk2 is a negative regulator of mitotic catastrophe. Oncogene 2004; 23: 4353-4361.

13 Coppe JP, Patil CK, Rodier F, Sun Y, Munoz DP, Goldstein J *et al*. Senescence-associated secretory phenotypes reveal cell-nonautonomous functions of oncogenic RAS and the p53 tumor suppressor. PLoS Biol 2008; 6: 2853-2868.

14 Correia-Melo C, Hewitt G, Passos JF. Telomeres, oxidative stress and inflammatory factors: partners in cellular senescence? Longev Healthspan 2014; 3: 1.

15 Cuadrado M, Martinez-Pastor B, Murga M, Toledo LI, Gutierrez-Martinez P, Lopez E *et al*. ATM regulates ATR chromatin loading in response to DNA double-strand breaks. J Exp Med 2006; 203: 297-303.

16 Czochor JR, Glazer PM. microRNAs in cancer cell response to ionizing radiation. Antioxid Redox Signal 2014; 21: 293-312.

17 Chao SK, Horwitz SB, McDaid HM. Insights into 4E-BP1 and p53 mediated regulation of accelerated cell senescence. Oncotarget 2011; 2: 89-98.

18 Chen H, Lee J, Kljavin NM, Haley B, Daemen A, Johnson L *et al*. Requirement for BUB1B/BUBR1 in tumor progression of lung adenocarcinoma. Genes Cancer 2015; 6: 106-118.

19 Chen RH. Phosphorylation and activation of Bub1 on unattached chromosomes facilitate the spindle checkpoint. EMBO J 2004; 23: 3113-3121.

20 Chen T, Xu XY, Zhou PH. Emerging molecular classifications and therapeutic implications for gastric cancer. Chin J Cancer 2016; 35: 49.

21 Cheng XJ, Lin JC, Tu SP. Etiology and Prevention of Gastric Cancer. Gastrointest Tumors 2016; 3: 25-36.

22 Cheung HW, Jin DY, Ling MT, Wong YC, Wang Q, Tsao SW *et al*. Mitotic arrest deficient 2 expression induces chemosensitization to a DNA-damaging agent, cisplatin, in nasopharyngeal carcinoma cells. Cancer Res 2005; 65: 1450-1458.

23 Chila R, Celenza C, Lupi M, Damia G, Carrassa L. Chk1-Mad2 interaction: a crosslink between the DNA damage checkpoint and the mitotic spindle checkpoint. Cell cycle 2013; 12: 1083-1090.

24 Dai Y, Jin S, Li X, Wang D. The involvement of Bcl-2 family proteins in AKT-regulated cell survival in cisplatin resistant epithelial ovarian cancer. Oncotarget 2016.

25 Dasari S, Tchounwou PB. Cisplatin in cancer therapy: molecular mechanisms of action. Eur J Pharmacol 2014; 740: 364-378.

26 Delbridge AR, Strasser A. The BCL-2 protein family, BH3-mimetics and cancer therapy. Cell Death Differ 2015; 22: 1071-1080.

27 Delbridge AR, Grabow S, Strasser A, Vaux DL. Thirty years of BCL-2: translating cell death discoveries into novel cancer therapies. Nat Rev Cancer 2016; 16: 99-109.

28 den Hoed CM, Kuipers EJ. Gastric Cancer: How Can We Reduce the Incidence of this Disease? Curr Gastroenterol Rep 2016; 18: 34.

29 Denisenko TV, Sorokina IV, Gogvadze V, Zhivotovsky B. Mitotic catastrophe and cancer drug resistance: A link that must to be broken. Drug Resist Updat 2016; 24: 1-12.

30 Digklia A, Wagner AD. Advanced gastric cancer: Current treatment landscape and future perspectives. World J Gastroenterol 2016; 22: 2403-2414.

31 Dobles M, Liberal V, Scott ML, Benezra R, Sorger PK. Chromosome missegregation and apoptosis in mice lacking the mitotic checkpoint protein Mad2. Cell 2000; 101: 635-645.

32 Dominguez-Brauer C, Thu KL, Mason JM, Blaser H, Bray MR, Mak TW. Targeting Mitosis in Cancer: Emerging Strategies. Molecular cell 2015; 60: 524-536.

33 Dotiwala F, Harrison JC, Jain S, Sugawara N, Haber JE. Mad2 prolongs DNA damage checkpoint arrest caused by a double-strand break via a centromere-dependent mechanism. Curr Biol 2010; 20: 328-332.

34 Du Y, Yin F, Liu C, Hu S, Wang J, Xie H *et al*. Depression of MAD2 inhibits apoptosis of gastric cancer cells by upregulating Bcl-2 and interfering mitochondrion pathway. Biochemical and biophysical research communications 2006; 345: 1092-1098.

35 Edifizi D, Schumacher B. Genome Instability in Development and Aging: Insights from Nucleotide Excision Repair in Humans, Mice, and Worms. Biomolecules 2015; 5: 1855-1869.

36 Fang Y, Liu T, Wang X, Yang YM, Deng H, Kunicki J *et al*. BubR1 is involved in regulation of DNA damage responses. Oncogene 2006; 25: 3598-3605.

37 Fung MK, Cheung HW, Ling MT, Cheung AL, Wong YC, Wang X. Role of MEK/ERK pathway in the MAD2-mediated cisplatin sensitivity in testicular germ cell tumour cells. British journal of cancer 2006; 95: 475-484.

38 Fung MK, Han HY, Leung SC, Cheung HW, Cheung AL, Wong YC *et al*. MAD2 interacts with DNA repair proteins and negatively regulates DNA damage repair. Journal of molecular biology 2008; 381: 24-34.

39 Furlong F, Fitzpatrick P, O'Toole S, Phelan S, McGrogan B, Maguire A *et al*. Low MAD2 expression levels associate with reduced progression-free survival in patients with high-grade serous epithelial ovarian cancer. J Pathol 2012; 226: 746-755.

40 Gadhikar MA, Sciuto MR, Alves MV, Pickering CR, Osman AA, Neskey DM *et al*. Chk1/2 inhibition overcomes the cisplatin resistance of head and neck cancer cells secondary to the loss of functional p53. Mol Cancer Ther 2013; 12: 1860-1873.

41 Garrison SP, Jeffers JR, Yang C, Nilsson JA, Hall MA, Rehg JE *et al*. Selection against PUMA gene expression in Myc-driven B-cell lymphomagenesis. Mol Cell Biol 2008; 28: 5391-5402.

42 Gewirtz DA, Alotaibi M, Yakovlev VA, Povirk LF. Tumor Cell Recovery from Senescence Induced by Radiation with PARP Inhibition. Radiat Res 2016; 186: 327-332.

43 Gottifredi V, Karni-Schmidt O, Shieh SS, Prives C. p53 down-regulates CHK1 through p21 and the retinoblastoma protein. Mol Cell Biol 2001; 21: 1066-1076.

44 Grabocka E, Commisso C, Bar-Sagi D. Molecular pathways: targeting the dependence of mutant RAS cancers on the DNA damage response. Clin Cancer Res 2015; 21: 1243-1247.

45 Grossi V, Peserico A, Tezil T, Simone C. p38alpha MAPK pathway: a key factor in colorectal cancer therapy and chemoresistance. World J Gastroenterol 2014; 20: 9744-9758.

46 Hanahan D, Weinberg RA. The hallmarks of cancer. Cell 2000; 100: 57-70.

47 Hanahan D, Weinberg RA. Hallmarks of cancer: the next generation. Cell 2011; 144: 646-674.

48 Hao X, Zhou Z, Ye S, Zhou T, Lu Y, Ma D *et al*. Effect of Mad2 on Paclitaxel-induced cell death in ovarian cancer cells. J Huazhong Univ Sci Technolog Med Sci 2010; 30: 620-625.

49 Hara M, Ozkan E, Sun H, Yu H, Luo X. Structure of an intermediate conformer of the spindle checkpoint protein Mad2. Proc Natl Acad Sci U S A 2015; 112: 11252-11257.

50 Hawryluk-Gara LA, Shibuya EK, Wozniak RW. Vertebrate Nup53 interacts with the nuclear lamina and is required for the assembly of a Nup93-containing complex. Molecular biology of the cell 2005; 16: 2382-2394.

51 Houten BV, Kuper J, Kisker C. Role of XPD in cellular functions: To TFIIH and beyond. DNA repair 2016; 44: 136-142.

52 Hu M, Liu Q, Song P, Zhan X, Luo M, Liu C *et al*. Abnormal expression of the mitotic checkpoint protein BubR1 contributes to the anti-microtubule drug resistance of esophageal squamous cell carcinoma cells. Oncol Rep 2013; 29: 185-192.

53 Huang ZL, Cao X, Luo RZ, Chen YF, Zhu LC, Wen Z. Analysis of ERCC1, BRCA1, RRM1 and TUBB3 as predictors of prognosis in patients with non-small cell lung cancer who received cisplatin-based adjuvant chemotherapy: A prospective study. Oncol Lett 2016; 11: 299-305.

54 Hurley PJ, Bunz F. ATM and ATR: components of an integrated circuit. Cell cycle 2007; 6: 414-417.

55 Inoue M, Tsugane S. Epidemiology of gastric cancer in Japan. Postgrad Med J 2005; 81: 419-424.

56 Jia S, Cai J. Update on Biomarkers in Development of Anti-angiogenic Drugs in Gastric Cancer. Anticancer Res 2016; 36: 1111-1118.

57 Joo J, Yoon KA, Hayashi T, Kong SY, Shin HJ, Park B *et al*. Nucleotide Excision Repair Gene ERCC2 and 5 Variants Increase Risk of Uterine Cervical Cancer. Cancer research and treatment : official journal of Korean Cancer Association 2015.

58 Jung Y, Lippard SJ. Direct cellular responses to platinum-induced DNA damage. Chem Rev 2007; 107: 1387-1407.

59 Kato T, Daigo Y, Aragaki M, Ishikawa K, Sato M, Kondo S *et al*. Overexpression of MAD2 predicts clinical outcome in primary lung cancer patients. Lung Cancer 2011; 74: 124-131.

60 Khedmat H, Taheri S. Gastroenterology in the developing countries: current situation, future outlook and our duty. Indian J Gastroenterol 2009; 28: 40; author reply 40-41.

61 Kim S, Sun H, Ball HL, Wassmann K, Luo X, Yu H. Phosphorylation of the spindle checkpoint protein Mad2 regulates its conformational transition. Proc Natl Acad Sci U S A 2010; 107: 19772-19777.

62 Kruiswijk F, Labuschagne CF, Vousden KH. p53 in survival, death and metabolic health: a lifeguard with a licence to kill. Nat Rev Mol Cell Biol 2015; 16: 393-405.

63 Lawrence KS, Chau T, Engebrecht J. DNA damage response and spindle assembly checkpoint function throughout the cell cycle to ensure genomic integrity. PLoS Genet 2015; 11: e1005150.

64 Lawrence KS, Engebrecht J. The spindle assembly checkpoint: More than just keeping track of the spindle. Trends Cell Mol Biol 2015; 10: 141-150.

65 Lentini L, Barra V, Schillaci T, Di Leonardo A. MAD2 depletion triggers premature cellular senescence in human primary fibroblasts by activating a p53 pathway preventing aneuploid cells propagation. J Cell Physiol 2012; 227: 3324-3332.

66 Li CY, Huang PM, Chu PY, Chen PM, Lin MW, Kuo SW *et al*. Predictors of Survival in Esophageal Squamous Cell Carcinoma with Pathologic Major Response after Neoadjuvant Chemoradiation Therapy and Surgery: The Impact of Chemotherapy Protocols. Biomed Res Int 2016; 2016: 6423297.

67 Li L, Xu DB, Zhao XL, Hao TY. Combination analysis of Bub1 and Mad2 expression in endometrial cancer: act as a prognostic factor in endometrial cancer. Arch Gynecol Obstet 2013; 288: 155-165.

68 Li X, Urwyler O, Suter B. Drosophila Xpd regulates Cdk7 localization, mitotic kinase activity, spindle dynamics, and chromosome segregation. PLoS Genet 2010; 6: e1000876.

69 Li X, Liang J, Liu YX, Wang Y, Yang XH, Bao H *et al*. Knockdown of the FoxM1 enhances the sensitivity of gastric cancer cells to cisplatin by targeting Mcl-1. Pharmazie 2016; 71: 345-348.

70 Li Z, Musich PR, Cartwright BM, Wang H, Zou Y. UV-induced nuclear import of XPA is mediated by importin-alpha4 in an ATR-dependent manner. PloS one 2013; 8: e68297.

71 Liu B, Qu J, Xu F, Guo Y, Wang Y, Yu H *et al*. MiR-195 suppresses non-small cell lung cancer by targeting CHEK1. Oncotarget 2015; 6: 9445-9456.

72 Liu J, Deng N, Xu Q, Sun L, Tu H, Wang Z *et al*. Polymorphisms of multiple genes involved in NER pathway predict prognosis of gastric cancer. Oncotarget 2016; 7: 48130-48142.

73 London N, Biggins S. Mad1 kinetochore recruitment by Mps1-mediated phosphorylation of Bub1 signals the spindle checkpoint. Genes & development 2014; 28: 140-152.

74 Lord CJ, Ashworth A. The DNA damage response and cancer therapy. Nature 2012; 481: 287-294.

75 Ma J, Shen H, Kapesa L, Zeng S. Lauren classification and individualized chemotherapy in gastric cancer. Oncol Lett 2016; 11: 2959-2964.

76 Ma Z, Yao G, Zhou B, Fan Y, Gao S, Feng X. The Chk1 inhibitor AZD7762 sensitises p53 mutant breast cancer cells to radiation in vitro and in vivo. Molecular medicine reports 2012; 6: 897-903.

77 Mandeville KL, Krabshuis J, Ladep NG, Mulder CJ, Quigley EM, Khan SA. Gastroenterology in developing countries: issues and advances. World J Gastroenterol 2009; 15: 2839-2854.

78 Mc Gee MM. Targeting the Mitotic Catastrophe Signaling Pathway in Cancer. Mediators Inflamm 2015; 2015: 146282.

79 McGranahan N, Burrell RA, Endesfelder D, Novelli MR, Swanton C. Cancer chromosomal instability: therapeutic and diagnostic challenges. EMBO Rep 2012; 13: 528-538.

80 Meek DW, Hupp TR. The regulation of MDM2 by multisite phosphorylation--opportunities for molecular-based intervention to target tumours? Semin Cancer Biol 2010; 20: 19-28.

81 Mei Z, Su T, Ye J, Yang C, Zhang S, Xie C. The miR-15 family enhances the radiosensitivity of breast cancer cells by targeting G2 checkpoints. Radiat Res 2015; 183: 196-207.

82 Michel LS, Liberal V, Chatterjee A, Kirchwegger R, Pasche B, Gerald W *et al*. MAD2 haplo-insufficiency causes premature anaphase and chromosome instability in mammalian cells. Nature 2001; 409: 355-359.

83 Mikhailov A, Cole RW, Rieder CL. DNA damage during mitosis in human cells delays the metaphase/anaphase transition via the spindle-assembly checkpoint. Curr Biol 2002; 12: 1797-1806.

84 Monks A, Harris ED, Vaigro-Wolff A, Hose CD, Connelly JW, Sausville EA. UCN-01 enhances the in vitro toxicity of clinical agents in human tumor cell lines. Invest New Drugs 2000; 18: 95-107.

85 Mossaid I, Fahrenkrog B. Complex Commingling: Nucleoporins and the Spindle Assembly Checkpoint. Cells 2015; 4: 706-725.

86 Nadkarni A, Burns JA, Gandolfi A, Chowdhury MA, Cartularo L, Berens C *et al*. Nucleotide Excision Repair and Transcription-coupled DNA Repair Abrogate the Impact of DNA Damage on Transcription. The Journal of biological chemistry 2015.

87 Nascimento AV, Singh A, Bousbaa H, Ferreira D, Sarmento B, Amiji MM. Mad2 checkpoint gene silencing using epidermal growth factor receptor-targeted chitosan nanoparticles in non-small cell lung cancer model. Mol Pharm 2014; 11: 3515-3527.

88 Nascimento AV, Gattacceca F, Singh A, Bousbaa H, Ferreira D, Sarmento B *et al*. Biodistribution and pharmacokinetics of Mad2 siRNA-loaded EGFR-targeted chitosan nanoparticles in cisplatin sensitive and resistant lung cancer models. Nanomedicine (Lond) 2016; 11: 767-781.

89 Nedaeinia R, Manian M, Jazayeri MH, Ranjbar M, Salehi R, Sharifi M *et al*. Circulating exosomes and exosomal microRNAs as biomarkers in gastrointestinal cancer. Cancer Gene Ther 2016.

90 O'Grady S, Finn SP, Cuffe S, Richard DJ, O'Byrne KJ, Barr MP. The role of DNA repair pathways in cisplatin resistant lung cancer. Cancer Treat Rev 2014; 40: 1161-1170.

91 Ofir M, Hacohen D, Ginsberg D. MiR-15 and miR-16 are direct transcriptional targets of E2F1 that limit E2F-induced proliferation by targeting cyclin E. Mol Cancer Res 2011; 9: 440-447.

92 Palou R, Palou G, Quintana DG. A role for the spindle assembly checkpoint in the DNA damage response. Curr Genet 2016.

93 Peralta-Sastre A, Manguan-Garcia C, de Luis A, Belda-Iniesta C, Moreno S, Perona R *et al*. Checkpoint kinase 1 modulates sensitivity to cisplatin after spindle checkpoint activation in SW620 cells. Int J Biochem Cell Biol 2010; 42: 318-328.

94 Pouliot LM, Chen YC, Bai J, Guha R, Martin SE, Gottesman MM *et al*. Cisplatin sensitivity mediated by WEE1 and CHK1 is mediated by miR-155 and the miR-15 family. Cancer Res 2012; 72: 5945-5955.

95 Qixing M, Gaochao D, Wenjie X, Rong Y, Feng J, Lin X *et al*. Predictive Value of Ercc1 and Xpd Polymorphisms for Clinical Outcomes of Patients Receiving Neoadjuvant Therapy: A Prisma-Compliant Meta-Analysis. Medicine (Baltimore) 2015; 94: e1593.

96 Rao S, Beckman RA, Riazi S, Yabar CS, Boca SM, Marshall JL *et al*. Quantification and expert evaluation of evidence for chemopredictive biomarkers to personalize cancer treatment. Oncotarget 2016.

97 Rechkunova NI, Lavrik OI. Nucleotide excision repair in higher eukaryotes: mechanism of primary damage recognition in global genome repair. Sub-cellular biochemistry 2010; 50: 251-277.

98 Royou A, Macias H, Sullivan W. The Drosophila Grp/Chk1 DNA damage checkpoint controls entry into anaphase. Curr Biol 2005; 15: 334-339.

99 Scharer OD. Nucleotide excision repair in eukaryotes. Cold Spring Harbor perspectives in biology 2013; 5: a012609.

100 Schvartzman JM, Duijf PH, Sotillo R, Coker C, Benezra R. Mad2 is a critical mediator of the chromosome instability observed upon Rb and p53 pathway inhibition. Cancer Cell 2011; 19: 701-714.

101 Sedgwick GG, Larsen MS, Lischetti T, Streicher W, Jersie-Christensen RR, Olsen JV *et al*. Conformation-specific anti-Mad2 monoclonal antibodies for the dissection of checkpoint signaling. MAbs 2016; 8: 689-697.

102 Seol HJ, Yoo HY, Jin J, Joo KM, Kim HS, Yoon SJ *et al*. The expression of DNA damage checkpoint proteins and prognostic implication in metastatic brain tumors. Oncol Res 2011; 19: 381-390.

103 Sotillo R, Schvartzman JM, Socci ND, Benezra R. Mad2-induced chromosome instability leads to lung tumour relapse after oncogene withdrawal. Nature 2010; 464: 436-440.

104 Spivak G. Nucleotide excision repair in humans. DNA repair 2015.

105 Sudo T, Nitta M, Saya H, Ueno NT. Dependence of Paclitaxel sensitivity on a functional spindle assembly checkpoint. Cancer Res 2004; 64: 2502-2508.

106 Sugitani N, Sivley RM, Perry KE, Capra JA, Chazin WJ. XPA: A key scaffold for human nucleotide excision repair. DNA repair 2016; 44: 123-135.

107 Suijkerbuijk SJ, Kops GJ. Preventing aneuploidy: the contribution of mitotic checkpoint proteins. Biochim Biophys Acta 2008; 1786: 24-31.

108 Sulli G, Di Micco R, d'Adda di Fagagna F. Crosstalk between chromatin state and DNA damage response in cellular senescence and cancer. Nat Rev Cancer 2012; 12: 709-720.

109 Swanton C, Tomlinson I, Downward J. Chromosomal instability, colorectal cancer and taxane resistance. Cell cycle 2006; 5: 818-823.

110 Taleei R, Girard PM, Nikjoo H. DSB repair model for mammalian cells in early S and G1 phases of the cell cycle: application to damage induced by ionizing radiation of different quality. Mutat Res Genet Toxicol Environ Mutagen 2015; 779: 5-14.

111 Teixeira JH, Silva P, Faria J, Ferreira I, Duarte P, Delgado ML *et al*. Clinicopathologic significance of BubR1 and Mad2 overexpression in oral cancer. Oral Dis 2015; 21: 713-720.

112 Thangavel C, Boopathi E, Ertel A, Lim M, Addya S, Fortina P *et al*. Regulation of miR106b cluster through the RB pathway: mechanism and functional targets. Cell cycle 2013; 12: 98-111.

113 Usanova S, Piee-Staffa A, Sied U, Thomale J, Schneider A, Kaina B *et al*. Cisplatin sensitivity of testis tumour cells is due to deficiency in interstrand-crosslink repair and low ERCC1-XPF expression. Mol Cancer 2010; 9: 248.

114 Vanoosthuyse V, Hardwick KG. Overcoming inhibition in the spindle checkpoint. Genes & development 2009; 23: 2799-2805.

115 Vogel C, Hager C, Bastians H. Mechanisms of mitotic cell death induced by chemotherapy-mediated G2 checkpoint abrogation. Cancer Res 2007; 67: 339-345.

116 Wang D, Lippard SJ. Cellular processing of platinum anticancer drugs. Nature reviews Drug discovery 2005; 4: 307-320.

117 Wang L, Yin F, Du Y, Chen B, Liang S, Zhang Y *et al*. Depression of MAD2 inhibits apoptosis and increases proliferation and multidrug resistance in gastric cancer cells by regulating the activation of phosphorylated survivin. Tumour Biol 2010; 31: 225-232.

118 Wang X, Jin DY, Wong YC, Cheung AL, Chun AC, Lo AK *et al*. Correlation of defective mitotic checkpoint with aberrantly reduced expression of MAD2 protein in nasopharyngeal carcinoma cells. Carcinogenesis 2000; 21: 2293-2297.

119 Weaver BA, Cleveland DW. Aneuploidy: instigator and inhibitor of tumorigenesis. Cancer Res 2007; 67: 10103-10105.

120 Westhorpe FG, Tighe A, Lara-Gonzalez P, Taylor SS. p31comet-mediated extraction of Mad2 from the MCC promotes efficient mitotic exit. J Cell Sci 2011; 124: 3905-3916.

121 Wittekind C. The development of the TNM classification of gastric cancer. Pathol Int 2015; 65: 399-403.

122 Wong OK, Fang G. Cdk1 phosphorylation of BubR1 controls spindle checkpoint arrest and Plk1-mediated formation of the 3F3/2 epitope. J Cell Biol 2007; 179: 611-617.

123 Wu B, Qiu W, Wang P, Yu H, Cheng T, Zambetti GP *et al*. p53 independent induction of PUMA mediates intestinal apoptosis in response to ischaemia-reperfusion. Gut 2007; 56: 645-654.

124 Wu X, Shell SM, Yang Z, Zou Y. Phosphorylation of nucleotide excision repair factor xeroderma pigmentosum group A by ataxia telangiectasia mutated and Rad3-related-dependent checkpoint pathway promotes cell survival in response to UV irradiation. Cancer Res 2006; 66: 2997-3005.

125 Xia L, Zhang D, Du R, Pan Y, Zhao L, Sun S *et al*. miR-15b and miR-16 modulate multidrug resistance by targeting BCL2 in human gastric cancer cells. Int J Cancer 2008; 123: 372-379.

126 Xiao S, Cui S, Lu X, Guan Y, Li D, Liu Q *et al*. The ERCC2/XPD Lys751Gln polymorphism affects DNA repair of benzo[a]pyrene induced damage, tested in an in vitro model. Toxicol In Vitro 2016; 34: 300-308.

127 Xu J, Li Y, Wang F, Wang X, Cheng B, Ye F *et al*. Suppressed miR-424 expression via upregulation of target gene Chk1 contributes to the progression of cervical cancer. Oncogene 2013; 32: 976-987.

128 Yang X, Xu W, Hu Z, Zhang Y, Xu N. Chk1 is required for the metaphase-anaphase transition via regulating the expression and localization of Cdc20 and Mad2. Life sciences 2014; 106: 12-18.

129 Yu J, Zhang L. PUMA, a potent killer with or without p53. Oncogene 2008; 27 Suppl 1: S71-83.

130 Yu L, Liu S, Guo W, Zhang B, Liang Y, Feng Q. Upregulation of Mad2 facilitates in vivo and in vitro osteosarcoma progression. Oncol Rep 2012; 28: 2170-2176.

131 Yuan B, Xu Y, Woo JH, Wang Y, Bae YK, Yoon DS *et al*. Increased expression of mitotic checkpoint genes in breast cancer cells with chromosomal instability. Clin Cancer Res 2006; 12: 405-410.

132 Yun M, Han YH, Yoon SH, Kim HY, Kim BY, Ju YJ *et al*. p31comet Induces cellular senescence through p21 accumulation and Mad2 disruption. Mol Cancer Res 2009; 7: 371-382.

133 Zannini L, Delia D, Buscemi G. CHK2 kinase in the DNA damage response and beyond. J Mol Cell Biol 2014; 6: 442-457.

134 Zhang Y, Hunter T. Roles of Chk1 in cell biology and cancer therapy. Int J Cancer 2014; 134: 1013-1023.

135 Zhou BB, Elledge SJ. The DNA damage response: putting checkpoints in perspective. Nature 2000; 408: 433-439.

136 Zhu W, Zhu D, Lu S, Wang T, Wang J, Jiang B *et al*. miR-497 modulates multidrug resistance of human cancer cell lines by targeting BCL2. Med Oncol 2012; 29: 384-391.

137 Zhuang M, Shi Q, Zhang X, Ding Y, Shan L, Shan X *et al*. Involvement of miR-143 in cisplatin resistance of gastric cancer cells via targeting IGF1R and BCL2. Tumour Biol 2015; 36: 2737-2745.

ANEXO I

N= 61		% LOW MAD2	% HIGH MAD2	X^2	*p*
AGE	Mean	56.8	57.9		*0.750*
SEX	Male	50	36.8		
	Female	50	63.2	0.814	*0.814*
STAGE	I	12.5	10		
	II	25	30		
	III	32.5	30		
	IV	30	30	3.846	*0.567*
GRADE	Good	10	0		
	Moderate	39	40		
	Poor	51	60	5.087	*0.079*
LAUREN	Intestinal	45	50		
	Difusse/mixt	55	50	0.176	*0.675*
NODULE M.	No	20	21.1		
	Yes	80	78.9	0.008	*0.929*
DISTANT M.	No	35	60		
	Yes	51	40	0.07	*0.782*
TREATMENT	None	34	40		
	RT	34	30		
	RT+CDDP	32	30	0.047	*0.923*
H.PYLORI	No	51	45		
	Yes	40	50	0.552	*0.458*
RECURRENCE	No	40	42.1		
	Yes	60	57.9	0.021	*0.884*
DEATH	No	43.3	10.5		
	Yes	56.7	89.5	5.894	*0.011*

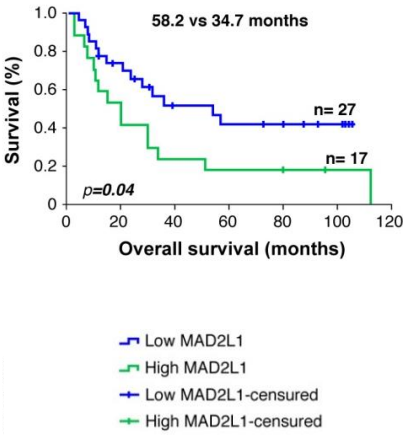

Table 1: **Association of MAD2 expression with the clinicopathological characteristics of Gastric Cancer patients.** Results from a total of 61 patient samples. Correlation between clinicopathological characteristics and MAD2 expression was assessed by *Chi2* or *Fisher* exact test and *t-test* to compare the mean age between groups. Statistical significance was considered when $p < 0.05$, using IBM SPSS Statistics 22.

Figure**: High MAD2L1 expression in tumor correlates with poor clinical outcome in human gastric cancer.**

A) Kaplan-Meier curves of overall survival (OS) period in patients with high or low expression of MAD2L1. Survival curves were statistically analyzed by the Log-Rank test. IBM SPSS Statistics 22 software.

ANEXO II

International Journal of Cancer and Oncology

OMMEGA Publishers
Answering Intelligence
www.ommegaonline.com

Mini Review

OPEN ACCESS

MAD2 in the Spotlight as a Cancer Therapy Regulator

Bargiela-Iparraguirre, J.[1,2], Fernandez-Fuente, M, Calés C[1] , Herrera, L.A[2] and Sanchez- Perez, I[1,2*]

[1]Departament de Bioquímica, Facultad Medicina, Instituto de Investigaciones Biomédicas Madrid CSIC-UAM; Madrid, Spain
[2]Unidad de Investigación Biomédica en Cáncer, Instituto Nacional de Cancerología (INCan)-Instituto de Investigaciones Biomédicas (IIB), Universidad Nacional Autónoma de México (UNAM), México; Instituto de Investigaciones Biomédicas, Universidad Nacional Autónoma de México, Circuito Escolar S/N, Ciudad Universitaria, Coyoacán, México

***Corresponding author:** Isabel Sanchez-Perez, PhD, Departament de Bioquímica, Facultad Medicina, Instituto de Investigaciones Biomédicas Madrid CSIC-UAM; C/Arturo Duperier 4, 28029 Madrid, Spain, Tel: (+34) 91-5854380/ Fax: (+34) 91-58544001, E-mail: misanchez@iib.uam.es; is.perez@uam.es

Abstract

MAD2 is a key protein required for mitotic checkpoint function and for the maintenance of accuracy on the mitotic process of every cell cycle. Deregulation of MAD2 is associated with both progression and poor prognosis in cancer disease. However, new evidence highlights the implication of MAD2 in other biological functions besides its classical Mitotic checkpoint implication, such as apoptosis, senescence and also DNA damage repair, which can ultimately define the response to a specific treatment. Development of novel therapeutic approaches and optimization of the existing therapies are now required for the design of successful treatments of cancer. MAD2 is emerging as a new key target for the design of more effective and personalized treatments in cancer disease.

Keywords: MAD2; Chemotherapy; Cell cycle; Mitosis; Cancer; SAC; Biomarker; Resistance

Abbreviations: SAC: Spindle Assembly Checkpoint; CIN: Chromosome Instability

Received Date: April 27, 2016
Accepted Date: May 27, 2016
Published Date: June 01, 2016

Citation: Sanchez- Perez, I., et al. MAD2 in the Spotlight as a Cancer Therapy Regulator. (2016) Int J Cancer Oncol 3(2): 1- 6.

DOI: 10.15436/2377-0902.16.889

Introduction

Mitosis is the last chance that cells have to avoid chromosome miss-segregation, and this can be achieved thanks to the activation of the spindle assembly checkpoint (SAC). SAC is a conserved mechanism, which ensures the fidelity of chromosome distribution in mitosis by preventing anaphase onset until the correct bipolar microtubule-kinetochore attachments are formed. SAC controls Metaphase-Anaphase transition and delays anaphase until correct bipolar attachment of sister chromatids to the mitotic spindle is achieved, thus ensuring accuracy of the chromosome segregation in mitosis[1]. This complex of proteins includes MAD1, MAD2, BUB1, BUB3, BUBR1, in association with the APC/C activator Cdc20[2]. When SAC is activated, it inhibits the anaphase-promoting complex/cyclosome (APC/C), ligase complex which induces degradation of specific cell cycle regulatory proteins, such as securin, an inhibitor of anaphase initiation activation, and Cyclin B. Degradation of this proteins ultimately leads to mitosis exit[3,4].

MAD2 has a central role in the modulation of the mitotic checkpoint: it activates the "waiting signal" when the microtubules are not correctly attached to the kinetochore in order to prevent unequal chromosome segregation[5]. The gene *MAD2L1* (mitotic arrest deficient-like 1) localized in 4q27 encodes MAD2, a small protein that is highly conserved from yeast to humans. The assembly and consequent activation of the Mitotic Checkpoint Complex (MCC) is initiated by the conversion of MAD2 from an open (O-MAD2) to a closed (C-MAD2) conformation, which then binds tightly to Cdc20. The C-MAD2–Cdc20 (MC) subcomplex associates then with BUBR1-BUB3 to form the mitotic checkpoint complex MCC[6]. Conversely, the disassembly of MCC that takes place when the checkpoint is turned off leads to the conversion of C-MAD2 back to O-MAD2[7,8]. Recently, a MAD2-inter-

acting protein, p31^{comet}, has been characterized as a spindle checkpoint silencer during mitosis[9-11]. This protein is a structural mimic of O-MAD2 (open state) and binds to C-MAD2 (closed state). Binding of p31^{comet} prevents dimerization of MAD2, which in turn inhibits the conformational change of O-MAD2 into C-MAD2, its active form, and ultimately triggers the exit from the mitotic process[9,10]. (FIGURE 1)

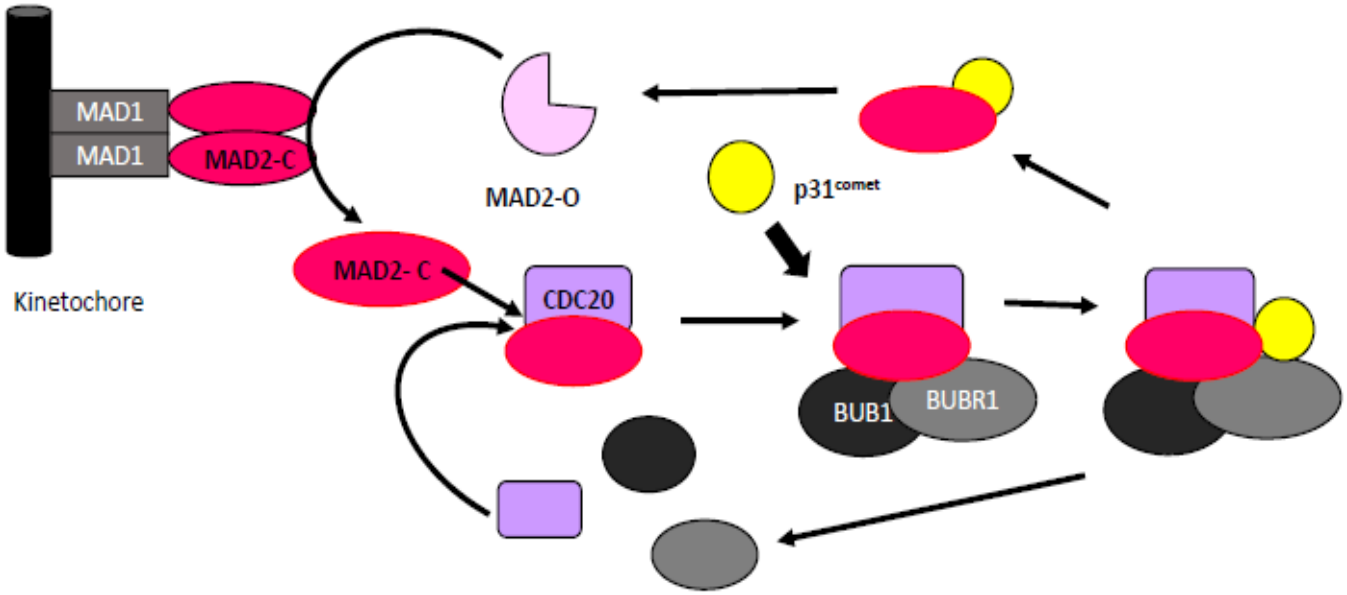

Figure 1:

The aim of this review is to highlight the relationship between MAD2 protein levels and chemotherapy response. Although the role of MAD2 as a prognostic factor in solid tumors is now well established, the data we analyze here suggest that MAD2 could be controlling other pathways apart from controlling SAC. These new functions could drive the ultimate fate of the cell: apoptosis, senescence or DNA repair, as a consequence of the treatment with drugs routinely included in the therapeutic regimen for patients. After careful analysis of this information, we discuss here the role MAD2 as a potential new therapeutic biomarker.

Deregulation of MAD2 levels in cancer and therapy response *in vitro* and *in vivo*

Deregulation of MCC protein level increases chromosome instability (CIN), a well known hallmark of cancer. Overexpression MAD2 is commonly found in gastric, colorectal, lung, breast and human ovary tumors, and many authors have demonstrated its correlation with tumorigenesis invasion and metastasis[12,13]. Using rodent models of the disease, it has been shown that reduced levels of MAD2[14], cause a mild increase in the onset of spontaneous tumors (around 30%). On the other hand, after generation of mice over-expressing MAD2[15], it was observed that all of them displayed high rates of spontaneous tumorigenesis. Despite the inherent variations associated with this approach, it is important to note that a common feature of the tumorigenic process observed in these mice models is that the tumors are always developed at old ages, which suggests that aneuploidy itself may be a promoting factor rather than a tumor initiator. However, the involvement of MAD2 on therapy response is still unclear, since some data suggest that over expression of MAD2 increases both sensitivity and resistance to a specific therapy.

In vitro analyses of tumor cell lines have shown that MAD2 levels influence chemotherapy response. Low levels of MAD2 increase resistance to platinum compounds, vincristine and γ- irradiation both in nasopharyngeal and Testicular Germ Cellular Tumor (TGCT) cancer cells[16,17]. In ovarian and gastric cancer cell lines, it has been demonstrated that through modulation of MAD2 levels using specific shRNAs, expression of p31^{comet} [18] or micro-RNAs, cells become more resistant to PTX[19-22]. Resistance to PTX seems to be correlated with apoptosis inhibition or senescence induction[19]. This evidence suggests that a nonfunctional SAC caused by insufficient kinetochore proteins would not be able to activate the apoptotic pathway. Moreover, we have also demonstrated that in MKN45 gastric cancer cells, reducing MAD2 protein levels confers resistance to PTX. Even though we did not observe any modifications in apoptotic induction pathways, we did note a significant induction of senescence accompanied by an elevation in IL 6 and IL-8 levels, of a consequence of MAD2 downregulation. (Figure 2)

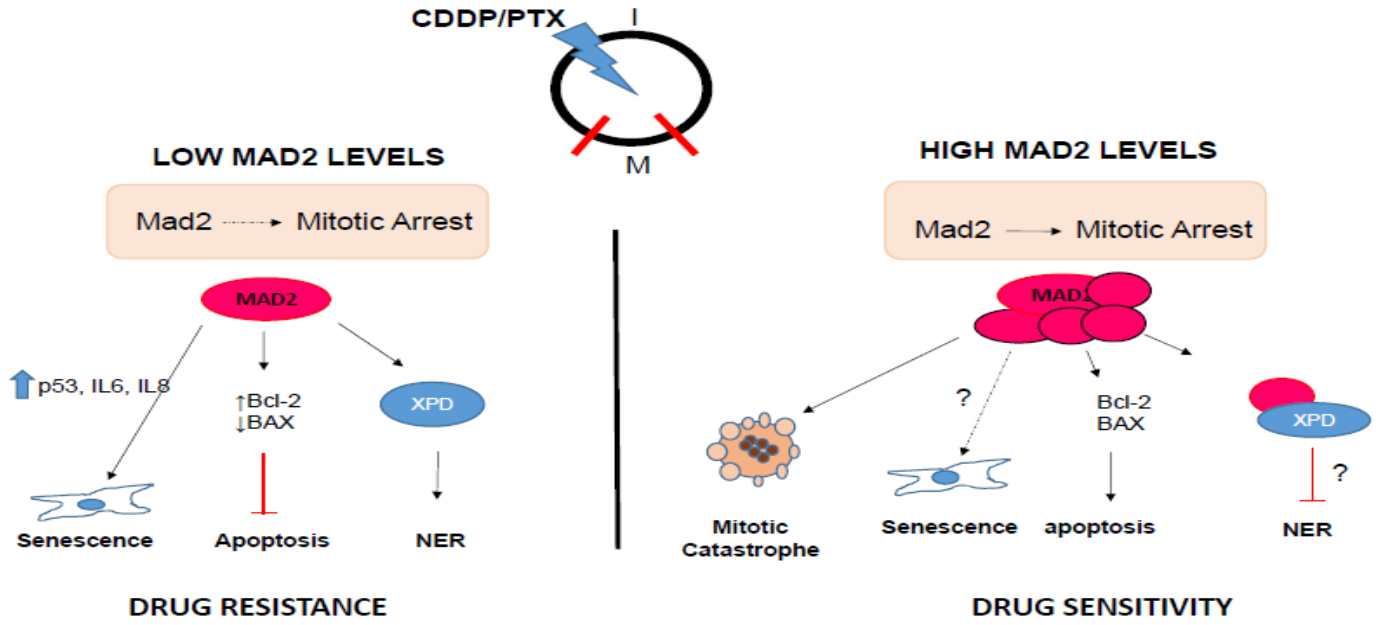

Figure 2:

It is important to be aware of the fact that the *in vitro* cellular systems do not always mimic the cellular processes that occur *in vivo*; tumors are subjected to multifactorial changes and undergo dramatically different developments between patients and therefore the expected response to a specific drug is not universal. Up until now, the available studies on MAD2 expression and chemotherapy response in patients have often been controversial. In general, taking into account the most relevant clinical studies, we can infer that elevated levels of MAD2 correlate with poor prognosis, evidenced by lower overall survival (OS) and or PFS (table 1). In contrast, immunohistochemical analysis of MAD2 within a series of high-grade serous epithelial ovarian cancer cell lines from patients who had previously been treated with CDDP and/or PTX, showed that low level MAD2 expressing patients had a shorter survival period and slower tumor progression[23]. It has also been shown that elevated MAD2 expression may lead to resistance to CDDP in advanced uterine cervical cancer patients, which is in clear disagreement with what seems to happen in the available *in vitro* studies with PTX[24]. However, we should take into account the following factors: On one hand, the criteria for gradation of MAD2 levels are not adequately standardized. This could explain the differences between the conclusions of the available studies. On the other hand, the cell type or the nature of the tissues analyzed in these previous studies should be taken as well in consideration.

Table 1:

TUMOR	MAD2 LEVELS	CLINICAL PARAMETERS	REFERENCES
Ovary	HIGH	tPFS	Furlong, Fitzpatrick et al., 2012
	LOW	tPFS	McGrogan B. et al. 2014
Colon	LOW	tos	Li y Zhang , 2004
Lung	LOW	tos	Sotillo , Schvartzman et al., 2010
	HIGH	tOS/WFS	Tatsuya Kato et al. 2011
Urothelial Bladder	HIGH	toS	Choi JW et al, 2013
Oral	HIGH	toS	Teixeira et al.,2015
Endometria l	HIGH	toS	Lin Li et al., 2013
Neuroblastoma	HIGH	toS	Kohei Otake et al., 2011

After careful analysis of all available data, we propose a potential model where MAD2 protein levels on the primary tumor, would decide the effect of the given treatment (Figure 3). In resectable primary tumors with low MAD2 expression, surgery followed by adjuvant chemotherapy continues to be the only curative option and presents a better outcome. However, in some cases, the tumor relapses due to resistance to apoptosis and/or senescent phenotype induction in these conditions, which can complicate the clinical landscape. On the contrary, resectable primary tumors with high MAD2 show a better clinical outcome after adjuvant therapy, suggesting that MAD2 is required for apoptosis induction in primary tumors diagnosed at early stages. However, in advanced stage tumors with high levels of MAD2, presenting metastasis and therefore poor prognosis, treatment is inefficient and our model suggests that downregulation of MAD2 could improve clinical outcome in this particular situation. (Figure 3)

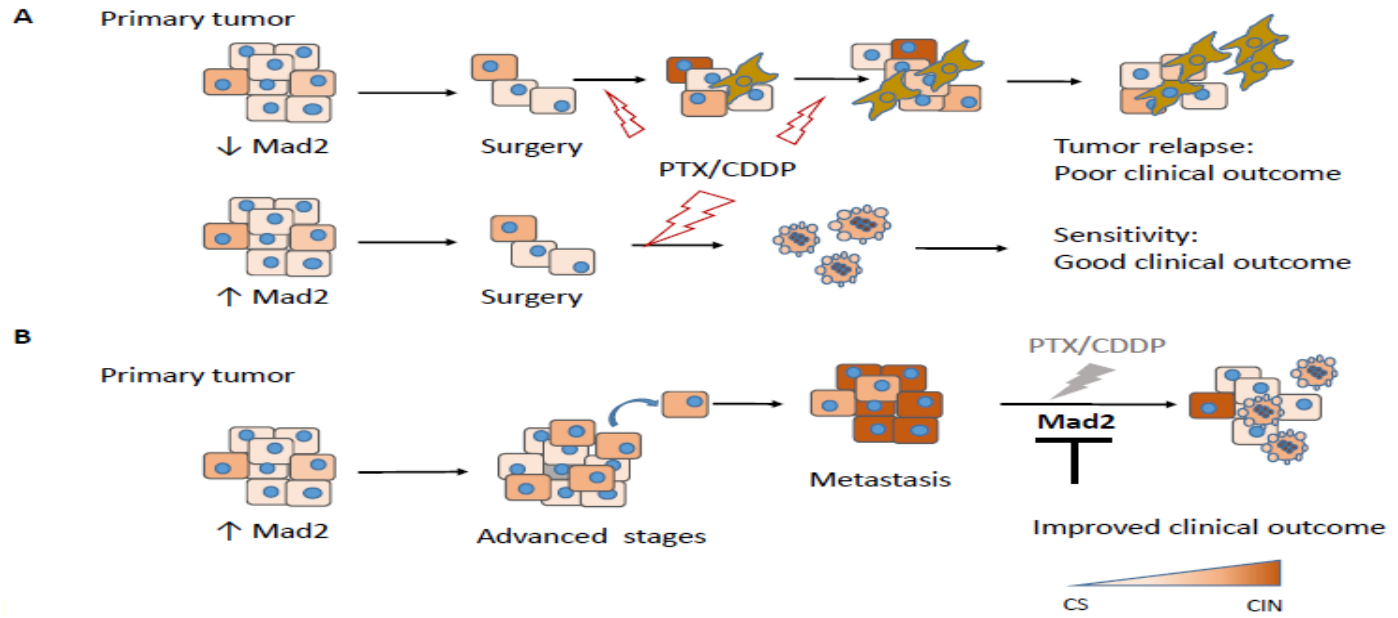

Figure 3:

The results available in the literature indicate that, although it is hard to predict the unique responses of a patient to therapy based on its levels of expression of MAD2 at the time of diagnosis, it is not clear whether altered MAD2 levels do affect therapy response, as this seems to depend on the origin of the tumor.

MAD2, more than a mitotic regulator?

The above data indicate that MAD2 is acting as an Oncogene, and could be used as a prognosis marker. However, the role of MAD2 in response to therapy is unknown, since the data available from the literature are contradictory and the majority of them are based on *in vitro* systems. MAD2 seems to be involved in various functions along the cell cycle, one of them being well characterized and specific to mitosis, and another one which is involved in the control of the interphase. Additional functions should be investigated, in relation with the control of cell fate after cellular damage, and also in the context of cancer therapy response.

The first evidence of MAD2 as a modulator of DNA damage response was obtained using Hela Cells, in a set of experiments where the authors demonstrated that the delay in mitosis induced by DNA damage is not due to an ATM-mediated DNA damage checkpoint pathway[25]. Other groups observed an interplay between ATM and SAC activation[26]. A novel connection between both processes has been described, where a physical interaction between nuclear MAD2 and Chk1 was detected in stress-free conditions, being this interaction stronger when cells presented DNA damage. One possibility to explain these findings is to consider that MAD2 plays a role controlling the translocation of DNA damage repair proteins to the nucleus[27]. In agreement with these results, MAD2 has been shown to be localized at the nuclear pore during interphase and to interact with TRp1 and Nup153 proteins[28]. For instance, in a work performed using HeLa cells, it was demonstrated that MAD2 interacts with XPD and ERCC1, two key proteins that participate in nucleotide excision repair pathway (NER). It was shown that in MAD2 overexpressing cells, XPD was localized in the cytoplasm and its recruitment to the nucleus after CDDP treatment was weak, whereas XPA was over expressed and accumulated in the nucleus. Some authors suggest that high levels of MAD2 can sensitize to CDDP through its ability to reorganize repair proteins, which could play a role sequestering XPD in the cytoplasm and therefore making the NER pathway weaker or inefficient. On the other hand, they did not find any relationship between MAD2 and Rad51, which are both involved in homologous recombination repair[24].

Other observations suggest a role for MAD2 within the apoptosis signaling pathway, for instance MAD2 downregulation correlates with a reduction on the expression of apoptotic proteins and on caspases activity within the mitotic cell population[29]. Supporting these data, in the germ tumor cell line (GCT) 1411HP, low levels of MAD2 correlate with an inhibition of the MEK/ERK and apoptotic pathways[17]. Furthermore, downregulation of MAD2 in GC and nasopharyngeal tumor cell lines increased cisplatin resistance due to the fact that the ratio of anti-apoptotic protein Bcl-2 levels and pro-apoptotic protein Bax was increased, whereas apoptosis was related to the expression of proteins such as cytochrome c, while cleaved caspase 3 maintained low levels[29,30].

The first observation that correlates MAD2 with senescence, came from a study in which low doses of Doxorrubicine induced senescence[31]. In other studies, depletion of MAD2 in human fibroblast cell line (IMR-90) confirmed the induction of senescence through the p53 signaling pathway[32]. These results suggest that aneuploidy induced by MAD2 depletion, is sensed as a stress signal by normal cells, which in turn will trigger premature cellular senescence that acts as a barrier to cell proliferation in cells with unbalanced karyotypes, and not related with DNA damage. Supporting this data it has also been proved that overexpressing $p31^{comet}$, which acts as a spindle checkpoint inhibitor, inducing tumor cell senescence by mediating accumulation of p21 (Waf1/Cip1) and MAD2 disruption[33]. In addition, our data corroborate this fact[20].

Conclusions and Future Perspectives

In this review, we have highlighted the relevant evidence of the implication of MAD2 protein levels as a marker which is in fact capable to define patients overall survival. To sum up, upregulation of MAD2 protein levels correlates with low survival, indicating that MAD2 is a good prognosis biomarker. It is clear that MAD2 plays other functions beyond mitosis; however further studies need to be done to clarify the partners and the real function of MAD2, since at the moment only *in vitro* correlations exist between survival /dead and MAD2 levels. There is a lack of in depth studies characterizing the molecular mechanism involved in this processes. The fact that MAD2 regulates the response to therapy, suggests that it could be a new therapeutic target. However, some concerns should be raised, in order to facilitate the development of drugs targeting MAD2. These doubts come from the *in vitro* analysis, where depletion of MAD2 confers senescence-like phenotype after treatment with agents used routinely in cancer therapy. Sadly there are no clinical trials corroborating the effect of MAD2 function in patients. However, the silencing MAD2 expression using siRNAs, increases sensitivity to chitosan in non-small cell lung model[34,35]. In addition, new synthetic antimitotic drugs showed that its main apoptotic potential is due to its ability to disrupt the SAC machinery and therefore provoking a mitotic catastrophe[36].

There are many gaps to fill in the current knowledge of the processes regulating cell fate, so future studies will need to answer some of this crucial question.

How is MAD2 regulated? Is it really the amount of protein what makes the difference or is it its availability to be in the right place and the right conformation state? And, is this balanced by its interactions with other SAC proteins?

Does MAD2 predict the potential response to therapy, or is it on the other hand specific for a certain drug and/or a certain type of tumor?

How do MAD2 levels influence the other mitotic complex proteins or its functionality?

Conflicts of Interest: The authors declare that they have no competing relationship or commercial affiliations or any financial interests.

Acknowledgments: This work was supported by a grant from UAM-SANTANDER CEAL-AL/2013-29. JBI was supported by a fellowship from Catedra Isaac Costero, funded by Banco Santander-UAM and is a doctoral student from Programa de Doctorado en Ciencias Biomédicas, Universidad Nacional Autónoma de México (UNAM) and received fellowship CVU:607546 from CONACYT.

References

1. Musacchio, A., Salmon, E.D. The spindle-assembly checkpoint in space and time. (2007) Nat Rev Mol cell Biology 8(5): 379-393.
2. Lara-Gonzalez, P., Westhorpe, F.G., Taylor, S.S. The spindle assembly checkpoint. (2012) Curr Biol 22(22): R966-R980.
3. Jia, L., Kim, S., Yu, H. Tracking spindle checkpoint signals from kinetochores to APC/C. (2013) Trends Biochem Sci 38(6): 302-311.
4. Chang, L., Barford, D. Insights into the anaphase-promoting complex: a molecular machine that regulates mitosis. (2014) Curr Opin Struct Biol 29:1-9.
5. Ballister, E.R., Lampson, M.A. Chromosomal Instability: Mad2 beyond the spindle checkpoint. (2012) Curr Biol 22(7): R233-R235.
6. Luo, X., Tang, Z., Xia, G., et al. The Mad2 spindle checkpoint protein has two distinct natively folded states. (2004) Nat Struct Mol Biol 11(4): 338-345.
7. Luo, X., Tang, Z., Rizo, J., et al. The Mad2 spindle checkpoint protein undergoes similar major conformational changes upon binding to either Mad1 or Cdc20. (2002) Mol cell 9(1): 59-71.
8. Luo, X., Fang, G., Coldiron, M., et al. Structure of the Mad2 spindle assembly checkpoint protein and its interaction with Cdc20. (2000) Nat Struct Mol Biol 7(3): 224-229.
9. Westhorpe, F.G., Tighe, A., Lara-Gonzalez, P., et al. p31comet-mediated extraction of Mad2 from the MCC promotes efficient mitotic exit. (2011) J cell sci 124(Pt 22): 3905-3916.
10. Habu, T., Matsumoto, T. p31(comet) inactivates the chemically induced Mad2- dependent spindle assembly checkpoint and leads to resistance to anti-mitotic drugs. (2013) SpringerPlus 2: 562.
11. Xia, G., Luo, X., Habu, T., et al. Conformation-specific binding of p31(comet) antagonizes the function of Mad2 in the spindle checkpoint. (2004) EMBO J 23(15): 3133-3143.
12. Kato, T., Daigo, Y., Aragaki, M., et al. Overexpression of MAD2 predicts clinical outcome in primary lung cancer patients. (2011) Lung Cancer 74(1): 124-131.
13. Zhang, S.H., Xu, A.M., Chen, X.F., et al. Clinicopathologic significance of mitotic arrest defective protein 2 overexpression in hepatocellular carcinoma. (2008) Hum Pathol 39(12): 1827-1834.
14. Li, M., Zhang, P. Spindle assembly checkpoint, aneuploidy and tumorigenesis. (2009) Cell cycle 8(21): 3440.
15. Sotillo, R., Hernando, E., Diaz-Rodriguez, E., et al. Mad2 overexpression promotes aneuploidy and tumorigenesis in mice. (2007) Cancer Cell 11(1): 9-23.
16. Wang, X., Jin, D.Y., Wong, Y.C., et al. Correlation of defective mitotic checkpoint with aberrantly reduced expression of MAD2 protein in nasopharyngeal carcinoma cells. (2000) Carcinogenesis 21(12): 2293-2297.
17. Fung, M.K., Cheung, H.W., Ling, M.T., et al. Role of MEK/ERK pathway in the MAD2-mediated cisplatin sensitivity in testicular germ cell tumour cells. (2006) Br J cancer 95(4): 475-484.
18. Date, D.A., Burrows, A.C., Venere, M., et al. Coordinated regulation of p31(Comet) and Mad2 expression is required for cellular proliferation. (2013) Cell cycle 12(24): 3824-3832.

19. Hao, X., Zhou, Z., Ye, S., et al. Effect of Mad2 on paclitaxel-induced cell death in ovarian cancer cells. (2010) J Huazhong Univ Sci Technolog Med Sci 30(5): 620-625.
20. Bargiela-Iparraguirre, J., Prado-Marchal, L., Pajuelo-Lozano, N., et al. Mad2 and BubR1 modulates tumourigenesis and paclitaxel response in MKN45 gastric cancer cells. (2014) Cell cycle 13(22): 3590-3601.
21. Otake, K., Uchida, K., Tanaka, K., et al. HsMAD2 mRNA expression may be a predictor of sensitivity to paclitaxel and survival in neuroblastoma. (2011) Pediatr Surg Int 27(2): 217-223.
22. Tambe, M., Pruikkonen, S., Maki-Jouppila, J., et al. Novel Mad2-targeting miR-493-3p controls mitotic fidelity and cancer cells' sensitivity to paclitaxel. (2016) Oncotarget 7(11): 12267-12285.
23. Furlong, F., Fitzpatrick, P., O'Toole, S., et al. Low MAD2 expression levels associate with reduced progression-free survival in patients with high-grade serous epithelial ovarian cancer. (2012) J Pathol 226(5): 746-755.
24. Morishita, M., Sumi, T., Nakano, Y., et al. Expression of mitotic-arrest deficiency 2 predicts the efficacy of neoadjuvant chemotherapy for locally advanced uterine cervical cancer. (2012) Exp Ther Med 3(2): 341-346.
25. Mikhailov, A., Cole, R.W., Rieder, C.L. DNA damage during mitosis in human cells delays the metaphase/anaphase transition via the spindle-assembly checkpoint. (2002) Curr Biol 12(21): 1797-1806.
26. Eliezer, Y., Argaman, L., Kornowski, M., et al. Interplay between the DNA damage proteins MDC1 and ATM in the regulation of the spindle assembly checkpoint. (2014) J Biol Chem 289(12): 8182-8193.
27. Chila, R., Celenza, C., Lupi, M., et al. Chk1-Mad2 interaction: a crosslink between the DNA damage checkpoint and the mitotic spindle checkpoint. (2013) Cell cycle 12(7): 1083-1090.
28. Mossaid, I., Fahrenkrog, B. Complex Commingling: Nucleoporins and the Spindle Assembly Checkpoint. (2015) Cells 4(4): 706-725.
29. Du, Y., Yin, F., Liu, C., et al. Depression of MAD2 inhibits apoptosis of gastric cancer cells by upregulating Bcl-2 and interfering mitochondrion pathway. (2006) Biochem Biophys Res Commun 345(3): 1092-1098.
30. Cheung, H.W., Jin, D.Y., Ling, M.T., et al. Mitotic arrest deficient 2 expression induces chemosensitization to a DNA-damaging agent, cisplatin, in nasopharyngeal carcinoma cells. (2005) Cancer Res 65(4): 1450-1458.
31. Eom, Y.W., Kim, M.A., Park, S.S., et al. Two distinct modes of cell death induced by doxorubicin: apoptosis and cell death through mitotic catastrophe accompanied by senescence-like phenotype. (2005) Oncogene 24(30): 4765-4777.
32. Lentini, L., Barra, V., Schillaci, T., et al. MAD2 depletion triggers premature cellular senescence in human primary fibroblasts by activating a p53 pathway preventing aneuploid cells propagation. (2012) J Cell Physiol 227(9): 3324-3332.
33. Yun, M., Han, Y.H., Yoon, S.H., et al. p31comet Induces cellular senescence through p21 accumulation and Mad2 disruption. (2009) Mol Cancer Res 7(3): 371-382.
34. Nascimento, A.V., Singh, A., Bousbaa, H., et al. Mad2 checkpoint gene silencing using epidermal growth factor receptor-targeted chitosan nanoparticles in non-small cell lung cancer model. (2014) Mol Pharm 11(10): 3515-3527.
35. Nascimento, A.V., Gattacceca, F., Singh, A., et al. Biodistribution and pharmacokinetics of Mad2 siRNA-loaded EGFR-targeted chitosan nanoparticles in cisplatin sensitive and resistant lung cancer models. (2016) Nanomedicine (Lond) 11(7): 767-781.
36. Masawang, K., Pedro, M., Cidade, H., et al. Evaluation of 2',4'-dihydroxy-3,4,5-trimethoxychalcone as antimitotic agent that induces mitotic catastrophe in MCF-7 breast cancer cells. (2014) Toxicol Lett 229(2): 393-401.

Ommega Online Publishers
Journal Title: International Journal of Cancer and Oncology (IJCO)
Journal Short Name: Int J Cancer Oncol
Journal ISSN: 2377-0902
E-mail: cancerandoncology@ommegaonline.com
Website: www.ommegaonline.org